ZooKeys 1076: 1–8 (2021)
doi: 10.3897/zookeys.1076.72802
https://zookeys.pensoft.net

RESEARCH ARTICLE

A peer-reviewed open-access journal
ZooKeys
Launched to accelerate biodiversity research

Neothelaxes pileata, a new species from China (Hemiptera, Sternorrhyncha, Aphididae, Thelaxinae)

Li-Yun Jiang[1], Xiao-Lu Zhang[1,2], Jing Chen[1], Yi-Fang Zhao[1], Ge-Xia Qiao[1,2]

1 *Key Laboratory of Zoological Systematics and Evolution, Institute of Zoology, Chinese Academy of Sciences, No. 1–5 Beichen West Road, Chaoyang District, Beijing 100101, China* **2** *College of Life Science, University of Chinese Academy of Sciences, No. 19, Yuquan Road, Shijingshan District, Beijing 100049, China*

Corresponding author: Ge-Xia Qiao (qiaogx@ioz.ac.cn)

Academic editor: Colin Favret | Received 10 August 2021 | Accepted 20 November 2021 | Published 8 December 2021

http://zoobank.org/0C7A4361-C435-404A-BEC7-8C5869593B50

Citation: Jiang L-Y, Zhang X-L, Chen J, Zhao Y-F, Qiao G-X (2021) *Neothelaxes pileata*, a new species from China (Hemiptera, Sternorrhyncha, Aphididae, Thelaxinae). ZooKeys 1076: 1–8. https://doi.org/10.3897/zookeys.1076.72802

Abstract

Neothelaxes pileata Qiao **sp. nov.**, found on *Pilea martinii* (Urticaceae) in China, is described and illustrated. *Neothelaxes* Chakrabarti & Quednau is also a new generic record for China.

Keywords

Aphid, new record, Tibetan plateau

Introduction

The aphid genus *Neothelaxes* was erected by Chakrabarti and Quednau (1996), with *Neothelaxes viticola* Chakrabarti & Quednau, 1996 as the type species. The generic diagnosis is based on the dorsal body setae arranged in single rows, not in groups, and the presence of minute wax gland pores on the sclerites. At present, there are only two known species, *Neothelaxes parthenocissi* Chakrabarti & Quednau, 1996 and *N. viticola* (Blackman and Eastop 2020; Favret 2020). Recently, some unusual specimens were collected on *Pilea martinii* (H. Lev) Hand-Mazz. (Urticaceae) in the Tibetan plateau, China, and they are here described as a new species, *Neothelaxes pileata* Qiao sp. nov. The genus *Neothelaxes* is newly recorded from China.

Materials and methods

The procedure used for processing and preparing the aphid specimens for microscopic study followsed that of Jiang et al. (2016). The descriptions and drawings provided here were produced from slide-mounted specimens using a Leica DM4000B with a drawing tube attached. The photomicrographic images were prepared with a Leica DM2500 using DIC illumination and processed with the Automontage and Photoshop software.

Aphid terminology in this paper generally follows that of Chakrabarti and Quednau (1996). The unit of measurement is millimetres (mm). The holotype and seven paratypes are deposited in the National Zoological Museum of China, Institute of Zoology, Chinese Academy of Sciences, Beijing, China (**NZMC**), and one paratype is deposited in the Natural History Museum, London, UK (**NHMUK**).

Taxonomy

The Thelaxinae (sensu Remaudière and Stroyan 1984) is a small group of aphids, at present comprising the genera *Thelaxes* Westwood, *Glyphina* Koch, *Kurisakia* Takahashi, and *Neothelaxes* Chakrabarti & Quednau. Species of the first three genera are associated with woody trees: *Thelaxes* includes oak-feeding species (Fagaceae), *Glyphina* species are associated with *Alnus* and *Betula* (Betulaceae), and *Kurisakia* species are associated with Juglandaceae and Fagaceae. On the other hand, *Neothelaxes* is recorded only on climbing woody rattan or herbaceous plants such as *Parthenocissus* (Vitaceae) (Chakrabarti & Quednau, 1996) and *Pilea martinii* (Urticaceae). Among the four genera, only *Neothelaxes* is covered with dorsal waxy plates. This genus has a restricted distribution, with the previously-described species occurring only in the Indian Northwest Himalaya and the new species restricted to the southern Tibetan plateau. Species of the genus are probably endemic to the region.

***Neothelaxes pileata* Qiao, sp. nov.**
http://zoobank.org/FE1B5156-4669-4410-9703-85D3D33C1834
Figures 1–28, Table 1

Specimens examined. *Holotype*: apterous viviparous female, **China**: Tibet Autonomous Region (Linzhi City: Motuo County, 29.697°N, 95.556°E, altitude 2678 m), 25 July 2019, No. 46755-1-1-1, on *Pilea martinii* coll. X.L. Zhang. ***Paratypes*:** 2 apterous viviparous females and 3 first instar nymphs with the same collection data as the holotype; 1 apterous viviparous female, No. 46755-1-2, with the same collection data as the holotype (NHMUK); 2 fourth instar apterous nymphs, China: Tibet Autonomous Region (Linzhi City: Motuo County, 29.697°N, 95.556°E, altitude 2678 m), 17 June 2021, No. 51097-1-1-1, on Pilea martinii coll. M. Qin and X.L. Zhang.

Etymology. The specific name *pileata* is an adjective based on the feminine generic name of the host plant.

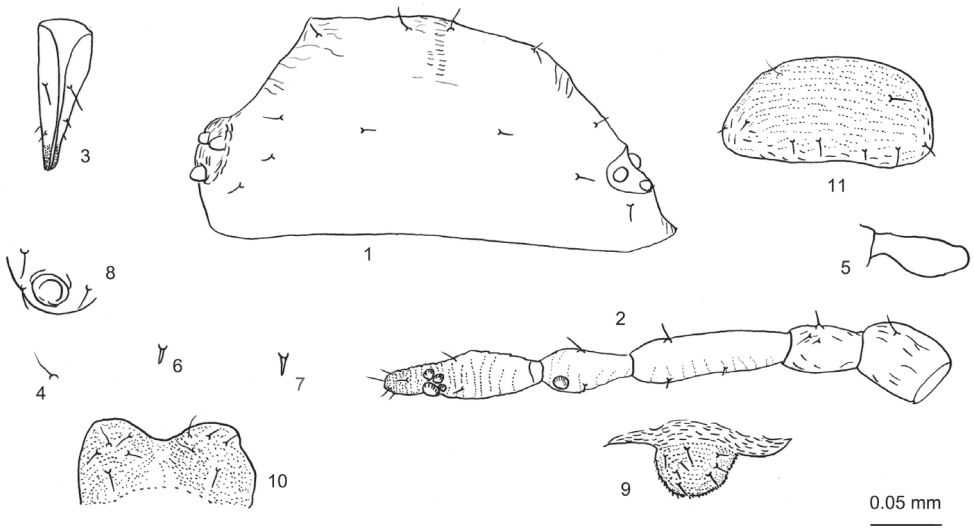

Figures 1–11. *Neothelaxes pileata* Qiao sp. nov. Apterous viviparous female: **1** dorsal view of head **2** antennal segments I–V **3** ultimate rostral segment **4** cephalic seta **5** mesosternal furca **6** marginal seta on abdominal tergite I **7** spinal seta on abdominal tergite VIII **8** siphunculi **9** cauda **10** anal plate **11** genital plate. Scale bars: 0.05 mm.

Description. Apterous viviparous female: Body small, oval (Figs 12, 23). Adults light dirty green, or dirty yellowish green, nymphs yellowish green, covered with white waxy powder in life (Fig. 23), and found in irregularly spherical galls on the leaves of the host plant. For morphometric data see Table 1.

Mounted specimens. Body dorsum pale brown (Fig. 12). Antennae, legs, cauda, anal plate, and genital plate brown, siphunculi and apex of rostrum dark brown. Head to abdominal segment VII fused, sometimes with intersegmental boundary on spinal area between head and pronotum and pronotum and mesonotum, and on spino-pleural areas of abdominal tergites; abdominal segment VIII free (Fig. 12). Dorsal setae of body spine-like (Figs 6, 7). Wax plates large, with many minute wax pores (Figs 15, 17–19). Vertex with one pair of wax plates, pronotum to abdominal tergites I–VII each with one pair of spinal and one pair of marginal wax plates, tergite VIII with a spino-pleural wax plate (Figs 15, 17–19). Spiracles small and round, spiracular plates small and oval, brown.

Head. Frons convex, eyes 3-faceted (Figs 1, 12, 15). Head dorsum with indistinct median suture. Dorsal setae on head short, fine and pointed (Figs 1, 15). Cephalic setae with two pairs, head with one pair of posterior spinal setae and three pairs of marginal setae; cephalic setae 0.78–1.13× basal diameter of antennal segment III (Figs 1, 4, 15). Eyes 3-faceted. Antennae 5-segmented (Figs 2, 13), segments III and IV with sparse spinulose imbrications, segment V with spinulose imbrications; 0.29–0.33× body; processus terminalis 0.30–0.40× base of the segment. Antennal setae sparse, very short and pointed; segments I–V with 2 or 3, 2, 1–4, 3, 2 setae, respectively; processus terminalis with five setae. Length of setae on segment III 0.50–0.80× basal diameter

Table 1. Morphometric data for apterous viviparous females of *Neothelaxes pileata* Qiao sp. nov. (n = 4, with means in brackets), the measurements are given in mm.

Characters	Apterous viviparous females (n = 4)
Body length	1.260–1.320 (1.288)
Body width	0.820–0.940 (0.868)
Antenna	0.359–0.418 (0.397)
Antennal segment I	0.052–0.064 (0.058)
Antennal segment II	0.047–0.059 (0.053)
Antennal segment III	0.094–0.119 (0.110)
Antennal segment IV	0.054–0.062 (0.059)
Base of antennal segment V	0.082–0.092 (0.087)
Processus terminalis	0.027–0.035 (0.030)
Ultimate rostral segment	0.104–0.109 (0.105)
Hind femur	0.257–0.319 (0.284)
Hind tibia	0.270–0.324 (0.295)
Second hind tarsal segment	0.079–0.084 (0.082)
Siphunculus	0.012–0.022 (0.015)
Basal width of siphunculus	0.054–0.069 (0.058)
Distal width of siphunculus	0.025–0.027 (0.025)
Cauda	0.015–0.037 (0.030)
Basal width of cauda	0.099–0.109 (0.101)
Basal diameter of antennal segment III	0.020–0.025 (0.022)
Widest width of hind femur	0.054–0.057 (0.056)
Width of hind tibia at mid length	0.032–0.040 (0.036)
Longest dorsal cephalic seta	0.017–0.022 (0.021)
Longest marginal seta on abdominal tergite I	0.012 (0.012)
Longest seta on abdominal tergite VIII	0.012–0.015 (0.014)
Longest seta on antennal segment III	0.010–0.020 (0.015)
Longest seta on hind tibia	0.020–0.027 (0.022)

of the segment. Primary rhinaria ciliated (Figs 2, 13). Rostrum (Figs 3, 14) reaching mid-coxae; ultimate rostral segment elongate wedge-shaped, stout at apex, 2.50–3.14× its basal width, 1.18–1.33× second hind tarsal segment, with two pairs of primary setae and two accessory setae, accessory setae longer than primary setae.

Thorax (Fig. 12). Pronotum with one pair of posterior spinal setae and two pairs of marginal setae; meso- and metanotum each with two pairs of marginal setae. Mesosternal furca with two arms separated (Fig. 5). Legs normal. Femur and trochanter fused (Fig. 12); hind femur and trochanter 4.52–5.61× widest width of this segment; 2.41–2.74× antennal segment III. Distal 1/3 of tibiae slightly expanded, with spinulose transverse stripes (Fig. 16); hind tibia 0.21–0.25× body. Setae on legs fine and pointed, length of setae on hind tibiae 0.43–0.73× middle diameter of the segment. First tarsal segments spinulose, segment II with spinulose short stripes (Fig. 16). First tarsal chaetotaxy: 4, 4, 2 or 3.

Abdomen. Abdominal tergites with two or three pairs of spinal and one pair of marginal setae; tergite VII with one pair of spinal and one pair of marginal setae (Fig. 19); tergite VIII with one pair of spinal and two pairs of marginal setae (Fig. 21). Length of marginal setae on tergite I 0.50–0.63× basal diameter of antennal segment III; dorsal setae on tergite VIII 0.56–0.75× basal diameter of antennal segment III. Siphunculi almost poriform (Figs 8, 18, 20), on tergite VI surrounded by three hair-

Figures 12–22. *Neothelaxes pileata* Qiao sp. nov. Apterous viviparous female: **12** dorsal view of body **13** antenna **14** ultimate rostral segment **15** dorsal view of head, with antennal segments I–II and dorsal setae **16** distal part of hind tibia and hind tarsal segment **17** marginal setae and marginal waxy plates on abdominal tergites II–V **18** siphunculus and marginal setae and marginal waxy plate on abdominal tergite V **19** spinal setae and waxy plates on abdominal tergite VII **20** siphunculus and dorsal view of abdominal tergites VI–VIII **21** dorsal setae on abdominal tergite VIII, cauda, and anal plate **22** cauda, anal plate and genital plate. Scale bars: 0.10 mm (**12, 17**); 0.05 mm (**13–16, 19–21**); 0.02 mm (**18, 22**).

like setae; 0.23–0.32× its basal width, 0.42–0.60× cauda. Cauda knob-shaped (Figs 9, 21–22), with spinulose short stripes; 0.27–0.38× its basal width, with six to eight long and short, finely pointed setae. Anal plate transversely oval (Figs 10, 21–22), indistinctly bilobed, with spinulose short stripes. Genital plate (Figs 11, 22) transverse oval, with sparse spinulose transverse lines; with two anterior setae and seven or eight posterior setae. Two gonapophyses, each with five shorter and pointed gonosetae.

***First instar nymph*:** Body oval, pale when macerated. Head and pronotum fused (Fig. 23). Vertex arc-shaped, head dorsum smooth, with distinct median suture (Fig. 24). Dorsal setae on head short and pointed, head with one pair of cephalic setae, two pairs of setae between antennae, three pairs of marginal setae and one pair of anterior spinal setae between eyes; length of cephalic setae 0.83× basal diameter of segment III. Eye 3-faceted. Antennae 5-segmented (Fig. 25), segments I–IV smooth, segment V with spinulose imbrications; antennal setae slightly long and pointed, segments I–V each with 2, 2, 0, 2–3, 2+5 setae, respectively; length of setae on segment IV 1.0× basal diameter of antennal segment III; segment III 0.032 mm, respective length in proportion of segments I–V as follows: 100, 100, 100, 77, 154+77; processus terminalis 0.50× base of the segment. Primary rhinaria round and ciliated. Rostrum reaching abdominal segment IV; ultimate rostral segment elongate wedge-shaped (Fig. 26), 2.82× its basal width, 1.35× hind second tarsal segment; with one pair of accessory setae and two pairs of primary setae. Dorsal setae of thorax and abdomen spine-like, similar to adults. Thorax dorsum each with one pair of spinal and one pair of marginal

wax plates, respectively. Pronotum with one pair of spinal and one pair of marginal setae, mesonotum and metanotum each with one pair of spinal, one pair of pleural and two pairs of marginal setae. Trochanter fused with femur. Distal half of tibiae and tarsi with spinulose stripes, the other half of tibiae smooth (Fig. 27). First tarsal chaetotaxy: 2, 2, 2. Abdominal tergites I–VII each with one pair of spinal and one pair of marginal wax plates (Fig. 28); tergite VIII covered with wax plate (Fig. 28). Abdominal tergites I–VII each with one pair of spinal and one pair of marginal setae (Fig. 28); tergite VIII with two dorsal setae (Fig. 28); length of marginal setae on tergite I and dorsal setae on tergite VIII 0.83× and 0.33× basal width of antennal segment III, respectively. Siphunculi invisible. Cauda circular at apex, with two setae (Fig. 28). Anal plate broadly circular, with four setae (Fig. 23). Cauda and anal plate with spinules.

Embryo **(in an aptera):** Eye 3-faceted. Antenna 5-segmented, segments I–IV smooth, segment V with spinulose imbrications. Frontal setae hair-like, the remainder of dorsal body setae stout, acute, almost spine-like. Vertex on each side with three anterior and two posterior setae. Pronotum with three pairs of marginal and one pair of spinal setae, anterior spinal setae missing. Meso- and metanotum each with two pairs of marginal, one pair of spinal, and one pair of pleural setae. Abdominal tergites I–VII each with one pair of spinal and one pair of marginal setae; tergite VIII with one pair of dorsal setae. Siphunculi hardly visible. Antennal segments I–IV with 2, 2, 0, 2 or 3 and 2+4 setae, respectively.

Host plant. *Pilea martinii* (H. Lev.) Hand-Mazz. (Urticaceae).

Biology. The specimens were found within an irregularly spherical gall on the leaves. Compared to the other two species in *Neothelaxes*, which are not known to form galls, the biology of this new species is unusual, interesting, but less well known.

Comments. According to some morphological features–3-faceted eye in apterae; fused head and thorax; 5-segmented antenna; processus terminalis shorter than base of the segment; antennal segment V, tarsi, and apices of tibiae spiculose; siphunculi poriform and surrounded by setae; cauda knob-shaped–the new species is regarded as belonging to the subfamily Thelaxinae. This new species is similar to those of *Neothelaxes* based on dorsum of body with waxy plates, dorsal body setae short and spine-like, and primary rhinaria ciliated. However, it differs from the type species of the genus, *N. viticola*, as follows: first tarsal segment chaetotaxy: 4, 4, 2 or 3 (in *N. viticola* first tarsal segments with 5-5-7 setae); dorsum of body pale brown, without distinct sclerites (in *N. viticola* vertex and spinal, marginal, and pleural sclerites of body dorsum distinct); antennae at most 1/3 of body length (in *N. viticola* 1/2 of body length); antennae of embryo 5-segmented (in *N. viticola* 4-segmented); infesting plants of *Pilea* (Urticaceae) (*N. viticola* infests the genus *Parthenocissus* (Vitaceae)).

Of the four known genera of Thelaxinae (sensu Remaudière and Stroyan 1984), *Thelaxes*, *Glyphina*, and *Kurisakia* are associated with woody trees (Fagaceae, Betulaceae, Juglandaceae), wheras *Neothelaxes* is known only from climbing woody rattan (Vitaceae: *Parthenocissus*) (Chakrabarti & Quednau, 1996). No species of

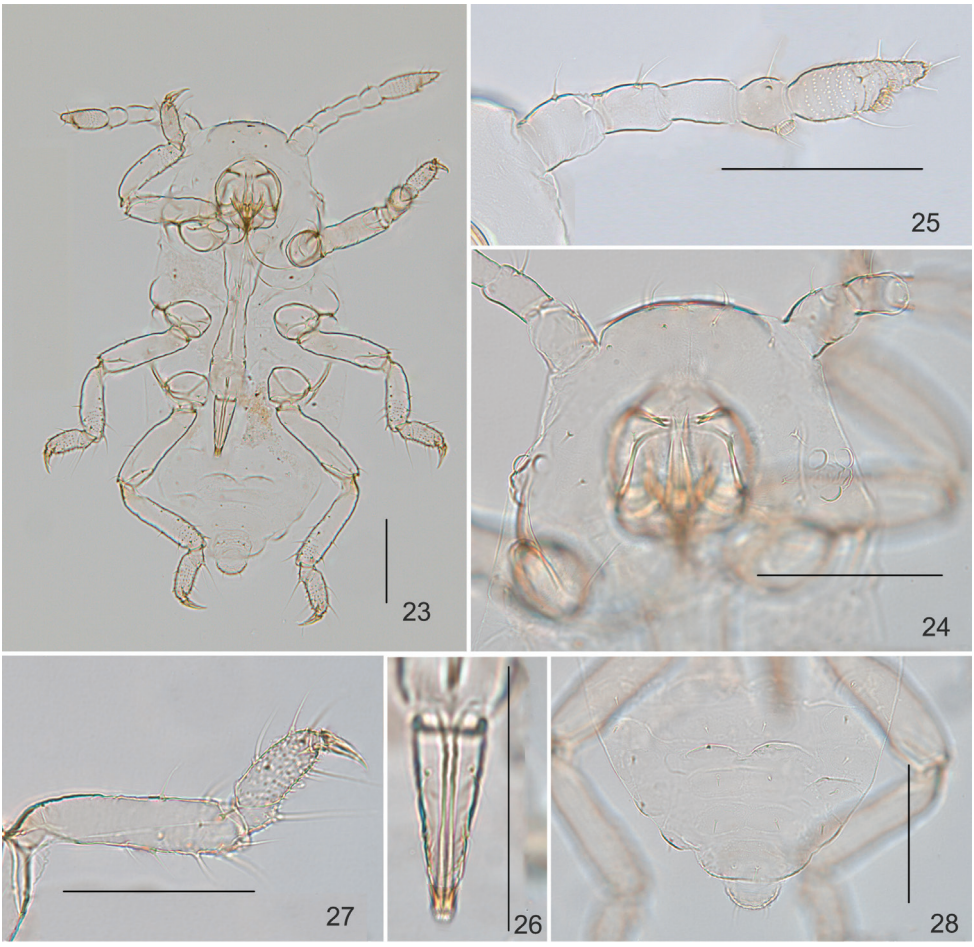

Figures 23–28. *Neothelaxes pileata* Qiao sp. nov. First instar nymph: **23** dorsal view of body **24** dorsal view of head, with antennal segments I–II and dorsal setae **25** antenna **26** ultimate rostral segment **27** hind tibia and hind tarsal segment **28** dorsal setae and waxy plates on abdominal tergites V–VIII, showing cauda. Scale bars: 0.10 mm.

Thelaxinae was previously known to live in galls. The new species is associated with an herbaceous plant and was found in leaf galls. These traits are very different from those of other species of Thelaxinae. The association with the galls is unusual and needs further confirmation from a full colony of aphids in a gall.

In view of the present findings on its host association and gall inducing nature as well as several other characters, the new species is placed in the genus *Neothelexes*. Further surveying and research on its biology, for example the rearing of additional adults (especially alatae) from additional galls, will be necessary to elucidate the appropriate taxonomic placement of the new species.

Acknowledgements

This work was supported by the National Natural Sciences Foundation of China (Grant Nos. 32030014, 31772492, 31970451), the Key Collaborative Research Program of the Alliance of International Science Organizations (Grant No. ANSO-CR-KP-2020-04), the Second Tibetan Plateau Scientific Expedition and Research (STEP) program (Grant No. 2019QZKK0501), and the Youth Innovation Promotion Association of Chinese Academy of Sciences (Grant No. 2020087).

References

Blackman RL, Eastop VF (2020) Aphids on the World's Plants. An online identification and information guide. [accessed 18 July 2021] http://www.aphidsonworldsplants.info/

Chakrabarti S, Quednau FW (1996) A new genus, *Neothelaxes*, and two new species of Thelaxinae from India (Homoptera: Aphididae). The Canadian Entomologist 128: 1005–1011. https://doi.org/10.4039/Ent1281005-6

Favret C (2020) Aphid Species File. Version 5.0/5.0. [accessed 18 Jul 2021] http://Aphid.SpeciesFile.org

Jiang LY, Chen J, Qiao GX (2016) *Yamatochaitophorus yichunensis*, a new species of aphid (Aphididae: Chaitophorinae) from northeast China. ZooKeys 612: 41–49. https://doi.org/10.3897/zookeys.612.7873

Remaudière G, Stroyan HLG (1984) Un *Tamalia* nouveau de Californie (U.S.A.). Discussion sur les Tamaliinae subfam. nov. (Hom. Aphididae). Les Annales de la Société Entomologique de France (N.S.) 20: 93–104.

Remaudière G, Remaudière M (1997) Catalogue of the World's Aphididae. Homoptera Aphidoidea. Institut National de la Recherche Agronomique, Paris, 473 pp.

ZooKeys 1076: 9–24 (2021)
doi: 10.3897/zookeys.1076.72835
https://zookeys.pensoft.net

RESEARCH ARTICLE

A peer-reviewed open-access journal
ZooKeys
Launched to accelerate biodiversity research

Designation of the neotype of *Triatoma dimidiata* (Latreille, 1811) (Hemiptera, Reduviidae, Triatominae), with full integrated redescription including mitogenome and nuclear ITS-2 sequences

Silvia Andrade Justi[1,2,3], Carolina Dale[4]

1 *Walter Reed Biosystematics Unit, Smithsonian Institution Museum Support Center, 4210 Silver Hill Road, Suitland, MD 20746, USA* **2** *Entomology Branch, Walter Reed Army Institute of Research, 503 Robert Grant Avenue, Silver Spring, MD 20910, USA* **3** *Department of Entomology, Smithsonian Institution National Museum of Natural History, Washington, DC 20560, USA* **4** *Laboratório de Biodiversidade Entomológica, Instituto Oswaldo Cruz, Fiocruz, Av. Brasil 4365, Rio de Janeiro, RJ, 21040-900, Brazil*

Corresponding author: Silvia Andrade Justi (justis@si.edu)

Academic editor: J. Oliveira | Received 10 August 2021 | Accepted 15 October 2021 | Published 8 December 2021

http://zoobank.org/046E83F4-C414-44F1-B5F0-EC77CA0BB184

Citation: Justi SA, Dale C (2021) Designation of the neotype of *Triatoma dimidiata* (Latreille, 1811) (Hemiptera, Reduviidae, Triatominae), with full integrated redescription including mitogenome and nuclear ITS-2 sequences. ZooKeys 1076: 9–24. https://doi.org/10.3897/zookeys.1076.72835

Abstract

The taxonomic status of *Triatoma dimidiata* (Latreille, 1811) is, by far, the most discussed within Triatominae. Molecular studies have recovered at least three independently evolving lineages in *T. dimidiata* across its range. The original description of *T. dimidiata* (as *Reduvius dimidiatus*) included few taxonomic characters, and no types were assigned. To define and describe the cryptic diversity within *T. dimidiata* sensu lato (s.l.), a neotype must be designated. For this purpose, all 199 specimens identified as *T. dimidiata* from the collections of the Smithsonian Institution – National Museum of Natural History and the American Museum of Natural History, ranging from Peru to Mexico, were studied. Only one specimen (from Tumbes, Peru) matched the combination of characters as listed in the original description, and it is herein formally designated as the neotype for *T. dimidiata*. The neotype is morphologically described and DNA sequences of its whole mitochondrial genome and the nuclear second internal transcribed spacer region (ITS2), commonly used in triatomine molecular systematics studies, are presented and compared to other publicly available sequences of *T. dimidiata* s.l. in GenBank. Our results suggest that *T. dimidiata* sensu stricto (s.s.) is somewhat rare and, therefore, unlikely to serve as a major vector of Chagas disease.

Keywords
Chagas disease, Latreille, Peru, South America, vector

Introduction

Triatoma dimidiata (Latreille, 1811) (Hemiptera, Reduviidae) has long been assumed to be the most widespread species of Triatominae, a reduviid subfamily of Chagas disease vectors. The long-standing discussion about its taxonomic status, however, is consequential of an original description with no type specimens defined and very few characters described by Latreille (1811).

Triatoma dimidiata was originally described as *Reduvius dimidiatus* by Latreille in Humboldt and Bonpland (1811), where the author only provided a drawing of the dorsal view of the described specimen (Fig. 1), a male specimen, pale yellow with body black, and no scale to size. Latreille highlighted the presence of 1+1 discal tubercles and 1+1 lateral tubercles on the pronotum, as well as 1+1 subapical "spines" on fore- and mid-femora. The locality was listed as Villa de Ybara, Peru (now Ecuador).

About 150 years after the description of *T. dimidiata*, two new species had been described, and later synonymized to *T. dimidiata*: *Triatoma capitata* Usinger, 1941 and *Triatoma maculipennis* Pinto, 1931. In their taxonomic revision of Triatominae, Lent and Wygodzinsky (1979), upon observation of 160 specimens from the whole geographic range (Mexico to Peru), highlighted the "highly variable" coloration and other morphological characters of the specimens observed. They concluded, however, that

Figure 1. Original drawing presented by Latreille (1811) illustrating the description of *Reduvius dimidiatus*.

these specimens have not segregated "into clearly separable allopatric populations"; synonimizing both *T. capitata* and *T. maculipennis* with *T. dimidiata.*

The availability of molecular sequencing techniques led to the discovery that *T. dimidiata*, when comprising the recently described *Triatoma mopan* Dorn, Justi & Dale, 2018 and *Triatoma huehuetenanguensis* Lima-Cordón & Justi, 2019, is a paraphyletic species complex (Justi et al. 2014b, 2016) which includes at least three independently evolving lineages (Bargues et al. 2008; Dorn et al. 2009, 2016; Justi et al. 2018).

Here we set out to assign and describe a neotype of *T. dimidiata* sensu stricto (s.s.) conforming to the original description of Latreille (1811) and from as close to the original locality as possible, in order to facilitate the understanding of the systematics of *T. dimidiata* sensu lato (s.l.). This solid taxonomic platform allows for the conduct of future studies to facilitate better understanding of the composition and internal systematics of species comprising *Triatoma dimidiata* s.l.. Given that most of the diversity in *T. dimidiata* s.l. is reported based on molecular rather than morphological data, the whole mitochondrial genome and nuclear rDNA sequences of the second internal transcribed spacer (ITS2) of the neotype specimen are also presented.

Methods

Examined material

To locate an optimal neotype in the absence of designated types in the original description of *T. dimidata* (Latreille, 1811), we examined all available specimens of *T. dimidiata* s.l. in the Hemiptera collections of the Smithsonian Institution-National Museum of Natural History (USNM) (n = 106) and of the American Museum of Natural History (AMNH) (n = 93). Following a first pass, all specimens were further compared to the original description and drawing by Latreille (1811). Where morphological deviations from the original description were observed, the examined specimen was discarded as a potential neotype. Associated metadata for all examined specimens are available as Suppl. material 1.

Once the specimen, suitable to be designated as neotype (i.e., showing no deviation from the characters originally described and collected close to the type locality) was identified, measurements were taken using a Dino-Lite Edge digital microscope. Whole specimen (habitus) and detailed character photos were taken at the NMNH Scanning Electron Microscopy Imaging Lab, using an Olympus DSX100 camera.

Mitochondrial genome and ITS-2 sequencing and assembly

Non-destructive DNA extraction, NGS library preparation, as well as mitochondrial genome and ITS2 sequencing and assembly were performed as previously described (Justi et al. 2021). References used for the sequence assemblies included *T. dimidiata* s.l. mitochondrial genome (GenBank accession AF01594) and *T. dimidiata* s.l. haplotype T-dim-H65 internal transcribed spacer 2 (GenBank accession KT874451).

Molecular barcode-like analysis

Two alignments were constructed to assess the relatedness of the neotype to the previously studied sequences: (1) all CytB sequences available on GenBank labeled as *T. dimidiata*; and (2) all ITS2 sequences available on GenBank labeled as *T. dimidiata*. Each of these public datasets were combined with the respective sequences from the neotype, *T. mopan*, and *T. huehuetenanguensis* and aligned using the Geneious alignment algorithm implemented in Geneious (Kearse et al. 2012). The GenBank accession number list for the sequences included is available as Suppl. material 2.

Pairwise Kimura 2-parameter (Kimura 1980) distances were calculated for comparison with previously published *T. dimidiata* s.l. sequences using the package ape (Paradis et al. 2004), and barcode-like gap analysis, followed by cluster analysis were performed for both markers, using a custom R script (R Development Core Team 2013). R code is available as Suppl. material 3. Briefly, pairwise distances are calculated for all sequences, and sorted from smallest to largest. The difference between the distances is successively calculated for each value, subtracting the previous value from the current value. The highest difference is identified. Then, the two distances that generated that difference are identified and assigned as the barcode-like gap. The barcode-like gap is then used to identify clusters, using the pairwise distances between the sequences.

Results

Examined material

Among the 199 specimens available in the collections of the AMNH and USNM, there were no exemplars from the original locality of Villa de Ybara (previously Peru; now part of Ecuador). Only one examined specimen presented the character combinations as per the original description of Latreille (1811): 1+1 discal tubercles, 1+1 lateral tubercles and, 1+1 subapical denticles on the femur on the front and mid leg. The male specimen (Fig. 2), from Tumbes, Peru, was previously illustrated in figure 63 in the review by Lent and Wygodzinsky (1979), and is herein designated as the neotype. As this was the only specimen determined to be *T. dimidiata* s.s., the character measurements refer only to the neotype specimen (Table 1).

Mitochondrial genome

The assembled mitochondrial genome (GenBank MT757852) comprises 16,087 nucleotides, with all 13 typical mitochondrial coding genes, 22 tRNA genes, and 12S and 16S ribosomal regions (Suppl. material 4). These were observed to follow the same arrangement as the reference used (GenBank AF01594; Fig. 3).

Figure 2. *Triatoma dimidiata* neotype. Male.

Table 1. Character measurements of the *Triatoma dimidiata* neotype.

Character	Length (mm)
Total body length	29.0
Width of the abdomen	11.5
Length of pronotum	5.5
Width of pronotum	7.2
Length of head (excludes neck)	5.0
Width of head across eyes	3.1
Synthlipsis	1.7
Width of eye in dorsal view	1.4
Anteocular region	3.5
Postocular region	1.7
Diameter of ocellus	0.5
Distance between ocellus-eye	0.2
Labium – Length of 1st visible segment	1.0
Labium – Length of 2nd visible segment	1.8
Labium – Length of 3rd visible segment	0.9

Molecular barcode-like analysis

Based on the calculated barcode-like gap clustering analysis for the mtDNA CytB alignment created, which comprised 105 sequences, only one sequence, from El Salvador [KT998327; Haplotype T.dim-Cytb.DKin (Dorn et al. 2016)] clustered with the neotype. For this mark-

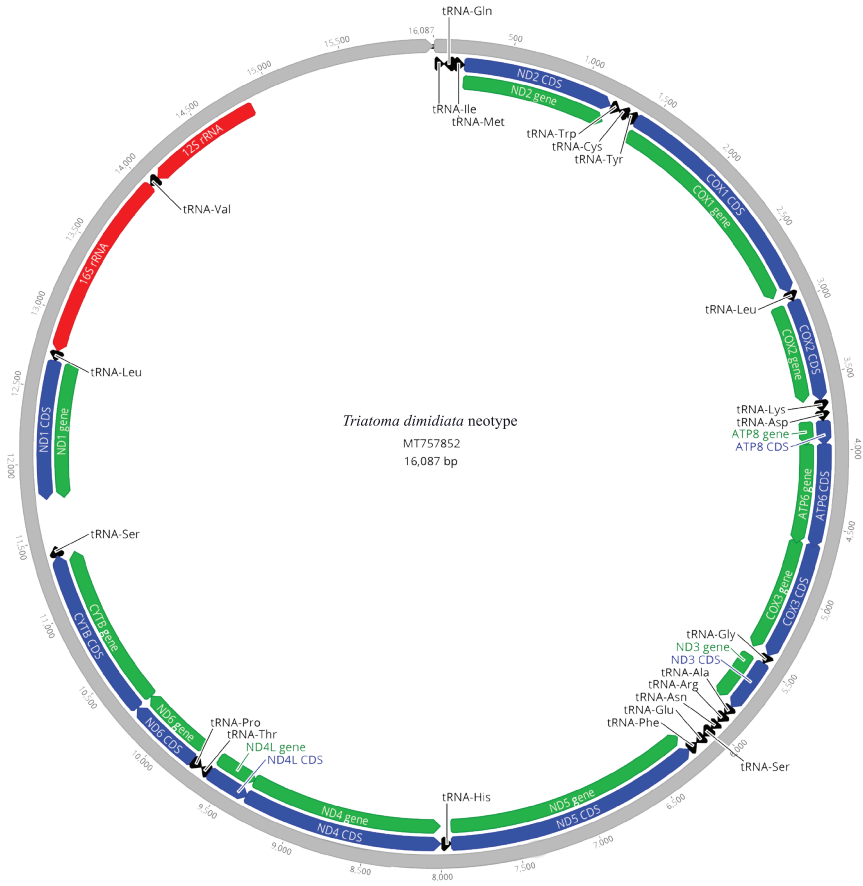

Figure 3. *Triatoma dimidiata* neotype (male) mitochondrial genome.

er, the lowest observed intra-cluster distance was zero, while the highest was 0.00334 (average 0.00115, SD ± 0.0014); while observed inter-cluster distance ranged from 0.00488–0.1754 (average 0.0881, SD ± 0.05446). Calculated CytB distances between the neotype and *T. mopan*, and the neotype and *T. huehuetenanguensis* were 0.1388 and 0.1580, respectively.

This diversity was further echoed through clustering analysis of all publicly available *T. dimidiata* nuclear rDNA ITS2 sequences (n = 128). Some 60 clusters were recovered, with 14 sequences, with geographic origin ranging throughout Central America (Table 2), clustering with the neotype.

The lowest observed intra-cluster distance for ITS-2 sequences was zero, while the highest was 0.00464 (average 0.00214, SD ± 0.0019); the lowest observed inter-cluster distance was 0.00674 and the highest 0.15164 (average 0.05998, SD ± 0.0267). Estimated ITS-2 distances between the neotype and *T. mopan*, and the neotype and *T. huehuetenanguensis* were 0.0326 and 0.0399, respectively.

A graphical representation of the calculated CytB and ITS-2 distances between the neotype and all other sequences is presented on Figure 4.

Table 2. List of GenBank accessions and geographic origin of specimens for which the ITS-2 sequence clustered with the neotype sequence.

GenBank species label	GenBank accession	Geographic origin as listed on the original publication for the sequence
Triatoma dimidiata	AM286696.1	Guatemala: Quiche
Triatoma dimidiata	DQ871355.1	El Salvador: Santa Ana
Triatoma dimidiata	AM286697.1	Ecuador: Guayaquil
Triatoma dimidiata	MN505087.1	Ecuador
Triatoma dimidiata	MN505088.1	Ecuador
Triatoma dimidiata	KT874433.1	Costa Rica
Triatoma dimidiata	KT874432.1	Costa Rica
Triatoma dimidiata	KF192843.1	Costa Rica
Triatoma dimidiata	AM286700.1	Guatemala: Pueblo Nuevo
Triatoma dimidiata	AM286693.1	Guatemala: Jutiapa
Triatoma dimidiata	AM286701.1	Honduras: Yoro Yoro
Triatoma dimidiata	AM286694.1	Honduras: Yoro Yoro
Triatoma dimidiata	MK248260.1	Mexico: Chiapas
Triatoma dimidiata	MK248261.1	Mexico: Chiapas

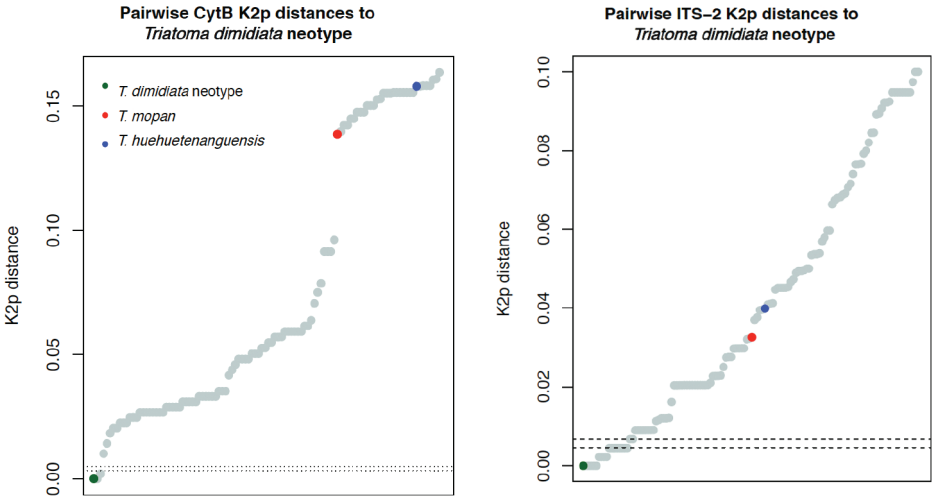

Figure 4. Pairwise Kimura 2-parameter distances between publicly available sequences and sequences from the neotype. Dashed lines indicate the barcode-like gap for each marker.

Description of the neotype

Taxonomy

Family Reduviidae Latreille, 1807
Subfamily Triatominae Jeannel, 1919

Genus *Triatoma* Laporte, 1832

Triatoma dimidiata (Latreille, 1811)
Reduvius dimidiatus Latreille, 1811
Conorhinus dimidiatus (Stål, 1859)
Conorrhinus dimidiatus (Champion, 1899)
Triatoma dimidiata (Neiva, 1914)

Type. ***Neotype*****:** male, designated herein. Cabezza de Lagartos, Tumbes, Peru. [= fig. 63 of Lent and Wygodzinsky (1979)].

Locality data: Cabezza de Lagartos, Tumbes, Peru [no date or collector attributes given].

Depository: American Museum of Natural History, specimen number AMNH_IZC 00319810.

DNA: neotype mitochondrial genome (GenBank MT757852); neotype nuclear ribosomal second internal spacer region (ITS2) (GenBank MT362613).

Diagnosis. The neotype can be immediately distinguished from the other observed *T. dimidiata* s.l. specimens by the following combination of character: pronotum with anterior lobe presenting 1+1 discal tubercles (one on each side of anterior lobe), pointed posteriorly, and 1+1 round, smaller lateral tubercles. Legs uniformly dark brown, one pair of subapical denticles on fore and middle femora; femur and tarsi setose with setae same color as tegument. Spongy fossula observed on fore- and mid-legs.

Description. ***Measurements*****:** Table 1. Coloration: generally brown, with connexivum and wings yellow. Head brown with setosity lighter than the tegument. Labium with first visible segment dark brown and second visible segment slightly paler than first. Neck brown, with 1+1 dark-yellow stripe. Pronotum brown, anterior lobe slightly darker than posterior lobe. Collar brown with anterolateral angles yellowish apically (Fig. 2A, B). Hemelytra with corium and most part of the clavus yellow and membrane smoky-brown. Basal portion of clavus brown, subcostal vein almost all yellow, except apex which bears a brown claw-shaped spot. Small dark oval spots adjacent (above, but not over) m-cu cross vein. Legs uniformly dark with femora and tarsi setosity with same color as tegument. Connexivum in dorsal view mostly yellow, with brown spots on first third of each segment adjacent to sutures (Fig. 2A). In ventral view, abdomen mostly brown on the center, with unique continuous yellow band separating the connexival segments and the center (brown) of the sternites (Fig. 2B).

Structure**:** head shallowly rugose on dorsal view, less than twice as long as width across the eyes (1: 0.62), and slightly shorter than the pronotum (1:1.1). Anteocular region about twice as long as the postocular region (1:0.48) (Fig. 5A). Eyes surpassing the ventral but not the dorsal margin of the head (Fig. 5B), in lateral view. Ratio of the width of eye to synthlipsis: 1:1.21. Ocelli larger than the distance from the eyes to ocelli (1:0.4) and inserted on conspicuous C-shaped protuberance (Fig. 5A).

Antenniferous tubercles subcylindrical, situated slightly after the posterior half of the anteocular region (Fig. 5A). First antennal segment not attaining to level of apex of

Figure 5. *Triatoma dimidiata* neotype head detail (male) **A** dorsal view **B** lateral view.

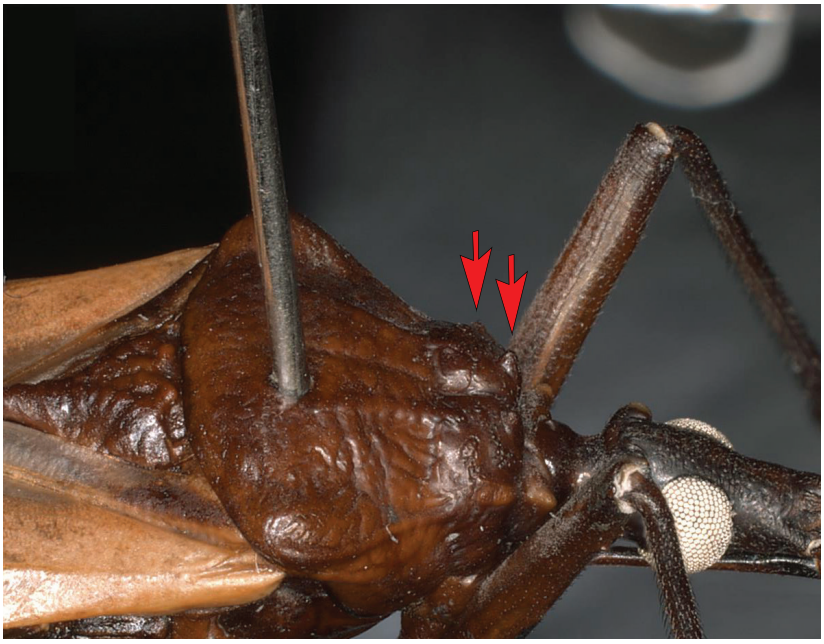

Figure 6. Pronotum of *Triatoma dimidiata* neotype (male). Detail of the anterior lobe of the pronotum, showing the discal tubercle (right arrow) and lateral tubercle (left arrow).

clypeus; other antennal segments missing (Fig. 5A). Labium slender, with first visible segment not reaching the level of the base of antenniferous tubercle; second visible segment extending to neck; third visible segment reaching the anterior third of stridulatory sulcus (Fig. 5B). Ratio of visible labium segments: 1:1.8:0.9.

Pronotum with anterior lobe presenting a distinct depression and with 1+1 discal tubercle, pointed posteriorly, and 1+1 round, smaller lateral tubercles (Fig. 6). Anterolateral angles presenting almost triangular, anterolaterally directed. Posterior lobe slightly rugose. Humeral angles slightly elevated and rounded. Scutellum rugose; posterior process of scutellum with rounded apex, shorter than basal portion of scutellum (Fig. 7).

Figure 7. *Triatoma dimidiata* neotype (male). Detail of head, pronotum, and scutellum in dorsal view

Hemelytra not reaching the posterior margin of VII urotergite (Fig. 2A). Legs with one pair of subapical denticles on fore and mid femora (Fig. 8); spongy fossae on the apices of fore- and mid-tibiae.

Abdomen ventrally convex, delicately striate transversally. Width of abdomen 0.39 times the total body length (1:0.39). Abdominal spiracles adjacent to connexival suture, surrounded by a round brown spot.

Discussion

The specific status of *Triatoma dimidiata* s.l., a major vector of Chagas disease in the New World, has long been debated among Triatominae systematists (Lent and Wygodzinsky 1979; Dorn et al. 2007, 2016; Bargues et al. 2008; Monteiro et al. 2013; Justi et al. 2018). Two taxa originally described as separate species and later designated as *T. dimidiata* subspecies-*Triatoma dimidiata maculipennis* (Neiva 1914) and *Triatoma dimidiata capitata* Usinger, 194–were synonymized with *T. dimidiata* by Lent and Wygodzinsky (1979). With the application of molecular approaches, it has become increasingly clear that the entity commonly described as *T. dimidiata* comprises several species, which may or may not differ in vector competency. Most recently, two other species-*T. mopan* and *T. huehuetenanguensis*-have been formally described within the *T. dimidiata* group. Adding to the incredible diversity and, at the same time, similarity of the *T. dimidiata* s.l. lineages, is the fact that when a cluster analysis is performed,

Figure 8. Legs of *Triatoma dimidiata* neotype (male) **A** detail of the pair of subapical denticles present on the forelegs **B** pair of subapical denticles present on the midlegs. Hindlegs do not present denticles.

over 50 distinct clusters are found, regardless of the marker used. However, when compared to other lineages within Triatominae, pairwise distances within *T. dimidiata* s.l. for both CytB and ITS2 are much lower.

The designation of a neotype was critical to fix the identity of *T. dimidiata* s.s. and better understand the component members of this very diverse and epidemiologically important group moving forward. In this study, our goal was to find a specimen as close

as possible as the one Latreille described in 1811. With Latreille's original specimens untraceable, we re-examined all USNM and AMNH *T. dimidiata* specimens used by Lent and Wygodzinky (1979) in their work, searching for the optimal specimen fitting the original description, to assign as the neotype. We noted that, while all exhibit a similar overall morphology, specimens markedly differed in several important taxonomic features from one locality to another, suggesting that the specimens used by Lent and Wygodzinsky (1979) in fact comprised several closely related taxa within *T. dimidiata* s.l.. These findings go some way to explaining the wide diversity of taxonomic characters, bionomics, and distribution currently attributed to *T. dimidiata* in the literature.

The most recent example of how deeper knowledge of *T. dimidiata* s.l. taxonomy is necessary, is the great effort by Rengifo-Correa et al. (2021). In this study, the authors performed a morphological review and published a long overdue diagnostic key to the species of the *T. phyllosoma* species group. Unfortunately, however, the taxonomic uncertainty regarding the status of *T. dimidiata* led the authors to include, as such, what seems to be at least three distinct lineages [see fig. 3D-F of Rengifo-Correa et al. (2021)]. Upon comparison of the diagnosis for *T. dimidiata* provided there, and the neotype, several disparities were found: (1) the anteocular region of the neotype is 2× the length of the postocular region, not 2.5–3× as stated by Rengifo-Correa et al., (2) the first antennal segment does not reach the apex of the clypeus on the neotype, (3) comparison of the images [fig. 3D-F of Rengifo-Correa et al. (2021)] shows disparities in the shape and coloration of the anterolateral angles; shape, color, and rugosity of the pronotum; and shape, color, and location of the wing spots, in relation to the neotype.

Despite examining all 199 available specimens housed in the AMNH and USNM collections, we found only one specimen that exactly matched Latreille's (1811) original description of *T. dimidata*. Similarly, only one of over 100+ publicly available mtDNA CytB sequences clustered with the neotype. Clustering analyses of ITS-2 sequences, however, showed the neotype sequence to be grouped with 14 other publicly available samples.

These observations are consistent with the hypothesis previously raised that *T. dimidiata* s.s. would have originated in northern Central America and been, somehow, introduced to South America (Bargues et al. 2008). Combined with the young age (<10 My) of the *T. dimidiata* s.l. lineage (Justi et al. 2016), these results show that the radiation of the group likely occurred very quickly and recently, like the radiation of south American *Triatoma* (Justi et al. 2016) that comprise several morphologically differentiable species, but for which current widely used molecular markers cannot be used for reliable species identification (Justi et al. 2014a).

With ITS-2 being a more conserved genetic marker, it is cautious to rely on CytB for the most accurate identification of such a young lineage, which lead us to conclude that true *T. dimidiata* is a rare species, with a seemingly limited range; contradicting current opinion that it is one of the most widespread species of the genus *Triatoma*, and consequently casting doubt on its perceived role as the major vector of Chagas' disease in the New World. Efforts are urgently needed to better assess the taxonomic status of the genetically diverse entities within the *T. dimidiata* s.l. and assess which of the component taxa are truly involved in transmission of this increasingly important disease in the New World.

Acknowledgements

We thank Thomas Henry (NMNH), Randall T. Schuh and Ruth Salas (AMNH) for unrestricted access to the archive specimens, and Yvonne-Marie Linton for her comments and suggestions on the original manuscript. This study was conducted while S.A.J. held a National Research Council Research Associateship at the Walter Reed Biosystematics Unit (WRBU) and Walter Reed Army Institute of Research (WRAIR). The study was funded by the Armed Forces Health Surveillance Division (AFHSD) – Global Emerging Infections Surveillance (GEIS) Branch core support to WRBU (P0030_21_WR to Yvonne-Marie Linton). The material published reflects the views of the authors and should not be misconstrued to represent those of the Department of the Army or the Department of Defense. The funders had no role in study design.

References

Bargues MD, Klisiowicz DR, Gonzalez-Candelas F, Ramsey JM, Monroy C, Ponce C, Salazar-Schettino PM, Panzera F, Abad-Franch F, Sousa OE, Schofield CJ, Dujardin JP, Guhl F, Mas-Coma S (2008) Phylogeography and genetic variation of *Triatoma dimidiata*, the main Chagas disease vector in Central America, and its position within the genus Triatoma. PLoS Neglected Tropical Diseases 2: e233. https://doi.org/10.1371/journal.pntd.0000233

Bonpland A, Humboldt A von (1811) In: Bonpland A, Humboldt A von (Eds) Voyage aux Regions Equinoxiales du Nouveau Continent. Recueil d'Observations de Zoologie et d'Anatomie Comparee faites dans l'Ocean Atlantique, dans l'Intedrieur du Nouveau Continent et dans la Mer du Sud. Recueil d'observations de zoologie et d'anatomie compar: faites dans l'ocn atlantique, dans l'intieur du nouveau continent et dans la mer du sud pendant les anns 1799, 1800, 1801, 1802 et 1803. Paris, 15–25. https://doi.org/10.5962/bhl.title.43770

Dorn PL, Calderon C, Melgar S, Moguel B, Solorzano E, Dumonteil E, Rodas A, de la Rua N, Garnica R, Monroy C (2009) Two distinct *Triatoma dimidiata* (Latreille, 1811) taxa are found in sympatry in Guatemala and Mexico. PLoS Neglected Tropical Diseases 3: e393. https://doi.org/10.1371/journal.pntd.0000393

Dorn PL, De NM, Axen H, Smith N, Richards BR, Charabati J, Suarez J, Woods A, Pessoa R, Monroy C, Kilpatrick CW, Stevens L (2016) Hypothesis testing clarifies the systematics of the main Central American Chagas disease vector, *Triatoma dimidiata* (Latreille, 1811), across its geographic range. Infection, Genetics and Evolution 44: 431–443. https://doi.org/10.1016/j.meegid.2016.07.046

Dorn PL, Monroy C, Curtis A (2007) *Triatoma dimidiata* (Latreille, 1811): a review of its diversity across its geographic range and the relationship among populations. Infection, Genetics and Evolution 7: 343–352. https://doi.org/10.1016/j.meegid.2006.10.001

Justi SA, Soghigian J, Pecor DB, Caicedo-Quiroga L, Rutvisuttinunt W, Li T, Stevens L, Dorn PL, Wiegmann B, Linton YM (2021) From e-voucher to genomic data: preserving archive specimens as demonstrated with medically important mosquitoes (Diptera: Culicidae) and kissing bugs (Hemiptera: Reduviidae). PLoS ONE 16: 1–13. https://doi.org/10.1371/journal.pone.0247068

Justi SA, Dale C, Galvão C (2014a) DNA barcoding does not separate South American *Triatoma* (Hemiptera: Reduviidae), Chagas Disease vectors. Parasites & Vectors 7: e519. https://doi.org/10.1186/s13071-014-0519-1

Justi SA, Galvão C, Schrago CG (2016a) Geological changes of the Americas and their influence on the diversification of the Neotropical kissing bugs (Hemiptera: Reduviidae: Triatominae). PLoS Neglected Tropical Diseases 10: e0004527. https://doi.org/10.1371/journal.pntd.0004527

Justi SA, Russo CAM, Mallet JRDS, Obara MT, Galvão C (2014b) Molecular phylogeny of Triatomini (Hemiptera: Reduviidae: Triatominae). Parasites and Vectors 7: e149. https://doi.org/10.1186/1756-3305-7-149

Justi SA, Cahan S, Stevens L, Monroy C, Lima-Cordón R, Dorn PL (2018) Vectors of diversity: Genome wide diversity across the geographic range of the Chagas disease vector *Triatoma dimidiata* sensu lato (Hemiptera: Reduviidae). Molecular Phylogenetics and Evolution 120: 144–150. https://doi.org/10.1016/j.ympev.2017.12.016

Kearse M, Moir R, Wilson A, Stones-havas S, Sturrock S, Buxton S, Cooper A, Markowitz S, Duran C, Thierer T, Ashton B, Meintjes P, Drummond A (2012) Geneious Basic: an integrated and extendable desktop software platform for the organization and analysis of sequence data. Bioinformatics 28: 1647–1649. https://doi.org/10.1093/bioinformatics/bts199

Kimura M (1980) A simple method for estimating evolutionary rates of base substitutions through comparative studies of nucleotide sequences. Journal of Molecular Evolution 16: 111–120. https://doi.org/10.1007/BF01731581

Latreille PA (1811) Insectes de l'Amedrique recueillis pendant le voyage de MM. In: Voyage aux Regions Equinoxiales du Nouveau Continent. Recueil d'Observations de Zoologie et d'Anatomie Comparee Faites dans l'Ocean Atlantique, dans l'Intedrieur du Nouveau Continent et dans la Mer du Sud. Paris, 197–397. https://doi.org/10.5962/bhl.title.43770

Lent H, Wygodzinsky P (1979a) Revision of the Triatomiane (Hemiptera, Reduviidae), and their significance as vectors of Chagas' disease. Bulletin of the American Museum of Natural History 163: 125–520.

Monteiro FA, Peretolchina T, Lazoski C, Harris K, Dotson EM, Abad-Franch F, Tamayo E, Pennington PM, Monroy C, Cordon-Rosales C, Salazar-Schettino PM, Gómez-Palacio AM, Grijalva MJ, Beard CB, Marcet PL (2013) Phylogeographic pattern and extensive mitochondrial DNA divergence disclose a species complex within the Chagas disease vector *Triatoma dimidiata*. PLoS Neglected Tropical Diseases 8: e70974. https://doi.org/10.1371/journal.pone.0070974

Paradis E, Claude J, Strimmer K (2004) APE: analyses of phylogenetics and evolution in R language. Bioinformatics 20: 289–290. https://doi.org/10.1093/bioinformatics/btg412

R Development Core Team (2008) R Development Core Team.

Rengifo-Correa L, Tellez-Rendon JL, Esteban L, Huerta H, Morrone J (2021) The *Triatoma phyllosoma* species group (Hemiptera: Reduviidae: Triatominae), vectors of Chagas disease: diagnoses and a key to the species. Zootaxa 5023: 335–365. https://doi.org/10.11646/zootaxa.5023.3.2

Supplementary material 1

Specimens metadata
Authors: Silvia Andrade Justi, Carolina Dale
Data type: COL

Link: https://doi.org/10.3897/zookeys.1076.72835.suppl1

Supplementary material 2

GenBank numbers list
Authors: Silvia Andrade Justi, Carolina Dale
Data type: molecular data

Link: https://doi.org/10.3897/zookeys.1076.72835.suppl2

Supplementary material 3

R code for barcode-like and cluster analyses 3
Authors: Silvia Andrade Justi, Carolina Dale
Data type: statistical data

Link: https://doi.org/10.3897/zookeys.1076.72835.suppl3

Supplementary material 4

Mitochondrial genome gene table

Authors: Silvia Andrade Justi, Carolina Dale

Data type: molecular data

Link: https://doi.org/10.3897/zookeys.1076.72835.suppl4

ZooKeys 1076: 25–41 (2021)
doi: 10.3897/zookeys.1076.73262
https://zookeys.pensoft.net

SHORT COMMUNICATION

A peer-reviewed open-access journal
ZooKeys
Launched to accelerate biodiversity research

Taxonomic and genetic assessment of captive White-Handed Gibbons (*Hylobates lar*) in Peninsular Malaysia with implications towards conservation translocation and reintroduction programmes

Millawati Gani[1*], Jeffrine J. Rovie-Ryan[1,2*], Frankie Thomas Sitam[1], Noor Azleen Mohd Kulaimi[1], Chew Cheah Zheng[1,3], Aida Nur Atiqah[1,3], Nur Maisarah Abd Rahim[1,4], Ahmad Azhar Mohammed[1]

1 *National Wildlife Forensic Laboratory, Ex-Situ Conservation Division, Department of Wildlife and National Parks, KM 10 Jalan Cheras, 56100 Kuala Lumpur, Malaysia* **2** *Faculty of Resource Science and Technology, Universiti Malaysia Sarawak, 94300 Kota Samarahan, Sarawak, Malaysia* **3** *Faculty of Science and Technology, Universiti Kebangsaan Malaysia, 43600 UKM, Bangi Selangor, Malaysia* **4** *Faculty of Science, Universiti Putra Malaysia, 43400 UPM Serdang, Selangor, Malaysia*

Corresponding author: Jeffrine J. Rovie-Ryan (rjeffrine@unimas.my)

Academic editor: Matthew Tocheri | Received 20 August 2021 | Accepted 25 October 2021 | Published 8 December 2021

http://zoobank.org/585E11C5-4430-4E40-B0E8-E882EFD7C3D5

Citation: Gani M, Rovie-Ryan JJ, Sitam FT, Kulaimi NAM, Zheng CC, Atiqah AN, Rahim NMA, Mohammed AA (2021) Taxonomic and genetic assessment of captive White-Handed Gibbons (*Hylobates lar*) in Peninsular Malaysia with implications towards conservation translocation and reintroduction programmes. ZooKeys 1076: 25–41. https://doi.org/10.3897/zookeys.1076.73262

Abstract

Conservation translocation and reintroduction for the purpose of repopulating and reinforcing extirpated or depleted populations has been recognised as an important conservation tool, particularly for gibbon conservation in the immediate future. Feasibility assessments involving multiple factors, including taxonomic and genetic assessment of rescued and captive gibbons, are imperative prior to translocation and reintroduction programmes. In this study, we attempt to determine the subspecies and origin of captive *Hylobates lar,* White-handed gibbons, from Peninsular Malaysia to assist in future translocation and reintroduction programmes. A total of 12 captive and rescued *H. lar* samples were analysed using the control region segment of mitochondrial DNA. Sequence analyses and phylogenetic trees constructed

* These authors have contributed equally to this work

using neighbour-joining, maximum likelihood, Bayesian inference, and network methods congruently differentiate all 12 captive individuals used in this study from other *H. lar* subspecies suggesting that these individuals belong to the *H. lar lar* subspecies. In addition, two populations of *H. l. lar* were observed: (1) a southern population consisting of all 12 individuals from Peninsular Malaysia, and (2) a possible northern population represented by three individuals (from previous studies), which might have originated from the region between the Isthmus of Kra, Surat Thani-Krabi depression, and Kangar-Pattani. Our findings suggest that the complete control region segment can be used to determine the subspecies and origin of captive *H. lar.*

Keywords

Control region, mitochondrial DNA, northern and southern *lar* populations, phylogenetic relationships, subspecies determination

Introduction

Small apes (family Hylobatidae), also known as lesser apes, consist of 20 species of gibbons inhabiting Southeast Asia which are grouped into four extant genera: *Hylobates*, *Hoolock*, *Nomascus*, and *Symphalangus*. Within the genus *Hylobates*, nine species are currently recognised (Roos 2016; IUCN 2021); *Hylobates abbotti* Kloss, 1929, *Hylobates agilis* F. Cuvier, 1821, *Hylobates albibarbis* Lyon, 1911, *Hylobates funereus* I. Geoffroy, 1850, *Hylobates klossii* (Miller, 1903), *Hylobates lar* (Linneaus, 1771), *Hylobates moloch* (Audebert, 1798), *Hylobates muelleri* Martin, 1841 and *Hylobates pileatus* (Gray, 1861); two species exist in Peninsular Malaysia namely *H. agilis* and *H. lar*. In Peninsular Malaysia, *H. lar* is distributed throughout except for a narrow region between Perak River (State of Perak) and Muda River (State of Kedah) that is inhabited by the congener, *H. agilis* (Brockelman & Geissmann 2020). Both species are categorised as 'Endangered' by the IUCN Red List of Threatened Species (Brockelman and Geissmann 2020; Geissmann et al. 2020) and are 'Totally Protected' under the Wildlife Conservation Act 2010 enforced in Peninsular Malaysia. Illegal hunting for the food and pet trade as well as habitat loss due to anthropogenic activities (forest clearing for development and agriculture) have been identified as the major causes of the decline of more than 50% of *H. lar* populations in the wild across its range (Brockelman and Geissmann 2020).

Large numbers of captive gibbons kept in zoological parks (including zoos and rescue centers) are individuals rescued from the illegal pet trade, private collectors, and plantations as their habitats are cleared (Cheyne 2009; Nijman et al. 2009). Due to the threat faced by *in-situ* populations, conservation translocation and reintroduction of ex-situ populations (of rescued and captive individuals) for the purpose of repopulating and reinforcing extirpated or depleted populations has been recognised as an important conservation tool, particularly for gibbon conservation in the immediate future (Cheyne 2009; IUCN/SSC 2013; Campbell et al. 2015). However, before such conservation actions are taken, feasibility assessments involving multiple factors in-

cluding taxonomic and genetic assessment of rescued and captive gibbons are imperative prior to any translocation and reintroduction programmes (Campbell et al. 2015).

To assess the taxonomic and genetic variation of gibbons, several molecular taxonomy studies have been conducted. However, most systematic studies on gibbons have focused mainly on interspecific variation (Chan et al. 2010, 2012, 2013; Israfil et al. 2011; Veeramah et al. 2015; Matsudaira and Ishida 2021) while only a few have investigated intraspecific variation (Andayani et al. 2001; Woodruff et al. 2005; Aifat and Md-Zain 2021). In particular, the taxonomic status of *H. lar* subspecies requires further examination as they are based on minor variations in body colour and fur polychromatism (Woodruff et al. 2005; Brockelman and Geissmann 2020). According to Roos et al. (2014), five subspecies of *H. lar* are currently recognised: *H. l. lar* (Linnaeus, 1771), *H. l. carpenteri* Groves, 1968, *H. l. entelloides* I. Geoffroy Saint-Hilaire, 1842, *H. l. vestitus* Miller, 1942, and *H. l. yunnanensis* Ma & Y. Wang, 1986. In this study, we employ the control region (CR) gene segment, a more variable gene segment of the mitochondrial DNA (mtDNA) (Roos and Geissmann 2001; Woodruff et al. 2005; Whittaker et al. 2007; Rovie-Ryan et al. 2014), to assess the taxonomic and genetic variation of white-handed gibbons in captivity.

Materials and methods

Samples and GenBank sequences

A total of 12 unrelated *H. lar* samples were used in this study. The approximate locality of the individuals is described in Table 1 and shown in Figure 1. All rescued individuals were of known locality. The localities of the confiscated and surrendered individuals were recorded at the location of the confiscation (from dealers or private owners) or the location of the Department of Wildlife and National Parks (DWNP) offices where the animals were brought in. Currently, all of these individuals are at the National Wildlife Rescue Centre (NWRC) at Sungkai (State of Perak) and are currently under-going rehabilitation.

Blood samples were collected during routine health checks by authorised veterinarians and personnel of DWNP where all sampling protocols adhere to the rules and regulations of the relevant authorities in Peninsular Malaysia. In addition, available mtDNA CR sequences of *Hylobates* were downloaded from GenBank including the outgroup species, *Symphalangus syndactylus* (Siamang), as summarised in Suppl. material 1.

DNA extraction, PCR amplification and DNA sequencing

Total genomic DNA was extracted from the blood samples using the QIAamp DNeasy Blood and Tissue Kit following the manufacturer's protocol (Qiagen, Germany). We designed two new pairs of oligonucleotides to amplify the complete CR region of the mtDNA as shown in Table 2.

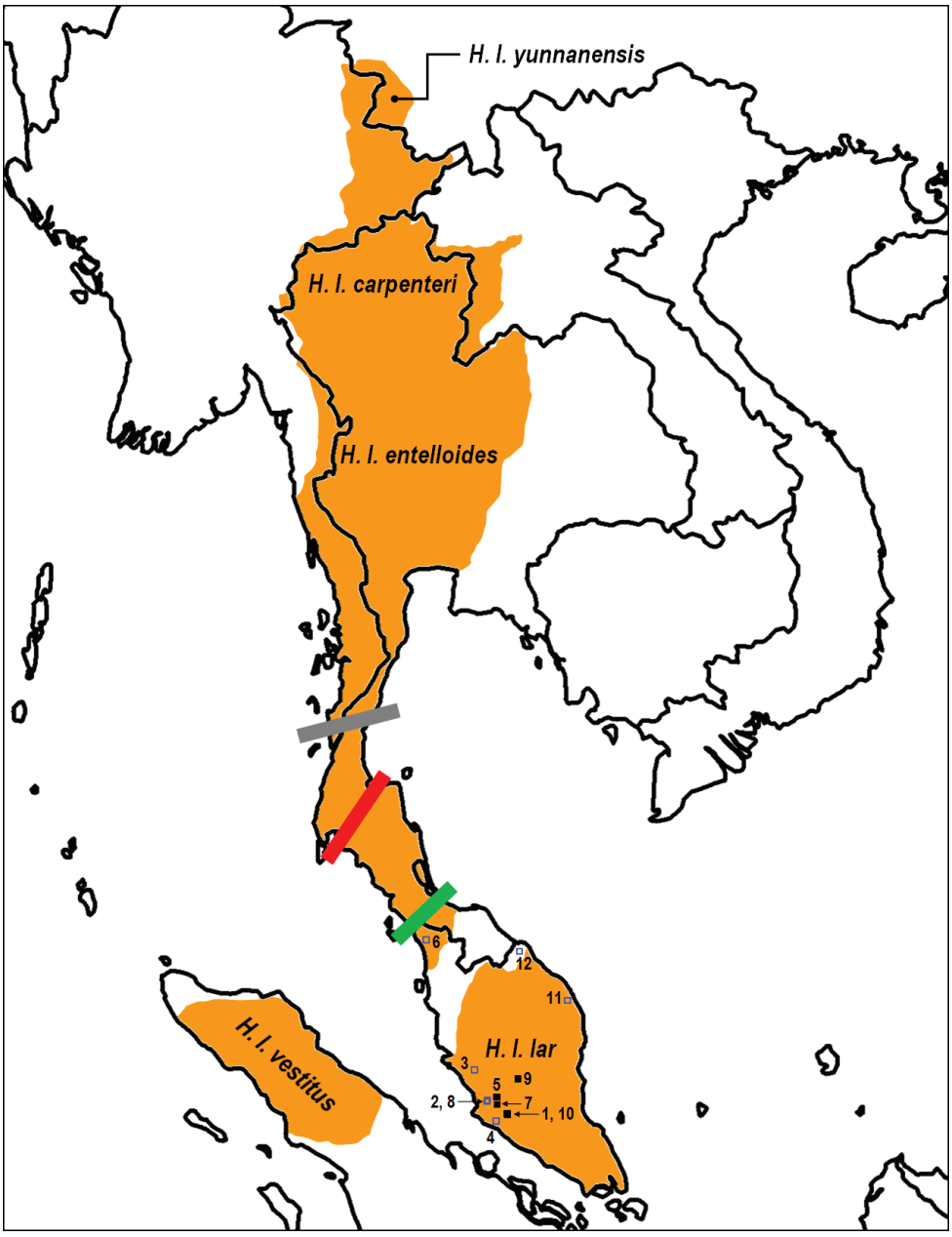

Figure 1. Geographical distribution of *Hylobates lar* subspecies throughout South-East Asia (adapted from Thinh et al. 2010; Brockelman and Geissmann, 2020). Black squares represent individuals of known exact locations while blue squares indicated the approximate locations of the confiscated and surrendered individuals used in this study. Numbers on the map corresponds to the location in Table 1. The approximate location of the Isthmus of Kra, the Surat Thani-Krabi depression, and the Kangar-Pattani line are indicated by the grey, red, and green lines, respectively, marking the possible break among the Indochinese (*carpenteri*, *entelloides*, and *yunnannesis*) from the *lar* subspecies.

Table 1. Information of *H. lar* individuals used in this study. DWNP, Department of Wildlife and National Parks, Malaysia

No.	Sample ID	Sex	Description of locality (village, district, state)
1	Betsy	F	Rescued from Kpg. Sg. Machang, Lenggeng, Negeri Sembilan*
2	Lucy	F	Surrendered to DWNP Shah Alam, Selangor
3	Chantiq	F	Confiscated from Sungai Dusun, Selangor
4	Daly	M	Surrendered from Sepang, Selangor
5	Keramat	F	Rescued from Taman Keramat, Kuala Lumpur*
6	Abu	M	Surrendered to DWNP Alor Setar, Kedah
7	Langat	F	Rescued from Hulu Langat, Selangor*
8	Luca	M	Surrendered to DWNP Shah Alam, Selangor
9	Daru	M	Rescued from Kpg. Asli Kuala Lompat, Krau, Pahang*
10	Bella	F	Rescued from Kpg. Jeram Kedah, Lenggeng, N. Sembilan*
11.	PetPet	M	Surrendered from Kpg. Perpat, Ajil, Terengganu
12.	Lola	F	Confiscated from Pasir Mas, Kelantan

*Rescued individual were animals of known locality

Table 2. Two pairs of newly designed oligonucleotides used in this study to amplify the complete control region gene segment of the mitochondrial DNA.

No.	Name	Oligonucleotide profile (5'–3')	Annealing temp. (°C)	Product size (bp)
1	CR1-15391F*	ACT TAA CTT CAC CCT CAG CAC C	50	550
	CR1-15887R	ACC CCC AAG TGT TGT ARG CC		
2	CR2-15810F*	YCC AGC ATC CTC CGT GAA AT	50	800
	CR2-56R*	GKG AGC CCG TCT CGA CAT TT		

*Used for DNA sequencing

PCR amplifications were conducted in 20 µl reactions using a T100 Thermal Cycler (Bio-Rad, USA) consisting of 1.0 µl of DNA template (~10 to 20 ng), 4X Green GoTaq Flexi Buffer (Promega, USA), 0.875 mM of $MgCl_2$, 0.1 mM of each dNTPs, 0.1mM of each primer, 1 unit of *Taq* polymerase, and added with ddH_2O to make up a total of 20 µl reaction mixtures. All amplifications were performed for 40 cycles each using the following profile: denaturation at 95 °C for 30 s, annealing at 50 °C for 30 s, and extension at 72 °C for 45 s, followed by a final extension step at 72 °C for 1 min. Successful PCR products were sent for sequencing on an ABI PRISM377 DNA Sequencer to a local sequencing service provider (Apical Scientific Pte. Ltd. Malaysia).

DNA sequence analysis

DNA sequences obtained were checked for quality and aligned using the software GENEIOUS PRIME 2021.1.1 (Biomatters 2020) before being examined manually. BLAST analysis (Altschul et al. 1990) showed sequence similarities ranging from 97.2% to 98.2% (with E-values less than or equal to 0) to *H. lar* from GenBank (AF311723), providing initial confirmation to rule out the chances of amplifying the nuclear copies of mitochondrial DNA (*Numts*). Secondly, as suggested by Sorenson and Quinn (1998), we designed our oligonucleotides using the gibbon reference sequence available in GenBank to maximise the chances of amplifying the CR segment and avoiding *Numts*. Thirdly, according to Spinks and Shaffer (2007), the presence

of multiple peaks in a sequenced chromatogram indicates the presence of *Numts*. We confirmed that the sequences obtained in this study showed clear single peaks indicating that our amplification has avoided amplifying *Numts*. All sequences were later registered with GenBank with the Accession Numbers MZ407482 - MZ407493.

In total, 101 CR sequences were included for subsequent analyses with aligned sequence lengths of 527-bp. DNA characteristics including conserved sites (CS), variable sites (VS), and parsimony informative sites (PIS) were checked using MEGA X (Kumar et al. 2018). Using DNASP 5.10.01 (Librado and Rozas 2009), DNA polymorphism analyses consisting of number of haplotypes (NHap), haplotype diversity (*Hd*), and nucleotide diversity, π (Nei 1987) were calculated. Genetic distances among the sequences were also calculated using the Kimura-2 parameter model (Kimura 1980) on MEGA X.

Phylogenetic tree construction

In MEGA X, phylogenetic trees were constructed using neighbour-joining (NJ; distance based method) and maximum likelihood (ML). For the ML analysis, the HKY85 substitution model with a discrete Gamma distribution (+G) with 5 rate categories (Hasegawa et al. 1985) was determined to be the best substitution model to run the ML tree, as calculated in MEGA X. The robustness of the NJ and ML trees were assessed by bootstrapping (Felsenstein 1985) with 1000 replicates. Bayesian inference (BI) was constructed using the BEAST 2.5 package (Bouckaert et al. 2019) on two independent runs each with 10 million Markov chain Monte Carlo (MCMC) generations and sub-sampled every 1000 generations using the following settings: HKY85 substitution model with five gamma category counts, strict clock, and Yule model (Heled and Drummond 2012). The convergence of the parameters was assessed using TRACER 1.7 (Rambaut et al. 2018). The log and tree files from both runs were then combined using LOGCOMBINER before TREEANNOTATOR (both software available within the BEAST package) was then used to create a consensus tree from the combined tree files with a burn-in of 10% and a posterior probability limit of 0.5. FIGTREE 1.4.4 (Rambaut 2018) was used to visualise the BI tree. Finally, to investigate the reticulate relationship among *H. lar* haplotypes, a median-joining network (MJN) tree analysis (Bandelt et al. 1999) was performed using NETWORK 10.2 (Fluxus Technology Ltd.).

Results

DNA sequence characteristics, DNA polymorphism, and genetic distances

Table 3 summarised the DNA characteristics and polymorphisms of the *Hylobates* species. Sequence characteristics of *H. lar* ($N = 57$) showed 88 VS and 46 PIS. In total, 49 *lar* haplotypes were observed with π of 2.10%. Haplotype mapping revealed that the 12 individuals of *H. l. lar* from Peninsular Malaysia are unrelated with an *Hd* of 0.99.

Table 3. DNA characteristics and polymorphisms calculated for the *Hylobates* used in this study. *N*= number of sequences; CV= conserved sites; VS= variable sites; PIS= parsimony informative sites; NHap= number of haplotypes; *Hd*= haplotype diversity; π= nucleotide diversity.

Species	*N*	DNA characteristics			DNA polymorphism		
		CV	VS	PIS	Nhap	*Hd*	π (%)
H. abbotti	2	464	24	0	2	1.00	4.92
H. agilis	8	412	83	41	8	1.00	6.31
H. albibarbis	3	460	31	0	3	1.00	4.24
H. klossii	8	460	29	14	8	1.00	2.07
H. lar	57	403	88	46	49	0.99	2.10
H. moloch	9	454	37	15	9	1.00	2.35
H. muelleri	5	443	49	20	5	1.00	4.59
H. pileatus	8	469	23	8	8	1.00	1.51
Total	100	273	227	176	89	1.00	7.52

Table 4. Genetic distances (in percentage, %) calculated among the species within the genus *Hylobates* using the Kimura-2 parameter model (Kimura 1980).

No.	Species	1	2	3	4	5	6	7	8
1	*H. abbotti*								
2	*H. agilis*	13.75							
3	*H. albibarbis*	14.06	7.23						
4	*H. klossii*	13.08	10.92	12.77					
5	*H. lar*	11.16	12.96	13.43	12.66				
6	*H. moloch*	10.32	11.13	12.76	9.41	10.46			
7	*H. muelleri*	8.48	12.96	14.51	13.95	11.64	11.05		
8	*H. pileatus*	18.60	18.59	19.93	17.95	14.31	15.81	16.54	
9	Outgroup*	25.94	24.45	26.43	22.58	23.63	22.57	25.90	24.90

*Symphalangus syndactylus

Interestingly, we observed two transversion mutations at nucleotide positions (np) 165 (thymine/cytosine to adenine) and 259 (thymine/cytosine to adenine) which differentiated all the 12 individuals used in this study from all other *H. lar* sequences (Suppl. material 2). In addition, a transition mutation at np 193 (adenine to guanine) differentiated all 12 individuals from Peninsular Malaysia, as well as three sequences from GenBank (AF311723, LC548024, and LC548028), from other sequences of *H. lar*. On the other hand, the subspecies *vestitus* (represented by a single sequence, LC548011) showed three transversion mutations (at np 264, 287, and 348) and 10 transition mutations (Suppl. material 2) which separated it from the other subspecies.

Pairwise genetic distances among the species of *Hylobates* are shown in Table 4. In summary, species within the genus *Hylobates* differ from each other from 7.2% (between *H. albibarbis* and *H. agilis*) to 19.93% (between *H. albibarbis* and *H. pileatus*). *Hylobates lar* differed from the other *Hylobates* species ranging from 10.46 – 14.31%. Genetic distances calculated for all *H. lar* ranged from 0.0 – 7.4% while distances among the 12 *H. lar* sequences from Peninsular Malaysia ranged from 0.2 – 3.4% (Suppl. material 3).

Phylogenetic trees and network analysis

The phylogenetic trees constructed using the NJ, ML (log likelihood= -4326.23), and BI produced similar topologies and thus was summarised using the NJ tree as shown in Figure 2. Each species formed its own monophyletic clade (with high bootstrap and posterior probability support) except for *H. albibarbis*, which clustered within the *H. agilis* clade. *Hylobates pileatus* was the basal species of the genus *Hylobates* although with low support (below 50% support). *Hylobates lar* was separated from all the other species with low to moderate support. *Hylobates abotti* and *H. muelleri* clustered together to form the Bornean species group (except for *H. albibarbis*) while *H. moloch*, *H. klossii* and *H. agilis* formed the Indonesian species group.

Within *H. lar*, we observed three possible subspecies groupings: (1) the basal *H. l. vestitus*, (2) *H. l. lar* (consisting of all 12 captive individuals from Peninsular Malaysia as well as the three sequences from GenBank mentioned above), and (3) a possible Indochinese subspecies group (representing *H. l. entelloides*, *H. l. carpenteri*, and *H. l. yunnanensis*). The Indochinese subspecies group did not show any obvious groupings according to subspecies. The *H. l. lar* group further splits with strong support (bootstrap and posterior probability) into two subgroups, which we tentatively define as representing northern and southern populations. The presumed northern *H. l. lar* population consists of three sequences from GenBank (of unknown origins) while the southern population consists of all 12 captive individuals from Peninsular Malaysia.

Similarly, the MJN tree constructed using the *H. lar* haplotypes ($N = 49$) produced similar groupings as the phylogenetic trees (Fig. 3). *Hylobates l. vestitus* differs from the Indochinese subspecies haplotypes and *H. l. lar* haplotypes (northern and southern) by at least 23 and 26 mutational steps, respectively. The northern *H. l. lar* haplotypes differ from the southern *H. l. lar* haplotypes by at least 10 mutational steps.

Discussion

A total of 1030-bp of the complete CR of mtDNA was successfully obtained from all 12 samples used in this study using the newly designed pairs of oligonucleotides. The CR segment of mtDNA is the most variable region and has been recommended as the appropriate segment to be used to infer gibbon phylogeny (Roos and Geissmann 2001; Woodruff et al. 2005; Whittaker et al. 2007; Matsudaira and Ishida 2010; Aifat and Md-Zain 2021). However, due to the lack of complete CR sequences of *Hylobates* in GenBank, a total of 527-bp of aligned dataset were analysed from 100 sequences representing all species of *Hylobates* except *H. funereus*. Our initial analysis of the complete CR sequence of *H. lar* (aligned sequence length of 1110-bp) showed an additional 59 VS and 34 PIS which may provide more informative data for the taxonomic and genetic assessment of *H. lar*. Therefore, we recommend the continued use of the complete CR segment in future studies of gibbon phylogeny and taxonomy.

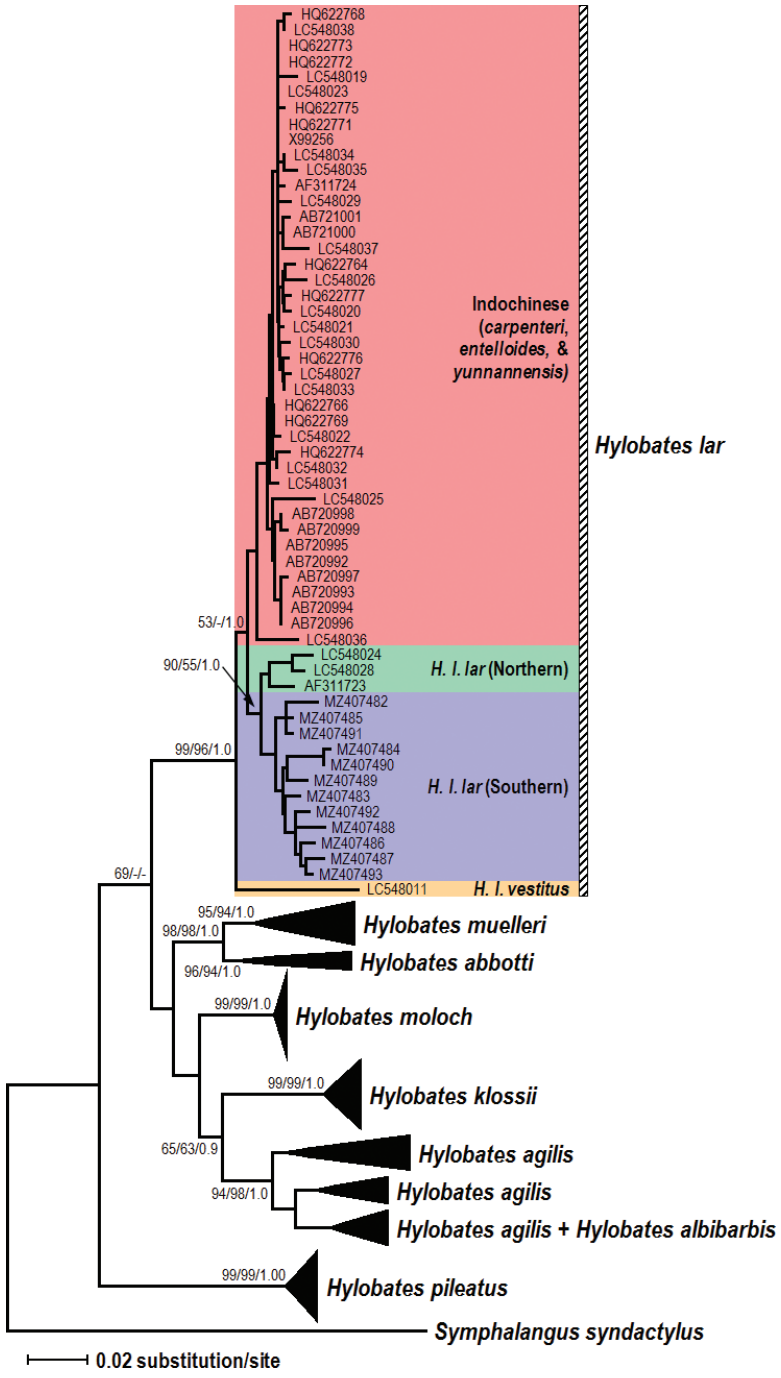

Figure 2. Phylogenetic relationships among the *Hylobates* species as represented by the NJ analysis. ML (Log Likelihood= -4326.23) and BI analysis produced similar topologies. Numbers above/below the branches represents bootstrap values for NJ, ML, and BI posterior probability, respectively. Only bootstrap values greater than 50% are shown.

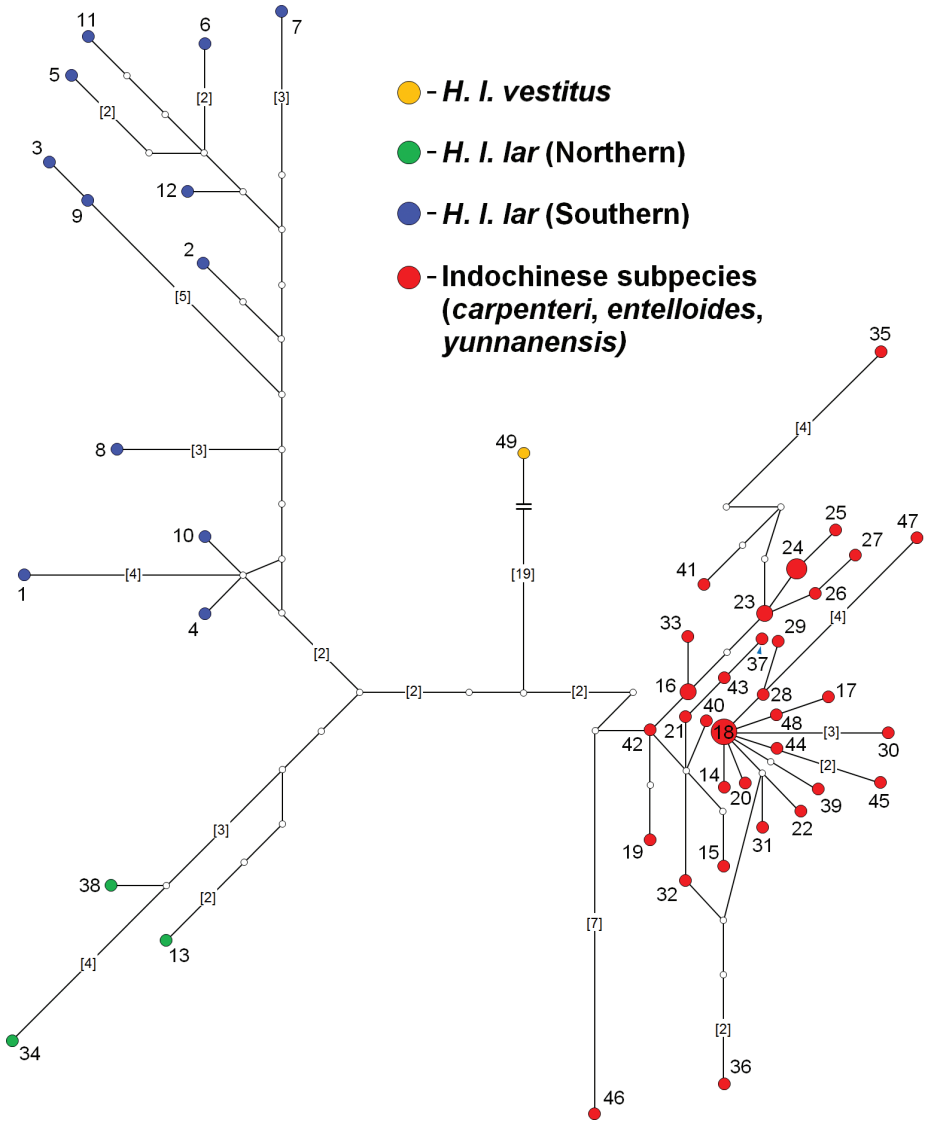

Figure 3. Median-joining network (MJN) constructed showing the relationships among the *H. lar* haplotypes. Each circle size is proportional to the number of individuals in each haplotype. The numbers next to the nodes correspond to the haplotype designation as listed in Supplementary Material, Table S1. The lines connecting the haplotypes represent single mutations unless indicated otherwise (numbers in parentheses). Hypothetical haplotypes (median vectors) are represented by white circles.

The phylogenetic relationships among *Hylobates* remain unresolved. Firstly, we observed *H. pileatus* as the basal species of *Hylobates* (although with low support), a result that is consistent with previous studies (Israfil et al. 2011; Chan et al. 2013; Matsudaira and Ishida 2021). Secondly, the relationships among the Sundaic species group (*abbotti*, *agilis*, *albibarbis*, *klossii*, *moloch*, and *muelleri*) remains conflated par-

ticularly with regard to the basal species of this group (Thinh et al. 2010; Chan et al. 2013; Matsudaira and Ishida 2021). In this study, the Bornean species group (*abbotti* and *muelleri*) diverged first followed by the Indonesian species group (*agilis*, *klossii*, and *moloch*). The clustering of *H. albibarbis* within the *H. agilis* clade is expected because the subspecies *albibarbis* was initially classified as a subspecies of *H. agilis* (Thinh et al. 2010; Matsudaira and Ishida 2021).

The phylogenetic positioning of *H. lar* within the genus *Hylobates* concurs with findings from previous studies (Israfil et al. 2011; Chan et al. 2013; Matsudaira and Ishida 2021). Our phylogenetic and network analysis showed that *H. l. vestitus* from Sumatra diverged first (Thinh et al. 2010; Aifat and Md-Zain 2021; Matsudaira and Ishida 2021) before the proto-*H. lar* bifurcated to form the *H. l. lar* clade and the possible Indochinese subspecies clade (*entelloides*, *carpenteri*, and *yunnanensis*). However, the Indochinese subspecies clade did not show any obvious subspecies groupings. Note that most of the sequences of the Indochinese subspecies clade were obtained from zoo individuals of unknown origin and locality (Suppl. material 1) except for sequences by Matsudaira et al. (2013) (AB720992 - AB721001) which originated from individuals from Khao Yai National Park, Thailand representing the subspecies *H. l. entelloides*. Thus, we deduce these following scenarios to explain the condition: (1) Indochinese *lar* gibbons are represented by only one subspecies (*entelloides*) instead of three, (2) sequences of *lar* gibbons from GenBank of unknown locality were derived from only one subspecies, *H. l. entelloides*, and (3) the CR segment is not powerful enough to differentiate among the Indochinese subspecies. In view of the lack of information regarding the origin of the zoo animals as well as the lack of reference samples of known locality, these proposed scenarios must be regarded as hypothetical and preliminary. Future studies should therefore use individuals of known localities to correctly assign captive and rescued gibbons to their geographical provenance and origin.

Finally, our findings revealed that all 12 captive individuals used in this study belong to the *H. l. lar* subspecies. Aifat and Md-Zain (2021) used partial cytochrome *b* gene segment of the mtDNA to successfully identify the subspecies of captive *H. lar* in Peninsular Malaysia but suggested that the CR segment be used in further studies on *H. lar*. The CR segment has been used in forensic investigations of various wildlife species to identify the subspecies and geographical origins of rescued or confiscated animals (Iyengar 2014). Interestingly, our results suggest the occurrence of two distinct populations of *H. l. lar*, as demarcated by two transversion mutations at np 165 and 259: (1) a southern population consisting of all 12 individuals from Peninsular Malaysia, and (2) a possible northern population of *H. l. lar* represented by three individuals from previous studies (AF311723, LC548024, and LC548028). These transversion mutations may be due to the prolonged isolation between the postulated southern and northern populations, which are separated by the presence of *H. agilis* in the narrow region between the Perak River and Muda River (Figure 1). Similar findings have been observed in other non-human primates, such as *Macaca* (Rovie-Ryan et al. 2021). Thus, these mutation sites should be used as genetic markers for future taxonomic and genetic assessments involving *lar* gibbons. The southern *H. l. lar* population likely

consists of all populations south of the Kangar-Pattani line (Fig. 1) and including the entirety of Peninsular Malaysia. In contrast, the northern population may exist in regions between the Isthmus of Kra and the Kangar-Pattani line. Several previous studies have demonstrated the role of the Isthmus of Kra, the Surat Thani-Krabi depression, and the Kangar-Pattani line as zoogeographical boundaries between Sundaland and Indochina (Baltzer et al. 2007; Woodruff 2010; Hughes et al. 2011; Rovie-Ryan et al. 2013; Abdul-Latiff et al. 2014).

Overall, our findings support the importance of conducting taxonomic and genetic assessments prior to any gibbon translocations and/or reintroductions. The distinguishable differences between the postulated northern and southern *H. l. lar* populations warrant their treatment as separate management units (MUs), a component within the Evolutionary Significant Unit (ESU) (Moritz 1994). Although treated as separate MUs, under the circumstance that the remnant populations of *lar* are showing signs of inbreeding depression or increased fragmentation, mixing (translocation) between MUs are permittable (Moritz 1999).

In summary, we conclude that using the CR segment of the mtDNA, we could taxonomically distinguish *H. l. lar* from the other *H. lar* subspecies, an important result for future translocation and reintroduction programs of rescued and captive gibbons in Peninsular Malaysia. Nevertheless, the use of nuclear DNA data for taxonomic and genetic assessments of captive and rescued gibbons should also be considered, especially for individuals of suspected hybrid origin. Further studies are currently on-going by DWNP (as the authority of wildlife conservation and management) to screen all captive *lar* gibbons in Peninsular Malaysia as well as to collect reference samples from the wild.

Acknowledgements

We wish to thank the Director General and Director of the Ex-situ Conservation Division of DWNP for the support and permission to conduct this study. Special thanks to the following personnel for their assistance during sampling: Dr David Magintan, Dr Zubaidah Kamarudin, Dr Siti Suzana Selamat, and the Primate Team of the NWRC of DWNP. The project was funded by the Government of Malaysia under the 12th Malaysia Plan Project: Strengthening Wildlife Forensics, Ex-Situ Conservation and Biobanking - Phase 2 (Project Code: P23071000810008) lead by JJRR. We also thank UNIMAS for the Publication Support Fee. MG and JJRR share the first authorship of the manuscript.

References

Abdul-Latiff MAB, Ruslin F, Faiq H, Hairul MS, Rovie-Ryan JJ, Abdul-Patah P, Yaakop S, Md-Zain BM (2014) Continental monophyly and molecular divergence of Peninsular Malaysia's *Macaca fascicularis fascic*ularis. BioMed Research International 2014: e897682. https://doi.org/10.1155/2014/897682

Aifat NR, Md-Zain BM (2021) Genetic identification of White-handed Gibbons (*Hylobates lar*) in captivity. Journal of Sustainability Science and Management 16(4): 316-326. https://doi.org/10.46754/jssm.2021.06.023

Altschul SF, Gish W, Miller W, Myers EW, Lipman DJ (1990) Basic Local Alignment Search Tool. Journal of Molecular Biology 215: 403–410. https://doi.org/10.1016/S0022-2836(05)80360-2

Andayani N, Morales JC, Forstner MRJ, Supriatna J, Melnick DJ (2001) Genetic variability in mtDNA of the silvery gibbon: Implications for the conservation of a critically endangered species. Conservation Biology 15(3): 770–775. https://doi.org/10.1046/j.1523-1739.2001.015003770.x

Baltzer JL, Davies SJ, Noor NSM, Kassim AR, LaFrankie JV 2007) Geographical distributions in tropical trees: Can geographical range predict performance and habitat association in co-occurring tree species? Journal of Biogeography 34(11): 1916–1926. https://doi.org/10.1111/j.1365-2699.2007.01739.x

Bandelt HJ, Forster P, Röhl A (1999) Median-joining networks for inferring intraspecific phylogenies. Molecular Biology and Evolution 16(1): 37–48. https://doi.org/10.1093/oxfordjournals.molbev.a026036

Biomatters (2020) Geneious – bioinformatics software for sequence data analysis. https://www.geneious.com/

Bouckaert R, Vaughan TG, Barido-Sottani J, Duchêne S, Fourment M, Gavryushkina A, Heled J, Jones G, Kühnert D, De Maio N, Matschiner M, Mendes FK, Müller NF, Ogilvie HA, du Plessis L, Popinga A, Rambaut A, Rasmussen D, Siveroni I, Suchard MA, Wu CH, Xie D, Zhang C, Stadler T, Drummond AJ (2019) BEAST 2.5: An advanced software platform for Bayesian evolutionary analysis. PLoS Computational Biology, 15(4): e1006650. https://doi.org/10.1371/journal.pcbi.1006650

Brockelman W, Geissmann T (2020) *Hylobates lar*. The IUCN Red List of Threatened Species 2020: eT10548A17967253. https://dx.doi.org/10.2305/IUCN.UK.2020-2.RLTS.T10548A17967253.en

Campbell CO, Cheyne SM, Rawson BM (2015) Best practice guidelines for the rehabilitation and translocation of gibbons. International Union for Conservation of Nature, Gland, Switzerland, 64 pp. https://doi.org/10.2305/iucn.ch.2015.ssc-op.51.en

Chan YC, Roos C, Inoue-Murayama M, Inoue E, Shih CC, Pei KJC, Vigilant L (2010) Mitochondrial genome sequences effectively reveal the phylogeny of *Hylobates* gibbons. PLoS One 5(12): e14419. https://doi.org/10.1371/journal.pone.0014419

Chan YC, Roos C, Inoue-Murayama M, Inoue E, Shih CC, Pei KJC, Vigilant L (2013) Inferring the evolutionary histories of divergences in *Hylobates* and *Nomascus* gibbons through multilocus sequence data. BMC Evolutionary Biology 13: e82. https://doi.org/10.1186/1471-2148-13-82

Chan C, Roos C, Inoue-Murayama M, Inoue E, Shih CC, Vigilant L (2012) A comparative analysis of Y chromosome and mtDNA phylogenies of the *Hylobates* gibbons. BMC Evolutionary Biology 12: e150. https://doi.org/10.1186/1471-2148-12-150

Cheyne SM (2009) The role of reintroduction in gibbon conservation: Opportunities and Challenges. In Whittaker D, Lappan S (Eds) The Gibbons. Developments in Primatol-

ogy: Progress and prospects. Springer, New York, 477–496. https://doi.org/10.1007/978-0-387-88604-6_23

Felsenstein J (1985) Confidence limits on phylogenies: An approach using the bootstrap. Evolution 39: 783–791. https://doi.org/10.1111/j.1558-5646.1985.tb00420.x

Geissmann T, Nijman V, Boonratana R, Brockelman W, Roos C, Nowak MG (2020) *Hylobates agilis*. The IUCN Red List of Threatened Species 2020: eT10543A17967655. https://dx.doi.org/10.2305/IUCN.UK.2020-2.RLTS.T10543A17967655.en

Hasegawa M, Kishino H, Yano T (1985) Dating of the human-ape splitting by a molecular clock of mitochondrial DNA. Journal of Molecular Evolution 22: 160–174. https://doi.org/10.1007/BF02101694

Heled J, Drummond AJ (2012) Calibrated tree priors for relaxed phylogenetics and divergence time estimation. Systematic Biology 61(1): 138–149. https://doi.org/10.1093/sysbio/syr087

Hughes AC, Satasook C, Bates PJ, Bumrungsri S, Jones G (2011) Explaining the causes of the zoogeographic transition around the Isthmus of Kra: using bats as a case study. Journal of Biogeography 38(12): 2362–2372. https://doi.org/10.1111/j.1365-2699.2011.02568.x

Israfil H, Zehr SM, Mootnick AR, Ruvolo M, Steiper ME (2011) Unresolved molecular phylogenies of gibbons and siamangs (Family: Hylobatidae) based on mitochondrial, Y-linked, and X-linked loci indicate a rapid Miocene radiation or sudden vicariance event. Molecular Phylogenetics and Evolution 58(3): 447–455. https://doi.org/10.1016/j.ympev.2010.11.005

IUCN (2021) Hylobatidae. The IUCN Red List of Threatened Species. Version 2021-1. https://www.iucnredlist.org

IUCN/SSC (2013). Guidelines for Reintroductions and Other Conservation Translocations. Version 1.0. IUCN Species Survival Commission, Gland, Switzerland, viiii + 57 pp. https://www.iucn.org/content/guidelines-reintroductions-and-other-conservation-translocations

Iyengar A (2014) Forensic DNA analysis for animal protection and biodiversity conservation: A review. Journal for Nature Conservation 22(3): 195–205. https://doi.org/10.1016/j.jnc.2013.12.001

Kimura M (1980) A simple method for estimating evolutionary rate of base substitutions through comparative studies of nucleotide sequences. Journal Molecular Evolution 16: 111–120. https://doi.org/10.1007/BF01731581

Kumar S, Stecher G, Li M, Knyaz C, Tamura K (2018) MEGA X: Molecular evolutionary genetics analysis across computing platforms. Molecular Biology and Evolution 35: 1547–1549. https://doi.org/10.1093/molbev/msy096

Librado P, Rozas J (2009) DnaSP v5: A software for comprehensive analysis of DNA polymorphism data. Bioinformatics 25: 1451–1452. https://doi.org/10.1093/bioinformatics/btp187

Matsudaira K, Ishida T (2010) Phylogenetic relationships and divergence dates of the whole mitochondrial genome sequences among three gibbon genera. Molecular Phylogenetics and Evolution 55(2): 454–459. https://doi.org/10.1016/j.ympev.2010.01.032

Matsudaira K, Ishida T (2021) Divergence and introgression in small apes, the genus *Hylobates*, revealed by reduced representation sequencing. Heredity 1–11. https://doi.org/https://doi.org/10.1038/s41437-021-00452-7

Matsudaira K, Reichard UH, Malaivijitnond S, Ishida T (2013) Molecular evidence for the introgression between *Hylobates lar* and *H. pileatus* in the wild. Primates 54: 33–37. https://doi.org/10.1007/s10329-012-0323-5

Moritz C (1994) Defining "evolutionary significant units" for conservation. Tree 9: 373–375.

Moritz C (1999) Conservation units and translocations: strategies for conserving evolutionary processes. Hereditas 130(3): 217–228. https://doi.org/10.1111/j.1601-5223.1999.00217.x

Nei M (1987) Molecular Evolutionary Genetics. Columbia University Press, New York, 514 pp. https://doi.org/10.7312/nei-92038

Nijman V, Martinez CY, Shepherd CR (2009) Saved from trade: Donated and confiscated gibbons in zoos and rescue centres in Indonesia. Endangered Species Research 9(2): 151–157. https://doi.org/10.3354/esr00218

Rambaut A (2018) FigTree: Tree figure drawing tool version 1.4.4. http://tree.bio.ed.ac.uk/software/figtree.

Rambaut A, Drummond AJ, Xie D, Baele G, Suchard MA (2018) Posterior summarisation in Bayesian phylogenetics using Tracer 1.7. Systematic Biology 67(5): 901–904. https://doi.org/10.1093/sysbio/syy032

Roos C (2016) Phylogeny and classification of gibbons (Hylobatidae). In Reichard UH, Hirai H, Barelli C (Eds) Evolution of gibbons and siamang. Developments in Primatology: Progress and prospects. Springer, New York, 151–164. https://doi.org/10.1007/978-1-4939-5614-2_7

Roos C, Boonratana R, Supriatna J, Fellowes JR, Groves CP, Nash SD, Rylands AB, Mittermeier RA (2014) An updated taxonomy and conservation status review of Asian primates. Asian Primates Journal 4(1): 2–38. http://paper.sci.ui.ac.id/jspui/handle/2808.28/108

Roos C, Geissmann T (2001) Molecular phylogeny of the major Hylobatid divisions. Molecular Phylogenetics and Evolution 19(3): 486–494. https://doi.org/10.1006/mpev.2001.0939

Rovie-Ryan JJ, Abdullah MT, Sitam FT, Abidin ZZ, Tan SG (2013) Y-chromosomal gene flow of *Macaca fascicularis* (Cercopithecidae) between the insular and mainland peninsula of Penang state, Malaysia. Journal of Science and Technology in the Tropics 9: 113–126.

Rovie-Ryan JJ, Abdullah MT, Sitam FT, Tan SG, Zainuddin ZZ, Basir MM, Abidin ZZ, Keliang C, Denel A, Joeneh E, Ali FM (2014) Genetic diversity of *Macaca fascicularis* (Cercopithecidae) from Penang, Malaysia as inferred from mitochondrial control region segment. Journal of Indonesian Natural History 2(1): 14–25. http://jinh.fmipa.unand.ac.id/index.php/jinh/article/view/27

Rovie-Ryan JJ, Khan FAA, Abdullah MT (2021) Evolutionary pattern of *Macaca fascicularis* in Southeast Asia inferred using Y-chromosomal gene. BMC Ecology and Evolution 21(1): 1–12. https://doi.org/10.1186/s12862-021-01757-1

Sorenson MD, Quinn TW (1998) Numts: A Challenge for Avian Systematics and Population Biology. The Auk 115(1): 214–221. https://doi.org/10.2307/4089130

Spinks PQ, Shaffer HB (2007) Conservation phylogenetics of the Asian box turtles (Geoemydidae, *Cuora*): Mitochondrial introgression, numts, and inferences from multiple nuclear loci. Conservation Genetics 8: 641–657. https://doi.org/10.1007/s10592-006-9210-1

Thinh VN, Mootnick AR, Geissmann T, Li M, Ziegler T, Agil M, Moisson P, Nadler T, Walter L, Roos C (2010) Mitochondrial evidence for multiple radiations in the evolutionary

history of small apes. BMC Evolutionary Biology 10: 74. https://doi.org/10.1186/1471-2148-10-74.

Veeramah KR, Woerner AE, Johnstone L, Gut I, Gut M, Marques-Bonet T, Carbone L, Wall JD, Hammer MF (2015) Examining phylogenetic relationships among gibbon genera using whole genome sequence data using an approximate Bayesian computation approach. Genetics 200(1): 295–308. https://doi.org/10.1534/genetics.115.174425

Whittaker DJ, Morales JC, Melnick DJ (2007) Resolution of the *Hylobates* phylogeny: Congruence of mitochondrial D-loop sequences with molecular, behavioral, and morphological data sets. Molecular Phylogenetics and Evolution 45(2): 620–628. https://doi.org/10.1016/j.ympev.2007.08.009

Woodruff DS (2010) Biogeography and conservation in Southeast Asia: How 2.7 million years of repeated environmental fluctuations affect today's patterns and the future of the remaining refugial-phase biodiversity. Biodiversity and Conservation 19(4): 919–941. https://doi.org/10.1007/s10531-010-9783-3

Woodruff DS, Monda K, Simmons RE (2005) Mitochondrial DNA sequence variation and subspecific taxonomy in the white-handed gibbon, *Hylobates lar.* Natural History Journal of Chulalongkorn University Supplement 1, 71–78.

Supplementary material 1

Table S1. Summary table of all used sequences used in this study

Authors: Millawati Gani, Jeffrine J. Rovie-Ryan, Frankie Thomas Sitam, Noor Azleen Mohd Kulaimi, Chew Cheah Zheng, Aida Nur Atiqah, Nur Maisarah Abd Rahim, Ahmad Azhar Mohammed

Data type: specimens data

Link: https://doi.org/10.3897/zookeys.1076.73262.suppl1

Supplementary material 2

Table S2. Variable regions observed among the *Hylobates lar* sequences

Authors: Millawati Gani, Jeffrine J. Rovie-Ryan, Frankie Thomas Sitam, Noor Azleen Mohd Kulaimi, Chew Cheah Zheng, Aida Nur Atiqah, Nur Maisarah Abd Rahim, Ahmad Azhar Mohammed

Data type: variable sites

Explanation note: Blue coloured boxed indicated transversion mutations while green boxes indicated transition mutations.

Link: https://doi.org/10.3897/zookeys.1076.73262.suppl2

Supplementary material 3

Table S3. Pairwise genetic distances among the *H. lar* sequences used in this study using Kimura-2 parameters (Kimura 1980)

Authors: Millawati Gani, Jeffrine J. Rovie-Ryan, Frankie Thomas Sitam, Noor Azleen Mohd Kulaimi, Chew Cheah Zheng, Aida Nur Atiqah, Nur Maisarah Abd Rahim, Ahmad Azhar Mohammed

Data type: genetic distance

Link: https://doi.org/10.3897/zookeys.1076.73262.suppl3

ZooKeys 1076: 43–65 (2021)
doi: 10.3897/zookeys.1076.75576
https://zookeys.pensoft.net

RESEARCH ARTICLE

A peer-reviewed open-access journal
ZooKeys
Launched to accelerate biodiversity research

Rediscovering the dancing semislug genus *Cryptosemelus* Collinge, 1902 (Eupulmonata, Ariophantidae) from Thailand with description of two new species

Arthit Pholyotha[1], Chirasak Sutcharit[1], Somsak Panha[1,2]

1 *Animal Systematics Research Unit, Department of Biology, Faculty of Science, Chulalongkorn University, Bangkok 10330, Thailand* **2** *Academy of Science, The Royal Society of Thailand, Bangkok 10300, Thailand*

Corresponding author: Somsak Panha (somsak.pan@chula.ac.th)

Academic editor: Frank Köhler | Received 21 September 2021 | Accepted 8 November 2021 | Published 8 December 2021

http://zoobank.org/5E314298-BAB5-4161-B96F-2ACE02EB390F

Citation: Pholyotha A, Sutcharit C, Panha S (2021) Rediscovering the dancing semislug genus *Cryptosemelus* Collinge, 1902 (Eupulmonata, Ariophantidae) from Thailand with description of two new species. ZooKeys 1076: 43–65. https://doi.org/10.3897/zookeys.1076.75576

Abstract

Knowledge of Thai semislugs remains scarce, especially the dancing semislug genus *Cryptosemelus.* Prior to the present study, only a single species has been recognized with little available information. To address this knowledge gap, we surveyed for semislugs in western and southern Thailand, which yielded three species belonging to the genus *Cryptosemelus*. The little-known type species *C. gracilis* is redescribed herein, including a comparison with the type specimens. Two additional species, *C. betarmon* **sp. nov.** and *C. tigrinus* **sp. nov.**, are described as new to science. All three species are characterized by differences in their genital anatomy, especially with respect to anatomical details of the penis, epiphallus, and spermatophore. In addition, *C. tigrinus* **sp. nov.** differs from *C. gracilis* and *C. betarmon* **sp. nov.** in the mantle color pattern.

Keywords

Diversity, endemic, land snail, limestone, Malay Peninsula, systematics, taxonomy

Introduction

Becoming a slug through the reduction of the shell has occurred multiple times among the stylommatophoran land snails; this has occurred particularly frequently within the limacoid snail families Ariophantidae Godwin-Austen, 1883, Helicarionidae Bourguignat, 1877, and Urocyclidae Simroth, 1889 (Solem 1966; Hausdorf 1998; Hyman et al. 2007; Hyman and Köhler 2020). This process, so-called 'limacization', has also produced intermediate forms between slugs and snails, known as 'semislugs', which are characterized by the presence of an external shell with a reduced number of whorls, and a loss of the ability to completely withdraw its body under the protective shell (Collinge 1902; Blanford and Godwin-Austen 1908; Solem 1966; Barker 2001; Schileyko 2003; Schilthuizen and Liew 2008; Hyman and Köhler 2020). In addition, semislugs tend to show extensive development of the mantle lobes that can completely cover its shell, providing an increased surface area for gaseous exchange (Tillier 1983; Barker 2001). Located in the center of the Indo-Burma biodiversity hotspot (Myers et al. 2000), Thailand harbors a large number of snails, slugs, and semislugs belonging to the Ariophantidae and Helicarionidae (Solem 1966; Panha 1996; Hemmen and Hemmen 2001), of which several semislug genera have never been systematically revised since the seminal work of Solem (1966).

In the past decade, knowledge of the species diversity of Thailand's ariophantid snails has dramatically improved, and many genera/species have been described and their systematics have been revised (i.e., Pholyotha et al. 2020, 2021). For the poorly known genus *Cryptosemelus* Collinge, 1902 such a systematic revision had been pending so far as there had been no additional records on this taxon since its first description. Collinge (1902) only gave a very brief description without providing any details on the genitalia, which bear important characters in semislug taxonomy (Blanford and Godwin-Austen 1908; Solem 1966; Hyman and Ponder 2010; Hyman and Köhler 2020). This monotypic genus was described based on specimens collected during the 'The University of Cambridge Expedition to the North-Eastern Malay States and Upper Perak', known as the 'Skeat Expedition, 1899–1900' (Gibson-Hill et al. 1953), which visited a region now situated in southern Thailand and the northern part of the Peninsular Malaysia. In addition, *Cryptosemelus* has been referred to as the 'dancing semislug' because of the fidgety or dance-like movement that it makes when it is disturbed or attacked (Collinge 1902).

The purely shell-based taxonomy of the semislug groups provides insufficient evidence for their systematic classification because the highly reduced and rather featureless shells provide a dearth of informative characters. Convergence in shell characters has been demonstrated in Australian helicarionids (Hyman and Köhler 2020). The lack of reproductive information has created a profound inaccuracy in their recognition and delimitation (e.g., Blanford and Godwin-Austen 1908; Solem 1966; Schilthuizen and Liew 2008; Hyman and Ponder 2010; Hyman and Köhler 2020). At present, anatomy-based approaches or those integrating molecular analyses are likely to

more successfully resolve these taxonomic problems. Because the systematic revision of *Cryptosemelus* has never been undertaken for over a century, to fill this gap, we present here valuable data on the genus *Cryptosemelus*, especially the genitalia, spermatophore, mantle extensions, and radula. This paper includes a re-description of its type species, *C. gracilis* Collinge, 1902, and the descriptions of two additional new species.

Materials and methods

This study is based on voucher specimens deposited in the Chulalongkorn University Museum of Zoology, Bangkok, Thailand and new materials collected during the rainy season from western and southern Thailand (Fig. 1). Prior to preservation, collected semislug specimens were photographed in life. Each semislug was then euthanized following the standard two-step method protocols (American Veterinary Medical Association 2020), and then fixed in 95% (v/v) ethanol for morphological work. Species identification was made based on the literature, i.e., Collinge (1902), Blanford and Godwin-Austen (1908), and Solem (1966), and then compared with available type specimens and the reference collection of the University Museum of Zoology, Cambridge. For the descriptive work, adult shells were measured for size using a vernier caliper and counting the number of whorls. Three to ten specimens of each species were dissected and examined under an Olympus SZX2-TR30 stereoscopic light microscope. Shell and genitalia were imaged using a Nikon camera (DSLR D850) with a Nikon 105 Macro lens (AF-S VR Micro-Nikkor 105 mm f/2.8G IF-ED) and the inner sculpture of the genitalia was imaged using a stereo microscope with Cell'D Imaging Software. Radulae were extracted, soaked in 10% (w/v) sodium hydroxide, cleaned with distilled water, and then imaged by scanning electron microscopy (SEM; JEOL, JSM-6610 LV).

Descriptions of all new species herein are attributed to the first author. Type material and other voucher specimens are deposited in the Chulalongkorn University Museum of Zoology (**CUMZ**), Bangkok, Thailand and additional paratype specimens are deposited at the Natural History Museum, London, United Kingdom (**NHM** or **NHMUK**–when citing specimen lots deposited in the NHM) and the Zoological Reference Collection (**ZRC**) of the Lee Kong Chian Natural History Museum, National University of Singapore, Singapore.

The following abbreviations were used as defined by Blanford and Godwin-Austen (1908), Solem (1966), Pholyotha et al. (2020), and Sutcharit et al. (2020): **at**, atrium; **de**, diverticulum of epiphallus; **e1**, portion of epiphallus nearer to penis; **e2**, portion of epiphallus nearer to retractor muscle; **fo**, free oviduct; **gd**, gametolytic duct; **gs**, gametolytic sac; **hf**, head filament; **p**, penis; **pc**, penial caecum; **ldl**, left dorsal lobe; **lsl**, left shell lobe; **prm**, penial retractor muscle; **ps,** penial sheath; **pv**, penial verge; **rdl**, right dorsal lobe; **rsl**, right shell lobe; **ss**, sperm sac; **tf**, tail filament; **v**, vagina; and **vd**, vas deferens.

In the descriptions of the genitalia, the term 'proximal' refers to the region closest to the genital opening, while 'distal' refers to the region farthest away from the genital opening.

Results

Systematic description

Superfamily Helicarionoidea Bourguignat, 1877
Family Ariophantidae Godwin-Austen, 1883
Subfamily Ostracolethinae Simroth, 1901

Genus *Cryptosemelus* Collinge, 1902

Cryptosemelus Collinge, 1902: 76. Blanford and Godwin-Austen 1908: 180. Thiele 1931: 640. Zilch 1959: 326. Vaught 1989: 97. Schileyko 2003: 1332. Bank 2017: 53. Inkhavilay et al. 2019: 75.

Type species. *Cryptosemelus gracilis* Collinge, 1902, by monotypy.

Description. Shell thin, subglobose to globose, and imperforate. Shell surface smooth, polished, and with pale yellowish to olive tinge or golden amber. Whorls 3½–4, rapidly increasing; body whorl large and rounded. Aperture oblique and crescentic with simple lip.

Animal with reticulated skin, pale grayish, brownish, blue-gray, and blackish body marked by conspicuous oblique lines running downwards and backwards. Mantle extensions well-developed and divided into two shell lobes and two dorsal lobes. Shell lobes entirely covering shell or retracted when disturbed; left and right shell lobes usually with same color as body and with or without irregular stripes; right shell lobe (rsl) broad and triangular; left shell lobe (lsl) narrow triangular and relatively small-sized. Right dorsal lobe (rdl) ovate to crescent-shaped and left dorsal lobe (ldl) undivided, larger, and crescent-shaped. Sole tripartite and lateral foot margin present. Caudal horn absent.

Genitalia with slightly short to moderately long penis, thin penial sheath, long to very long epiphallus, penial retractor muscle attached to epiphallus, and short to slightly long gametolytic duct. Epiphallic caecum, flagellum, and dart apparatus absent. Spermatophore with complex branching spines.

Radular teeth arranged in a wide U-shape with symmetrical tricuspid central tooth, asymmetrical tricuspid lateral teeth with square to oblong base-plate, and bicuspid marginal teeth with oblong plate.

Remarks. Originally, Collinge (1902) referred this genus to the family Girasiidae, but later it was suggested to be placed under the subfamily Parmarioninae of the family Zonitidae (Blanford and Godwin-Austen 1908). Thiele (1931) then reclassified this genus, placing it under the subfamily Helicarioninae of the family Ariophantidae. This familial classification was then widely accepted and followed by subsequent authors except with the distinct subfamilial classification in which Zilch (1959) and Vaught (1989) placed *Cryptosemelus* as a member of the subfamily Macrochlamydinae, while Schileyko (2003) arranged it under the subfamily Parmarioninae. Regardless of the phylogenetic study, the higher classification of *Cryptosemelus* is still equivocal. Therefore, in this study, we follow the most recent gastropod classification that placed *Cryptosemelus* under the Ostracolethinae of the Ariophantidae (Bouchet et al. 2017).

Collinge (1902) additionally described another two monotypic semislug genera, *Apoparmarion* and *Paraparmarion*, from Peninsular Malaysia based on specimens from the Skeat Expedition. These two genera differ from the genus *Cryptosemelus* mainly based on the number of shell whorls and mantle extensions, shape of the caudal horn, and genital structure. The genus *Apoparmarion* has a very reduced shell with about two whorls, with mantle extensions rising upon the shell on all sides with the right shell lobe posteriorly large, wing-like, and covering the apex of the shell, a prominent caudal horn, and genitalia with both a flagellum and dart apparatus (Fig. 2A, B; Collinge 1902). In contrast, *Cryptosemelus* has a reduced shell of about 3 to 4 whorls, with well-developed mantle extensions with the right shell lobe covering the apex and larger than the left shell lobe, a tail with no caudal horn, and genitalia without flagellum and dart apparatus. For further comparison, *Paraparmarion* and *Cryptosemelus* share a similar reduction in the number of shell whorls and the disappearance of the caudal horn, but *Paraparmarion* has only a right shell lobe (Fig. 2E, F; Collinge 1902), whereas *Cryptosemelus* has both right and left shell lobes (Fig. 2C, D; Collinge 1902). Unfortunately, the genitalia of the genus *Paraparmarion* have never been examined for comparison. A future search for additional specimens of the genus *Paraparmarion* is necessary for elucidating its relationship with the genus *Cryptosemelus*.

Cryptosemelus gracilis Collinge, 1902

Figs 1, 2C, D, 3A, B, 4, 5, 10A

Cryptosemelus gracilis Collinge, 1902: 76, pl. 5, figs 37–39. Type locality: Bukit Besar, State of Nawng Chik [Nong Chik District, Pattani Province, Thailand]. Laidlaw 1933: 221. Benthem Jutting 1949: 71. Zilch 1959: 326. Maassen 2001: 112. Schileyko 2003: 1332.

Type material. ***Syntype*** UMZC I.66448 (one specimen in spirit; Fig. 2D) from Bukit Besar, Patani [Pattani Province, Thailand], Malay Peninsula.

Other material examined. Ton Din, Khuan Don District, Satun Province, Thailand (6°43'N, 100°09'E): CUMZ 7954.

Diagnosis. Shell globose and pale golden amber. Animal with blue-gray body. Genitalia with large vagina and elongated epiphallus with two small diverticula. Inner sculpture of penis with a small papilla near atrium. Spermatophore with a head filament of several spines and long tail filament with a cluster of small spines at the tip.

Description. ***Shell*** (Fig. 3A, B). Shell globose, small size (width up to 6.6 mm, height up to 4.2 mm), thin, smooth, polished, and pale golden amber. Whorls 3½–4, rapidly increasing; body whorl large and well-rounded at periphery. Spire slightly elevated; suture little impressed. Aperture oblique, diagonal, and roundly ovate; peristome simple and thin. Columellar margin simple. Umbilicus imperforate.

Genital organs (Figs 4B–D, 5). Atrium (at) short. Penis (p) rather short, cylindrical, and with thin penial sheath covering entire penis. Internal penis surface

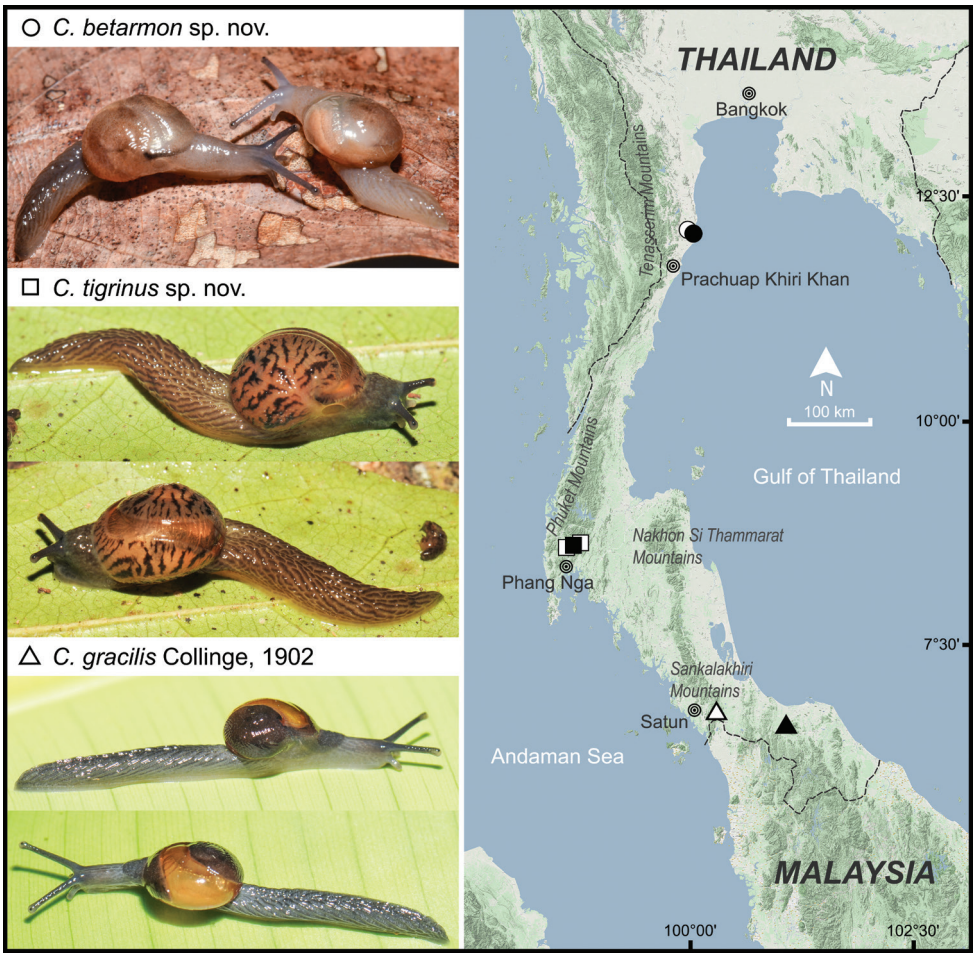

Figure 1. Geographic distribution and living animals of *Cryptosemelus gracilis*, *C. betarmon* sp. nov., and *C. tigrinus* sp. nov. based on the specimens examined herein. All not to scale. Black symbols indicate type locality and white symbols indicate other localities.

nearly smooth, with small papilla (protruded tissue) near atrium (yellow arrow in Fig. 4C). Epiphallus (e1+e2) approximately three times total penis length; e1 cylindrical and gradually smaller in diameter (Fig. 4B); proximal e2 enlarged with irregularly undulated surface patch; and distal e2 generally smooth surface. Diverticulum (de) having two caeca: one small and one more muscular, thicker, and slightly larger (Fig. 4D). Penial retractor muscle (prm) thin and attached at junction between e1 and e2. Vas deferens (vd) thin tube connected between distal epiphallus and free oviduct (Fig. 4B).

Vagina (v) large, cylindrical, and approximately half of penis length. Gametolytic sac (gs) bulbous (Fig. 4B with spermatophore); gametolytic duct (gd) rather

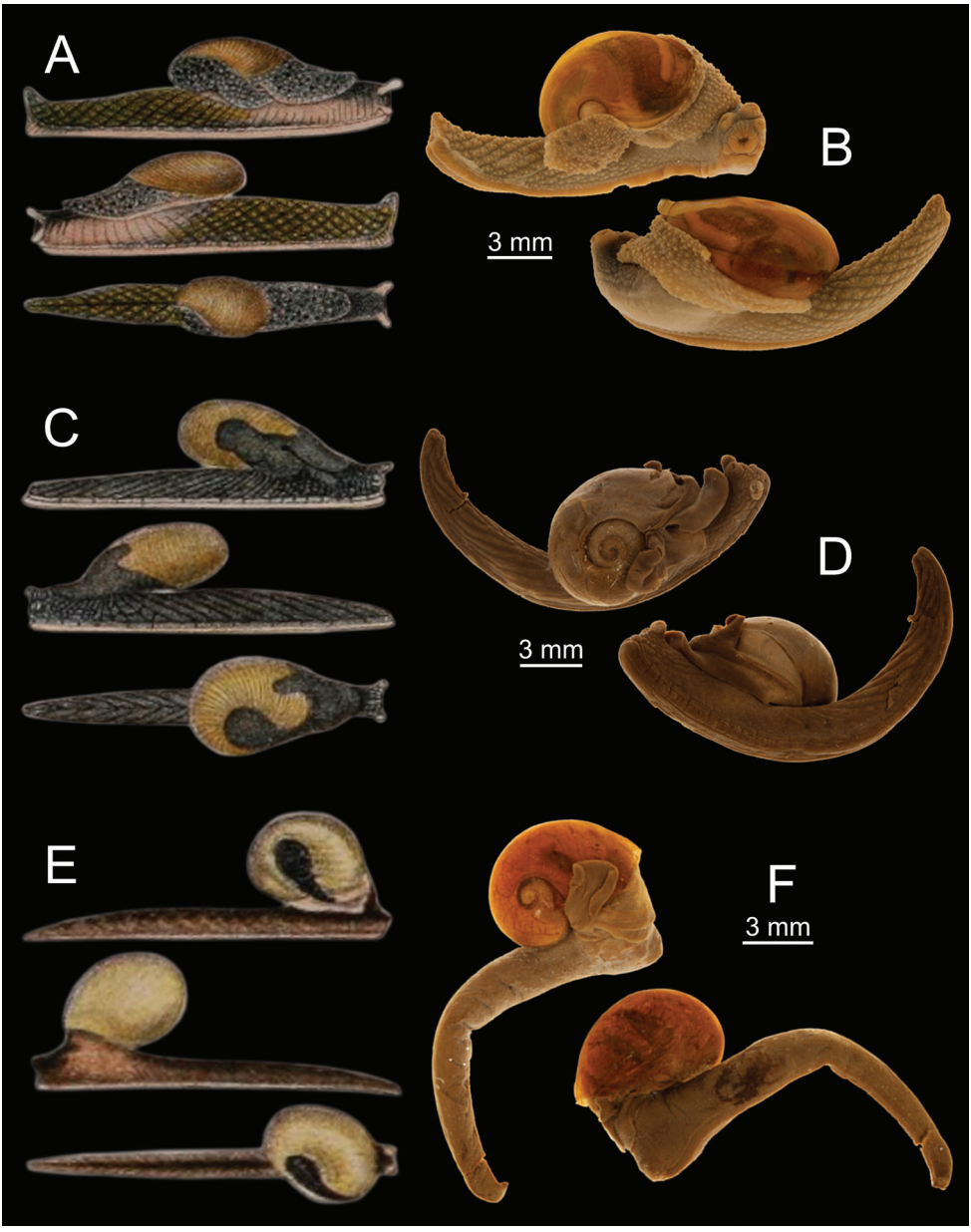

Figure 2. Comparison of shell and mantle lobes among the three monotypic semislugs described by Collinge (1902) **A, B** *Apoparmarion partridgii* Collinge, 1902 **A** original illustration and **B** syntype UMZC I.66414 **C, D** *Cryptosemelus gracilis* Collinge, 1902 **C** original illustration and **D** syntype UMZC I.66448 **E, F** *Paraparmarion elongatus* Collinge, 1902 **E** original illustration **F** syntype UMZC I.66522. Credits: **A, C, E** after Collinge (1902) and **B, D, F** online catalogues of the UMZC, Cambridge.

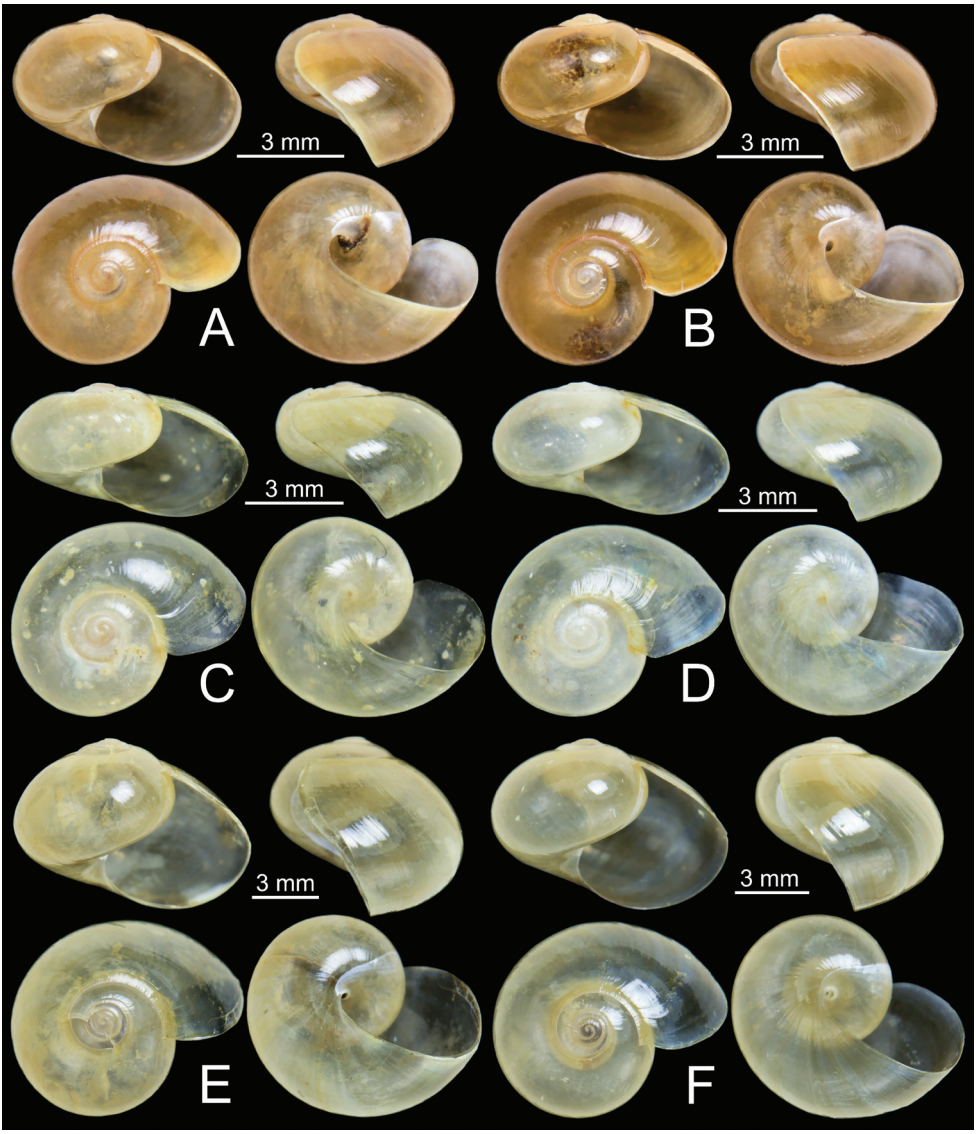

Figure 3. Shells **A, B** *Cryptosemelus gracilis* specimen CUMZ 7954 **C, D** *C. betarmon* sp. nov. **C** holotype CUMZ 7959, and **D** paratype CUMZ 7960 **E, F** *C. tigrinus* sp. nov. **E** holotype CUMZ 7955, and **F** paratype CUMZ 7956.

short, cylindrical, and somewhat broader at its base. Free oviduct (fo) cylindrical, approximately one and a half times penis length, and encircled with thick tissue in middle (Fig. 4B).

Spermatophore long (Fig. 5). Sperm sac (ss) enlarged and elongate ovalate. Head filament (hf) large and divided into two major branches located opposite: first branch bearing one small bifid spine, and second branch containing several bifid spines

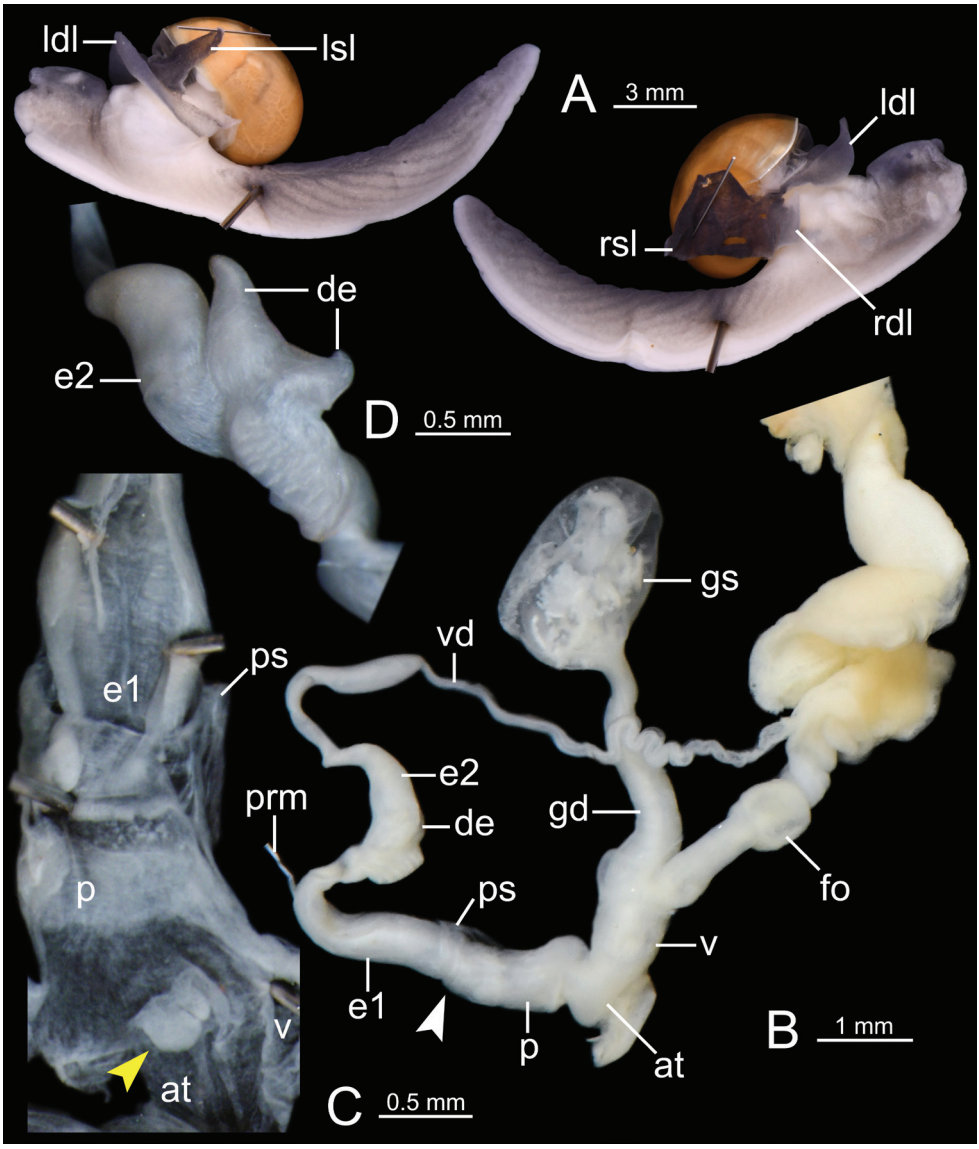

Figure 4. *Cryptosemelus gracilis* specimen CUMZ 7954 **A** both sides of animal showing four lobes of mantle and **B–D** genitalia: **B** general view of the genital system **C** internal structure of the penis, and **D** external structure of epiphallus (e2). White arrow indicates the end of the penis. Yellow arrow indicates the protruded tissue inside the penis near the atrium.

(Fig. 5B). Tail filament (tf) very long tube; terminal part about two-thirds of its length containing a series of tiny spines arranged in spiral rows (Fig. 5D–F).

Radula (Fig. 10A). Teeth arranged in a wide U-shape with half row formula: 1–(19–20)–38 teeth. Central tooth square base-plate with symmetrical tricuspid; mesocone large and triangular shape; ectocones small and pointed cusps. Lateral teeth

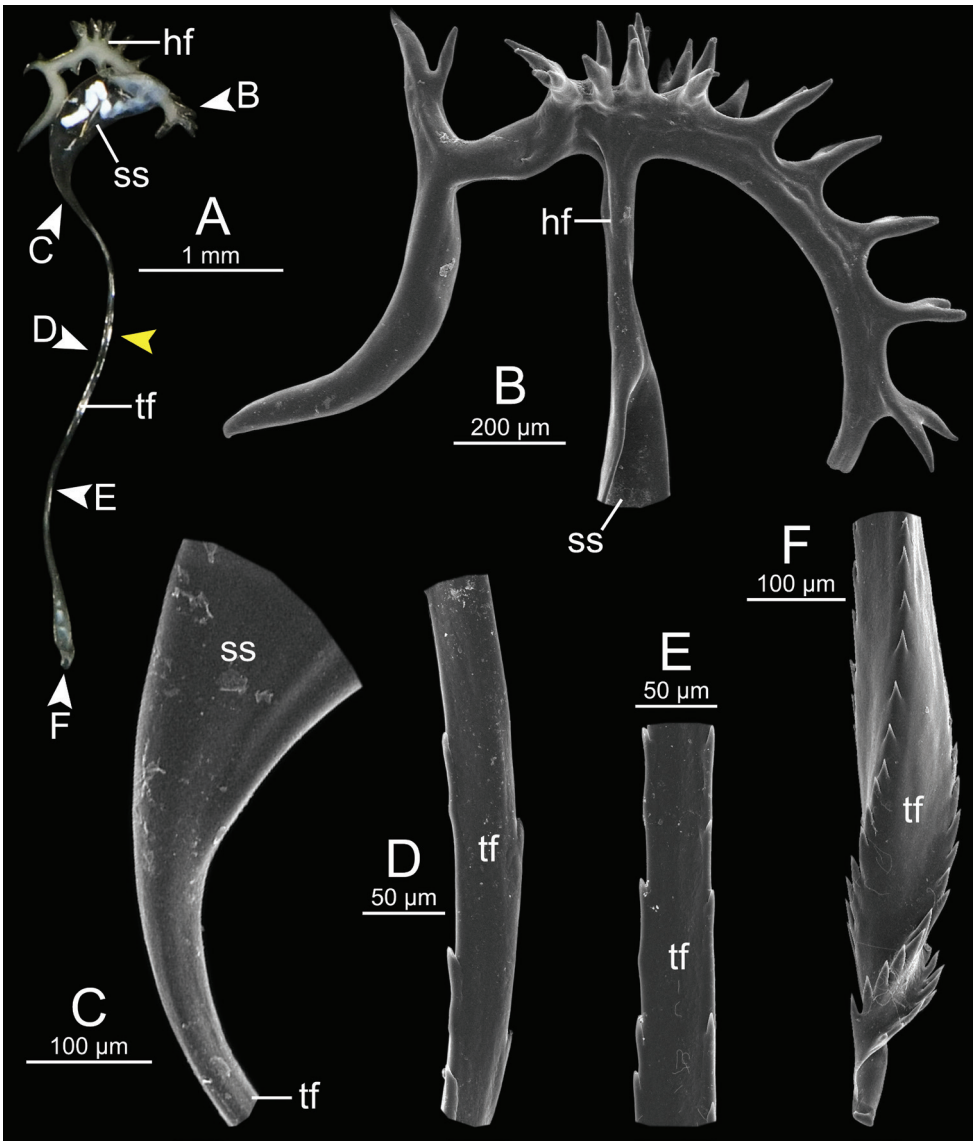

Figure 5. Spermatophore of *Cryptosemelus gracilis* specimen CUMZ 7954 **A** general view of the spermatophore **B–F** SEM images **B** head filament showing branching spines **C** region of tail filament near sperm sac showing no spine **D** alternate-spined region of tail filament near the end of spines from the tip **E** opposite-spined region of tail filament near the tip region, and **F** tail filament showing branching spines on the tip region. Yellow arrow indicates the end of spines from the tip.

asymmetrical tricuspid, inner teeth square base-plate and then gradually become elongate-shaped at outer teeth. Inner lateral teeth with mesocone large, triangular, and with pointed cusp; ectocone larger than endocone and located near tooth base. Outer lateral teeth: mesocone and ectocone large and pointed tip; endocone very small to nearly

absent. Marginal teeth starting at approximately teeth numbers 19 to 20 with obliquely elongate bicuspid; endocone large and pointed tip; ectocone small lanceolate shape with pointed cusp. Outermost marginal teeth shorter and smaller than inner teeth.

External appearance (Figs 1, 2C, D, 4A). Living animal with reticulated skin, blue-gray to blackish body marked by conspicuous oblique grooves running downwards. Four mantle extensions well-developed and same color as body. Shell lobes enlarged to cover entire shell; left shell lobe (lsl) smaller than right shell lobe (rsl); left dorsal lobe (ldl) larger than right dorsal lobe (rdl). Sole divided into three parts longitudinally. Caudal horn absent.

Distribution, habitat, and behavior observations. *Cryptosemelus gracilis* can be found in Satun, Yala, Songkhla, and Pattani Provinces in southern Thailand (Fig. 1). We searched after rain and found the semislug populations normally hiding under the slope of rocks or the tree trunks, and sometimes climbing on the rocks or low branches of plants. When the semislug are disturbed, they escape by quickly flipping and wagging their tail, and then falling on the floor. Information on its natural predators and parasites remains scarce, but the carnivorous slug genus *Atopos* and streptaxid snails were found sympatrically with this semislug.

Remarks. A specimen of *C. gracilis* was first discovered from 'Bukit Besar', the Malay Language, which means 'Big Mountains' in Thai Language (Skeat 1901; Annandale and Robinson 1906). However, this type locality is now referred to as the Namtok Sai Khao National Park area that is situated on the boundary of Pattani, Yala, and Songkhla Provinces in southern Thailand.

In this study, we examined specimens from Satun Province, which are identical to the syntype in having a blue-gray body with prominent oblique lines running downwards on the posterior body, large right shell lobes that covered the apex of the shell, and no caudal horn. Benthem Jutting (1949) provisionally attributed three semislug specimens from Telom Valley, Gunong Siku, Pahang State (1,000 m altitude) as *C. gracilis* s.l., but this was without any description or illustration. Based on our observation, all recognized *Cryptosemelus* species generally have a restricted distribution, and tend to occur at low altitudes near the mean sea level. Therefore, we consider that those semislug specimens from Pahang State probably belong to a distinct taxon from *C. gracilis* s.s. However, this semislug population needs to be re-examined to confirm their taxonomic status.

Cryptosemelus betarmon Pholyotha, sp. nov.

http://zoobank.org/11AF3310-99EB-402D-8A3C-68AD48B349DE
Figs 1, 3C, D, 6, 7, 10B

Type material. *Holotype*. CUMZ 7959 (Fig. 3C, width 7.4 mm, height 4.1 mm).

***Paratypes*.** Same locality as holotype: CUMZ 7960 (Fig. 3D, width 7.3 mm, height 4.1 mm), NHMUK (two shells), and ZRC (two shells). Limestone outcrops at Sam Roi Yot District, Prachuap Khiri Khan Province, Thailand (12°14'N, 99°55'E): CUMZ 7961.

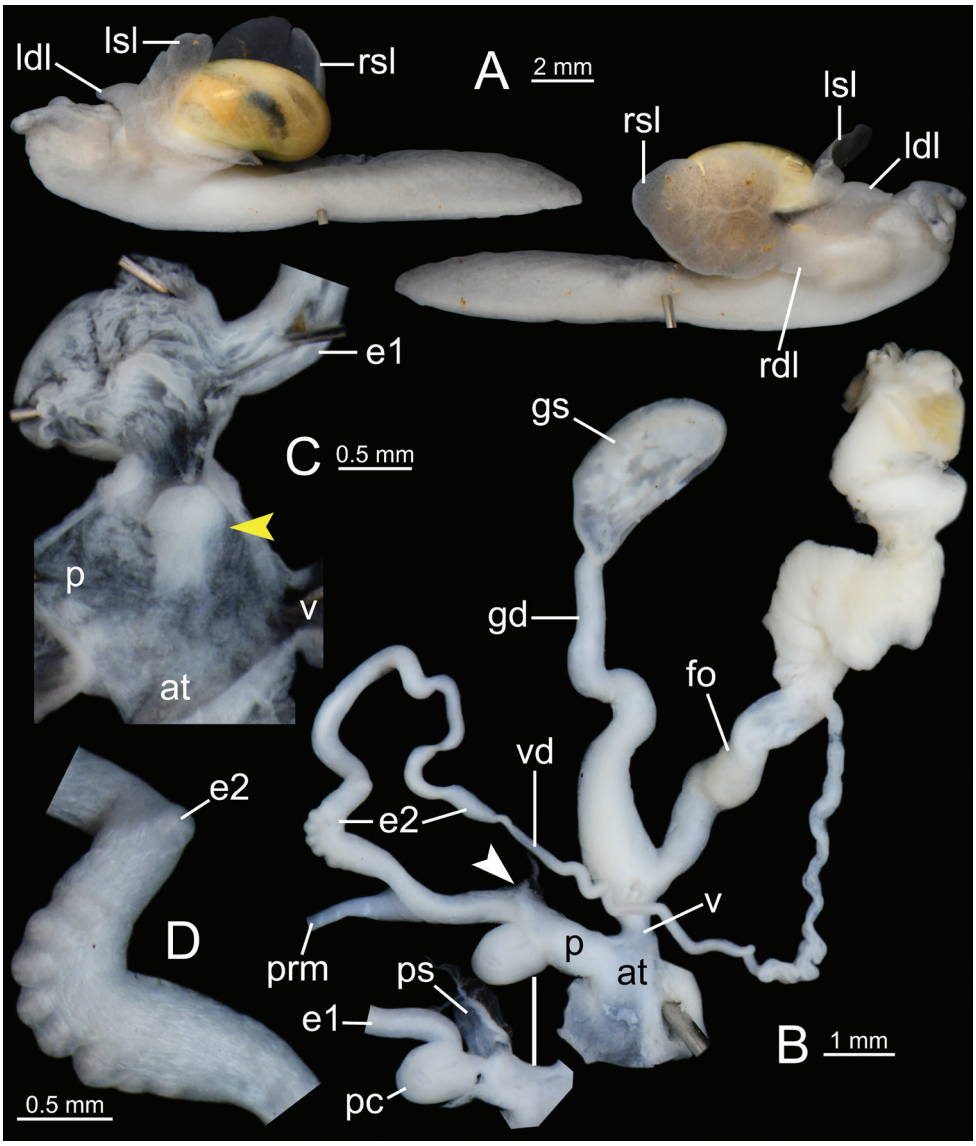

Figure 6. *Cryptosemelus betarmon* sp. nov. paratype CUMZ 7960 **A** both sides of animal showing four lobes of mantle **B–D** genitalia **B** general view of the genital system **C** internal structure of the penis, and **D** external structure of epiphallus (e2). White arrow indicates the end of the penis. Yellow arrow indicates the protruded tissue inside the penis near the atrium.

Type locality. Limestone outcrop at Wat Bang Pu, Sam Roi Yot District, Prachuap Khiri Khan Province, Thailand (12°12'N, 100°00'E).

Diagnosis. Shell depressedly subglobose and pale yellowish. Animal with grayish body. Genitalia with penial caecum, small vagina, and elongated epiphallus. Inner sculpture of penis with papilla and penial caecum. Spermatophore with a row of branching spines.

Description. ***Shell*** (Fig. 3C, D). Shell depressedly subglobose, small size (width up to 7.4 mm, height up to 4.1 mm), thin, smooth, polished, pale yellowish with olive tinge. Whorls 3½–4, rapidly increasing; body whorl large and well-rounded at periphery. Spire slightly elevated; suture little impressed. Aperture oblique, diagonal, roundly ovate; peristome thin, simple. Columellar margin simple. Umbilicus imperforate.

Genital organs (Figs 6B–D, 7). Atrium (at) short. Penis (p) somewhat short, cylindrical, and with thin penial sheath (ps) covering most of the penis; penial caecum (pc) enlarged and bulbous. Internal sculpture of proximal penis covered by nearly smooth surface and with thickened papilla (protruded tissue); and in penial caecum covered by irregularly folds (Fig. 6C). Epiphallus (e1+e2) approximately four times total penis length; e1 shorter than e2 and cylindrical; proximal e2 enlarged and with undulated surface (Fig. 6D) and then gradually reduced diameter to distal end (Fig. 6B). Penial retractor muscle (prm) thick, enlarged at base and attached at junction between e1 and e2. Vas deferens (vd) thin tube connected between distal epiphallus and free oviduct (Fig. 6B).

Vagina (v) cylindrical, and slightly shorter than a half of penis length. Gametolytic sac (gs) bulbous (Fig. 6B with spermatophore); gametolytic duct (gd) cylindrical, enlarged at base, and then gradually reduced in diameter to gametolytic sac. Free oviduct (fo) long, cylindrical, approximately two times total penis length, and encircled with thick tissue in middle (Fig. 6B).

Spermatophore incomplete (sperm sac and tail filament missing). Head filament (hf) with nine branching spines arranged in a single row along the head filament section (Fig. 7).

Radula (Fig. 10B). Teeth arrangement and shape similar to those of *C. gracilis*. Teeth with half row formula: 1–(27–28)–37 teeth. Central tooth square base-plate with symmetrical tricuspid. Inner lateral teeth square base-plate with asymmetrical tricuspid; outer lateral teeth oblong to elongate tricuspid. Marginal teeth elongate bicuspid. Marginal teeth starting at about teeth numbers 27–28; outermost teeth shorter and smaller than inner teeth.

External appearance (Figs 1, 6A). Living animal with reticulated skin, pale to dark grayish body marked by prominent, oblique, pale brownish lines running downwards. Four mantle extensions well-developed and same color as body. Shell lobes enlarged to cover almost entire shell; right shell lobe (rsl) larger than left shell lobe (lsl); right dorsal lobe (rdl) smaller than left dorsal lobe (ldl). Foot sole divided into median and lateral planes. Caudal horn absent.

Etymology. The specific name "*betarmon*" is from the Greek word meaning a dancer and refers to the fidgety movements or dance-like movements of living semislugs found in the field after being disturbed.

Distribution, habitat, and behavior observations. *Cryptosemelus betarmon* sp. nov. is restricted to the limestone outcrops in Prachuap Khiri Khan Province, Thailand (Fig. 1). During the rainy season, but with low precipitation, the semislugs were found inactive under the decaying leaf litter or sometimes inside the hole of decaying wood. This semislug species also moved quickly as well as quickly flipping and wagging its tail to escape after being disturbed. The data on its natural enemies are unknown, but the

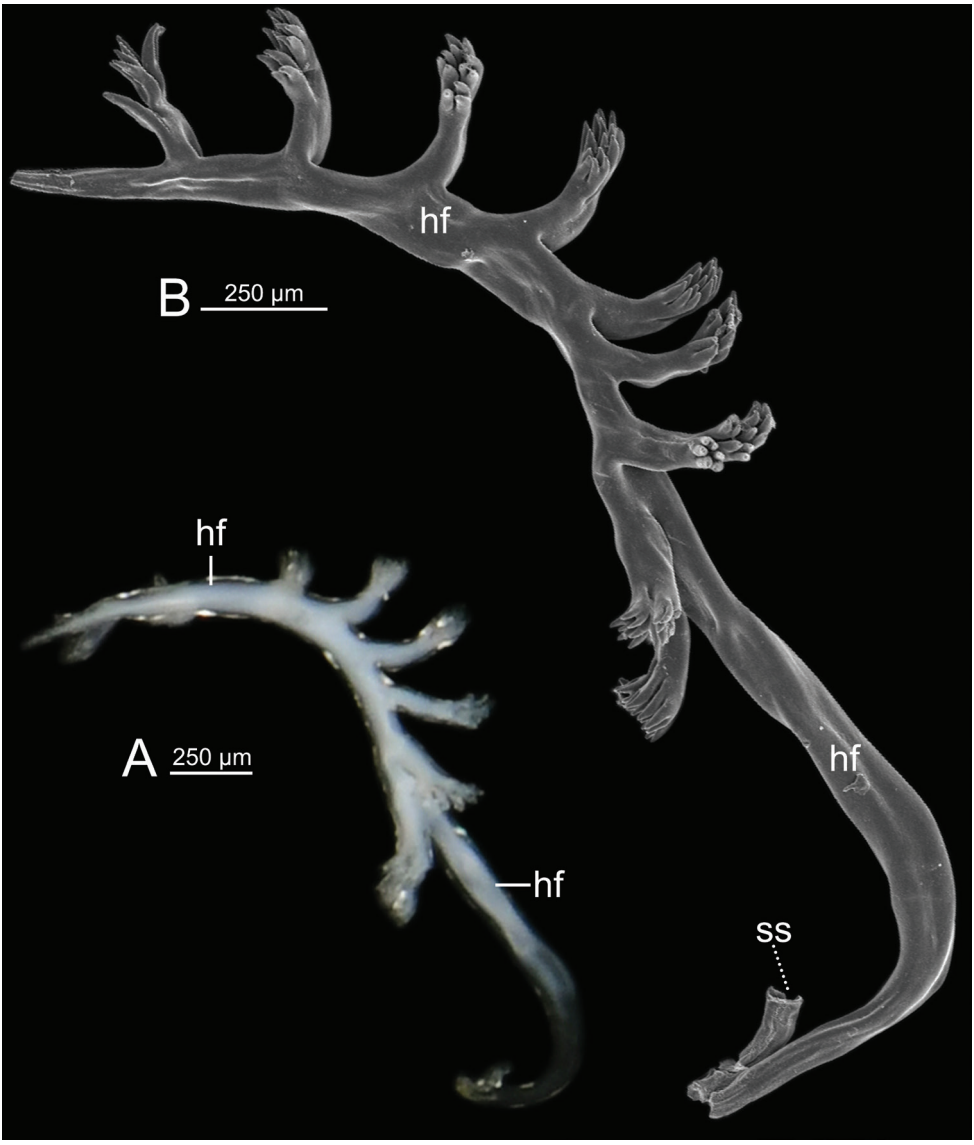

Figure 7. Spermatophore of *Cryptosemelus betarmon* sp. nov. paratype CUMZ 7960 **A** General view of head filament and **B** SEM images of head filament showing branching spines.

carnivorous snail, *Haploptychius* sp. (Streptaxidae), was found at a high abundance in the type locality.

Remarks. This new species is a small-sized *Cryptosemelus* species which has a subglobose and pale yellowish shell with an olive tinge, and genitalia with a penial caecum and without an epiphallic diverticulum. Compared to the type species, this species has a globose and pale golden amber shell, genitalia with two small diverticula on the epiphallus, and no penial caecum.

***Cryptosemelus tigrinus* Pholyotha, sp. nov.**
http://zoobank.org/98028C74-C2C5-4464-AE95-23FD93F25846
Figs 1, 3E, F, 8, 9, 10C

Type material. *Holotype*. CUMZ 7955 (Fig. 3E; width 10.7 mm, height 7.6 mm). ***Paratypes*.** Same locality as holotype: CUMZ 7956 (Fig. 3F; width 9.8 mm, height 6.8 mm), NHMUK (two shells), and ZRC (two shells). Limestone outcrops at Wat Suwan Khuha, Takua Thung District, Phang-Nga Province, Thailand (8°25'N, 98°28'E): CUMZ 7957. Limestone outcrops at Wat Tham Bang Toei, Mueang District, Phang-Nga Province, Thailand (8°27'N, 98°34'E): CUMZ 7958.

Type locality. Limestone outcrop at Tham Phung Chang, Mueang District, Phang-Nga Province, Thailand (8°26'N, 98°30'E).

Diagnosis. Shell globose, pale yellowish. Animal with brownish body, shell lobes pale yellowish-orange and flanked with irregular black bands. Genitalia with long penis and vagina and epiphallus with granulated surface near vas deferens; penial caecum and penial verge present. Inner sculpture of penis: proximal part with one thickened longitudinal fold; distal part with irregular folds. Spermatophore with smooth head filament and long tail filament with several delicate, branching spines.

Description. ***Shell*** (Fig. 3E, F). Shell globose, medium-sized (width up to 10.7 mm, height up to 7.6 mm), thin, smooth, polished, pale yellowish with an olive tinge. Whorls 4–4½, rapidly increasing; last whorl large and rounded at periphery. Spire elevated; suture little impressed. Aperture oblique, diagonal, roundly ovate; peristome thin, simple. Columellar margin simple. Umbilicus imperforate.

Genital organs (Figs 8B–D, 9). Atrium (at) short. Penis (p) moderately long, cylindrical with thin penial sheath (ps) covering nearly half of its length; penial caecum (pc) small. Internal wall of penis: proximal part covered with very thin longitudinal folds and one thickened longitudinal fold; distal part with irregularly zigzag folds surrounding the penial verge. Penial verge (pv) elongate ovate shape and smooth surface (Fig. 8C). Epiphallus (e1+e2) equal to penis length; e1 slightly shorter than e2 and cylindrical; proximal e2 cylindrical and smooth surface (Fig. 8B); distal e2 cylindrical with prominently granulated surface (Fig. 8D). Penial retractor muscle (prm) thick, enlarged at base and attached at junction between e1 and e2. Vas deferens (vd) thin tube connected between distal epiphallus and free oviduct (Fig. 8B).

Vagina (v) long, slender, and approximately half of penis length. Gametolytic sac (gs) bulbous (Fig. 8B with spermatophore); gametolytic duct (gd) somewhat enlarged and cylindrical. Free oviduct (fo) cylindrical, about half of penis length, and encircled with thick tissue in middle (Fig. 8B).

Spermatophore long and twisted cylindrical tube (Fig. 9). Head filament (hf) elongate tube with smooth surface (Fig. 9B). Sperm sac (ss) enlarged, elongate ovate with unclear boundary between sperm sac and tail filament. Tail filament (tf) very long and enlarged tube with series of long and delicate branching spines arranged in a row, and then near the tip having multiple rows of short branching spines (Fig. 9C, D).

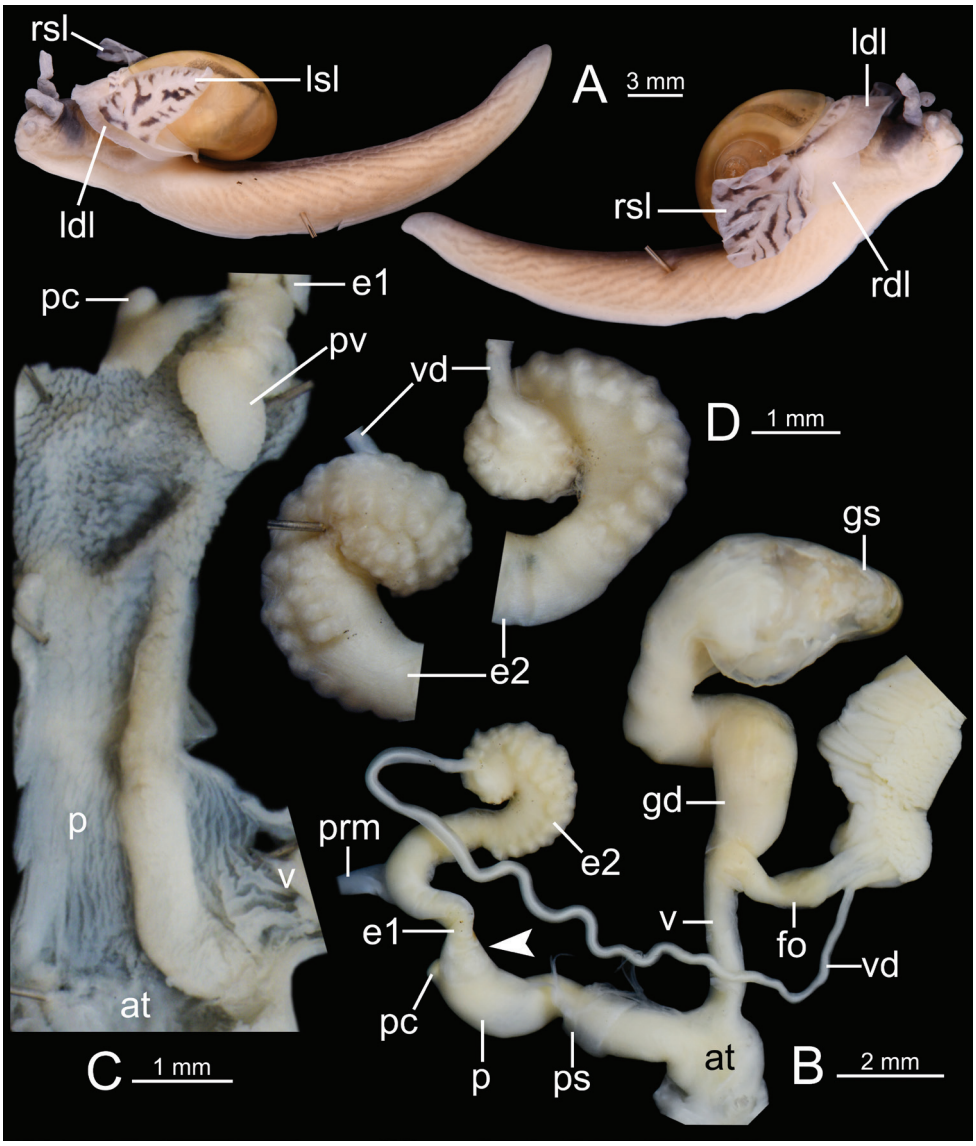

Figure 8. *Cryptosemelus tigrinus* sp. nov. paratype CUMZ 7956 **A** both sides of animal showing four lobes of mantle **B–D** genitalia **B** general view of the genital system **C** internal structure of the penis, and **D** external structure of epiphallus (e2). White arrow indicates the end of the penis.

Radula (Fig. 10C). Teeth arrangement and shape similar to those of *C. gracilis*. Teeth with half row formula: 1–(38–39)–44 teeth. Central tooth square base-plate with symmetrical tricuspid. Inner lateral teeth square base-plate with asymmetrical tricuspid; outer lateral teeth with oblong to elongate teeth with tricuspid. Marginal teeth elongate bicuspid. Marginal teeth starting at about teeth numbers 38–39; outermost teeth shorter and smaller than inner teeth.

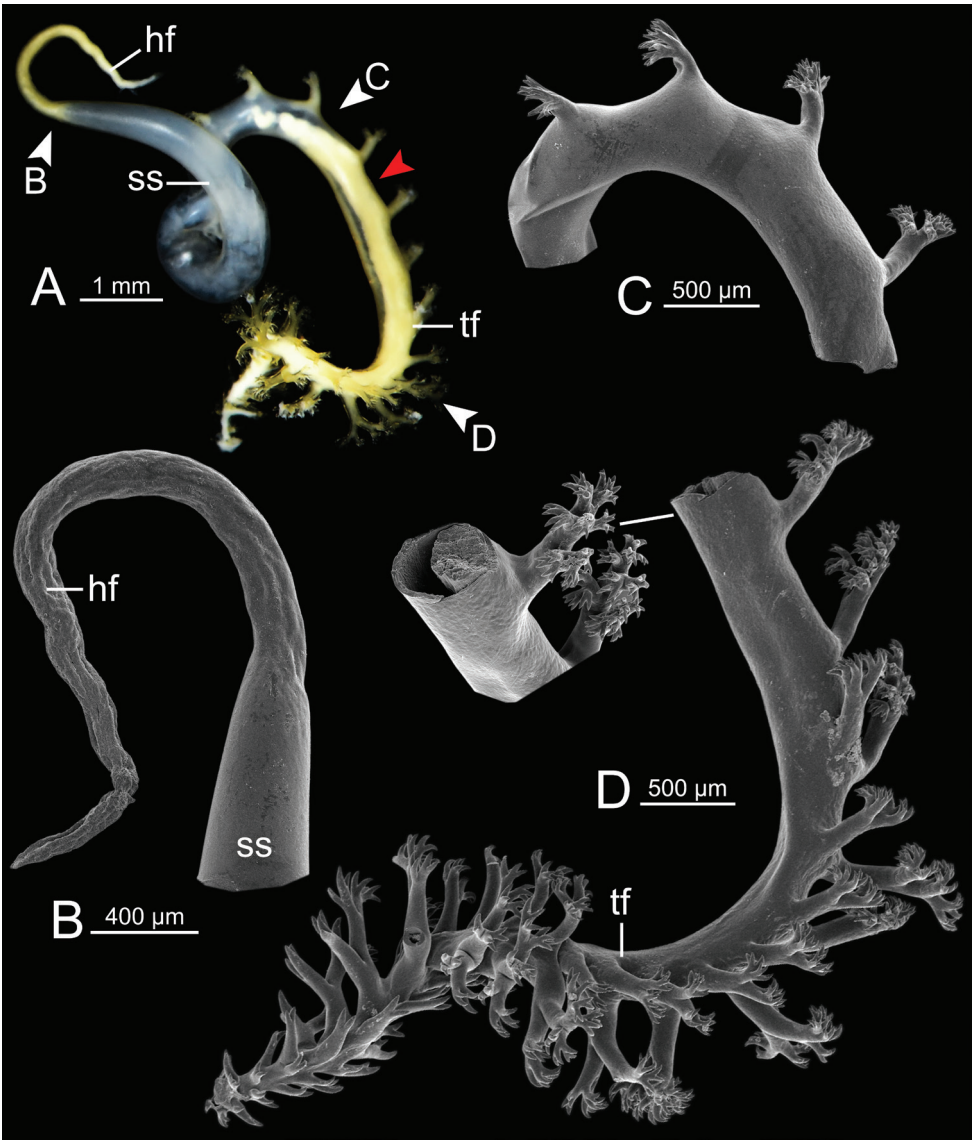

Figure 9. Spermatophore of *Cryptosemelus tigrinus* sp. nov. paratype CUMZ 7956 **A** general view of the spermatophore **B–D** SEM images **B** head filament without spine **C** branching spines on the unclear boundary between sperm sac and tail filament, and **D** tail filament showing branching spines; inset showing cross section of tail filament. Red arrow indicates position of cross section of tail filament.

External appearance (Figs 1, 8A). Living animal with reticulated skin, pale to dark brownish body marked with prominent, oblique, dark brownish lines running downwards. Mantle extensions well-developed. Shell lobes pale yellowish-orange, painted with irregular black stripes, and enlarged to cover entire shell; right shell lobe (rsl) large (square shape in preserved specimen); left shell lobe (lsl) small (triangular

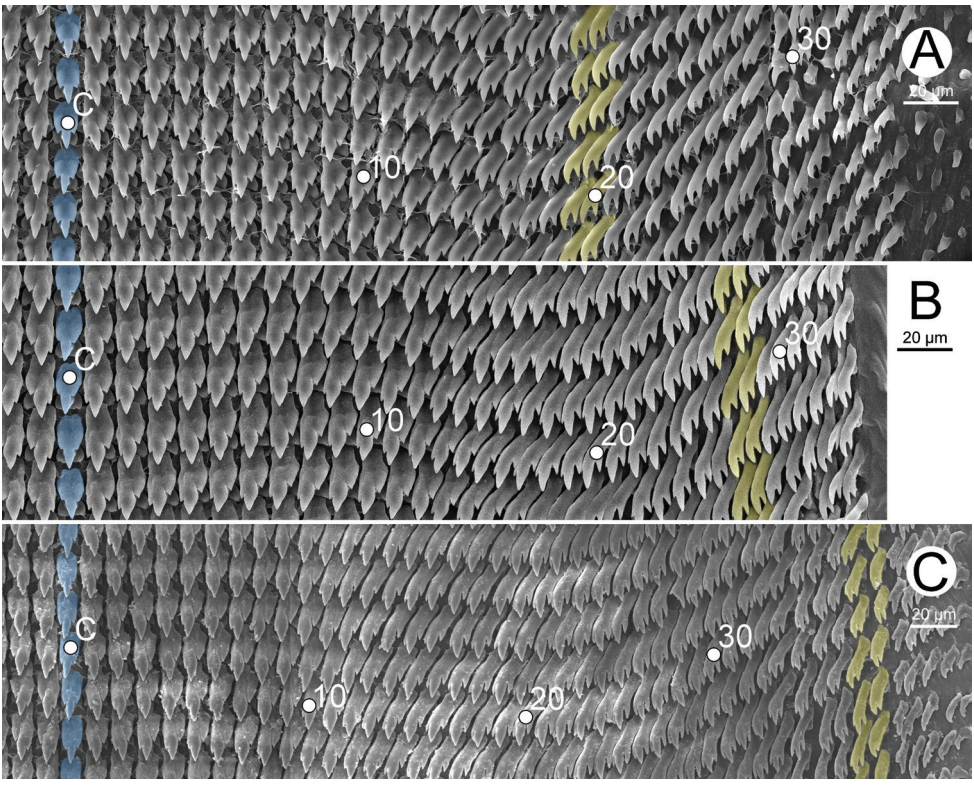

Figure 10. Representative SEM images of the radula **A** *Cryptosemelus gracilis* specimen CUMZ 7954 **B** *C. betarmon* sp. nov. paratype CUMZ 7960, and **C** *C. tigrinus* sp. nov. paratype CUMZ 7956. Central tooth indicated by 'C'; blue color indicates central tooth row; yellow color indicates the transition of outer lateral to marginal teeth.

shape in preserved specimen); left dorsal lobe (ldl) larger than right dorsal lobe (rdl). Foot sole divided into median and lateral planes. Caudal horn absent.

Etymology. The specific name is a Latin word "*tigrinus*", a noun in apposition referring to the dark stripes on shell lobes, which is similar to the color pattern of the tiger.

Distribution, habitat, and behavior observations. *Cryptosemelus tigrinus* sp. nov. can be found on the limestone hills in Phang-Nga Province (Fig. 1). This new semislug species has a high activity level, and is abundant in moist weather conditions after rain. They were seen hanging, crawling, or slowly climbing on the wet surface of the limestone rocks, tree trunks, and limestone shrubs. This new species also has an escape behavior similar to the other congeners. Its predators are unknown, but the carnivorous slug *Atopos* sp. (Rathuisiidae) and *Discartemon* sp. (Streptaxidae) were sympatric with the new species.

Remarks. *Cryptosemelus tigrinus* sp. nov. differs from *C. gracilis* and *C. betarmon* sp. nov. in having pale yellow-orange banded shell lobes and a well-developed penial verge, whereas *C. gracilis* and *C. betarmon* sp. nov. have monochrome shell lobes and do not have a penial verge.

Discussion

The three character states of (i) reduced shell, (ii) presence of the stimulator with a calcareous dart, and (iii) attachment of the penial retractor muscle directly to the epiphallus rather than to the epiphallic caecum are characteristic for members of the Ostracolethinae, family Ariophantidae (Hausdorf 1998). This study contains the first anatomical investigation of *Cryptosemelus* and we found that its genital anatomy is consistent with a membership in this subfamily. This finding is corroborated by evidence from shell and reproductive characters as outlined above (dart possibly secondarily reduced). With regard to the absence of a dart apparatus, this character together with the epiphallic caecum and flagellum appears to have been lost and gained repeatedly and convergently among the Ariophantidae and the limacoid snails in general (Hausdorf 1998; Schileyko and Semenyuk 2018).

The shell morphology of the genus *Cryptosemelus* is similar to that of several semislug genera on mainland Southeast Asia that consist of *Apoparmarion*, *Cryptaustenia* Cockerell, 1891, *Durgella* Blanford, 1863, and *Paraparmarion*. However, the absence of a caudal horn, which is a unique character shared between *Cryptosemelus* and *Paraparmarion*, distinguishes these two semislug genera from the others (Collinge 1902; Blanford and Godwin-Austen 1908; Solem 1966; Schileyko 2002, 2003).

Cryptosemelus was stated to differ from *Paraparmarion* in that the left shell lobe is well-developed, whereas it is missing in the latter (Collinge 1902). However, the presence and absence of the left shell lobe can simultaneously occur within congeneric species in the ariophantid snail genus *Sarika* Godwin-Austen, 1907 (Pholyotha et al. 2020). Hence, the relationship between *Cryptosemelus* and *Paraparmarion* remains uncertain since they were consecutively described in the same publication without genital information (Collinge 1902). However, the genitalia of *Cryptosemelus* have been examined herein and its generic status is confirmed. The genital morphology of all species of *Cryptosemelus* examined herein all show no epiphallic caecum, flagellum, and dart apparatus. In comparison, a flagellum occurs only in *Apoparmarion*, while an epiphallic caecum occurs only in *Durgella* (Collinge 1902; Blanford and Godwin-Austen 1908; Solem 1966; Schileyko 2002, 2003).

Regarding the dart apparatus, the main role of which is for stimulation during courtship behaviour, this character has been used as a distinguishing character among the limacoid genera, i.e., *Hemiplecta* Albers, 1850 (with dart apparatus) vs. *Falsiplecta* Schileyko & Semenyuk, 2018 (without dart apparatus), or *Macrochlamys* Gray, 1847 (with dart apparatus) vs. *Syama* Godwin-Austen, 1908 (without dart apparatus). These sibling genera have a similar external appearance except for the dart apparatus (Blanford and Godwin-Austen 1908; Schileyko 2002, 2003; Schileyko and Semenyuk 2018). However, it is widely accepted that the dart apparatus could be present or absent within the same genus, i.e., *Cryptaustenia* and *Durgella* (Blanford and Godwin-Austen 1908; Solem 1966; Schileyko 2002, 2003). Moreover, no molecular phylogeny has been implemented to test the monophyly of the genera *Cryptaustenia* and *Durgella*.

In this study, the shell lobes and genitalia (penis and epiphallus) are considered as taxonomically informative and these can be used to distinguish all *Cryptosemelus* species. In addition, these characters might reflect the relationships among three species of *Cryptosemelus.* Our results indicated that *C. gracilis* is closely related to *C. betarmon* sp. nov. even though the distribution of *C. gracilis* is closer to *C. tigrinus* sp. nov. (Fig. 1). In support, the shell lobes of *C. gracilis* and *C. betarmon* sp. nov. have a monotone color and the internal wall of the penis has a papilla located close to atrium, whereas *C. tigrinus* sp. nov. has shell lobes with dark stripes and a large, conical penial verge. In addition, the undulated surface on the epiphallus of the two species is located close to the penial retractor muscle, while in *C. tigrinus* sp. nov. this character is located near the vas deferens. Furthermore, the color pattern of the shell lobes and the reproductive tracts of *C. tigrinus* sp. nov. are very distinct and unique, which could possibly be recognized as different subgenera or genera. However, we refrain from nominating this because at present it is without support from a molecular framework. Thus, future studies need more materials from other members of *Cryptosemelus* and will also require combining with molecular phylogenetic analyses to investigate this hypothesis.

Predator-prey interactions are recognized as major processes promoting morphological and behavioral diversity (Vermeij 1987; Chiba 2007; Morii et al. 2016; Sugiura 2016; Le Ferrand and Morii 2020). Land snails are preyed upon by a wide range of predators (e.g., rodents, birds, snakes, insects, and molluscs). Their own anti-predator adaptations, a passive defense by pulling their body into their shell and an active behavior by swinging their shell around, are well documented and are potentially associated with differences in shell traits (Vermeij 1987, 1993; Chiba 2007; Baalbergen 2014; Liew and Schilthuizen 2014; Morii et al. 2016; Morii and Wakabayashi 2017; Le Ferrand and Morii 2020). In contrast, the evolution of slug and semislug forms have sacrificed the protection offered by possession of a shell for the mobility, fast body movements, and ability to occupy very small spaces afforded by the reduction or elimination of the shell (Solem 1974; Barker 2001; Wiktor 2002; Dedov et al. 2019). In our study, this dancing semislug genus showed an anti-predator behavior by quick dance-like movements or the sudden flipping and wagging tail movement and the fast movement away from the location of threat. This behavior has also been recorded in several helicarionid semislugs: *Cryptaustenia* species in Papua-New Guinea, *Laocaia* species in Vietnam, and *Muangnua* species in Thailand (Wiktor 2002; Dedov et al. 2019; Tumpeesuwan and Tumpeesuwan 2019).

Acknowledgements

We are grateful to all members of the Animal Systematics Research Unit, Chulalongkorn University for their kind help during field trips and technical support. We are also grateful for the financial support that we received from the Thailand Research Fund (TRF-DPG628001) and Center of Excellence on Biodiversity (BDC–PG2–161002). In addition, this research was supported by the Ratchadapisek Somphot Fund for Postdoctoral Fellowship, Chulalongkorn University to S.P. and A.P. This study was

approved by the Chulalongkorn University Animal Care and Use Committee (CU-ACUC) under the approval number 1723018. Additionally, special thanks go to anonymous reviewers for providing valuable comments and suggestions on the manuscript.

References

American Veterinary Medical Association (2020) AVMA Guidelines for the Euthanasia of Animals: 2020 Edition. 121 pp. https://www.avma.org/sites/default/files/2020-01/2020-Euthanasia-Final-1-17-20.pdf [accessed 12 Feb 2020]

Annandale N, Robinson HC (1906) Fasciculi Malayenses: anthropological and zoological results of an expedition to Perak and the Siamese Malay states, 1901–1902 Vol 3: supplement: itinerary in Perak, Selangor, and the Siamese Malay states. University Press of Liverpool, London, 180 pp.

Baalbergen E, Helwerda R, Schelfhorst R, Castillo Cajas RF, van Moorsel CHM, Kundrata R, Welter-Schultes FW, Giokas S, Schilthuizen M (2014) Predator-prey interactions between shell-boring beetle larvae and rock-dwelling land snails. PLoS ONE 9(6): e100366. https://doi.org/10.1371/journal.pone.0100366

Bank RA (2017) Classification of the Recent terrestrial Gastropoda of the World. Last update: July 16th, 2017.

Barker GM (2001) The Biology of terrestrial molluscs. CABI publishing, United Kingdom, 560 pp. https://doi.org/10.1079/9780851993188.0000

Benthem Jutting WSS van (1949) On a collection of non-marine Mollusca from Malaya in the Raffles Museum, Singapore, with an appendix on cave shells. Bulletin of Raffles Museum Singapore 19: 50–77.

Blanford WT, Godwin-Austen HH (1908) The Fauna of British India, including Ceylon and Burma. Mollusca. Testacellidae and Zonitidae. Taylor and Francis, London, 311 pp.

Bouchet P, Rocroi JP, Hausdorf B, Kaim A, Kano Y, Nützel A, Parkhaev P, Schrödl M, Strong EE (2017) Revised classification, nomenclator and typification of gastropod and monoplacophoran families. Malacologia 61(1–2): 1–526. https://doi.org/10.4002/040.061.0201

Chiba S (2007) Morphological and ecological shifts in a land snail caused by the impact of an introduced predator. Ecological Research 22: 884–891. https://doi.org/10.1007/s11284-006-0330-3

Collinge WE (1902) On the non-operculated land- and freshwater molluscs collected by the members of the "Skeat Expedition" in the Malay Peninsula, 1899–1900. The Journal of Malacology 9(3): 71–95.

Dedov I, Schneppat U, Vu MQ, Huy NQ (2019) A new semislug of the genus *Laocaia* (Gastropoda, Pulmonata, Helicarionidae) from Vietnam. ZooKeys 846: 19–30. https://doi.org/10.3897/zookeys.846.34372

Gibson-Hill CA, Skeat WW, Laidlaw FF (1953) The Cambridge University Expedition to the North-Eastern Malay States, and to Upper Perak, 1899–1900. Journal of the Malayan Branch of the Royal Asiatic Society 26: 3–174.

Hausdorf B (1998) Phylogeny of the Limacoidea sensu lato (Gastropoda: Stylommatophora). Journal of Molluscan Studies 64: 35–66. https://doi.org/10.1093/mollus/64.1.35

Hemmen J, Hemmen C (2001) Aktualisierte Liste der terrestrischen Gastropoden Thailands. Schriften zur Malakozoologie aus dem Haus der Natur-Cismar 18: 35–70.

Hyman IT, Köhler F (2020) Feeling sluggish: The extreme semislugs of Australia (Stylommatophora, Helicarionidae) Journal of Zoological Systematics and Evolutionary Research 58: 1021–1057 https://doi.org/10.1111/jzs.12376

Hyman IT, Ponder WF (2010) A morphological phylogenetic analysis and generic revision of Australian Helicarionidae (Gastropoda: Pulmonata: Stylommatophora), and an assessment of the relationships of the family. Zootaxa 2462: 1–148. https://doi.org/10.11646/zootaxa.2462.1.1

Hyman IT, Ho SY, Jermiin LS (2007) Molecular phylogeny of Australian Helicarionidae, Euconulidae and related groups (Gastropoda: Pulmonata: Stylommatophora) based on mitochondrial DNA. Molecular Phylogenetics and Evolution 45(3): 792–812. https://doi.org/10.1016/j.ympev.2007.08.018.

Inkhavilay K, Sutcharit C, Bantaowong U, Chanabun R, Siriwut W, Srisonchai R, Pholyotha A, Jirapatrasilp P, Panha S (2019) Annotated checklist of the terrestrial molluscs from Laos (Mollusca, Gastropoda). ZooKeys 834: 1–166. https://doi.org/10.3897/zookeys.834.28800

Laidlaw FF (1933) A list of the land and fresh-water Mollusca of the Malay Peninsula. Journal of the Malaysian Branch of the Royal Asiatic Society 11: 211–234.

Le Ferrand H, Morii Y (2020) Structure-behaviour correlations between two genetically closely related snail species. Royal Society Open Science 7: e191471. https://doi.org/10.1098/rsos.191471

Liew T-S, Schilthuizen M (2014) Association between shell morphology of micro-land snails (genus *Plectostoma*) and their predator's predatory behaviour. PeerJ 2: e329. https://doi.org/10.7717/peerj.329

Maassen WJM (2001) A preliminary checklist of the non-marine molluscs of West-Malaysia. "A Handlist". De Kreukel, Amsterdam, 155 pp.

Morii Y, Prozorova L, Chiba S (2016) Parallel evolution of passive and active defence in land snails. Scientific Reports 6: e35600. https://doi.org/10.1038/srep35600

Morii Y, Wakabayashi H (2017) Do native rodents prey on land snails? An experimental and quantitative study in Hokkaido, Japan. Zoological Science 34: 275–280. https://doi.org/10.2108/zs170018

Myers N, Mittermeier RA, Mittermeier CG, da Fonseca GAB, Kent J (2000) Biodiversity hotspots for conservation priorities. Nature 403: 853–858. https://doi.org/10.1038/35002501

Panha S (1996) A checklist and classification of the land terrestrial pulmonate snail in Thailand. Walkerana 8: 31–40.

Pholyotha A, Sutcharit C, Tongkerd P, Jeratthitikul E, Panha S (2021) Integrative systematics reveals the new land-snail genus *Taphrenalla* (Eupulmonata: Ariophantidae) with a description of nine new species from Thailand. Contributions to Zoology 90: 21–69. https://doi.org/10.1163/18759866-bja10013

Pholyotha A, Sutcharit C, Tongkerd P, Panha S (2020) Integrative taxonomic revision of the land snail genus *Sarika* Godwin-Austen, 1907 in Thailand, with descriptions of nine new species (Eupulmonata, Ariophantidae). ZooKeys 976: 1–100. https://doi.org/10.3897/zookeys.976.53859

Schileyko AA (2002) Treatise on recent terrestrial pulmonated mollusks. Part 9. Helicarionidae, Gymnarionidae, Rhysotinidae, Ariophantidae. Ruthenica, Supplement 2: 1167–1307.

Schileyko AA (2003) Treatise on recent terrestrial pulmonate molluscs. Part 10. Ariophantidae, Ostracolethidae, Ryssotidae, Milacidae, Dyakiidae, Staffordiidae, Gastrodontidae, Zonitidae, Daudebardiidae, Parmacellidae. Ruthenica Supplement 2: 1309–1466.

Schileyko AA, Semenyuk I (2018) *Falsiplecta integripedia* gen. et sp. nov. from Vietnam (Gastropoda, Pulmonata, Helicarionidae). Ruthenica 28: 125–129. https://doi.org/10.35885/ruthenica.2018.28(3).5

Schilthuizen M, Liew T-S (2008) The slugs and semislugs of Sabah, Malaysian Borneo (Gastropoda, Pulmonata: Veronicellidae, Rathouisiidae, Ariophantidae, Limacidae, Philomycidae). Basteria 72: 287–306.

Skeat WW (1901) List of a collection of snakes, crocodiles, and chelonians from the Malay Peninsula, made by members of the "Skeat Expedition," 1899–1900. With an appendix containing a list of the names of the places visited by the "Skeat Expedition". Proceedings of the Zoological Society of London 71(2): 575–586. https://doi.org/10.1111/j.1469-7998.1902.tb08188.x

Solem A (1966) Some non-marine mollusks from Thailand. Spolia Zoologia Musei Hauniensis 24: 1–110.

Solem A (1974) The shell makers, introducing mollusks. John Wiley & Sons Inc, New York.

Sugiura S (2016) Impacts of introduced species on the biota of an oceanic archipelago: the relative importance of competitive and trophic interactions. Ecological Research 31: 155–164. https://doi.org/10.1007/s11284-016-1336-0

Sutcharit C, Jeratthitikul E, Pholyotha A, Lin A, Panha S (2020) Molecular phylogeny reveals high diversity and endemism in the limestone karst-restricted land snail genus *Sophina* Benson, 1859 from Myanmar (Eupulmonata: Helicarionidae), with description of four new species. Journal of Zoological Systematics and Evolutionary Research 58: 957–981. https://doi.org/10.1111/jzs.12420

Thiele J (1931) [1929–1935] Handbuch der systematischen Weichtierkunde. Erster Band, Tiel 2, Gastropoda: Ophisthobranchia and Pulmonata [English translation: Bieler & Mikkelsen (1992–1998)]. Gustav Fischer Verlag, Jena.

Tillier S (1983) Structures respiratoires et excrétrices secondaries des limaces (Gastropoda: Pulmonata: Stylommatophora). Bulletin de la Société Zoologique de France 108: 9–19.

Tumpeesuwan C, Tumpeesuwan S (2019) *Muangnua arborea*, a new semislug (Gastropoda, Stylommatophora, Helicarionidae, Durgellininae) from Loei Province, northeastern Thailand. ZooKeys 894: 19–32. https://doi.org/10.3897/zookeys.894.38327

Vaught KC (1989) A classification of the living Mollusca. American Malacologist, Inc., Melbourne, 189 pp.

Vermeij GJ (1987) Evolution and escalation. Princeton University Press, Princeton, 527 pp.

Vermeij GJ (1993) A natural history of shells. Princeton University Press, Princeton, 207 pp.

Wiktor A (2002) Terrestrial gastropods of the province of Madang in Papua-New Guinea (Part II) – Two species of *Cryptaustenia* Cockerell, 1898 (Pulmonata: Helicarionidae) new to the science. Folia Malacologica 10(4): 225–231. https://doi.org/10.12657/folmal.010.014

Zilch A (1959) Gastropoda, Euthyneura. In: Schindewolf OH (Ed.) Handbuch der Paläozoologie, Band 6, Gastropoda. Gebrüder Borntraeger, Berlin, 400 pp.

ZooKeys 1076: 67–81 (2021)
doi: 10.3897/zookeys.1076.37278
http://zookeys.pensoft.net

RESEARCH ARTICLE

A peer-reviewed open-access journal
ZooKeys
Launched to accelerate biodiversity research

First record of the genus *Discorhabdella* (Porifera, Demospongiae, Poecilosclerida, Crambeidae) from Sagami Bay, Japan with description of two new species

Yuji Ise[1], Jean Vacelet[2], Takato Izumi[3], Sau Pinn Woo[1], Shau Hwai Tan[1]

1 *Centre for Marine & Coastal Studies (CEMACS), Universiti Sains Malaysia, 11800 USM, Penang, Malaysia* **2** *Institut Méditerranéen de Biodiversité et d'Ecologie Marine et Continentale, CNRS, Aix Marseille Université, IRD, Avignon Université, Station Marine d'Endoume, Marseille, France* **3** *Department of Biological Sciences, The University of Tokyo, Bunkyo-ku, Tokyo 113-0033, Japan*

Corresponding author: Yuji Ise (yujiise@usm.my)

Academic editor: *Pavel Stoev* | Received 13 June 2019 | Accepted 6 November 2019 | Published 9 December 2021

http://zoobank.org/D361D247-440F-4846-8AFB-7D3EE2CFD1EC

Citation: Ise Y, Vacelet J, Izumi T, Woo SP, Tan SH (2021) First record of the genus *Discorhabdella* (Porifera, Demospongiae, Poecilosclerida, Crambeidae) from Sagami Bay, Japan with description of two new species. ZooKeys 1076: 67–81. https://doi.org/10.3897/zookeys.1076.37278

Abstract

Two new species of *Discorhabdella* are described from Sagami Bay, Japan. *Discorhabdella* has been suggested to have an ancient Tethyan origin according to discovery of their unique pseudoastrose acanthostyles from late Eocene to Oligocene deposits. This is the first record of the genus from the northwest Pacific and first record of the family Crambeidae from Japan. *Discorhabdella hispida* **sp. nov.** is distinctive within the genus by possession of special sigmoid microscleres and C-shaped isochelae with short alae. *Discorhabdella misakiensis* **sp. nov.** is characterized by short choanosomal subtylostyles, and their length overlapped with that of the ectosomal subtylostyles. Only one other species, *Discorhabdella tuberosocapitata* (Topsent, 1890), has the same spicule composition. However, all spicule types are larger in *D. tuberosocapitata* than those of *D. misakiensis* **sp. nov.**, and the shape of the isochelae is different: the alae are more widely opened in *D. tuberosocapitata*. An identification key to species of the genus *Discorhabdella* is also provided. The discovery of two new species from warm temperate northwest Pacific extends the geographical distribution of the genus *Discorhabdella*.

Keywords

biodiversity, Central Kuroshio Current, northwest Pacific, relict species, sponge taxonomy, Tethys Sea

Introduction

Sponges of the genus *Discorhabdella* Dendy, 1924 are characterized by the possession of smooth ectosomal subtylostyles, long choanosomal styles/subtylostyles with swollen lumpy bases, and tuberculate club-shaped pseudoastrose or heavily spined acanthostyles that form an erect hymedesmioid skeleton and various cheloid microscleres (Maldonado et al. 2001, Van Soest 2002). It has been suggested that *Discorhabdella* originated in the Tethys Sea (Boury-Esnault et al. 1992, Maldonado and Uriz 1996, Maldonado et al. 2001), as their unique pseudoastrose acanthostyles were discovered from the late Eocene to Oligocene deposits in New Zealand (Hinde and Holmes 1892, Łukowiak 2015, 2016). Seven extant species are currently known from the genus (Van Soest et al. 2019). Of these, *Discorhabdella incrustans* Dendy, 1924 is reported only from its type locality Three King's Islands, New Zealand. *Discorhabdella littoralis* Maldonado, Carmona, Van Soest & Pomponi, 2001 and *D. urizae* Maldonado, Carmona, Van Soest & Pomponi, 2001 are reported from off the Pacific coast of Panama. *Discorhabdella urizae* is also reported from Gulf of California (Aguilar-Camacho and Carballo 2012). *Discorhabdella hindei* Boury-Esnault, Pansini & Uriz, 1992 is reported from the Alboran Sea, and *D. tuberosocapitata* (Topsent, 1890) is reported from Azores, Canaries and Madeira (Van Soest 2002, Van Soest et al. 2019). Two recently described species have been discovered from north of Madagascar (*D. pseudaster* Vacelet & Cárdenas, 2018) and Gulf of Mexico (*D. ruetzleri* Díaz & Pomponi, 2018). A recent faunal survey of benthic animals in Sagami Bay, Japan yielded several undescribed species of the family Crambeidae (Ise 2017), and the descriptions of two new species of *Discorhabdella* are provided herein.

Materials and methods

The sponges described in the present study were collected by dredging from the R/V Rinkai-maru of Misaki Marine Biological Station, the University of Tokyo. The sampling was carried out at the northeastern part of Sagami Bay during the period of 10–13 January 2012 (Fig. 1). The specimens were kept alive in seawater for several hours and directly preserved in 90% ethanol afterwards. Dry fragments of the sponge were digested using hydrogen peroxide in order to obtain clean spicules. They were then cleaned using distilled water, centrifuged, and resuspended three times. Cleaned spicules were then placed on glass slides, dried, embedded in mounting medium Eukitt® (O. Kindler), cover-slipped, and then observed under a light microscope. Spicules were also placed on copper stub, coated with 400Å platinum, and observed by scanning electron microscope (JEOL JSM-6380LV). Spicules were measured with calibrated ocular micrometer directly under a microscope. Measurements were carried out along randomly chosen transects across the slide, ignoring unfocused, broken, or malformed spicules. Measurements of choanosomal subtylostyles of *Discorhabdella hispida* sp. nov. were only taken from the width of base and shaft as they are usually

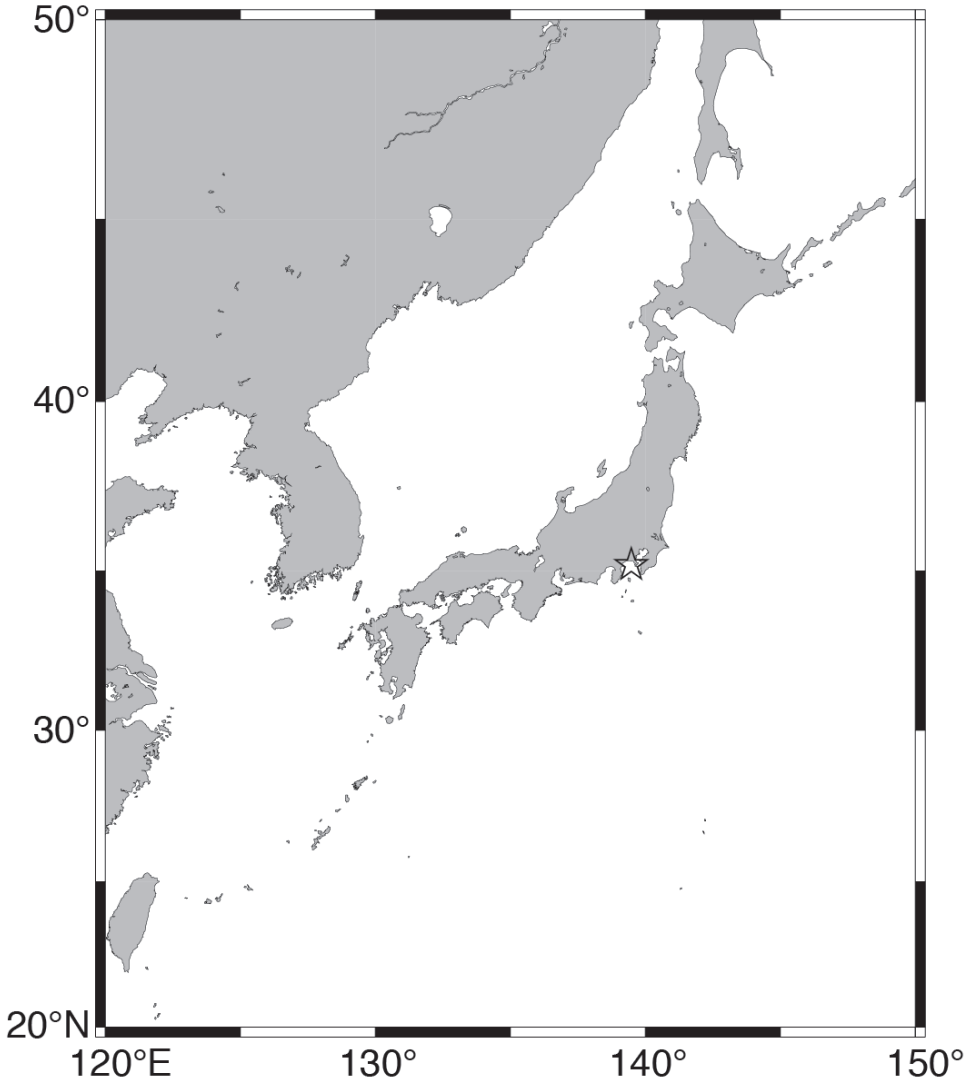

Figure 1. Location of sampling site. Open star indicates Sagami Bay.

broken during spicule preparation steps. About 30 spicules for each type of spicule were measured. Spicule sizes are given as a range, followed by the mean in parenthesis. Spicule and morphological nomenclature follows Boury-Esnault and Rützler (1997), and terminology of cheloid microscleres follows Hajdu et al. (1994). Terminology for geographical distribution of each species basically follows descriptions of the original references; however, the data are corrected in Table 1 according to Marine Ecoregions of the World (Spalding et al. 2007). Specimens were deposited in National Museum of Nature and Science, Tsukuba, Japan (NSMT).

Table 1. Morphological comparison of spicules and geographical distribution of extant *Discorhabdella* species. Locality is described as ecoregions and province following Spalding et al. (2007). Spicule sizes are given as the range, followed by the mean in parenthesis. All spicule measurements in μm.

Species	Locality	Depth (m)	Ectosomal subtylostyle	Choanosomal style/subtylostyle	Pseudoastrose acanthostyle or acanthostyle	Isochelae	Sigma	spined microxea	Other microsclere	Reference
			length × width	length × width	length × base width	length, number of alae	length × width	length × width	length	
D. hindei Boury-Esnault et al., 1992	Alboran Sea, Mediterranean Sea	534–604	276–445 (367) × 5.2	855–1556 (1086) × 34–52 (43)	43–57 (48) × 36–39 (38.5)	22–27 (23), 8 alae	11–16 (12) × 1–1.3 (1.3)	none	none	Boury-Esnault et al. 1992
D. incrustans Dendy, 1924	Three King's North Cape, Northern New Zealand	180	357–592 (496.8) × 10–15 (12.6)	900–1700 × 28–61 (43.1)	36–53 (45.4) × 32–43 (37.2)	33–51 (44), up to 7 alae	none	26–34 (31.4)	none	Van Soest 2002
D. littoralis Maldonado et al., 2001	Nicoya, Tropical East Pacific	10–30	130–180 × 2.5–4	117–300 × 5–10	26–40 × 10–18.5	none	13–15 × 1	none	none	Maldonado et al. 2001
D. pseudaster Vacelet & Cárdenas, 2018	Western and Northern Madagascar, Western Indian Ocean	346–349	240–370, 9–10	more than 600 × 40–56	35–45 × 35–45	12–15, 4–5 alae	none	none	pseudoaster, 12.5–18 in diameter	Vacelet and Cárdenas 2018
D. ruetzleri Díaz & Pomponi, 2018	Floridian, Tropical Northwestern Atlantic	60–80	260–340 (300) × 3–7.55 (4)	470–810 (598) × 5–13 (10.5)	17–40 (29.6) × 7.5–20 (15)	20–25, unknown	12–18	15–18	none	Díaz and Pomponi 2018
D. tuberosocapitata (Topsent, 1890)	Azores Canaries Madeira, Lusitanian	550–736	330	c.a. 650 × c.a. 28	c.a. 130	25, 4–8 alae	none	none	none	Boury-Esnault et al. 1992, Van Soest 2002
D. urizae Maldonado et al., 2001	Nicoya, Tropical East Pacific	55–73	180–220 × 5–7	380–750 × 19–42	23–37 × 15–26	26–29, 5 alae	13–16 × 1	19–26 × 2–3	none	Maldonado et al. 2001
	Cortezian, Warm Temperate Northeast Pacific	344	175–220 (197.5) × 2.5–7.5 (4.75)	220–610 (423.3) × 17.5–35 (25.8)	30–42.5 (36.6) × 23–37	35–42 (36.6), 3 alae	15–20 (17.1)	15–22.5 (21.6)	none	Aguilar-Camacho and Carballo 2012
D. hispida **sp. nov.**	Central Kuroshio Current, Warm Temperate Northwest Pacific	113–223	292.2–392.5 (335.4) × 13.4–16.7 (15.2)	814–1500 × 42.0–56.5 (50.3)	84–127.5 (103.6) × 41.1–57.7 (48.0)	27.3–38 (31.7), 3–7 alae	none	none	sigmoid microsclere 20.7–31.2 (26.3)	this study
D. misakiensis **sp. nov.**	Central Kuroshio Current, Warm Temperate Northwest Pacific	255–318	203–257 (232) × 10.6–14.1 (11.7)	252.0–336.4 (295.2) × 18.6–26.6 (22.6)	73.0–91.3 (82.0) × 27.9–42.0 (34.2)	17.5–21.9 (19.8), 6 alae	none	none	none	this study

Results

Phylum Porifera Grant, 1836
Class Demospongiae Sollas, 1885
Order Poecilosclerida Topsent, 1928
Family Crambeidae Lévi, 1963

Genus *Discorhabdella* Dendy, 1924

Diagnosis. Smooth ectosomal subtylostyles, long choanosomal styles/subtylostyles with swollen lumpy bases and tuberculate club-shaped pseudoastrose or heavily spined acanthostyles forming erect hymedesmioid skeleton; microscleres anchorate unguiferous isochelae and may include spined microxea with two lumpy swellings or sigma-like spicules (slightly modified from Van Soest 2002).

Type species. *Discorhabdella incrustans* Dendy, 1924: 376 (by monotypy).

***Discorhabdella hispida* sp. nov.**
http://zoobank.org/025E3E24-8A78-4AD1-9BD6-44FD92B55A35
Figs 2A–C, 3, 4

Material examined. ***Holotype*.** NSMT-Po-2489. Off Misaki, eastern part of Sagami Bay (Fig. 1), Japan (35°7.484'N, 139°33.212'E to 35°7.504'N, 139°33.625'E), 223–113 m depth, dredge, 13 January 2012.

Description of holotype. ***External morphology*.** Thinly encrusting, surface hispid due to protruding choanosomal large subtylostyles. Color greenish ochre in life, grayish white in ethanol. Size, 22 × 17 mm, about 0.3 mm thick (Fig. 2A–C). Oscules not observed in the living specimen; probably contracted in preserved state. Ostia observed only in preserved specimen, rounded, evenly distributed, 150–300 μm in diameter.

***Skeleton*.** Hymedesmioid skeleton made by large choanosomal subtylostyles making the sponge surface hispid and by perpendicular acanthostyles with their bases attached on substrate. Ectosomal subtylostyles arranged perpendicular to surface with tips outward. Anchorate unguiferous isochelae and sigmoid microscleres roughly dispersed throughout the sponge.

***Spicules*.** Choanosomal subtylotyles (Fig. 3A, B), long slightly curved near the base, maximum diameter at the base gradually tapering to sharp point (Fig. 3A). Base smooth and slightly lumpy (Fig. 3B). Size, 814–1500 μm in length, 42.0–56.5 (50.3) μm in shaft width, 52.4–70.8 (61.7) μm in base width.

Ectosomal subtylostyles (Fig. 3C–F), fusiform, smooth and straight; with smooth and slightly swollen base (Fig. 3D). Maximum diameter at middle region, then gradually tapering to a sharp point (Fig. 3E). Microspined sparsely around the shaft and densely around the tip (Fig. 3F). Size, 292.2–392.5 (335.4) μm in length, 13.4–16.7 (15.2) μm in shaft width, 10.7–14.0 (12.9) in tyle width.

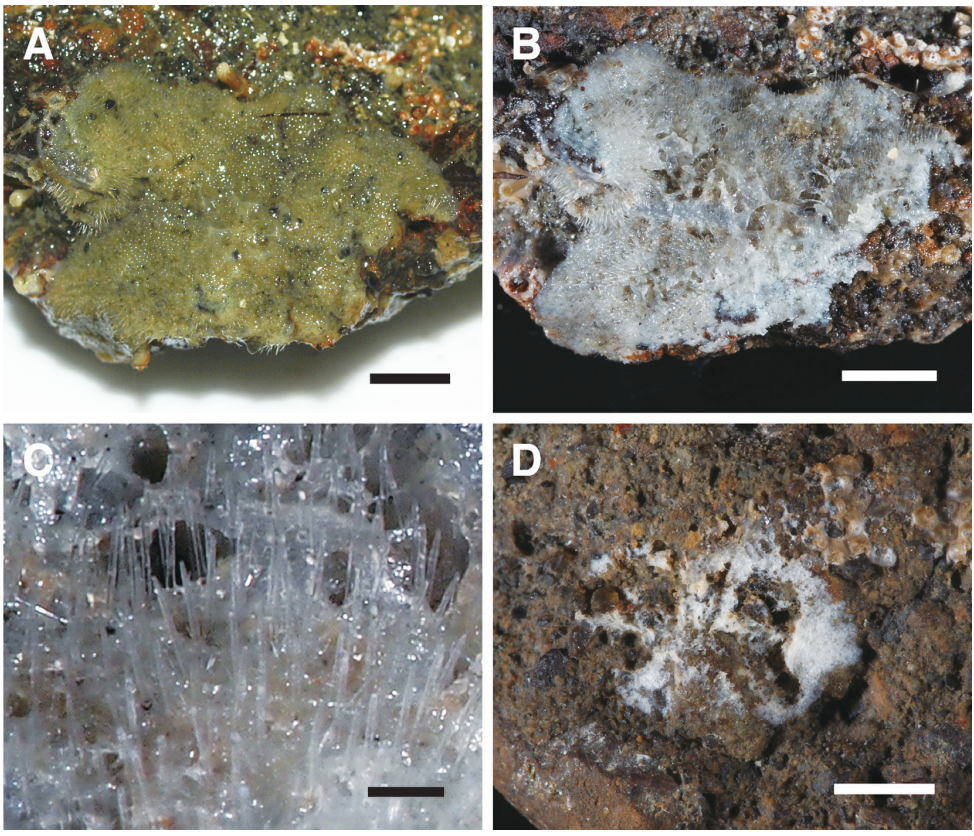

Figure 2. A–C External view of *Discorhabdella hispida* sp. nov., holotype (NSMT-Po-2489). **A** Alive **B** in ethanol preserved **C** magnified view of surface of preserved specimen. Note a number of choanosomal subtylostyles vertically protruding with their tips outward **D** external view of *Discorhabdella misakiensis* sp. nov., holotype (NSMT-Po-2490) in ethanol preserved state. Note most part of the sponge was already used for spicule preparation. Scale bars: 5 mm (**A, B**); 500 μm (**C**); 3 mm (**D**).

Acanthostyles (Fig. 4A), club-shaped head with conical spines having blunt ends. Shaft straight, fusiform, and densely covered with prominent spines with tips sharply pointed, devoid of spines on the last 10–20 μm towards extremity. Terminal holes or orifices of spines especially around head could be detected. Size, 84.0–127.5 (103.6) μm in length, 41.1–57.7 (48.0) μm in head width including spines, 26.3–42.4 (31.1) μm in head width without spines, 24–35.9 (27.8) μm in width of shaft including spine, 16.2–27.5 (21.3) μm in width of shaft without spine.

Anchorate unguiferous isochelae (Fig. 4B, C), strongly curved C-shaped shaft with lateral expansion that forming a pair of fimbriae along its entire length. Both extremities bearing 3–7 short and unequal shaped alae. The alae closest to the lateral fimbriae sometimes reduced or nearly absent, and connected to the fimbriae. Size, 27.3–38.0 (31.7) μm in length, 2.9–4.0 (3.5) μm in shaft width.

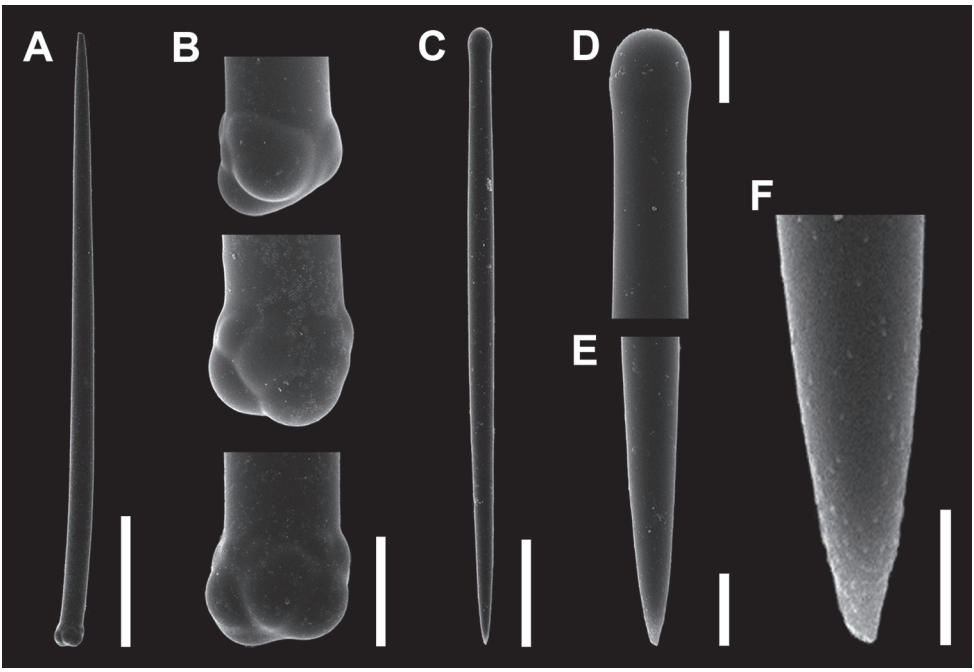

Figure 3. Spicules of *Discorhabdella hispida* sp. nov., holotype (NSMT-Po-2489). **A** Choanosomal subtylostyle **B** magnified view of base of subtylostyle **C–E** ectosomal subtylostyle **D** tyle **E** tip **F** magnified view of tip. Note the surface is microspined. Scale bars: 300 μm (**A**); 50 μm (**B**); 10 μm (**D, E**); 5 μm (**F**).

Sigmoid microscleres (Fig. 4D), strongly curved shaft and irregular in shape. Size, 20.7–31.2 (26.3) μm in length, 0.7–1.0 (0.8) μm in shaft width.

Distribution. Known only from type locality, Misaki, eastern part of Sagami Bay, Japan.

Etymology. Specific epithet refers to its hispid surface appearance.

Remarks. The present species appears well characterized by its spicule complement, especially its microscleres. The isochelae have a unique shape, with a strongly curved shaft compared to all other species of *Discorhabdella*, which have a straight or feebly curved shaft. However, the isochelae of *D. hispida* sp. nov. are similar to the anchorate isochelae of *Monanchora unguiculata* (Dendy, 1922) (see also Lévi 1961, Vacelet et al. 1976). The presence of a sigmoid microsclere that is different from the true sigma, is also distinctive. Sigmas are present in four other *Discorhabdella* species: *D. hindei*; *D. littoralis*; *D. ruetzleri* and *D. urizae*; however, in these species, there are several differences in the other spicule characters (see Table 1).

Discorhabdella hispida sp. nov. differs from *D. hindei* by having acanthostyle (length: 84.0–127.5 μm) instead of pseudoastrose acanthostyles (length: 43–57 μm) in *D. hindei*, a less tuberculated base of the choanosomal styles and a less developed tyle of the ectosomal subtylostyles. It differs from *D. littoralis* by larger choanosomal subtylostyles (814–ca 1500 μm vs 117–300 μm), by having acanthostyles instead of pseudoastrose

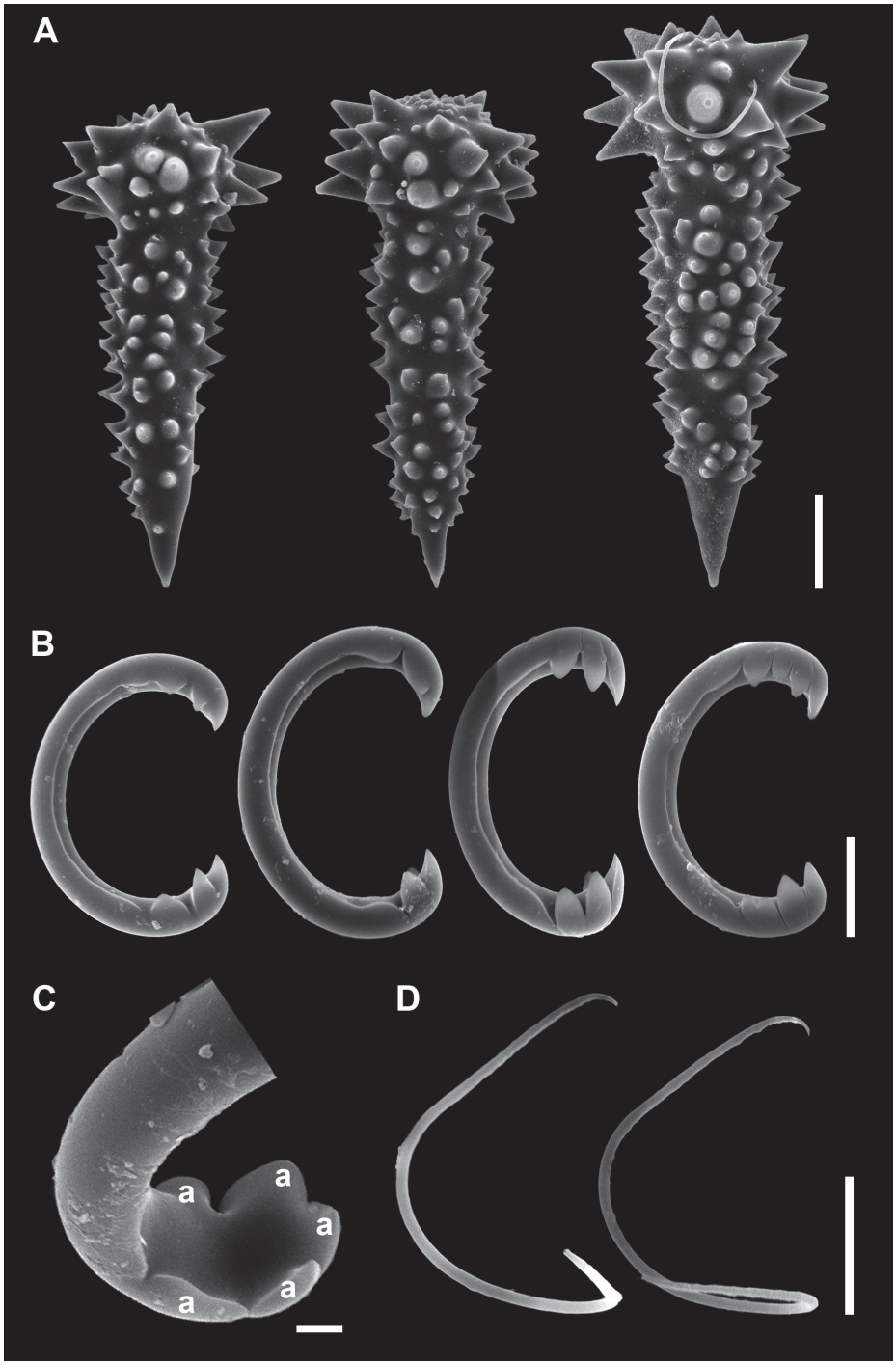

Figure 4. Spicules of *Discorhabdella hispida* sp. nov., holotype (NSMT-Po-2489). **A** Acanthostyles **B** isochelae **C** magnified view of one extremity of isochelae. a, alae **D** sigmoid microscleres. Scale bars: 20 μm (**A**); 10 μm (**B, D**); 2 μm (**C**).

acanthostyles, and a more tuberculated base of choanosomal subtylostyles. It differs from *D. ruetzleri* by larger choanosomal subtylostyles (814–1500 μm vs 470–810 μm), larger acanthostyles (84.0–127.5 μm vs 17–40 μm), larger isochelae (27.3–38.0 μm vs 20–25 μm), absence of spined microxea. It differs from *D. urizae* by larger choanosomal subtylostyles (814–1500 μm vs 220–750 μm in length), absence of spined microxeas and a less tuberculated base of the choanosomal styles. Acanthostyles that are more than 90 μm long have been observed only in *D. tuberosocapitata* and in *D. misakiensis* sp. nov. described in this study. But both species lack sigmoid microscleres and have choanosomal subtylostyles with a well-developed lumpy base. Tubercles around the base of choanosomal subtylostyles are not well developed in *D. hispida* sp. nov. and can be comparable with those recently found in *D. pseudaster* and *D. ruetzleri*. However, *D. hispida* sp. nov. totally lacks peculiar pseudoaster of *D. pseudaster* and also lacks spined microxea of *D. ruetzleri*.

***Discorhabdella misakiensis* sp. nov.**
http://zoobank.org/636E3E9C-BF02-45D5-8CEE-222468D4C945
Figs 2D, 5, 6

Material examined. ***Holotype.*** NSMT-Po-2490. Off Misaki, eastern part of Sagami Bay (Fig. 1), Japan (35°7.734'N, 139°34.133'E to 35°7.714'N, 139°34.061'E), 318–255 m depth, dredge, 10 January 2012.

Description of holotype. ***External morphology.*** Small, very thinly encrusting sponge, about 0.2 mm thick, with velvet surface, white in alcohol. Size, 8 × 5 mm (Fig. 2D). Ostia and oscules not observed either in live or in the preserved specimen.

Skeleton. Hymedesmioid skeleton made by choanosomal subtylostyles and acanthostyles. Choanosomal subtylostyles mostly arranged perpendicular to surface with tips oriented upward. Anchorate unguiferous isochelae distributed in whole body.

Spicules. Choanosomal subtylostyles (Fig. 5A–C), straight, almost uniform in thickness along shaft gradually tapering to a sharp point (Fig. 5C). Lumpy base bearing many prominent smooth projections (Fig. 5B). Size, 252– 336.4 (295.2) μm in length, 18.6– 26.6 (22.6) μm in shaft width, 33.2–45.6 (40.2) μm in base width.

Ectosomal subtylostyles (Fig. 5D–F), fusiform, smooth and straight, with smooth and slightly swollen tyle (Fig. 5E). Maximum diameter at middle region, then gradually tapering to sharp point (Fig. 5F). Size, 203–257 (232) μm in length, 10.6–14.1 (11.7) μm in shaft width, 7.9–9.9 (8.9) μm in tyle width.

Acanthostyles (Fig. 6A, B), straight, surface covered with prominent spines especially at club-shaped head with longer spines. Spines on shaft slightly recurved with tips sharply pointed. Shaft devoid of spines from extremity up to ca. 10–20 μm. Size, 73–91.3 (82.0) μm in length, 27.9–42.0 (34.2) μm in head width including spines, 15.6–21.8 (19.8) μm in head width without spines.

Anchorate unguiferous isochelae (Fig. 6B–D), shaft nearly straight, with a pair of fimbriae along whole shaft; bearing 6 alae (Fig. 6B–D). Size, 17.5–21.9 (19.8) μm in total length, 2.0–2.7 (2.2) μm in shaft width, 6.7–8.0 (7.3) μm in alae length.

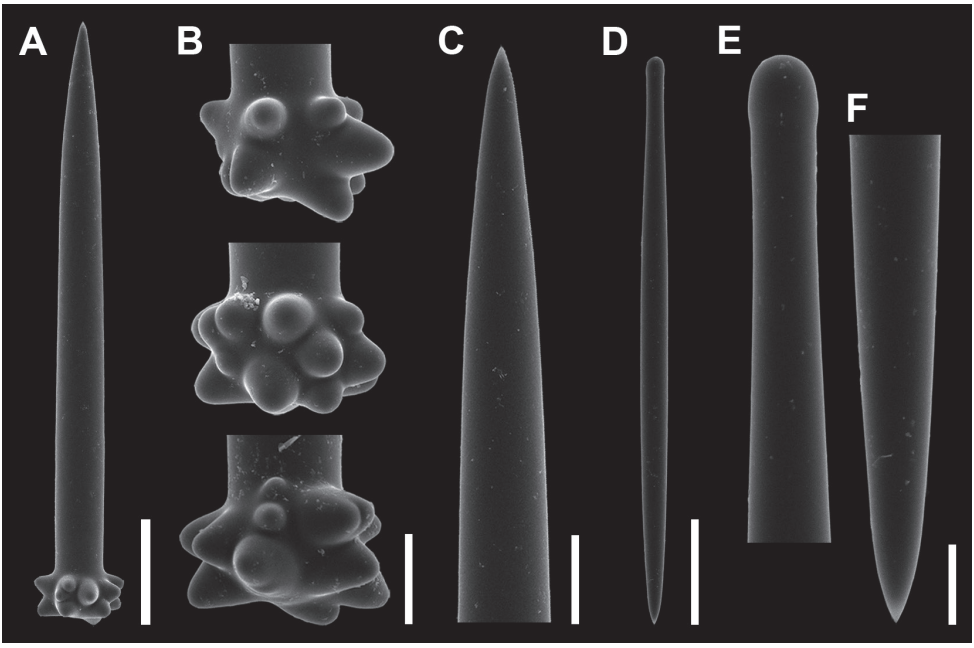

Figure 5. Spicules of *Discorhabdella misakiensis* sp. nov., holotype (NSMT-Po-2490). **A–C** Choanosomal subtylostyle **B** magnified view of base of subtylostyle with prominent lumpy projections **C** tip **D–F** ectosomal subtylostyle **E** tyle **F** tip. Scale bars: 50 μm (**A, D**); 20 μm (**B, C**); 10 μm (**E, F**).

Distribution. Known only from type locality, Misaki, eastern part of Sagami Bay, Japan.

Etymology. Specific epithet refers to type locality: Misaki.

Remarks. *Discorhabdella misakiensi*s sp. nov. has only isochelae as microscleres. This composition of spicules can be found in one other species of the genus, *D. tuberosocapitata* from Azores, Canaries and Madeira (Van Soest 2002, Van Soest et al. 2019). The two species can be clearly differentiated by the size of their spicules: all spicules are smaller in *D. misakiensis* sp. nov. (see Table 1). In addition, they can be differentiated by the shape of their isochelae. Although the isochelae of *D. tuberosocapitata* and *D. misakiensis* sp. nov. have similar number of alae, the alae in *D. tuberosocapitata* are more widely opened. The reported number of isochelae alae in *D. tuberosocapitata* is rather confusing because different authors reported different number of alae despite all of them observing the same type material: four in Boury-Esnault et al. (1992), four to five in Van Soest (2002) and seven to eight in Maldonado and Uriz (1996). This is possibly due to differences in the interpretation of the fused alae. Boury-Esnault et al. (1992) and Van Soest (2002) considered the two alae fused at the base as one, while Maldonado and Uriz (1996) counted them as two. The alae number of *D. misakiensis* sp. nov. is here counted as six; however, the two frontal alae seem to fuse at the base or might be regarded as one ala divided into two (Fig. 6D). Further evidence of separation of these two species is their distant geographical distribution: *D. tuberosocapitata* is reported from Azores, Canaries and Madeira (Van Soest 2002, Van Soest et al. 2019)

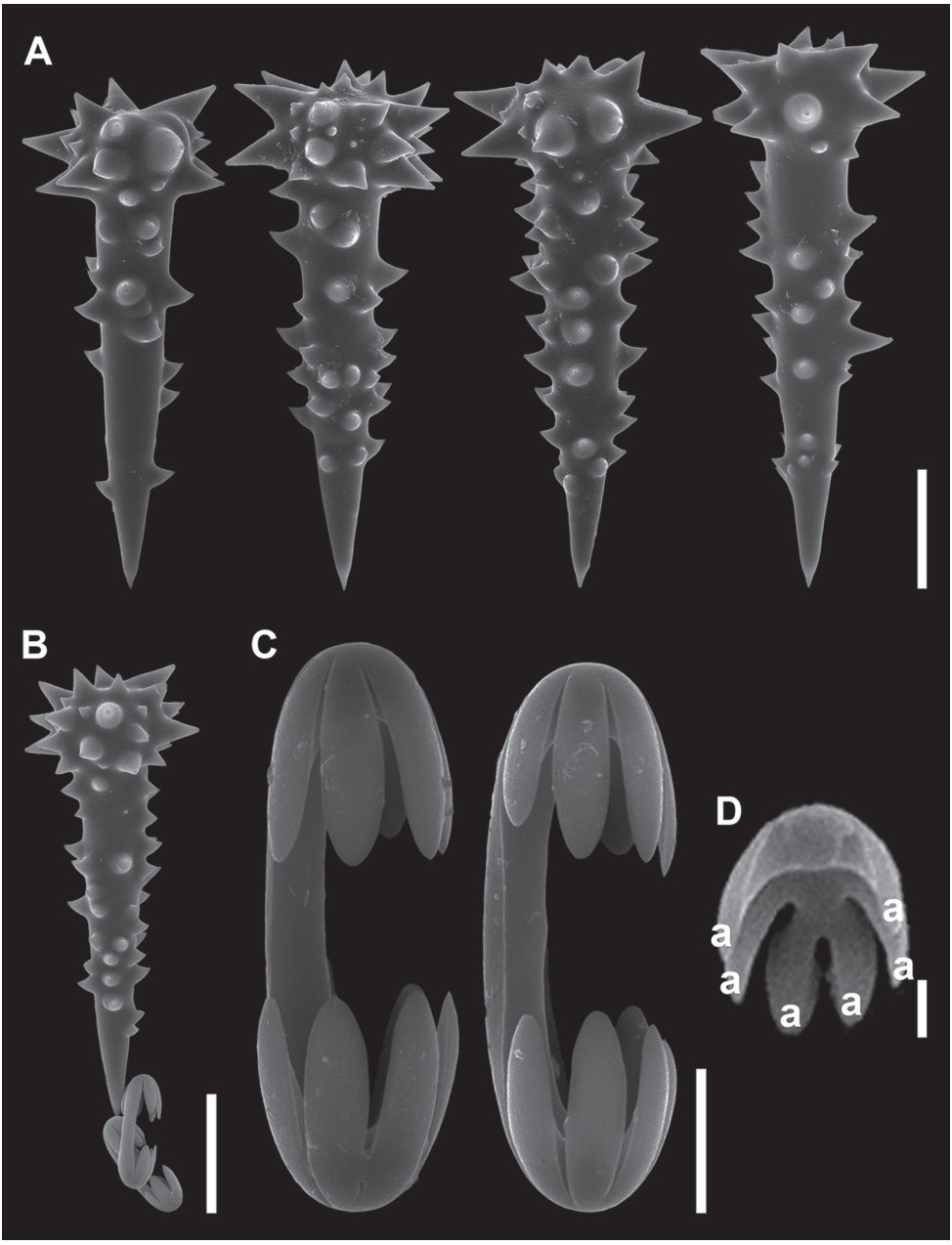

Figure 6. Spicules of *Discorhabdella misakiensis* sp. nov., holotype (NSMT-Po-2490). **A** Acanthostyles **B** comaparative view of acanthostyle and isochelae **C** isochelae **D** back side view of broken isochelae. a, alae. Scale bars: 20 μm (**A, B**); 5 μm (**C**); 2 μm (**D**).

but *D. misakiensis* sp. nov. is found only from the type locality, Sagami Bay, Japan. The dichotomous central ala is also found from "eight-toothed isochelae" of *D. hindei* (Maldonado and Uriz 1996); however, *D. misakiensis* sp. nov. and *D. hindei* are clearly

separated by the possession of sigma in the latter species. Furthermore, *D. hindei* has been reported only from Alboran Sea (Maldonado and Uriz 1996), which is very distant from type locality of *D. misakiensis* sp. nov.

The choanosomal subtylostyles of the new species are relatively small, and their length overlapped with that of the ectosomal subtylostyles. In *Discorhabdella*, this pattern is found only in *D. littoralis* (see Table 1). However, *D. littoralis* and *D. misakiensis* sp. nov. are clearly separated by the size of acanthostyles (26–40 μm vs 73.0–91.3 in length), the presence of isochelae (absent in *D. littoralis*), and of sigmas (absent in *D. misakiensis* sp. nov.). *D. littoralis* has been only reported from off the Pacific coast of Panama (Maldonado et al. 2001), which also exhibits distant geographical distribution from type locality of *D. misakiensis* sp. nov.

Discussion. The present study adds two new species to the genus *Discorhabdella*, which now has nine species. This is the first record of the genus and family Crambeidae from Japanese waters. Thus the discovery of these two new species from warm temperate northwest Pacific extends the geographical distribution of the genus (see Table 1).

Vacelet and Cárdenas (2018) raised doubts to the hypothetical polyaxial nature of the choanosomal styles/subtylostyles and the pseudoastrose acanthostyles that has been proposed by Uriz and Maldonado (1995) and Maldonado and Uriz (1996). The authors proposed instead, a monaxonal origin for the spicule shaft with secondary axes for bulges. In our study, we could not precisely distinguish axes on the choanosomal subtylotyles or the acanthostyles.

Feeble microspines around the distal tips of ectosomal subtylostyles have been first reported from *Crambe tuberosa* Maldonado & Benito, 1991 and later considered as a possible common character of the genera *Discorhabdella* and *Crambe*, both in the family Crambeidae (Maldonado and Uriz 1996). In this study, this character was observed in *D. hispida* sp. nov. (e.g. Fig. 3F) but seems to be absent in *D. misakiensis* sp. nov. (Fig. 5F). This character was not mentioned in the recently described species, *D. pseudaster* and *D. ruetzleri* (Vacelet and Cárdenas 2018, Díaz and Pomponi 2018). The actual affinity between *Discorhabdella* and *Crambe* has not been revealed as yet (Maldonado and Uriz 1996), but the feeble microspines around the distal tips of the ectosomal subtylostyles may be a symplesiomorphy for these two genera.

The evolutionary aspect of morphological divergence among sphaeroclones, pseudoastrose acanthostyles, and typical acanthostyles has long been discussed and the question remains as to whether the amount of change between sphaeroclones and astrose acanthostyles is more important than the whole set of shared morphological features in determining the phylogenetic relationships between *Crambe* and *Discorhabdella* (Uriz and Maldonado 1995, Maldonado and Uriz 1996). Our findings on the two new species add more knowledge on acanthostylose derivatives in *Discorhabdella*. To date, long acanthostyles have been found only in *D. tuberosocapitata* (with ca 130 μm in length), but in all other species of *Discorhabdella* they are less than 60 μm (see Table 1) and thus regarded as pseudoastrose acanthostyle because of the putative polyaxial nature contrasting the monoaxial nature of typical acanthostyles of other

demosponge taxa (Uriz and Maldonado 1995, Maldonado and Uriz 1996). In the two new species, acanthostyles are longer than 70 μm in length, which means the alleged possession of long acanthostyles differing from typical pseudoastrose acanthostyles, is not unusual in *Discorhabdella*. They also provide clues for solving the trait of gradual morphological divergence between sphaeroclones, pseudoastrose acanthostyles, and acanthostyles along with pseudoaster recently found from *D. pseudaster* (Vacelet and Cárdenas 2018). A molecular phylogenetic study is necessary to unravel the diversification of sphaeroclones, pseudoastrose acanthostyles, acanthostyles and pseudoasters as well as the affinity of *Discorhabdella* and *Crambe* within the order Poecilosclerida (Maldonado and Uriz 1996, Vacelet and Cárdenas 2018).

Identification key to species of extant *Discorhabdella*

1	Pseudoasters present	***D. pseudaster***
–	Pseudoasters absent	**2**
2	Chelae present	**3**
–	Chelae absent	***D. littoralis***
3	Microscleres isochelae only	**4**
–	More types of microscleres in addition to isochelae	**5**
4	Size of choanosomal subtylostyles much larger than those of ectosomal subtylostyles	***D. tuberosocapitata***
–	Size of choanosomal subtylostyles overlapping with those of ectosomal subtylostyle	***D. misakiensis* sp. nov.**
5	Standard sigmas present	**6**
–	Standard sigmas absent	7
6	Spinose microxea present	**8**
–	Spinose microxea absent	***D. hindei***
7	Other sigmoid microscleres present	***D. hispida* sp. nov.**
–	Other sigmoid microscleres absent	***D. incrustans***
8	Ectosomal subtylostyles longer than 250 μm	***D. ruetzleri***
–	Ectosomal subtylostyles shorter than 250 μm	***D. urizae***

Acknowledgements

We are grateful to the captain and crews of R/V *Rinkai-maru* for the collection of samples, to Toshihiko Fujita for using scanning electron microscope and registration of specimens to National Museum of Nature and Science, Tsukuba, Japan. The editor and four referees greatly improved the manuscript. This study was supported in part by Grant-in-Aid for Young Scientist (B) (No.15 K18594) from the Ministry of Education, Culture, Sports, Science, and Technology, Japan to YI.

References

Aguilar-Camacho JM, Carballo, JL (2012) New and little-known poecilosclerid sponges from the Mexican Pacific Ocean. Zoological Studies 51: 1139–1153.

Boury-Esnault N, Pansini M, Uriz MJ (1992) A new *Discorhabdella* (Porifera, Demospongiae), a new Tethyan relict of pre-Messinian biota? Journal of Natural History 26: 1–7. https://doi.org/10.1080/00222939200770011

Boury-Esnault N, Rützler K (1997) Thesaurus of Sponge Morphology. Smithsonian Contributions to Zoology 596: 1–55. https://doi.org/10.5479/si.00810282.596

Dendy A (1922) Report on the Sigmatotetraxonida collected by H.M.S.'Sealark' in the Indian Ocean. Reports of the Percy Sladen Trust Expedition to the Indian Ocean in 1905, Vol. 7. Transactions of the Linnean Society of London (2)18: 1–164. https://doi.org/10.1111/j.1096-3642.1922.tb00547.x

Dendy A (1924) Porifera. Part I. Non-Antarctic sponges. Natural History Report. British Antarctic (Terra Nova) Expedition, 1910–1913. Zoology 6: 269–392.

Díaz MC, Pomponi SA (2018) New Poecilosclerida from mesophotic coral reefs and the deep-sea escarpment in the Pulley Ridge region, eastern Gulf of Mexico: *Discorhabdella ruetzleri* n.sp. (Crambeidae) and *Hymedesmia (Hymedesmia) vaceleti* n.sp. (Hymedesmiidae). Zootaxa 4461: 229–237. https://doi.org/10.11646/zootaxa.4466.1.17

Hajdu E, Van Soest RWM, Hooper JNA (1994) Proposal for a phylogenetic subordinal classification of poecilosclerid sponges. In: Van Soest RWM, Van Kempen, TMG, Braekman J-C (Eds) Sponge in Time and Space: Biology, Chemistry, Paleontology. Balkema, Rotterdam, 123–139.

Hinde GJ, Holmes WM (1892) On the sponge remains in the Lower Tertiary Strata near Oamaru, New Zealand. Journal of the Linnean Society of London, Zoology 24: 177–262. https://doi.org/10.1111/j.1096-3642.1892.tb02480.x

Ise Y (2017) Taxonomic review of Japanese sponges (Porifera). In: Motokawa M, Kajihara H (Eds) Species Diversity of Animals in Japan Springer Japan. Springer, Tokyo, 343–382. https://doi.org/10.1007/978-4-431-56432-4_13

Lévi C (1961) Résultats scientifiques des campagnes de la 'Calypso'. XIV. Champagne 1954 dans l'Océan Indien. 2. Les spongiaires de l'Ile Aldabra. Annales de l'Institut Océanographique de Monaco 39: 3–32.

Łukowiak M (2015) Late Eocene siliceous sponge fauna of southern Australia: reconstruction based on loose spicules record. Zootaxa 3917: 1–65. https://doi.org/10.11646/zootaxa.3917.1.1

Łukowiak M (2016) Fossil and modern sponge fauna of southern Australia and adjacent regions compared: interpretation, evolutionary and biogeographic significance of the late Eocene 'soft' sponges. Contributions to Zoology 85: 13–35. https://doi.org/10.1163/18759866-08501002

Maldonado M, Benito J (1991) *Crambe tuberosa* n. sp. (Demospongiae, Poecilosclerida): a new Mediterranean poecilosclerid with lithistid affinities. Cahiers de Biologie Marine 32: 323–332.

Maldonado M, Carmona MC, Van Soest RWM, Pomponi SA (2001) First record of the sponge genera *Crambe* and *Discorhabdella* for the eastern Pacific, with description of three new species. Journal of Natural History 35: 1261–1276. https://doi.org/10.1080/002229301750384293

Maldonado M, Uriz MJ (1996) Skeletal morphology of two controversial poecilosclerid genera (Porifera, Demospongiae): *Discorhabdella* and *Crambe*. Helgoländer Meeresuntersuchungen 50: 369–390. https://doi.org/10.1007/BF02367110

Spalding MD, Fox HE, Allen GR, Davidson N, Ferdaña ZA, Finlayson M, Halpern BS, Jorge MA, Lombana A, Lourie SA, Martin KD, McManus E, Molnar J, Recchia CA, Robertson J. (2007) Marine ecoregions of the world: a bioregionalization of coastal and shelf areas. BioScience 57: 573–583. https://doi.org/10.1641/B570707

Van Soest RWM (2002) Family Crambeidae Lévi, 1963. In: Hooper JNA, Van Soest RWM (Eds) Systema Porifera: a guide to the classification of sponges. Vol. 1. Kluwer Academic/Plenum Publishers, New York, 547–555. https://doi.org/10.1007/978-1-4615-0747-5_58

Van Soest RWM, Boury-Esnault N, Hooper JNA, Rützler K, de Voogd NJ, Alvarez B, Hajdu E, Pisera AB, Manconi R, Schönberg C, Klautau M, Picton B, Kelly M, Vacelet J, Dohrmann M, Díaz MC, Cárdenas P, Carballo JL, Ríos P, Downey R (2019) World Porifera database. http://www.marinespecies.org/porifera [on 2019-04-29]

Topsent E (1890) Notice préliminaire sur les spongiaires recueillis durant les campagnes de l'Hirondelle. Bulletin de la Société zoologique de France 15: 26–32, 65–71. https://doi.org/10.5962/bhl.part.18721

Topsent E (1892) Contribution à l'étude des Spongiaires de l'Atlantique Nord (Golfe de Gascogne, Terre-Neuve, Açores). Résultats des campagnes scientifiques accomplies par le Prince Albert I. Monaco 2: 1–165.

Uriz MJ, Maldonado M (1995) A reconsideration of the relationship between polyaxonid and monaxonid spicules in Demospongiae: new data from the genera *Crambe* and *Discorhabdella*. Biological Journal of the Linnean Society 55: 1–15. https://doi.org/10.1016/0024-4066(95)90025-X

Vacelet J, Vasseur P, Lévi C (1976) Spongiaires de la Pente Externe des Récifs coralliens de Tulear (sud-ouest de Madagascar). Mémoires du Muséum National d'Histoire Naturelle Série A, Zoologie 99: 1–116.

Vacelet J, Cárdenas P (2018) When is an aster not an aster? A new deep-sea *Discorhabdella* (Demospongiae, Poecilosclerida) with asters, from the Mozambique Channel. Zootaxa 4461: 197–204. https://doi.org/10.11646/zootaxa.4466.1.15

ZooKeys 1076: 83–107 (2021)
doi: 10.3897/zookeys.1076.76123
https://zookeys.pensoft.net

RESEARCH ARTICLE

A peer-reviewed open-access journal
ZooKeys
Launched to accelerate biodiversity research

Two new Cypridopsinae Kaufmann, 1900 (Crustacea, Ostracoda) from southern Africa

Agata Szwarc[1], Koen Martens[2,3], Tadeusz Namiotko[1]

1 *Laboratory of Biosystematics and Ecology of Aquatic Invertebrates, Department of Evolutionary Genetics and Biosystematics, Faculty of Biology, University of Gdansk, Wita Stwosza 59, 80–308 Gdansk, Poland* **2** *Royal Belgian Institute of Natural Sciences (RBINS), Natural Environments, Vautierstraat 29, 1000 Brussels, Belgium* **3** *Ghent University, Department of Biology, K.L. Ledeganckstraat 35, 9000 Ghent, Belgium*

Corresponding author: Agata Szwarc (agata.szwarc@ug.edu.pl)

Academic editor: Ivana Karanovic | Received 4 October 2021 | Accepted 22 November 2021 | Published 9 December 2021

http://zoobank.org/0C119DBA-476B-473B-B06A-AFF22B950D89

Citation: Szwarc A, Martens K, Namiotko T (2021) Two new Cypridopsinae Kaufmann, 1900 (Crustacea, Ostracoda) from southern Africa. ZooKeys 1076: 83–107. https://doi.org/10.3897/zookeys.1076.76123

Abstract

Two new Cypridopsinae ostracods, *Potamocypris meissneri* **sp. nov.** and *Sarscypridopsis harundineti* **sp. nov.** are described. Both were found only as asexual (all-female) populations in temporary waters of southern Africa. *Potamocypris meissneri* was collected from a small pan in the North-West Province of South Africa. It is approximately 0.5 mm long and belongs to the species group with long swimming setae on the second antennae. However, the species has a somewhat isolated position in the genus owing to the conspicuously reticulated carapace, which is furthermore densely covered by prominent conuli with normal pores carrying long sensilla, as well as to the wide anterior and posterior flanges on the left valve. To allow identification of the new species in relation to its closest congeners, a key to the species of the genus *Potamocypris* Brady, 1870 from southern Africa is provided. The genus *Sarscypridopsis* McKenzie, 1977 mostly has an Afrotropical distribution with only few species occurring in other regions. *Sarscypridopsis harundineti* was collected from floodplains of the outskirts of the Okavango Delta in Botswana. It is approximately 0.4 mm long and can be distinguished from congeners mainly by the smaller and more oval-shaped valves. We conclude that southern African Cypridopsinae urgently need integrated taxonomic revision, by means of both morphological characters and DNA-sequence data.

Keywords

Afrotropical, Cyprididae, microcrustaceans, morphology, taxonomy, temporary waters

Introduction

Ostracods, small bivalved crustaceans, have an impressive taxonomic diversity and functional specialisation of their appendages, which are used for locomotion, feeding, and reproduction (Meisch 2000; Smith et al. 2015). They commonly occur in both marine and non-marine habitats, from the oceans and estuaries, over deep lakes to small temporary pools, phytotelmata or troughs, as well as subterranean waters and even semi-terrestrial environments (Mesquita-Joanes et al. 2012; Smith et al. 2015). Ostracoda differ from (most) other crustaceans by a combination of two main features: firstly, by their body oligomerisation with no true body segmentation and secondly, by the strong development of the carapace consisting of two calcified valves hinged along the dorsal margin, and with central adductor muscles attached to the inner part of the valves, crossing the body from one valve to the other and creating characteristic internal muscle scar patterns on them.

Ostracoda are the extant arthropod group with the most abundant fossil record. Although much less diversified than marine lineages, freshwater ecosystems are home to ~ 2300 Recent (living) species and 270 genera (Meisch et al. 2019). Sixteen families have representatives in non-marine habitats, the most diverse family being the Cyprididae Baird, 1845. It includes 24 subfamilies of which the subfamily Cypridopsinae Kaufmann, 1900 is the richest (Meisch et al. 2019) with 22 genera (Savatenalinton 2018; Meisch et al. 2019; Savatenalinton 2020; Almeida et al. 2021). Cypridopsinae are mostly small animals (< 1.0 mm), characterised by a strong reduction of the caudal ramus, which is usually flagellum-like (or even missing) in females, and integrated in the hemipenes in males (Martens and Meisch 1985).

Potamocypris Brady, 1870, is after *Cypridopsis* Brady, 1867, the second most abundant genus within the subfamily (Meisch et al. 2019). The 46 species it includes are characterised by 1) asymmetrical valves, with the right valve overlapping the left one dorsally and ventrally, 2) a distinguishing spatula-like shape of the distal palp segment of the maxillula, and 3) a distally tapering caudal ramus. The genus has nearly cosmopolitan distribution, but only 10 species have so far been recorded from the Afrotropical region, and only five from southern Africa (Martens 2001; Meisch et al. 2019).

Sarscypridopsis McKenzie, 1977 is mostly distributed in South Africa, with 13 out of the 17 known species described from this country (Sars 1924a, 1924b). Similar to *Potamocypris*, in *Sarscypridopsis* the right valve overlaps the left valve anteriorly, ventrally and posteriorly, but the terminal segment of the maxillular palp is cylindrical and the base of the caudal ramus is triangular (McKenzie 1977).

Here, we describe one species each belonging to *Potamocypris* and to *Sarscypridopsis*. The present paper also constitutes a contribution to the knowledge of the poorly known freshwater ostracod fauna of southern Africa and presents the first comprehensive description of a species of the genus *Sarscypridopsis* with full illustration of valves and appendages.

Materials and methods

Samples were collected from temporary waters in South Africa and Botswana (Fig. 1) using a hand-net (mesh size of 120 μm) to sweep the bottom surface and among vegetation at the depth of < 50 cm. Sediment samples were rinsed in the field, placed in plastic jars and preserved in 96% ethanol. Physical and chemical properties of the pond water (temperature, pH and electrical conductivity) were measured in situ using a hand-held multi-parameter probe WTW Multi 350i. In the laboratory, samples were thoroughly rewashed with tap water through a 120 μm-mesh sieve, placed in plastic jars and preserved in fresh 96% ethanol. Specimens were sorted, counted, dissected, and mounted using a binocular and light transmission microscope according to Namiotko et al. (2011). Soft parts of dissected ostracods were mounted in glycerin or Hydro-Matrix mounting medium, whereas valves were stored dry on micropalaeontological slides. Species identification was performed using the keys published in McKenzie (1977), Meisch (2000), and Martens (2001), and taxonomical descriptions in Meisch et al. (2019). Drawings of soft parts were made with a camera lucida on a transmission light microscope Nikon Eclipse 50i (Univ. Gdansk, Poland). Carapaces and valves were gold-coated and observed under the scanning electron microscope, Fei Qanta 200 ESEM, at the Royal Belgian Institute of Natural Sciences, Brussels, Belgium as well as under a transmission light microscope Nikon Eclipse 50i (Univ. Gdansk, Poland).

The type specimens are deposited in the Collection of the Royal Belgian Institute of Natural Sciences, Brussels (**RBINS**, general I.D. 3439) and in the Ostracod Collection of the Laboratory of Biosystematics and Ecology of Aquatic Invertebrates, Department of Evolutionary Genetics and Biosystematics, University of Gdansk (**OC-UG**).

Chaetotaxy of the limbs follows the model proposed by Broodbakker and Danielopol (1982), revised for the second antenna by Martens (1987). Names for the limbs were used according to Meisch (2000) except for caudal ramus, which follows Meisch (2007).

Abbreviations used in text and figures

Limbs:

A	anterior
a, a'	two setae on Pr of T1
A1	first antenna (antennule)
A2	second antenna
alfa (α)	special seta on the 1st podomere of Md palp
beta (β)	special seta on the 2nd podomere of Md palp

CR	caudal ramus
D	distal
d1, **d2**, **dp**	setae on Pr of T2 or T3
E	endopod
e	setae on EI of T2 and T3
EI-EIV	1st to 4th podomeres of E
Ex	exterior
Exo	exopod
f	setae on EII of T2 and T3
g	setae on EIII of T2 and T3
gamma (γ)	special seta on 3rd podomere of Md palp
GM (**Gm**)	major (minor) claw on EIV of A2
G1–3	anterior and internal claws (or setae) on EIII of A2
h1–3	setae (or claws) on EIV of T2 and T3
In	interior
l	large (relative length of setae or claws)
m	medium (relative length of setae or claws)
Mastic	masticatory process on Pr of T1
Md	mandibula
Mx1	maxillula
P	posterior
pl	plumed
Pr	protopod
s	small (relative length of setae or claws)
S1–2	plumed setae on 1st podomere of Md palp
ser	serrated
T1	first thoracopod (maxilliped)
T2	second thoracopod (walking leg)
T3	third thoracopod (cleaning leg)
t1–4	internal setae on EII of A2
Y	aesthetasc on EI of A2
y1–3	aesthetascs on EII, EIII and EIV of A2 respectively
ya	aesthetasc on the terminal podomere of A1
z1–3	external setae (or claws) on EIII of A2

Valves and carapace:

Cp	carapace
H	valve height
L	valve length
LV	left valve
RV	right valve

Figure 1. Localities of *Potamocypris meissneri* sp. nov. (purple star SA-9) in the North-West Province of South Africa and *Sarscypridopsis harundineti* sp. nov. (red dots SA-96 to SA-103) in the outskirts south of the Okavango Delta in Botswana. The type locality of *Sarscypridopsis harundineti* sp. nov. (SA-103) is marked with a dark red dot.

Taxonomy

Class Ostracoda Latreille, 1802
Subclass Podocopa Sars, 1866
Order Podocopida Sars, 1866
Suborder Cypidocopina Baird, 1845
Superfamily Cypridoidea Baird, 1845
Family Cyprididae Baird, 1845
Subfamily Cypridopsinae Kaufmann, 1900
Genus *Potamocypris* Brady, 1870

***Potamocypris meissneri* sp. nov.**
http://zoobank.org/03D4496-F0A1-4C66-B481-BFDE1F939B4D
Figures 2–4

Material examined. Type locality: South Africa, North-West Province, small temporary open pan (SA-9) near the village of Ganalaagte (Fig. 1, Suppl. material 1: Fig. 1A); 26°26'45"S, 25°32'19"E, elevation 1380 m a.s.l.; 1 Apr. 2011; T. Namiotko leg.

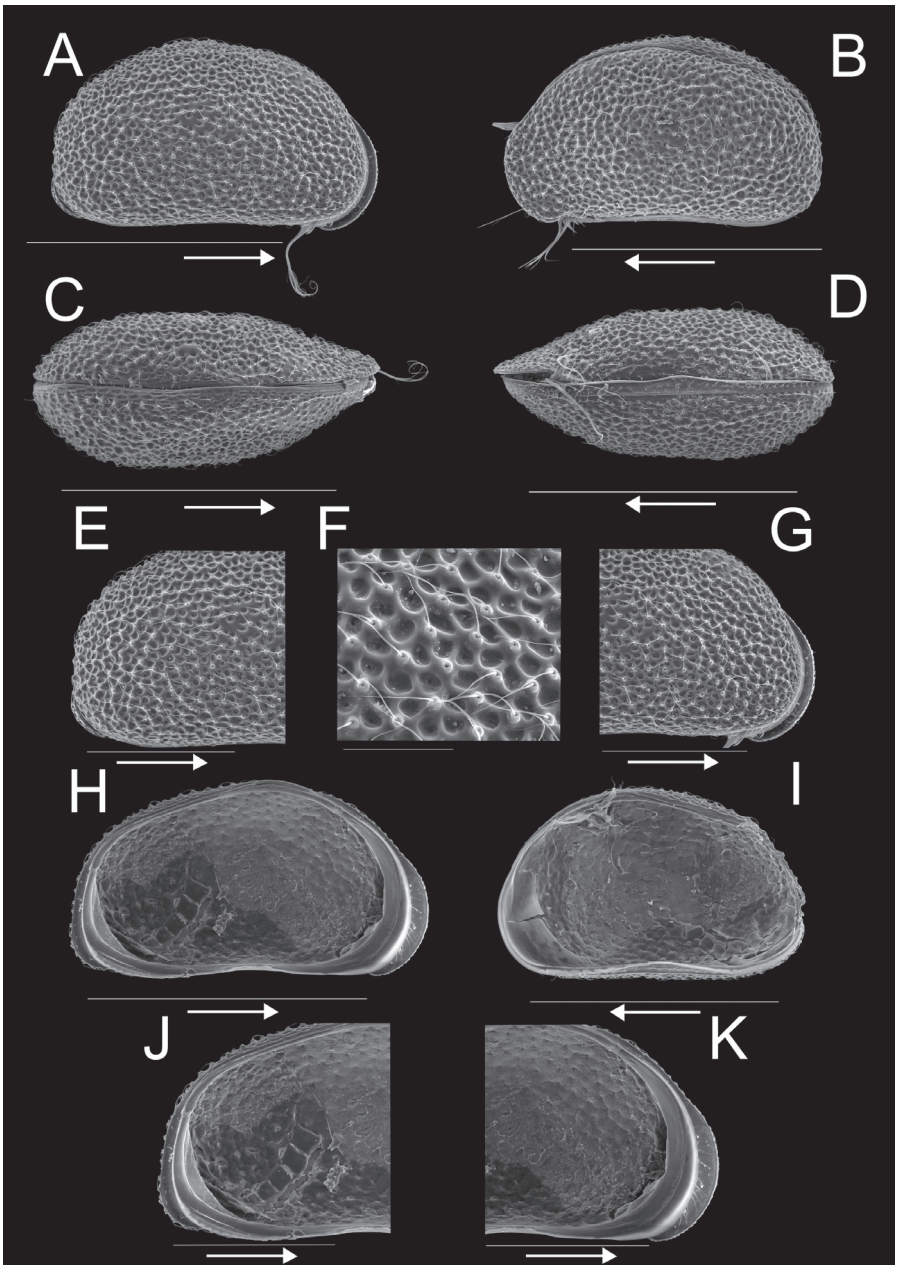

Figure 2. Carapace and valves of *Potamocypris meissneri* sp. nov. ♀ **A** RBINS INV.159060 **B** RBINS INV.159062 **C** RBINS INV.159061 **D** RBINS INV.159063 **E–G** RBINS INV.159060 **H–K** RBINS INV.159059. **A** carapace right view **B** carapace left view **C** carapace dorsal view **D** carapace ventral view **E** carapace right view of posterior end, detail of A **F** detail of external surface of A **G** carapace right view of anterior end, detail of A **H** left valve internal view **I** right valve internal view **J** left valve internal view of posterior part, detail of H **K** left valve internal view of anterior part, detail of H. Scale bars: 400 μm (**A–D, H, I**); 200 μm (**E, G, J, K**); 50 μm (**F**); arrows indicate anterior end.

***Holotype*:** • 1 ♀ (adult); dissected female stored on a permanent microscopic slide and valves stored dry on a micropalaeontological slide (RBINS INV.159058). ***Paratypes*:** South Africa • 2 ♀♀ (adults); same collection data as for holotype (OC-UG 110401-9A2L and OC-UG 110401-9A3L) • 136 ♀♀ (adults), 78 juv.; same collection data as for holotype: 115 ♀♀ and 78 juv. preserved in 96% ethanol; 16 ♀♀ stored as the holotype; 5 ♀♀ stored with carapaces stored on micropalaeontological slides (RBINS INV.159059–INV.159063); repositories: RBINS and OC-UG. **Accompanying ostracod fauna:** *Hemicypris* cf. *inversa* (Daday, 1913); *Limnocythere* cf. *stationis* Vávra, 1891.

Etymology. This species is named after Dr Włodzimierz Meissner, Professor of ornithology at the University of Gdansk, Poland, a long-standing friend of TN who provided unrelenting support in the collection of ostracods from all over the world and who has encouraged and helped TN to join various scientific expeditions for collecting ostracods.

Diagnosis. Carapace in lateral view somewhat ovoid, broadly rounded dorsally, with both extremities more or less equally rounded, ventral margin weakly concave, and maximum height situated at mid-length. Valves distinctly asymmetrical, with LV overlapping RV anteriorly and posteriorly, RV overlapping LV dorsally and ventrally. Anterior and posterior margins on LV with marginal flange, anterior one larger than posterior one. Carapace external surface hirsute, strongly ornamented with ridges, set with thickly rimmed pores with long sensilla. Antenna with long swimming setae. Terminal segment of maxillula palp spatulate with five claws. T1 with two hirsute branchial rays. CR of whip-like shape with elongated base, fused with distal long flagellum-like seta and set with additional short subapical seta.

Description. Female. Cp in lateral view (Fig. 2A, B) with posterior extremity more broadly rounded than anterior one, dorsal margin broadly rounded, ventral margin weakly concave, almost straight. Maximum height situated at mid-length. Valves distinctly asymmetrical, with LV overlapping RV along anterior and posterior margins with flanges (Fig. 2E, G). Carapace of hirsute appearance with reticulate external surface bearing numerous thickly rimmed normal pores with long sensilla (Fig. 2F). Cp in dorsal (Fig. 2C) and ventral view (Fig. 2D) with posterior extremity slightly rounded, anterior extremity more pointed. Greatest width situated slightly behind mid-length. RV slightly overlapping LV dorsally and ventrally. LV in internal view (Fig. 2H) subtriangular, with greatest height situated in front of mid-length, posterior part of dorsal margin straight and sloping towards the posterior side; anterior margin rounded, posterior margin almost straight, ventral margin slightly sinuous at mid-length. Anterior and posterior margins with marginal flanges, extending beyond inwardly displayed selvage along anterior and posterior margins, but peripheral along ventral margin (Fig. 2H, J–K). Flanges particularly expanded in the lower two-thirds of the anterior and posterior margins, with LV overlapping RV (Fig. 2A). Anterior and posterior calcified inner lamella narrow with one inner list, the latter not reaching halfway posterior margin. RV in internal view (Fig. 2I) ovoid, with maximum height situated in front of mid-length, anterior margin rounded, posterior

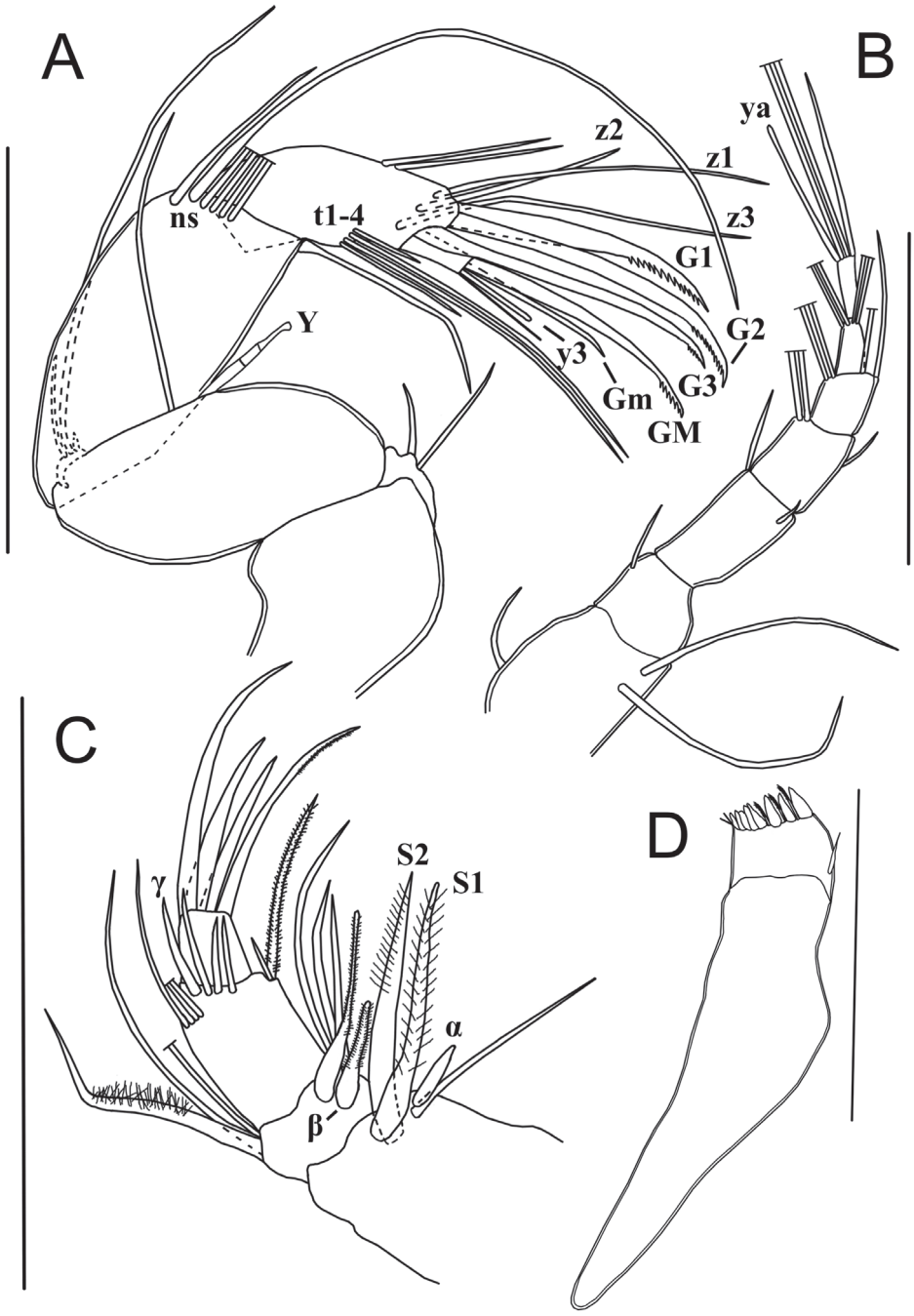

Figure 3. Limbs of *Potamocypris meissneri* sp. nov. ♀. Holotype (OC-UG 110401-9A1L) **A** second antenna **B** first antenna **C** mandibular palp **D** mandibular coxa. Scale bars: 100 μm. Abbreviation: ns = natatory setae.

margin less so. Anterior calcified inner lamella wide without inner list, but with submarginal peripheral selvage.

A1 (Fig. 3B) 7-segmented. First segment with one short subapical dorsal seta (not reaching tip of segment) and two long ventral setae. Second segment subquadrate with one short antero-dorsal seta. Rome organ not seen. Third segment ~ 2× as long as wide, with two setae, one short antero-dorsal (reaching tip of next segment) and one very short antero-ventral seta. Fourth segment with two long antero-dorsal setae and one short antero-ventral seta (reaching 1/3 of next segment). Fifth segment bearing two long antero-dorsal setae and two ventral setae, one long and one of medium length (reaching beyond tip of terminal segment). Penultimate segment with four long apical setae. Terminal segment distally with three (two long and one medium-length) setae and an aesthetasc ya, length of aesthetasc ya ~ 5/6 of that of medium seta.

Chaetotaxic formula: I: A-1s, P-2l / II: A-1s / III: A-1s, P-1s / IV: A-2l, P-1s / V: A-2l, P-1l-1m / VI: A-4l / VII: D: 2l-1m-ya.

A2 (Fig. 3A) with protopodite, exopodite and 3-segmented endopodite. Basal segment of protopodite with two short ventro-apical setae. Second segment of protopodite with one long apical seta, reaching beyond first endopodal segment. Exopodite reduced to a small plate with three setae, two short and one long, the latter reaching halfway second endopodal segment. Endopodite 3-segmented. First endopodal segment with one long ventro-apical seta, extending beyond tip of terminal segment and one aesthetasc Y of medium length, divided in three parts, distal sensorial part with conspicuously sunken appearance; antero-dorsal with five long natatory setae (reaching tips of terminal claws) and one shorter (6^{th}) seta reaching half of next segment. Second endopodal segment undivided, with two subequal medio-dorsal setae and four medio-ventral setae (t1-t4), two long, one medium and one short; distally with three z-setae, z1 and z3 long, z2 ~ 1/2 the length of z1 and z3, and three long serrated G-claws: G1 thick and apically strongly serrated, G2 and G3 more slender. Terminal endopodal segment subquadrate, with a long serrated claw GM, a shorter (~ 2/3 length of GM) smooth claw Gm and an aesthetasc y3 fused with slightly longer accompanying seta. Aesthetascs y1, y2 and seta g not seen, the latter almost certainly absent as typical of the subfamily.

Chaetotaxic formula: Pr: 1l / Exo: 1l-2s / EI: A-5l-1m, P: Y-1l / EII+III: A-2m, P-1m(t1)-2l(t2,3)-1s(t4), D-2l(z1,z3)-1m(z2)-3l(G1,2,3: ser) / EIV: 1l(GM: ser)-1m(Gm)-y3–1m

Md with sclerotised coxa (Fig. 3D) and 4-segmented palp (Fig. 3C). First palp-segment ventro-apically with two long plumed setae (S1 and S2), one long slender and smooth seta and a short but stout, smooth α-seta. Second segment antero-dorsally with two long slender and smooth setae and one thick plumed seta; ventrally with three unequally long smooth setae, one long hirsute seta and a stout and hirsute β-seta. Third segment antero-ventrally with one long hirsute seta and one short smooth seta; medio-dorsally with four setae, two reaching tip of terminal segment, and two longer setae, one of these smooth γ-seta; antero-dorsally with four setae reaching beyond tips of terminal segment. Terminal segment with four claws, two ~ 3× as long as length

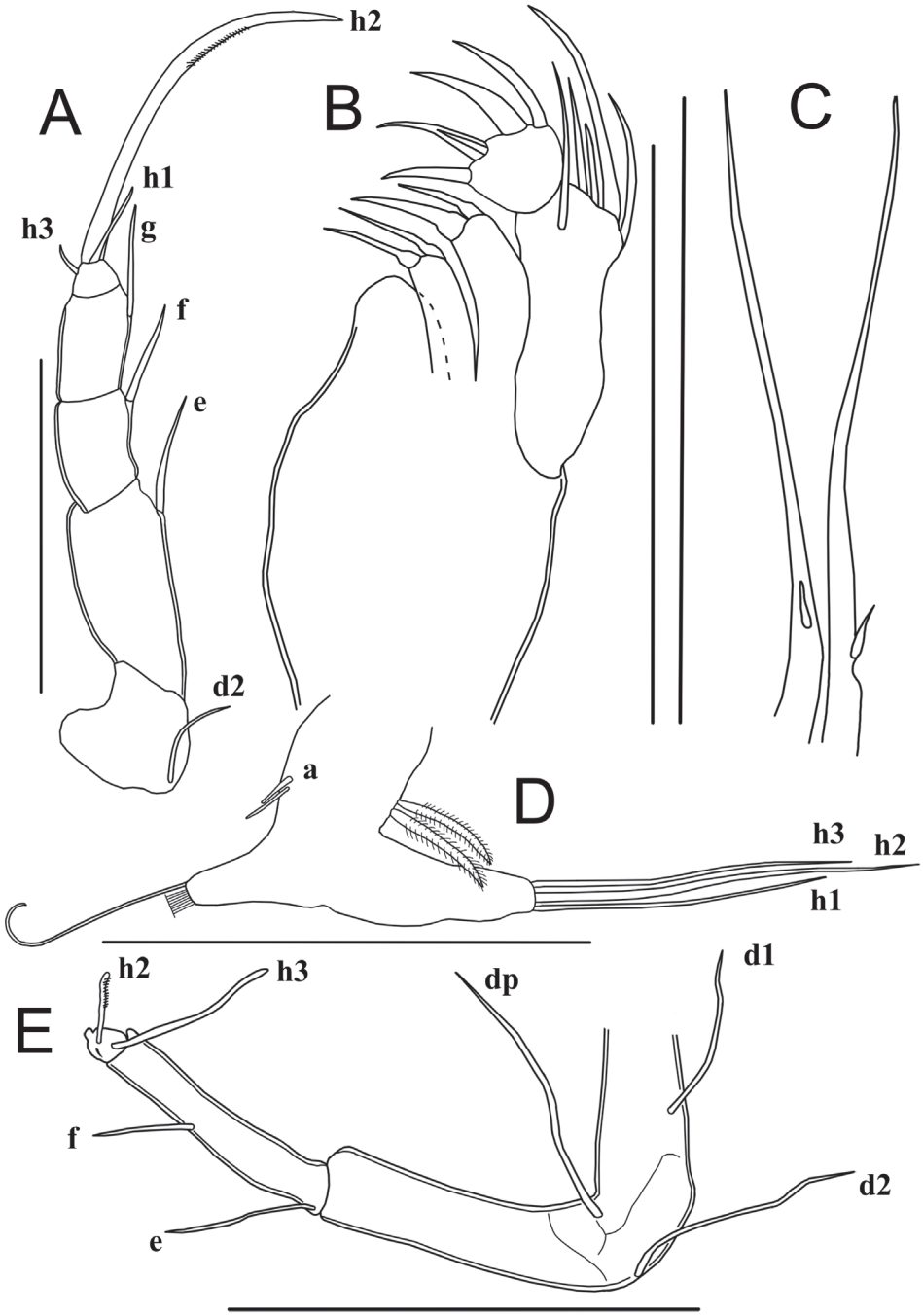

Figure 4. Limbs of *Potamocypris meissneri* sp. nov. ♀ **A, B, C** holotype (OC-UG 110401-9A1L) **D** paratype (OC-UG 110401-9A3L) **E** paratype (OC-UG 110401-9A2L) **A** second thoracopod (walking leg) **B** maxillula **C** caudal ramus **D** first thoracopod (maxilliped) **E** third thoracopod (cleaning leg). Scale bars: 100 μm.

of terminal segment, one of these serrated, and two shorter claws. Md coxa typically elongated, distally with rows of teeth and small setae, and with one short smooth seta situated near the insertion place of the palp.

Chaetotaxic formula: Palp: I: In-1s(alfa)-1l-2l(S1,S2: pl) / II: In-1s(beta: pl)-1l(pl)-2m-1l, Ex:1l(pl)-2l / III: In-1l(pl)-1s, D-3m-1m(gamma), Ex-4m / IV: 2m-1l-1l(ser)

Mx1 (Fig. 4B) with three endites (with chaetotaxy incompletely illustrated), a 2-segmented palp and a large respiratory plate (not illustrated). Third endite with two smooth teeth bristles (Zahnborsten). First palp-segment dorso-apically with four unequal setae; medio-dorsally with one long, subapical seta, reaching beyond tip of terminal segment. Second palp-segment spatulate, apically with four stout claws (~ 1.5× as long as terminal segment) and one shorter claw (~ 1/2 length of others).

Chaetotaxic formula: Palp: I: Ex-3s-1l, In-1m / II: D-5s

T1 (Fig. 4D). Protopodite with two short a-setae; b-, c-, and d-setae absent, endite distally with a dozen apical setae (exact number not determined). Endopod elongated, apically with one long seta (h2) and two shorter setae (h1 and h3) of differing lengths. Respiratory plate with two hirsute rays.

Chaetotaxic formula: Pr: A-2s(a and a') / Mastic: D-? / Exo: 2m(pl) / E: D-3l

T2 (Fig. 4A) a walking limb. Protopodite with seta d2 of medium length, seta d1 absent. First three endopodal segments each with one ventro-apical seta. Setae e and f reaching tip of the next segment, seta g ~ 3× as long as terminal segment. Fourth segment with one short seta (h3), one medium seta of length (h1) and a long claw, distally serrated (h2), the latter ~ 3× as long as the second endopodal segment.

Chaetotaxic formula: Pr: A-1s(d2) / EI: A-1m / EII: A-1m / EIII: A-1m / EIV: P-1s(h3), D-1m(h1)-1l(h2 G:ser)

T3 (Fig. 4E) a cleaning limb. First segment with two long apical setae (dp and d2) and one shorter medio-ventral seta (d1). Second segment fused with third segment, with e-seta of medium length, and with f-seta reaching tip of segment. Distal part of limb consisting of a pincer-organ (fusion between tip of third segment and fourth segment), bearing a seta (h3) of medium length and a short, serrated seta (h2); h3 ~ 2/3 of the length of penultimate segment, h2 ~ 1/3 of length of h3.

Chaetotaxic formula: Pr: A-1l(d2)-1m(d1), P-1l(dp) / EI: A-1m(e) / EII + III: A-1s(f) / EIV: 1s(h2: ser)-1m(h3)

CR (Fig. 4C). Reduced to a whip-like structure, with elongated base fused with long flagellum-like seta and bearing a short subapical seta.

Remark. It should be noted that juveniles of this species do not have tubercles on the valves (see discussion).

Measurements (in μm). Cp (n = 4): L = 512–526, H = 305–306; LV (n = 11): L = 510–530, H = 278–298; RV (n = 11): L = 498–517, H = 301–319.

Male unknown.

Ecology. *Potamocypis meissneri* was collected only from the type locality in the North-West Province of South Africa. This is an open temporary pan with the following physical and chemical water properties: pH = 7.0, electrical conductivity = 36 μS/cm and water temperature 25.8°C.

Key to southern African *Potamocypris* species (partly based on Martens 2001):

1	Natatory setae of A2 short (not reaching tips of terminal claws ..... ***P. paludum* Gauthier, 1939**
–	Natatory setae of A2 long **2**
2	Cp elongated (L ≥ 2× H), crescent-shaped ..... ***P. mastigophora* (Methuen, 1910)**
–	Cp compressed (L < 2× H), differently shaped, not crescent-shaped **3**
3	Cp subtriangular, dorsally arched with blunt angle .... ***P. gibbula* (Sars, 1924)**
–	Cp with dorsal margin broadly rounded or straight on a long distance and sloping down to the posterior **4**
4	Cp with posterior margin rounded; maximum height at mid-length ..... ***P. meissneri* sp. nov.**
–	Cp with posterior margin straight; maximum height in front of mid-length.... **5**
5	RV with wide dorsal overlap of LV..... ***P. deflexa* (Sars, 1924)**
–	Dorsal overlap of RV minute or lacking..... ***P. humilis* (Sars, 1924)**

Genus *Sarscypridopsis* McKenzie, 1977

***Sarscypridopsis harundineti* sp. nov.**
http://zoobank.org/45D19D9C-FD3E-4D1E-8C2C-65F14004373F
Figures 5–7

Material examined. Type locality: Botswana, North-West District, floodplains south of Okavango Delta (SA-103); grassy shore of seasonal pond near the city of Maun (Fig. 1, Suppl. material 1: Fig. 1B), 19°52'12"S, 23°20'23"E, elevation ca. 940 m a.s.l.; 15 Sept. 2012; T. Namiotko leg.

***Holotype*:** • 1 ♀ (adult); dissected female stored on a permanent microscopic slide and valves stored dry on a micropalaeontological slide (RBINS INV.159064). ***Paratypes*:** BOTSWANA • 27 ♀♀ (adults); same data as for holotype; 2 ♀♀ stored as the holotype (OC-UG 120915-3A2L, 120915-3A3L); 22 ♀♀ preserved in 96% ethanol (120915-30); 3 ♀♀ stored on micropalaeontological slides (RBINS INV.159065–INV.159067); repositories: RBINS and OC-UG. **Accompanying ostracod fauna:** *Heterocypris oblonga* (Sars, 1924); *Limnocythere* cf. *stationis*; *Plesiocypridopsis newtoni* (Brady and Robertson 1870).

Additional material. Botswana – North-West District: • **SA-96** (Fig. 1, Suppl. material 1: Fig. 1C): 1 juv.; endorheic Lake Ngami; 20°28'57"S, 22°42'08"E; elevation ca. 930 m a.s.l.; 12 Sept. 2012; accompanying ostracod fauna: *Hemicypris inversa*; *Heterocypris giesbrechti* (G.W. Müller, 1898) • **SA-97** (Fig. 1, Suppl. material 1: Fig. 1D): 11 ♀♀ and 1 juv.; Thamalakane river near the city of Maun; 19°55'52"S, 23°30'38"E; elevation ca. 940 m a.s.l.; 13 Sept. 2012; accompanying ostracod fauna: *Candonopsis navicula* Daday, 1910; *Chrissia perarmata* (Brady, 1904); *Heterocypris oblonga*; *Isocypris* cf. *priomena* G.W. Müller, 1908; *Limnocythere* cf. *stationis*; *Physocypria* cf. *capensis*

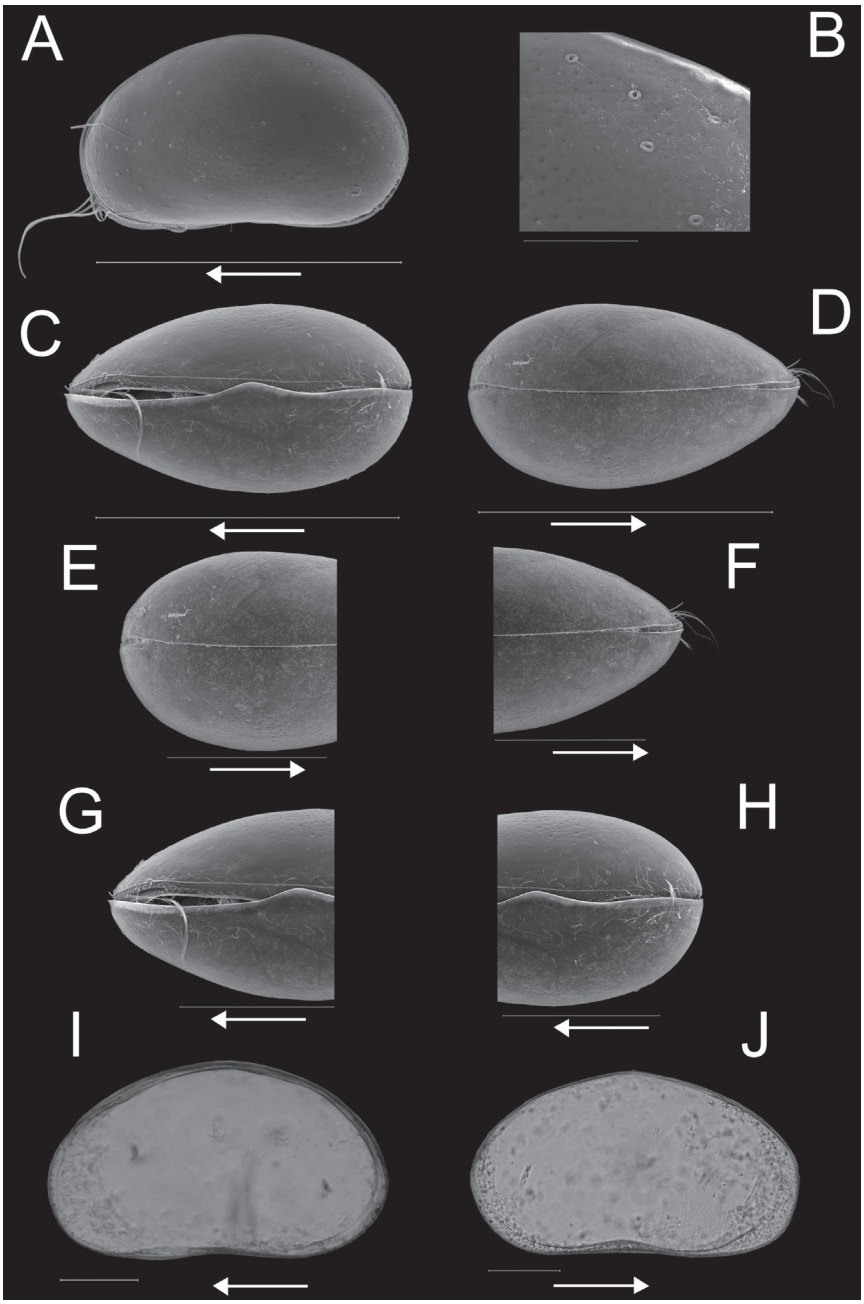

Figure 5. Carapace and valves of *Sarscypridopsis harundineti* sp. nov. ♀ **A, B** RBINS INV.159066 **C** RBINS INV.159067 **D, E, F** RBINS INV.159065 **G, H** RBINS INV.159067 **A** carapace left view **B** detail of external surface of A **C** carapace ventral view **D** carapace dorsal view **E** carapace posterior part, detail of D **F** carapace anterior part, detail of D **G** carapace anterior part, detail of C **H** carapace posterior part, detail of C **I** left valve external view **J** right valve external view Scale bars: 400 μm (**A, C, D**); 50 μm (**B**); 200 μm (**E–H**); 100 μm (**I, J**); arrows indicate anterior end.

(Sars, 1895); *Potamocypris mastigophora* (Methuen, 1910); *Sarscypridopsis* cf. *elizabethae* (Sars, 1924); *Sclerocypris* sp., *Stenocypris malayica* Victor & Fernando, 1981; *Strandesia* cf. *prava* Klie, 1935 • **SA-98** (Fig. 1, Suppl. material 1: Fig. 1E): 6 ♀♀; floodplains south of Okavango Delta, temporary channel near the city of Maun; 19°52'15"S, 23°21'06"E; elevation ca. 940 m a.s.l.; 14 Sept. 2012; accompanying ostracod fauna: *Heterocypris giesbrechti* • **SA-99** (Fig. 1, Suppl. material 1: Fig. 1F): 16 ♀♀ and 1 juv.; floodplains south of Okavango Delta, temporary channel near the city of Maun; 19°52'15"S, 23°20'45"E; elevation ca. 940 m a.s.l.; 14 Sept. 2012; accompanying ostracod fauna: *Heterocypris oblonga*; *Potamocypris deflexa* (Sars, 1924); *Potamocypris mastigophora*; *Zonocypris costata* (Vávra, 1897) • **SA-100** (Fig. 1, Suppl. material 1: Fig. 1G): 11 ♀♀; floodplains south of Okavango Delta, flooded swamp and grassland near the city of Maun; 19°52'04"S, 23°20'38"E; elevation ca. 940 m a.s.l.; 14 Sept. 2012; accompanying ostracod fauna: *Heterocypris oblonga*; *Stenocypris malayica*; *Zonocypris tuberosa* G.W. Müller, 1908 • **SA-101** (Fig. 1, Suppl. material 1: Fig. 1H): 6 ♀♀; floodplains south of Okavango Delta, isolated pool in flooded grassland near the city of Maun; 19°51'39"S, 23°19'41"E; elevation ca. 940 m a.s.l.; 15 Sept. 2012; accompanying ostracod fauna: *Heterocypris oblonga* • **SA-102** (Fig. 1, Suppl. material 1: Fig. 1I): 1 ♀; floodplains south of Okavango Delta, floodplain channel near the city of Maun; 19°52'06"S, 23°20'41"E; elevation ca. 940 m a.s.l.; 15 Sept. 2012; accompanying ostracod fauna: *Heterocypris oblonga*.

All individuals collected by T. Namiotko; 51 ♀♀ and 3 juv. are stored in 96% ethanol and 3 ♀♀ are stored as holotype. Repositories: RBINS and OC-UG.

Etymology. This species is named after the term "reed-bed" (Latin: *harundinetum*), the original meaning of the name of the town Maun in Botswana close to the sites from where *Sarscypridopsis harundineti* was collected. The name Maun is derived from the language of Bantu-speaking people and translates as "the place of river reeds".

Diagnosis. Carapace in lateral view with anterior and posterior margins nearly symmetrically rounded, dorsal margin almost evenly rounded with greatest height situated just behind mid-length, ventral margin almost straight. RV overlapping LV anteriorly, posteriorly and ventrally, LV slightly overlapping RV dorsally. Carapace surface smooth (with fine reticulation in the central area), with rare thickly rimmed normal pores with short sensilla, situated mostly in the posterior and postero-dorsal parts. Antenna with long swimming setae, and supporting aesthetasc Y with distinctive distal bulbous sensory part. Terminal segment of maxillular palp elongated, ~ 2× as long as wide, bearing four long claws. T1 with four branchial rays. CR reduced, with elongated, triangular base.

Description. Female. Cp in left lateral view (Fig. 5A) with anterior and posterior margins nearly symmetrically rounded, dorsal margin almost evenly rounded, with greatest height situated just behind mid-length; ventral margin almost straight. RV overlapping LV anteriorly and posteriorly. LV slightly overlapping RV dorsally, RV overlapping LV ventrally (Fig. 5E–H). External surface smooth with fine reticulation in the central area; with rare, thickly rimmed pores with extending sensilla situated mostly

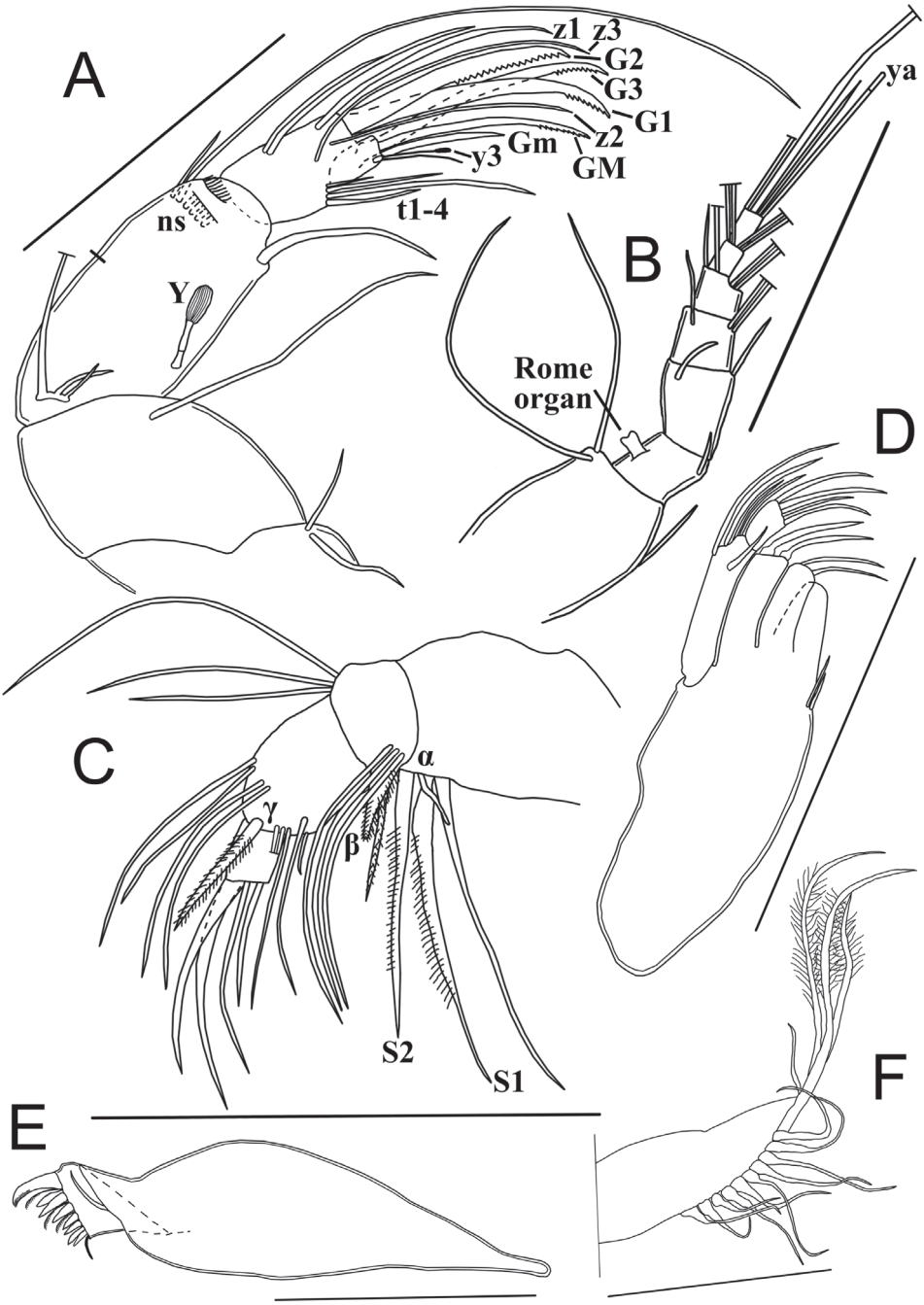

Figure 6. Limbs of *Sarscypridopsis harundineti* sp. nov. ♀. **A, B, E, F** holotype (OC-UG 120915-3A1L) **C, D** paratype (OC-UG 120915-3A3L) **A** Second antenna **B** First antenna **C** Mandibular palp **D** Maxillula **E** Mandibular coxa **F** Maxillular respiratory plate. Scale bars: 100 μm. Abbreviation: ns = natatory setae.

in the anterior and postero-dorsal parts (Fig. 5B). Cp in dorsal (Fig. 5D) and ventral views (Fig. 5C) sub-elliptical, lateral margins unevenly rounded, widening posteriorly; posterior edge broadly rounded, anterior one more pointed. Greatest width situated behind mid-length. LV in internal view (Fig. 5I) ovoid, with greatest height situated at mid-length. Anterior and posterior margins almost equally rounded, ventral margin slightly sinuous at mid-length. Anterior and posterior calcified inner lamella narrow with marginal selvage. RV in internal view (Fig. 5J) with posterior margin broadly rounded, anterior margin more pointed and with ventral margin almost straight. Anterior and posterior calcified inner lamella wider than on LV; no selvage or inner list.

A1 (Fig. 6B) 7-segmented. First segment with one short subapical dorsal seta (reaching beyond tip of segment) and two long ventro-apical setae. Second segment with one short dorso-apical seta (reaching 1/3 of length of next segment) and a large ventral Rome organ. Third segment ~ 0.5× as long as wide, with two apical setae, one short dorsal seta (reaching beyond tip of next segment) and one short ventral seta (not reaching tip of next segment). Fourth segment with two long dorso-apical setae and one short ventro-apical seta (reaching 1/3 of penultimate segment). Fifth segment bearing two long ventro-apical setae and two dorso-apical setae, one long and one short (the latter nearly reaching tip of terminal segment). Penultimate segment with four long apical setae. Terminal segment with three (two long and one medium) setae and one aesthetasc ya, the latter slightly longer than the seta of medium length.

Chaetotaxic formula: I: A-1s, P-2l / II: A-1s, P-r / III: A-1s, P-1s / IV: A-2l, P-1s / V: A-2l, P-1l-1s / VI: A-4l / VII: D: 2l-1m-ya.

A2 (Fig. 6A) with protopodite, exopodite and 3-segmented endopodite. Basal segment of protopodite with two short ventro-apical setae. Second segment of protopodite with one long ventro-apical seta. Exopodite reduced to a small plate with three setae, two short and one long. Endopodite 3-segmented. First endopodal segment with long ventro-apical seta, extending beyond tip of terminal segment; a large aesthetasc Y with a distinct distal bulbous sensory part; dorso-apically with five long natatory setae (reaching far beyond tips of terminal claws) and one shorter (6^{th}) seta reaching 1/3 of length of next segment. Second endopodal segment undivided, medio-dorsally with two subequally long setae and medio-ventrally with four unequal setae (t1-t4), one long and three short; distally with three long z-setae (z1, z2, z3) and three long serrated G-claws: G2 thick and apically strongly serrated, G1 and G3 more slender. Terminal (third) endopodal segment subquadrate with a long serrated claw GM, a shorter (~ 1/2 length of GM) smooth claw Gm and an aesthetasc y3 fused with slightly longer accompanying seta. Aesthetascs y1, y2 and seta g not seen, the latter almost certainly absent as typical of the subfamily.

Chaetotaxic formula: Pr: 1l / Exo: 1l-2s / EI: A-5l-1s, P-Y-1l / EII+III: A-2l, P-1s(t1)-1l(t2)-2s(t3,4), D-3l(z1,z2,z3)-3l(G1,2,3: ser) / EIV: 1l(GM: ser)-1m(Gm)-y3–1s

Md with sclerotised coxa (Fig. 6E) and 4-segmented palp (Fig. 6C). Md-coxa elongated, distally with rows of teeth and small setae, and with one short, smooth seta situated near the palp. First palp-segment ventro-apically with two long plumed setae (S1 and S2), one long, slender seta and a short smooth α-seta, situated in between the two

S-setae. Second segment dorso-apically with three unequally long slender setae; ventrally with three long, smooth setae, one medium hirsute seta and hirsute, cone-shaped β-seta. Third segment ventro-apically with one long and one short seta; medio-apically with three setae, all reaching tip of terminal segment and a hirsute and long γ-seta; dorso-apically with four setae, all extending far beyond tips of terminal segment. Terminal segment bearing four claws, three ~ 4× as long as terminal segment and one shorter.

Chaetotaxic formula: Palp: I: In-1s(alfa)-1l-2l(S1,S2: pl) / II: In-1s(beta: pl)-1m(pl)-3l, Ex-3l / III: In-1l-1s, D-3l-1l(gamma: pl), Ex-4l / IV: 3l-1m

Rake-like organs (food-rakes) (Fig. 7A) T-shaped, each with nine apical teeth.

Mx1with three endites and 2-segmented palp (Fig. 6D) and a large respiratory plate (Fig. 6F). First endite with two short setae near its base. Third endite with two smooth teeth bristles. First palp-segment with four unequal dorso-apical setae, one long, one medium and two short; medio-apically with one seta (reaching 1/2 length of terminal segment). Second segment elongated (~ 2× as long as wide), apically with four unequal but long claws (~ 2× as long as terminal segment). Respiratory plate large and elongate, distally with a row of more than eleven smooth rays and three long plumose rays.

Chaetotaxic formula: Palp: I: Ex-2s-1m-1l, In-1s / II: D-4m

T1 (Fig. 7B). Protopodite with two short unequal a-setae; b-, c- and d-setae absent, endite distally with a dozen apical setae (exact number not determined). Endopod elongated, apically with one long seta (h2) and two shorter setae (h1 and h3). Respiratory plate with four long rays with swollen bases.

Chaetotaxic formula: Pr: A-2s(a and a') / Mastic: D-? / Exo: 4l / E: D-3l

T2 (Fig. 7C, D) a walking limb. Protopodite with seta d2 of medium length, seta d1 absent. First two endopodal segments with one long antero-apical seta each. Seta e reaching half of the penultimate segment and seta f reaching tip of terminal segment. Third endopodal segment with two antero-apical setae, one medium length g-seta and one very short seta. Fourth segment with one very short seta (h3), one short seta (h1) and long, strongly curved and serrated claw (h2); distal claw ~ 3× as long as the second endopodal segment.

Chaetotaxic formula: Pr: A-1m(d2) / EI: A-1l / EII: A-1l / EIII: A-1m-1s / EIV: P-1s(h3), D-1s(h1)-1l(h2 G:ser)

T3 (Fig. 7E) a cleaning limb. Protopodite with two long setae (dp and d2) and one shorter seta (d1). First endopodal segment with short subapical e-seta. Second and third endopodal segments fused, with short f-seta not reaching tip of segment. Terminal part (fusion between distal part of third and fourth segment) a pincer organ, bearing a medium length seta (h3), a short serrated seta (h2), and a very short seta (h1), length of seta h3 ~ 2/3 that of fused segment, seta h2 ~ 1/2 length of seta h3.

Chaetotaxic formula: Pr: A-1l(d2)-1m(d1), P-1l(dp) / EI: A-1s(e) / EII + III: A-1s(f) / EIV: 1s(h2: ser)-1m(h3)

CR (Fig. 7F). Reduced, with elongated, triangular base; distally with long flagellum-like seta and subapically with a short seta.

Measurements (in μm). Cp (n = 3): L = 433–464, H = 259–282; LV (n = 6): L = 430–461, H = 250–272; RV (n = 6): L = 444–473, H = 261–275.

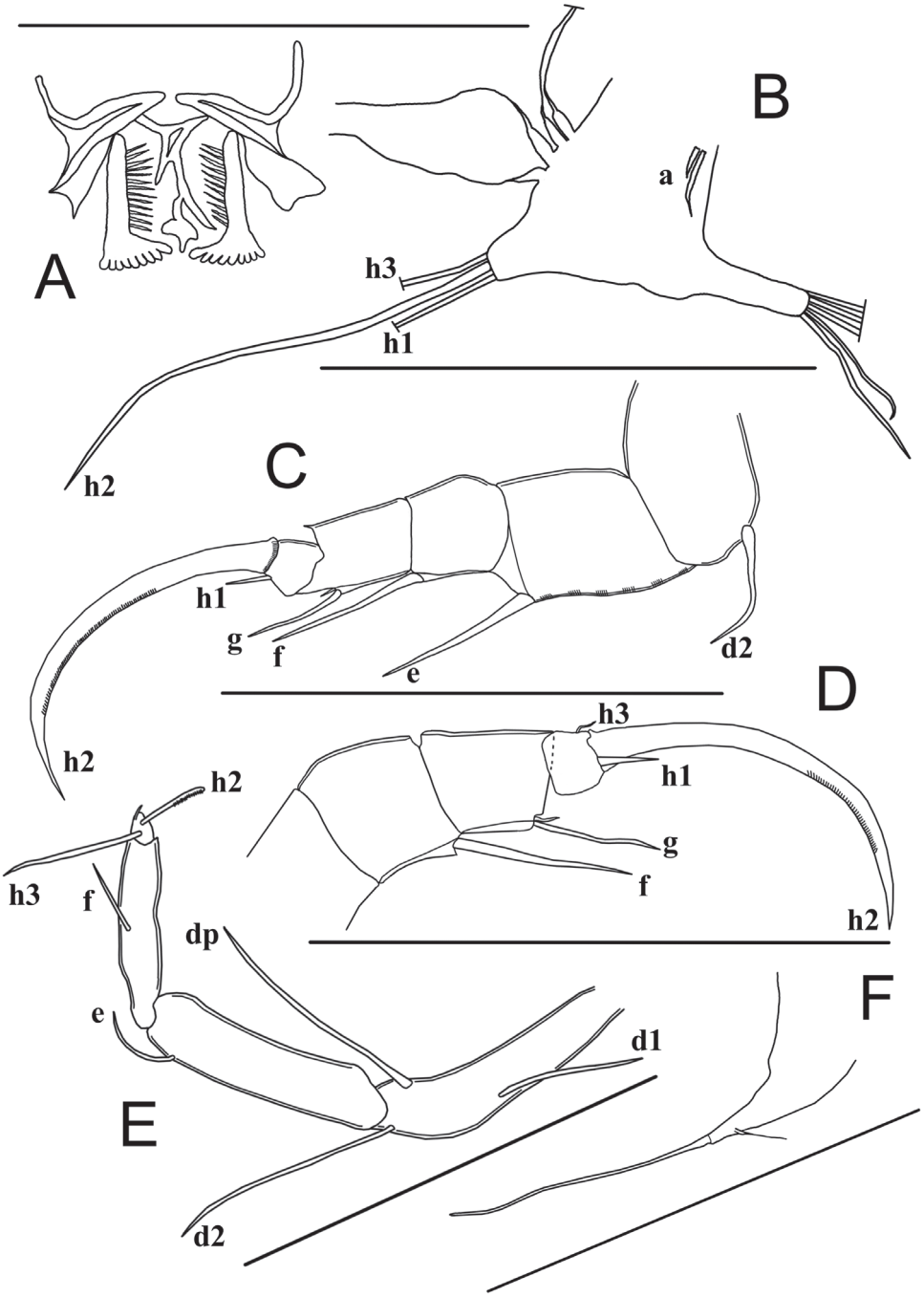

Figure 7. Limbs of *Sarscypridopsis harundineti* sp. nov. ♀ **A, B, C, F** paratype (OC-UG 120915-3A3L) **D** paratype (OC-UG 120915-3A2L) **E** holotype (OC-UG 120915-3A1L) **A** Food-rake **B** First thoracopod (maxilliped) **C** Second thoracopod (walking leg) **D** Second thoracopod distal end **E** Third thoracopod (cleaning leg) **F** Caudal ramus. Scale bars: 100 μm.

Male unknown.

Ecology. *Sarscypridopsis harundineti* was found in eight temporary waterbodies of the vast floodplains south of the Okavango Delta in northern Botswana. Habitats include both lotic (river side channel, floodplain channel) and lentic waters (flooded swamp, grassland, isolated pool) as well as the endorheic Lake Ngami. The species occurred at the pH range of 6.5–7.7, the electrical conductivity range of 102–464 μS/cm, and the water temperature range of 19.8–33.7 °C.

Discussion

Potamocypris and *Cyprilla* Sars, 1924

Sars (1924a) described the genus *Cyprilla*, based on the carapace shape and presence of large flanges on the left valve, causing a noticeable LV > RV overlap. Five species were assigned to this genus, all raised from dry mud or obtained from water samples, from South Africa: *C. arcuata* Sars, 1924, *C. deflexa* Sars, 1924, *C. gibbula* Sars, 1924, *C. humilis* Sars, 1924 and *C. producta* Sars, 1924. In the same publication, Sars (1924a) noticed that *Cyprilla* differs from *Potamocypris* "in the general appearance of the shell and in the mutual relation of the valves, as also apparently in the sculpture", but shares with *Potamocypris* reduced caudal rami and a spatulate terminal segment of the Mx1 palp. According to Gauthier (1939), these features cannot be considered diagnostic, and thus he transferred the five *Cyprilla* species to *Potamocypris*, automatically synonymising *Cyprilla* with *Potamocypris*. The same view was supported by Meisch (1984, 1985) and George and Martens (2002). While redescribing *P. humilis* from the Outer Hebrides off the west coast of Scotland, Horne and Smith (2004) noticed prominent tubercules on juvenile carapaces, the trait not yet described in any *Potamocypris*. They partly agreed with Purasjoki (1948) who considered the presence of tubercules in juveniles a *Cyprilla* trait, in this way questioning the previously proposed synonymisation of the two genera. This merits a further study, but we confirm that none of the juveniles of *P. meissneri* we collected had tubercules. Therefore, we feel confident in describing the new species as a member of *Potamocypris*.

Potamocypris meissneri differs from other species of the genus by the presence of a conspicuously reticulate carapace, densely covered by prominent conuli carrying rimmed pores with long extending sensilla, and by wide anterior and posterior flanges on the left valve. Out of five southern African *Potamocypris* species only one, *P. paludum* Gauthier, 1939 (nom. nov. pro *Cyprilla arcuata* Sars, 1924 nec Sars, 1903 – *fide* Gauthier, 1939), has short swimming setae on the second antennae, which clearly distinguishes it from the new species described here. Two further species, *P. mastigophora* (of which *Cyprilla producta* Sars, 1924 is a synonym – *fide* McKenzie, 1971) and *P. gibbula* have different carapace shapes from *P. meissneri*: more elongated and crescent-shaped in *P. mastigophora*, and more subtriangular, and dorsally arched with a blunt angle in *P. gibbula*. The remaining two species (i.e., *P. humilis* and *P. deflexa*)

are more similar to *Potamocypris meissneri* as they also have ornamented carapaces. However, unlike in *Potamocypris meissneri*, the posterior part of the dorsal margin in the two species is almost straight, sloping down and making a distinct angle with the characteristically truncated and almost straight posterior margin. In addition, none of the presently known species of *Potamocypris* has this type of pronounced external valve ornamentation. *Potamocypris narayanani* George & Martens, 2002 carries conspicuous stiff setae and has a pitted valve surface, but lacks the prominent ridges and has a huge dorsal hump on the left valve.

Sarscypridopsis

The originally assigned type species, *S. gregaria* (Sars, 1895), was placed into the synonymy of *S. aculeata* (Costa, 1847) by Sywula (1966), and both were originally assigned to the genus *Cypridopsis*, which originally included all cypridinid ostracods with a flagellate CR. However, over time, as more species with this trait had been found, new genera were distinguished, *Sarscypridopsis* being one of those. McKenzie (1977) ignored the synonymy proposed by Sywula (1966) and made *S. gregaria* the type species of his genus *Sarscypridopsis*. The status of *S. gregaria* has to be rechecked on type material, to clearly determine which is the true type species of this genus: *S. aculeata* with *S. gregaria* being its junior synonym, or *S. gregaria* as a valid species. Nominally, of course, *S. gregaria* will always remain the designated type species.

According to McKenzie (1977) and Meisch (2000) *Sarscypridopsis* is diagnosed by the following morphological characters: carapace rather small (< 0.9 mm), subtriangular in shape with smooth or pitted surface; RV overlapping LV ventrally, anteriorly and posteriorly; calcified inner lamella broad anteriorly and narrower posteriorly; distal segment of Mx1 palp cylindrical and ramus of the CR triangular. As our new species show all of these characteristics, we herewith assign it to the genus *Sarscypridopsis*. However, compared to other congeners, the base of the CR is unusually elongated.

Sarscypridopsis is mostly an Afrotropical genus (Meisch et al. 2019). Of the 17 species presently assigned to this genus, only three are known to occur also outside the African continent. *Sarscypridopsis aculeata* is nearly cosmopolitan (Meisch et al. 2019), *S. lanzarotensis* (Mallwitz, 1984) has been found in Spain including Canary Islands (Mallwitz 1984; Meisch 2000; Castillo-Escrivà et al. 2016), Italy (Pieri et al. 2015), and Morocco (Scharf and Meisch 2014), while *S. ochracea* (Sars, 1924), except for the Afrotropical region, has also been reported from the Oriental and Australian regions (Meisch et al. 2019), although these latter identifications seem unlikely from a zoogeographical point of view and need confirmation.

Most of the *Sarscypridopsis* species are poorly described and only for the following three species the morphology of the soft parts is (partly) known: *S. aculeata*, *S. katesae* (Hartmann, 1957) and *S. lanzarotensis*. In all three of these species, the respiratory plate of T1 carries five rays, while *S. harundineti* has only four rays, although admittedly this character is often very difficult to observe. Another difference between the new species and *S. aculeata* and *S. lanzarotensis* is the presence of two smooth teeth

bristles on the third endite of Mx1 in *S. harundineti*. In the other two species the proximal bristle is serrated as is the neighboring one (Mallwitz 1984; Meisch 2000). In *Sarscypridopsis katesae* these teeth bristles are also smooth (Hartmann 1957).

Despite of the lack of comparative characters, *Sarscypridopsis harundineti* can be easily distinguished from its South African congeners by the unique, more rounded valves shape, and the smaller carapace (L = 0.43–0.47 mm versus 0.54–0.80 mm). The greatest height is situated just behind mid-length in the new species, unlike in *S. clavata* (Sars, 1924), *S. echinata* (G.W. Müller, 1908), *S. elizabethae*, *S. hirsuta* (Sars, 1924), *S. punctata* (Sars, 1924), *S. reniformis* (Sars, 1924) and *S. striolata* (Sars, 1924) in which the dorsal margin of the carapace is more arched and the greatest height is situated more to the front. *Sarscypridopsis ochracea* (Sars, 1924), *S. pyramidata* (Sars, 1924), *S. tonsa* (Sars, 1924) and *S. trigonella* (Sars, 1924) have sub-triangular carapaces, while *S. glabrata* (Sars, 1924) has more elongated one. The carapace size and the shape in the lateral view of *Sarscypridopsis harundineti* is most similar to *S. brevis* (Sars, 1924) and *S. sarsi* (Klie, 1935). The former can be distinguished by a very hirsute external surface of the carapace, while the latter has a distinctly globular carapace in dorsal view (Sars 1924a, 1924b).

Taking into account the mentioned gaps in information on taxonomic traits, we conclude that southern African Cypridopsinae, especially representatives of the genus *Sarscypridopsis*, urgently need integrated taxonomic revision, i.e., by means of both morphological characters (including redescriptions based on both the type and newly collected material) and DNA-sequence data.

Acknowledgements

This study was partly funded by the University of Gdansk under internal grants no. L-155-4-0089-1 and 531-D090-D818-21 attributed to TN. Julien Cillis (RBINS, Brussels, Belgium) offered technical assistance with the SEM. We also thank Malwina Laskowska, Mateusz Krawczuk and Lucyna Namiotko (University of Gdansk, Poland) for their assistance in sample processing and preliminary identification of ostracods. Anna Karolewska (Warsaw, Poland) is acknowledged for making the names of our new species conform to the rules of Latin grammar. We thank both reviewers, Renate Matzke-Karasz and Claude Meisch, for their positive reviews and encouraging comments.

References

Almeida NM, Higuti J, Ferreira VG, Martens K (2021) A new tribe, two new genera and three new species of Cypridopsinae (Crustacea, Ostracoda, Cyprididae) from Brazil. European Journal of Taxonomy 762: 1–48. https://doi.org/10.5852/ejt.2021.762.1451

Baird W (1845) Arrangement of the British Entomostraca, with a list of species, particularly noticing those which have as yet been discovered within the bounds of the Club. Transac-

tions of the Berwickshire Naturalists' Club 2(13): 145–158. https://www.biodiversitylibrary.org/part/9791

Brady GS (1867) A synopsis of the recent British Ostracoda. Intellectual Observer 12: 110–130.

Brady GS (1870) Notes on Entomostraca taken chiefly in the Northumberland and Durham District (1869). Natural History Transactions of Northumberland and Durham 3(1868–1870): 361–373.

Brady GS (1904) On Entomostraca collected in Natal by Mr James Gibson. Proceedings of the Zoological Society of London 1904: 121–128. https://doi.org/10.1111/j.1469-7998.1904.tb08317.x

Brady GS, Robertson D (1870) The Ostracoda and Foraminifera of tidal rivers. Part I. Annals and Magazine of Natural History ser 4, 6: 1–33. https://doi.org/10.1080/00222937008696200

Broodbakker NW, Danielopol DL (1982) The chaetotaxy of Cypridacea (Crustacea, Ostracoda) limbs: proposals for a descriptive model. Bijdragen tot de Dierkunde 52(2): 103–120. https://doi.org/10.1163/26660644-05202003

Castillo-Escrivà A, Rueda J, Zamora L, Hernández R, del Moral M, Mesquita-Joanes F (2016) The role of watercourse versus overland dispersal and niche effects on ostracod distribution in Mediterranean streams (eastern Iberian Peninsula). Acta Oecologica 73: 1–9. https://doi.org/10.1016/j.actao.2016.02.001

Costa OG (1847) Entomostraci, Ostracodi. Fauna del Regno di Napoli, ossia enumerazione di tutti gli animali che abitano la diverse regioni di questo Regno a le acque che le bagnano: Animali Articolati, Crostacei 1: 7–12.

Daday E (1910) Untersuchungen über die Süßwasser-Mikrofauna Deutsch-Ost-Africas. Zoologica, Original-Abhandlungen aus dem Gesamtgebiete der Zoologie 23: 1–314. https://doi.org/10.5962/bhl.title.11655

Daday E (1913) Cladoceren und Ostracoden aus Süd- und Südwestafrika. Denkschriften der Medizinisch-Naturwissenschaftlichen Gesellschaft zu Jena 17(2): 89–102.

Gauthier H (1939) Sur la structure de la coquille chez quelques cypridopsines à furca réduite et sur la validité du genre *Cyprilla* (Ostracodes). Bulletin de la Societé zoologique de France 64: 203–228.

George S, Martens K (2002) On a new species of *Potamocypris* (Crustacea, Ostracoda) from Chalakkudy River, Kerala (India), with a checklist of the *Potamocypris*-species of the world. Zootaxa 66: 1–15. https://doi.org/10.11646/zootaxa.66.1.1

Hartmann G (1957) Ostrakoden aus dem Namaland und Transvaal. Veröffentlichungen des Naturwissenschaftlichen Vereins zu Osnabrück 28: 50–60.

Horne DJ, Smith RJ (2004) First British record of *Potamocypris humilis* (Sars, 1924), a freshwater ostracod with a disjunct distribution in Europe and southern Africa. Bollettino della Società Paleontologica Italiana 43(1–2): 297–306.

Kaufmann A (1900) Cypriden und Darwinuliden der Schweiz. Revue suisse de Zoologie 8: 209–423. https://doi.org/10.5962/bhl.part.10584

Klie W (1935) Voyage de Ch Alluaud et PA Chappuis en Afrique occidentale française (Dec 1930-Avril 1931): VIII. Ostracoda aus dem tropischen Westafrika. Archiv für Hydrobiologie 28: 35–68

Latreille PA (1802) Histoire naturelle, générale et particulière des Crustacés et des Insectes. Histoires des Cypris et des Cytherées 8(4): 232–254. https://doi.org/10.5962/bhl.title.15764

Mallwitz J (1984) *Cypridopsis lanzarotensis* n. sp., ein neuer Ostracode von Lanzarote (Kanarische Inseln) (Crust.: Ostracoda: Podocopida). Mitteilungen aus dem Hamburgischen Zoologischen Museum und Institut 81: 171–176.

Martens K (1987) Homology and functional morphology of the sexual dimorphism in the antenna of *Sclerocypris* Sars, 1924 (Crustacea, Ostracoda, Megalocypridinae). Bijdragen tot de Dierkunde 57(2): 183–190.

Martens K (2001) Ostracoda. In: Day JA, de Moor IJ, Stewart BA, Louw AE (Eds) Guides to the freshwater invertebrates of Southern Africa. Volume 3: Crustacea II. Water Research Commission Report TT 148/01: 9–77.

Martens K, Meisch C (1985) Description of the male of *Potamocypris villosa* (Jurine, 1820) (Crustacea, Ostracoda). Hydrobiologia 127: 9–15. https://doi.org/10.1007/BF00004658

McKenzie KG (1971) Species list of South African freshwater Ostracoda, with an appendix listing museum collections and some further determinations. Annals of the South African Museum 57: 157–213.

McKenzie KG (1977) Illustrated generic key to South African continental Ostracoda. The Annals of the South African Museum 74(3): 45–103.

Meisch C (1984) Revision of the Recent Western Europe species of genus *Potamocypris* (Crustacea, Ostracoda). Part I. Species with short swimming setae on the second antennae. Travaux scientifiques du Musée d'Histoire naturelle de Luxembourg 3: 1–55.

Meisch C (1985) Revision of the Recent West European species of the genus *Potamocypris* (Crustacea, Ostracoda). Part II. Species with long swimming setae on the second antennae. Travaux scientifiques du Musée d'Histoire naturelle de Luxembourg 6: 1–95.

Meisch C (2000) Freshwater Ostracoda of Western and Central Europe. In: Schwoerbel J, Zwick P (Eds) Süßwasserfauna von Mitteleuropa 8(3). Spektrum Akademischer Verlag, Heidelberg, Berlin, 522 pp.

Meisch C (2007) On the origin of the putative furca of the Ostracoda (Crustacea). Hydrobiologia 585: 181–200. https://doi.org/10.1007/s10750-007-0637-2

Meisch C, Smith RJ, Martens K (2019) A subjective global checklist of the extant non-marine Ostracoda (Crustacea). European Journal of Taxonomy 492: 1–135. https://doi.org/10.5852/ejt.2019.492

Mesquita-Joanes F, Smith AJ, Viehberg FA (2012) The ecology of Ostracoda across levels of biological organisation from individual to ecosystem: A review of recent developments and future potential. Developments in Quaternary Sciences 17: 15–35. https://doi.org/10.1016/B978-0-444-53636-5.00002-0

Methuen PA (1910) On a collection of freshwater Crustacea from the Transvaal. Proceedings of the Zoological Society of London 1910: 148–166. https://doi.org/10.1111/j.1096-3642.1910.tb01889.x

Müller GW (1898) Ergebnisse einer zoologischen Forschungsreise in Madagaskar und Ost-Afrika 1889–1895 von Dr. A. Voeltzkow: Die Ostracoden. Abhandlungen der Senckenbergischen Naturforschenden Gesellschaft 21(2): 255–296.

Müller GW (1908) Die Ostracoden der Deutschen Südpolar-Expedition 1901–1903. Deutsche Südpolar-Expedition 10: 51–182. https://www.biodiversitylibrary.org/bibliography/2166

Namiotko T, Danielopol DL, Baltanás A (2011) Soft body morphology, dissection and slide-preparation of Ostracoda: A primer. Joannea Geologie und Paläontologie 11: 327–343. https://www.zobodat.at/pdf/JoanGeo_011_0327-0343.pdf

Pieri V, Martens K, Meisch C, Rossetti G (2015) An annotated checklist of the Recent non-marine ostracods (Ostracoda: Crustacea) from Italy. Zootaxa 3919(2): 271–305. https://doi.org/10.11646/zootaxa.3919.2.3

Purasjoki KJ (1948) *Cyprilla humilis* G.O. Sars, an interesting ostracod discovery from Finland. Societas Scientiarum Fennica, Commentationes Biologicae 10(3): 1–7.

Sars GO (1866) Oversigt af Norges marine Ostracoder. Forhandliger I Videnskabs-Selskabet I Christiania 1865: 1–130.

Sars GO (1895) On some South-African Entomostraca raised from dried mud. Skrifter udg af Videnskabsselskabet i Christiania 8: 1–56.

Sars GO (1903) On the crustacean fauna of central Asia. Part 3: Copeopoda and Ostracoda. Annuaire du Musée zoologique de l'Académie impériale de St.-Pétersbourg 8(2): 195–264.

Sars GO (1924a) The fresh-water Entomostraca of Cape Province (Union of South Africa). Part 2. Ostracoda. Annals of the South African Museum 20: 105–193.

Sars GO (1924b) The contributions to a knowledge of the fauna of South-West Africa (Union of South Africa). Part 3. Annals of the South African Museum 20: 194–211.

Savatenalinton S (2018) New genus of subfamily Cypridopsinae Kaufmann, 1933 (Crustacea: Ostracoda) from Thailand. European Journal of Taxonomy 487: 1–17. https://doi.org/10.5852/ejt.2018.487

Savatenalinton S (2020) A new cypridopsine genus (Crustacea, Ostracoda) from Thailand. European Journal of Taxonomy 631: 1–16. https://doi.org/10.5852/ejt.2020.631

Scharf S, Meisch C (2014) New records of nonmarine Ostracoda (Crustacea) from Gran Canaria (Canary Island), with an updated checklist of the nonmarine Ostracoda of the Canary Island. Bulletin de la Societe des Naturalistes Luxembourgeois 115: 259–270.

Smith AJ, Horne DJ, Martens K, Schön I (2015) Class Ostracoda. In: Thorp JH, Rogers Ch (Eds) Ecology and General Biology. Thorp and Covich's Freshwater Invertebrates. Volume I. Elsevier, Amsterdam, 757–780. https://doi.org/10.1016/B978-0-12-385026-3.00030-9

Sywula T (1966) Notes on Ostracoda. I. On some Polish species. Bulletin de l'Académie Polonaise des Sciences, Série des Sciences Biologiques, Cl. II 13(11–12): 647–652.

Vávra W (1891) Monographie der Ostracoden Böhmens. Archiv der naturwissenschaftlichen Landesdurchforschung von Böhmen 8(3) (I–IV): 1–116.

Vávra W (1897) Die Süßwasser-Ostracoden Deutsch-Ost-Afrikas. In: Möbius K (Ed.) Die Tierwelt Ost-Afrikas und der Nachbargebiete 4(2–3): 1–28.

Victor R, Fernando CH (1981) Freshwater Ostracoda of the genera *Chrissia* Hartmann, 1957 and *Stenocypris* Sars, 1889 from Malaysia, Indonesia and the Philippines. Mitteilungen aus dem Hamburgischen Zoologischen Museum und Institut 78: 151–168.

Supplementary material 1

Pictures of the sites from where new species *Potamocypris meissneri* sp. nov. and *Sarscypridopsis harundineti* sp. nov. were collected

Authors: A. Szwarc, K. Martens, T. Namiotko

Data type: Images

Explanation note: Pictures of the sites from where *Potamocypris meissneri* sp. nov. and *Sarscypridopsis harundineti* sp. nov. were collected in the North-West Province of South Africa (A) and in the floodplains south of the Okavango Delta near the town of Maun (except C) in the North-West District of Botswana (B-I), respectively. **A** SA-9: a small temporary open pan near the village of Ganalaagte **B** SA-103: grassy shore of a seasonal pond **C** SA-96: endorheic Lake Ngami **D** SA-97: Thamalakane river **E** SA-98: a temporary channel **F** SA-99: a temporary channel **G** SA-100: a flooded swamp and grassland **H** SA-101: an isolated pool in flooded grassland **I** SA-102: a floodplain channel.

Link: https://doi.org/10.3897/zookeys.1076.76123.suppl1

ZooKeys 1076: 109–124 (2021)
doi: 10.3897/zookeys.1076.73103
https://zookeys.pensoft.net

RESEARCH ARTICLE

A peer-reviewed open-access journal
ZooKeys
Launched to accelerate biodiversity research

New relictual genera in Cyrtoquediini and Indoquediini (Coleoptera: Staphylinidae: Staphylininae)

Adam J. Brunke[1]

1 *Agriculture and Agri-Food Canada, Canadian National Collection of Insects, Arachnids and Nematodes, 960 Carling Avenue, Ottawa, Ontario, Canada*

Corresponding author: Adam J. Brunke (adam.j.brunke@gmail.com)

Academic editor: Volker Assing | Received 17 August 2021 | Accepted 16 October 2021 | Published 9 December 2021

http://zoobank.org/7A0C4169-2065-4FD9-AC8D-4470A0468B63

Citation: Brunke AJ (2021) New relictual genera in Cyrtoquediini and Indoquediini (Coleoptera: Staphylinidae: Staphylininae). ZooKeys 1076: 109–124. https://doi.org/10.3897/zookeys.1076.73103

Abstract

Sundaquedius **gen. nov.** (Cyrtoquediini) and *Fluviphirus* **gen. nov.** (Indoquediini) are described from southeast Asia and western North America, respectively, resulting in the new combinations *Sundaquedius nigropolitus* (Cameron) and *Fluviphirus elevatus* (Hatch). *Sundaquedius abbreviatus* **sp. nov.** is described from Vietnam. The phylogenetic positions of these genera within Staphylininae are supported by morphology and recently published phylogenomic evidence. New keys to the world genera of Cyrtoquediini and Indoquediini are provided. A new country record for *Alesiella lineipennis* (Cameron) is provided for Thailand, based on the first available specimen in more than 100 years.

Keywords

Rove beetles, Nearctic, Oriental, taxonomy, systematics, identification keys

Introduction

The tribe Quediini (formerly Quediina, see Materials and methods) was previously a convenient dumping ground for plesiomorphy-rich taxa in Staphylininae, and its largest genus, *Quedius*, was the destination for most of these species (summarized by Solodovnikov 2006a). Numerous phylogenetic analyses using both morphological and molecular evidence have sought to identify monophyletic lineages within this heterogeneous assemblage and a number of higher taxa have been created to represent

these separately from Quediini and *Quedius* (e.g., Chatzimanolis et al. 2010; Brunke et al. 2016, 2019, 2021). With a diverse monophyletic core of Quediini largely now delimited, Brunke et al. (2021) assembled a phylogenomic dataset to resolve the position of remaining Staphylininae *incertae sedis* taxa and identify any remaining *Quedius* species that may belong to other tribes. These analyses revealed that two species of *Quedius*, *Q. elevatus* (Hatch) from western North America and an undescribed species from Vietnam, very closely related to *Q. nigropolitus* (Cameron) from East Java, clearly belonged to Indoquediini and Cyrtoquediini, respectively and represented undescribed genera. These species were also found to share morphological synapomorphies with other members of their tribe, though they were geographically quite distant from their closest relatives. Several Staphylininae *incertae sedis* genera were also recovered by Brunke et al. (2021) as Cyrtoquediini and Indoquediini, resulting in significant changes to the composition and morphological diagnoses of these tribes. This paper aims to formally describe and illustrate these two genera, and provide the first keys to the world genera of Indoquediini and Cyrtoquediini as recently revised by Brunke et al. (2021).

Materials and methods

Depositories:

cHay Personal collection of Y. Hayashi, Kawanishi City, Japan
NMUK Natural History Museum, London, U.K. (M. Geiser, M. Barclay)
CNC Canadian National Collection of Insects, Arachnids and Nematodes, Ottawa, Ontario, Canada
ZIN Zoological Institute, Russian Academy of Sciences, St. Petersburg, Russia (via A. Solodovnikov)

Specimen data

Type label data are given verbatim, with labels separated by "/" and comments indicated in square brackets. Non-type label data were standardized to improve clarity. Specimens were georeferenced using Google Earth or Google Maps.

Microscopy, illustration, and photography

All specimens were examined dry using a Nikon SMZ25 stereomicroscope. Genitalia and terminal segments of the abdomen were dissected and placed in glycerin filled vials, pinned with their respective specimens. Line illustrations were made from standard images and then digitally inked in Adobe Illustrator CC-2020. All imaging, including photomontage was accomplished using a motorized Nikon SMZ25 microscope and NIS Elements BR v4.5. Photos were post-processed in Adobe Photoshop CC-2020.

Measurements and character variability

All measurements were made using a live measurement module within NIS Elements BR v4.5. Measurements were taken as listed below, but only proportional (HW/HL, PW/PL, EW/EL, PW/HW) and forebody measurements are stated directly in descriptions. Total body length is generally difficult to standardize for Staphylinidae and was not measured due to the contractile nature of the abdomen.

HL Head Length, at middle, from the anterior margin of frons to the nuchal ridge.
HW Head Width, the greatest width, including the eyes.
PL Pronotum Length, at middle.
PW Pronotum Width, greatest width.
EL Elytral Length, greatest length taken from level of the anterior most large, lateral macroseta to apex of elytra. EL approximates the length of the elytra not covered by the pronotum and therefore contributing to the forebody length.
EW Elytral Width, greatest width.
Forebody HL + PL + EL.

Terminology and higher classification

Morphological terminology follows that of Brunke et al. (2019, 2021). Recent phylogenetic studies (Tihelka et al. 2020; Żyła and Solodovnikov 2020) have proposed alternate solutions for the limits of subfamily Staphylininae (i.e., including or excluding the xantholinine group, Arrowinini and genus *Coomania* Cameron). In the stricter sense (sensu Żyła & Solodovnikov 2020), the xantholinine group, *Arrowinus*+*Platyprosopus*, *Coomania* and the remaining Staphylininae are each treated at the subfamily level with diagnostic character states. The system proposed by Żyła & Solodovnikov (2020) is preferred here for its greater diagnostic value and therefore Cyrtoquediini, Quediini, etc. are treated as tribes of Staphylininae herein.

Taxonomy

Staphylininae Latreille, 1802

Cyrtoquediini Brunke & Solodovnikov, 2016

Diagnosis. Cyrtoquediini (as recently redefined by Brunke et al. (2021)) can be recognized among other Staphylininae based on the following combination of characters: microsculpture on disc of head and pronotum absent; obvious presence of both posterior frontal and basal punctures (Brunke et al., 2019: fig. 1); profemora with apical row of lateroventral spines (near joint with protibia) (Brunke et al. 2021: fig. 8B); protibia

without subapical notch (Brunke et al. 2021: fig. 8C); metatarsomeres 1–4 flattened and trapezoidal, not elongate and cylindrical. Most genera in Cyrtoquediini can also be recognized by the unique row of coarse, impressed setose punctures on the elytral epipleuron (Brunke et al. 2016: fig. 4).

Key to world genera of Cyrtoquediini

1 Last segment of maxillary and labial palpi strongly dilated to a truncate apex; mandibles without teeth; West Palaearctic ..... ***Astrapaeus*** **Gravenhorst (*A. ulmi* (Rossi))**

– Last segment of maxillary and labial palpi not strongly dilated to truncate apex; mandibles with at least one tooth each; Nearctic, Neotropical, East Palaearctic and Oriental Regions **2**

2 Eyes relatively small, eye no more than 1.5 × longer than temple **3**

– Eyes relatively large, eye nearly 3 × as long as temple or larger, temple usually very small **6**

3 Dorsal head and pronotum entirely covered in fine setae; inside termite nests (*Nasutitermes* Dudley); known only from South America; 2 spp., key in Solodovnikov (2006b) ..... ***Sedolinus*** **Solodovnikov**

– Dorsal head and pronotum glabrous except for macrosetae **4**

4 Antennomeres 1–3 without tomentose pubescence; body small (< 6.0 mm); ventral head with infraorbital ridge extending to base of mandibles; mesoscutellum without micropunctures; associated with fungusy rotting wood in older stages of decomposition (Hu and Bogri 2020); 5 spp., key in Hu et al. (2013) ..... ***Quwatanabius*** **Smetana**

– Antennomeres 1–4 without tomentose pubescence; body large (approx. 1 cm or more); ventral head with infraorbital ridge restricted to basal third of head length or less; mesoscutellum with micropunctures; associated with early, fermenting stages of decay such as rotting *Agave* or *Myrtillocactus* (Navarrete et al. 2002), or under the bark of sappy logs **5**

5 Abdomen bicolored red (basal three segments) and black (apical two segments); mesoventrite with horn-like projection; Oriental Region, known from Myanmar and northern Thailand ..... ***Alesiella*** **Brunke & Solodovnikov (*A. lineipennis* (Cameron))**

– Abdomen uniformly dark; mesoventrite without horn-like projection; Neotropical Region, known from Mexico to Costa Rica; 2 spp., notes in Brunke and Solodovnikov (2013) ..... ***Quediomacrus*** **Sharp**

6 Elytra with irregular, coarse and asetose macropunctures; antennomeres 1–5 without tomentose pubescence; 78 spp., keys in Brunke and Solodovnikov (2014), Brunke (2017) ..... ***Bolitogyrus*** **Chevrolat**

– Elytral with macropunctures setose, organized in rows, surface sometimes with scattered micropunctures; antennomeres 1–3 without tomentose pubescence (tomentose pubescence sometimes partly missing on antennae 4) **7**

7 Head with two or more parocular punctures (Fig. 1B, E); infraorbital ridge incomplete, not reaching base of mandible; pronotum with at least two punctures in dorsal row (Fig. 1C, F); Oriental Region.... ***Sundaquedius*** **Brunke, gen. nov.**

– Head with only one parocular puncture; infraorbital ridge complete, reaching base of mandible; pronotum with only one puncture in dorsal row (marginal puncture); Nearctic and Neotropical Regions..... **8**

8 Head, pronotum and elytra distinctly flattened; meso- and metatarsomeres markedly bilobed, transverse; tarsomere 4 reaching half the length of tarsomere 5; occurs under the bark of decaying trees (Brèthes 1900); known only from the Buenos Aires area, Argentina..... ***Parisanopus*** **Brèthes (*P. castaneipennis* Brèthes)**

– Forebody distinctly convex; meso- and meta tarsomeres less strongly bilobed, not transverse; tarsomere 4 not reaching half the length of tarsomere 5; southern half of Nearctic Region and broadly distributed within the Neotropical Region; 23 extant spp., listed in Brunke et al. (2016)..... ***Cyrtoquedius*** **Bernhauer**

Alesiella lineipennis (Cameron, 1932)

Quedius (*Quedionuchus*) *lineipennis* Cameron, 1932
Quedius lineipennis Cameron: Smetana 1988
Alesiella lineipennis (Cameron): Brunke and Solodovnikov 2013

Type locality. Mogok [= Ruby Mines], Mandalay, Myanmar

Non-type material. Thailand: Chiang Rai: Wiang Pa Pao District [no specific locality], 17–21.V.2015, K. Takahashi (1 male, aedeagus missing, cHay).

Diagnosis. Only one species of *Alesiella* is known and can be recognized by characters in the above key to genera. The specimen from Thailand does not differ from the type material (previously studied by the author), though the aedeagus was lost during mounting (Y. Hayashi, pers. comm.).

Distribution. Myanmar and Thailand (new country record).

Bionomics. Nothing is known about this species' microhabitat preferences but it probably occurs under the bark of dead trees in the earlier fermentation states of decay, as does its sister group *Quediomacrus*.

Comments. The above specimen is a new record of the genus and species from Thailand, and represents the first available material in more than 130 years (since 1890). The above record also indicates that the species is certainly still extant and rather widespread, though its elevational range remains unknown. Although the type series only bears the information 'Ruby Mines, Doherty', the diaries of William Doherty (reproduced in Hartert 1901) indicate that they were collected somewhere along the route (1150–1800 m) between the towns of Mogok (= 'Ruby Mines') and Bernardmyo, during 1890. This montane rainforest elevational range is compatible with the general locality of the specimen from Thailand.

***Sundaquedius* Brunke, gen. nov.**
http://zoobank.org/B1952B22-6F67-4717-9C69-74F8C5E5498D
Figs 1A–F, 2A–G

Type species. *Sundaquedius abbreviatus* Brunke, sp. nov.

Etymology. The generic name refers to the Sunda Plate and *Quedius*, with which members of this genus and closely related genus *Cyrtoquedius* were associated with for a long time. Much of the Sunda Plate is currently below sea level but had connected terrestrial species on Borneo, Sumatra, Java and the present southeast Asian mainland in multiple episodes, from about the Eocene to as recently as the Pleistocene (e.g., Inger and Voris 2001). Noun in apposition.

Diagnosis. Among other Oriental Cyrtoquediini, *Sundaquedius* is easily recognized by a combination of the large eyes (more than 3 × as long as temples) (Fig. 1B, E), incomplete infraorbital ridge and elytra with rows of setose punctures. It can be distinguished from its putative close relatives *Cyrtoquedius* and *Parisanopus* by any one of: more than one puncture in the dorsal row of the pronotum (Fig. 1C, F), two or more parocular punctures on the head (Fig. 1B, E), the incomplete infraorbital ridge and presence of peg setae on the paramere (Fig. 2B).

Description. With the character states of Cyrtoquediini (see Brunke et al. 2021) and the following: head with basal puncture present but not doubled; two or three parocular punctures present; antennae non-geniculate, antennomeres 1–3 sparsely pubescent and without tomentose pubescence, antennomere 4 with some tomentose pubescence but much sparser than 5; labrum with two usual lobes and moderately incised median emargination; apical maxillary and labial palpi fusiform, apical labial palpomere with sparse, short setae; mandibles slender in apical half and markedly broad in basal half, bearing a single proximal tooth; gular sutures convergent, separate but running extremely close in basal half; infraorbital ridge/nuchal ridge incomplete, reaching ~ 1/3 to 1/2 the distance to mandible base; pronotum strongly convex, non-explanate and slightly elongate, with 2–8 punctures in the dorsal row, 'second' puncture present; basisternum with pair of macrosetae at middle; mesoscutellum glabrous and without micropunctures; disc of elytra without microsculpture and glabrous, except for three rows of coarse setose macropunctures (one sutural, two discal), rows slightly disorganized due to extra punctures in *S. nigropolitus*; elytra with epipleuron bearing row of coarse, setose macropunctures, epipleuron with additional rows and clusters of coarse setae; epipleural margin not thickened; mesocoxae contiguous; metatibia spinose, with three spines on outer face, inner face without spines; pro- and metatarsomeres with setae on disc, setae not restricted to margins; metatarsomere 4 with ventral setae distinctly interrupted medially and removed from apical margin; abdominal tergite IV with impression but punctures only slightly more impressed, not markedly coarser in impression (as in *Bolitogyrus*); abdominal sternite III with basal transverse line sharply produced posteriad forming an acute angle at middle; abdominal sternite IV with basal transverse line not pro-

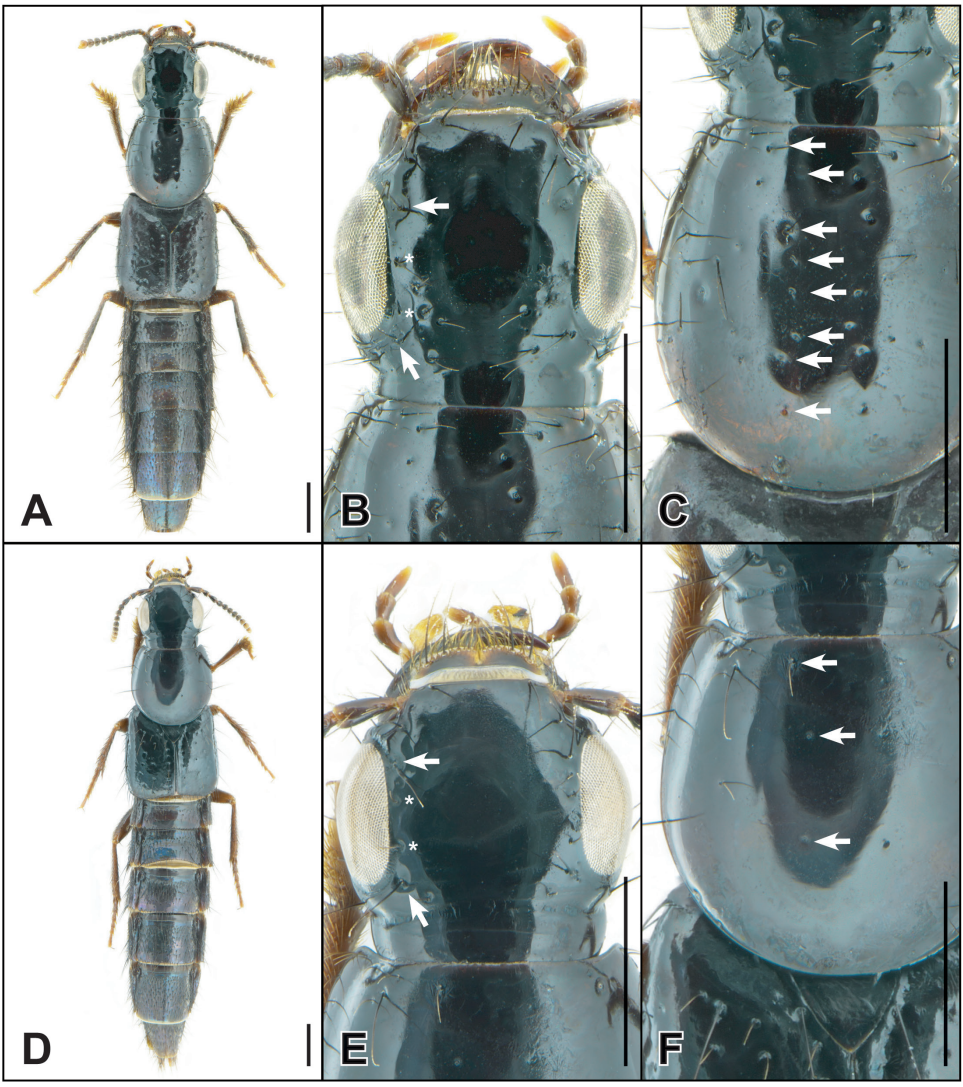

Figure 1. *Sundaquedius* Brunke **A–C** *S. nigropolitus* (Cameron) **D–F** *S. abbreviatus* Brunke **A, D** habitus **B, E** dorsal head, arrows indicating anterior and posterior frontal punctures, asterisks indicating parocular punctures **C, F** dorsal pronotum, arrows indicating punctures of the dorsal row. Scale bars: 1 mm.

duced; aedeagus with single fused paramere bearing well-developed peg setae, internal sac with ventral, paired copulatory sclerites, with an additional sclerotized structure similar to dorsal copulatory piece, but singular, and more weakly sclerotized compared to *Cyrtoquedius* or *Parisanopus*, and held within spinose internal sac.

Distribution. *Sundaquedius* is presently known only from central Vietnam and East Java but likely occurs at medium elevations across southeast Asia, west of Wallace's line.

Bionomics. Nothing is known about the bionomics of this genus, except that both species were collected in lower montane forests (700–1500 m). *Sundaquedius* might be collected by sifting moist litter, like many species of the related genus *Cyrtoquedius*.

Comments. In recent phylogenomic analyses, *Sundaquedius* was recovered as the sister group of Nearctic/Neotropical genus *Cyrtoquedius* with high support, though few genera of Cyrtoquediini were included in the taxon sample (Brunke et al. 2021). *Sundaquedius* is probably most closely related to *Cyrtoquedius*, or perhaps *Cyrtoquedius*+*Parisanopus*, based on morphological similarity (see above key).

Key to species of *Sundaquedius* Brunke, gen. nov.

1 Pronotum with 2 or 3 punctures in the dorsal row (Fig. 1F); head without additional macropunctures (Fig. 1E); elytra with discal rows organized and without scattered punctures between (Fig. 1D); Vietnam ..... ***S. abbreviatus* Brunke sp. nov.**

– Pronotum with 7 or 8 punctures in the dorsal row (1C); head with additional macropunctures (Fig. 1B); elytra with discal rows slightly disorganized, with additional scattered punctures between (Fig. 1A); East Java ..... ***S. nigropolitus* (Cameron)**

***Sundaquedius nigropolitus* (Cameron), comb. nov.**
Figs 1A–C, 2G

Quedius (*Sauridus*) *nigropolitus* Cameron, 1937
'*Quedius*' *nigropolitus* Cameron: Brunke et al. (2021) (in undescribed genus of Cyrtoquediini)

Type locality. Blawan [sometimes 'Belawan'], Ijen Plateau [no specific locality, ca. -7.98, 114.17], Bondowoso Regency, East Java, Indonesia.

Type material. ***Holotype*** (female, NMUK): Type [circular label with red border] / leg H. Lucht, K.O. Blawan, Idjen-Plateau [Ijen Plateau] Java, 900-1500 mr., 12.I.1934 [printed label] / Q. nigropolitus Type Cameron [handwritten] / M. Cameron, Bequest, B.M. 1955-147. [printed label] / AJB0001486 [printed label] / HOLOTYPE *Quedius nigropolitus* Cameron, det. A. Brunke 2021 [red label] / *Sudaquedius nigropolitus* (Cameron) [white label], det. A. Brunke 2021

Diagnosis. *Sundaquedius nigropolitus* can be easily recognized by the dorsal rows of the pronotum, which have seven or eight punctures in each row. The only other known species is allopatric.

Redescription. Measurements ♀ (n = 1): HW/HL 1.23; PW/PL 0.94; EW/EL 1.06; PW/HW 1.13; forebody length 4.8 mm.

Body highly glossy, entirely black, except for yellowish brown apical antennomere, tarsi and apical maxillary and labial palpomeres, abdomen with iridescent sheen ranging from violet to blue.

Head distinctly transverse, with two or three additional punctures mediad of posterior frontal puncture (Fig. 1B). Antennomeres 1–3 elongate, 4 subquadrate, 5 and 6

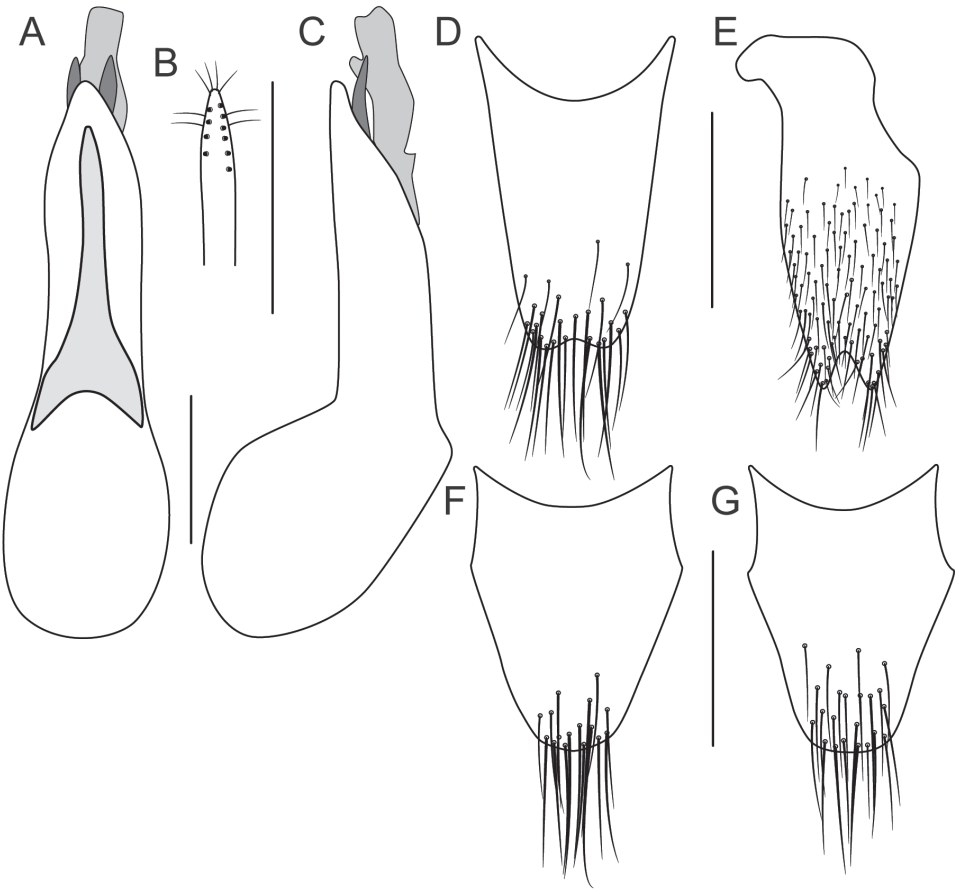

Figure 2. *Sundaquedius* Brunke **A–F** *S. abbreviatus* Brunke **G** *S. nigropolitus* (Cameron) **A** aedeagus, ventral view **B** apex of paramere, underside **C** aedeagus, lateral view (paramere removed) **D** male tergite X **E** male sternite IX **F, G** female tergite X. Scale bars: 0.25 mm (**A–C**); 0.5 mm (**D–G**).

weakly transverse, 7–10 strongly transverse, 10 ~ 2 × as wide as long. Pronotum slightly elongate with seven or eight punctures in the dorsal row, with additional groups of scattered punctures between dorsal and sublateral rows, and between sublateral row and lateral margin (Fig. 1C). Elytra transverse, with additional scattered punctures between the two discal rows (Fig. 1A). Abdominal tergites III–IV with distinct basal impression, tergites III–V with median or medioapical glabrous or sparsely punctate areas, these areas successively becoming smaller toward the apex; abdominal punctures generally coarse, nearly all separated by at least their diameters; tergites with exceedingly fine and dense microsculpture of transverse waves.

Male unknown. Female with tergite X triangular, with slightly narrowed but broadly rounded apex, apical half with many long setae (Fig. 2G).

Distribution. Known only from the type locality in East Java, which is at the northern edge of the plateau.

Bionomics. Nothing is known about this species' microhabitat preferences.

Comments. The holotype of this species was one of the few specimens included from East Java in Cameron's (1937) 'Fauna Javanica'. This region is still extremely poorly collected for Staphylinidae, even more so than West or Central Java.

***Sundaquedius abbreviatus* Brunke, sp. nov.**
http://zoobank.org/CBC36A0B-D8DC-46C0-BB10-84D68131930E
Figs 1D–F, 2A–F

Type locality. 35 km north of An Khê, near Buôn Lưới village, Gia Lai, Vietnam [ca. 14.32, 108.58].

Type material. ***Holotype*** (male, CNC): Vietnam, 35 km N An Khe, Buon Luoi, 2.VII.1984 / AJB0001487 [white label] / HOLOTYPE *Sundaquedius abbreviatus* Brunke, des. A. Brunke 2021 [red label] ***Paratypes*** (5, ZIN): same data as the holotype but with labels: PARATYPE *Sundaquedius abbreviatus* Brunke, des. A. Brunke 2021 [yellow label]. Identifiers: AJB0001334, AJB0001488–1491

Etymology. The species epithet means 'shortened' or 'reduced', and refers to the shorter dorsal rows of punctures on the pronotum compared to *S. nigropolitus*.

Diagnosis. *Sundaquedius abbreviatus* can be distinguished by the presence of only two or three punctures in the dorsal row of the pronotum.

Description. Measurements. Male (n = 2): HW/HL 1.30–1.35; PW/PL 1.06–1.08; EW/EL 1.22–1.24; PW/HW 1.14–1.19; forebody length 4.9–5.4 mm. Female (n = 4): HW/HL 1.25–1.29; PW/PL 1.03–1.10; EW/EL 1.13–1.15; PW/HW 1.21–1.23; forebody length 4.7–5.0 mm.

Similar to *S. nigropolitus* and differing only in the following: antennomeres dark except apical three segments paler, becoming successively paler to antennal apex; maxillary and labial palpi paler, entirely medium reddish brown; head, without additional punctures between named punctures, distinctly transverse, more so in males, head also broader relative to pronotum in males; antennae overall more robust, with apical segments less strongly transverse; pronotum slightly to distinctly transverse, with two or three punctures in the dorsal row, third puncture, when present, smaller, sometimes rudimentary and without seta; elytra more transverse than in *S. nigropolitus*, and even more so in males, with two discal rows and without scattered additional punctures; abdominal tergites III and IV with distinct impressions, V with only vague impression; abdominal punctation slightly denser but punctures generally still well separated.

Male with sternite VII broadly but shallowly emarginate; sternite VIII with slightly deeper emargination and distinct, triangular impressed and glabrous area; tergite X elongate, with distinct shallow emargination, with many long setae at apex (Fig. 2D); sternite IX with bulky, asymmetrical base, apex deeply emarginate (Fig. 2E); median lobe of aedeagus in ventral view subparallel sided, narrowing to rounded, acute apex, paramere with broad base, becoming slender to strongly acute apex (Fig. 2A); median lobe in lateral view with nearly straight ventral face, with short, rounded apical part (Fig. 2C); apex of paramere with short, sparse paired row of marginal peg setae (Fig. 2B); aedeagus with ventral paired copulatory sclerites broadest at base and strongly

narrowed to sharp apex. Female tergite X similar to that of *S. nigropolitus* but with slightly narrower apex (Fig. 2F).

Distribution. Known only from the type locality in the central highlands of Vietnam.

Bionomics. Nothing specific is known about this species but the type locality is at approximately 700–800 m, so this species likely occurs elsewhere in lower montane forests of central Vietnam and possibly adjacent Cambodia.

Indoquediini Brunke & Solodovnikov, 2016

Diagnosis. Indoquediini (as recently redefined by Brunke et al. (2021)) can be recognized among other Staphylininae by the combination of: head with obvious presence of both posterior frontal and basal punctures (Brunke et al. 2019: fig. 1); protibiae subapically with distinct and unique notch (Brunke et al. 2021: fig. 8C); all antennomeres longer than wide.

Key to world genera of Indoquediini

1 Head with interocular punctures present on frons (Brunke et al. 2019: fig. 1); eyes small, less than half the length of temples; pronotum with four punctures in dorsal row; empodial setae absent; Nepal, Pakistan and China ..... ***Strouhalium* Scheerpeltz (*S. gracilicorne* Scheerpeltz)**

– Head without interocular punctures on frons; eyes large, clearly longer than temples; pronotum with two punctures in dorsal row; empodial setae present; western Nearctic, East Palaearctic and Oriental Regions **2**

2 Head and pronotum without microsculpture, highly glossy; head with bulging eyes occupying nearly all of lateral head; East Palaearctic and Oriental Regions; 39 spp., listed by Brunke et al. (2016)..... ***Indoquedius* Blackwelder**

– Head and pronotum with meshed microsculpture creating dull (especially head) appearance; head with eyes smaller and less convex, occupying ~ 2/3 of lateral head (Fig. 3A); western Nearctic.... ***Fluviphirus* Brunke, gen. nov. (*F. elevatus* (Hatch))**

Fluviphirus Brunke, gen. nov.

http://zoobank.org/9E8CF744-6B68-484A-A4D1-4003CF0D291F
Fig. 3A–G

Type species. *Fluviphirus elevatus* (Hatch), comb. nov.

Etymology. The generic name is a combination of the Latin word *fluvium* (river, stream) and *Raphirus* (a subgenus of *Quedius*), where the only species of *Fluviphirus* was previously classified and to which it bears a superficial resemblance. Noun in apposition.

Diagnosis. Among other Indoquediini, *Fluviphirus* is easily recognized by the combination of meshed microsculpture on the forebody and the absence of interocular punctures on the head. It is also the only genus of Nearctic Indoquediini.

Description. With the character states of Indoquediini (see Brunke et al. 2021) and the following: disc of head and pronotum with meshed microsculpture; eyes moderately convex, not strongly bulging, large, distinctly larger than temples (Fig. 3A); head with single basal puncture, interocular punctures absent, temples with numerous smaller punctures, with single parocular puncture; antennomere 3 with dense but not tomentose pubescence; apical maxillary palpomere glabrous; penultimate labial palpomere with brush of dense setae (but sparser than that of *Indoquedius*); pronotum with two punctures in dorsal row, 'second' puncture present (Fig. 3A); postcoxal process fused across inferior marginal line; elytra with sub-basal ridge reduced to horizontal fragment, with evidence of mesoscutellar collar; humeral spines absent; protibia without lateral spines (Fig. 3A); metatibia with only two thin spines on outer face (Fig. 3A); pretarsi of all legs with one pair of empodial setae; abdominal sternite III with basal transverse carina produced posteriad at a sharp angle.

Distribution. Western North America, broadly distributed along the western cordilleras at a variety of elevations.

Bionomics. The single species of *Fluviphirus* is strongly associated with debris along the margins of rivers and larger creeks.

Comments. Smetana (1971a) placed *Q. elevatus* in its own species group as it was "quite isolated within the subgenus [*Quedius* (*Raphirus*)]". The subgenus *Raphirus* remains a convenient dumping ground for many unrelated taxa (Brunke et al. 2021) because of its broad definition, with many plesiomorphic character states, including the absence of certain features typical of other clades within Quediini. Recent phylogenomic analyses recovered *Q. elevatus* as a member of Indoquediini, as the sister group of either *Strouhalium* (coalescent analyses) or *Indoquedius* (concatenated analyses). *Fluviphirus* shares a number of character states with both genera but more densely sampled, total evidence analyses are needed to determine its sister group.

***Fluviphirus elevatus* (Hatch), comb. nov.**
Fig. 3A–G

Quedius (*Sauridus*) *elevatus* Hatch, 1957
Quedius (*Raphirus*) *elevatus* Hatch: Smetana 1971a, b (subgenus *Raphirus*, *elevatus* species group)
'*Quedius*' *elevatus* Hatch: Brunke et al. 2021 (in undescribed genus of Indoquediini)

Type locality. Snoqualmie, Washington, United States.

Type material. The type material of this distinctive species was not examined.

Non-type material. Canada: British Columbia: 8 mi W Creston, ex. river debris, 10.VI.1968, J.M. Campbell & A. Smetana (8, CNC); 20 mi E Hope, ex. river debris, 3.VI.1968, J.M. Campbell & A. Smetana (1, CNC); 4 mi W Midway, ex. river debris, 6.VI.1968, J.M. Campbell & A. Smetana (6, CNC); 16 mi W Osoyoos, ex. river debris, 5.VI.1968, J.M. Campbell & A. Smetana (1, CNC); Paulson, beaver house,

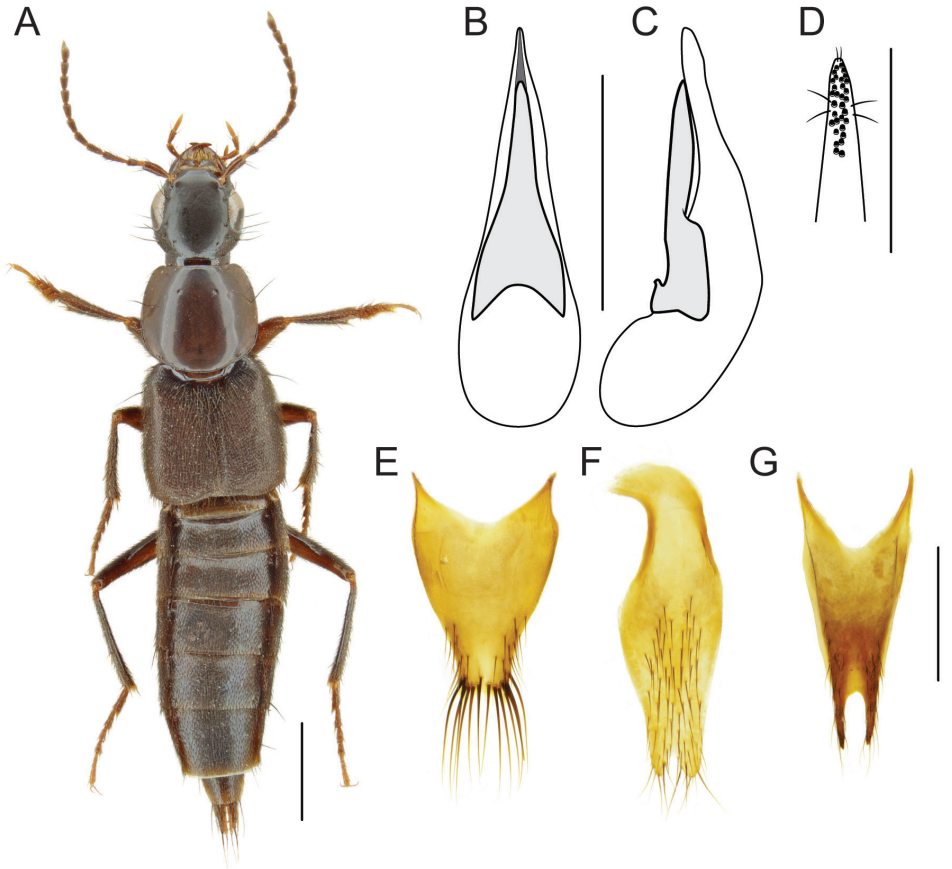

Figure 3. *Fluviphirus elevatus* (Hatch) **A** habitus **B** aedeagus, ventral view **C** aedeagus, lateral view **D** apex of paramere, underside **E** male tergite X **F** male sternite IX **G** female tergite X. Scale bars: 1 mm (**A**); 0.5 mm (**B–C, E–G**); 0.25 mm (**D**).

7.VI.1968, J.M. Campbell & A. Smetana (1, CNC); 4 mi W Rossland, 9.VI.1968, J.M. Campbell & A. Smetana (2, CNC); 2 mi S Salmo, ex. river debris, 9.VI.1968, J.M. Campbell & A. Smetana (3, CNC); 2 mi E Burnt Flats [Burnt Flat Junction], 9.VI.1968 (2, CNC). **United States: California**: *Marin Co.*, Lagunitas Creek at Tocaloma, 18.III.1983, A. Smetana (17, CNC); same except 19.III.1983 (6, CNC). **Oregon**: Union Co., Blue Mts., Phillips Creek Road, 9 km NW Elgin (2, CNC).

Diagnosis. As given above for the genus.

Redescription. The species was redescribed by Smetana (1971a) but this is here supplemented with additional characters specific to the male and female: male with sternite VII unmodified; sternite VIII with broad shallow emargination; tergite X constricted in apical half, with weakly emarginate apex, apical half with short fine setae on lateral parts of disc and strong, coarse setae along apical margin (Fig. 3E); sternite IX

with moderately slender, asymmetrical base, elongate with deep and narrow emargination (Fig. 3F); median lobe of aedeagus in ventral view narrowed to sharp apex, apical portion with longitudinal median excavation (Fig. 3B), paramere with broad base, with elongate triangular apical part and narrow apex (Fig. 3B); aedeagus in lateral view with paramere swollen, slightly deflexed dorsad, median lobe sinuate, narrow, with finlike apex (Fig. 3C); apex of paramere with longitudinal, median cluster of peg setae, extended basad on slight ridge (Fig. 3D). Female with tergite X narrowly elongate, with two-pronged apex, prongs separated by U-shaped emargination (Fig. 3G).

Distribution. Canada: BC. **United States:** CA, ID, NV, OR, WA

Bionomics. Smetana (1971a, b) reported this species from debris near water, especially along larger creeks and rivers. Longer series were found in river drift left behind after periods of high water levels. Several specimens have been found in beaver houses, but it is not known whether they regularly occur there.

Comments. The paratype specimens mentioned by Hatch (1957) from Lenore, Idaho and Pullman, Washington were not examined but indicate this species' distribution is rather broad across the entire Western Cordillera. The occurrence of *F. elevatus* along large river banks at a wide range of elevations suggests a single broadly distributed species. Specimens from California were paler than most of those from British Columbia and Oregon but no consistent differences were observed in the aedeagus.

Acknowledgements

I would like to thank the curators listed in Materials and methods for making specimens under their care available for study. I would also like to thank Aleš Smetana (CNC) for his assistance with Latin and general nomenclature. This study received financial support from A-base funding from the Government of Canada (Agriculture and Agri-food Canada: Systematics of Beneficial Arthropods – J-002276). Two reviewers are thanked for their input, which improved the manuscript.

References

Brèthes FJ (1900) *Parisanopus*, un nouveau genre de Staphylins (Quediaria). Comunicaciones del Museo Nacional de Buenos Aires 1: 215–219.

Brunke AJ (2017) A revision of the Oriental species of *Bolitogyrus* Chevrolat (Coleoptera, Staphylinidae, Staphylininae). ZooKeys 664: 1–97. https://doi.org/10.3897/zookeys.664.11881

Brunke A, Solodovnikov A (2013) *Alesiella* gen.n. and a newly discovered relict lineage of Staphylinini (Coleoptera: Staphylinidae). Systematic Entomology 38: 689–707. https://doi.org/10.1111/syen.12021

Brunke A, Solodovnikov A (2014) A revision of the Neotropical species of *Bolitogyrus* Chevrolat, a geographically disjunct lineage of Staphylinini (Coleoptera, Staphylinidae). ZooKeys 423: 1–113. https://doi.org/10.3897/zookeys.423.7536

Brunke AJ, Chatzimanolis S, Schillhammer H, Solodovnikov A (2016) Early evolution of the hyperdiverse rove beetle tribe Staphylinini (Coleoptera: Staphylinidae: Staphylininae) and a revision of its higher classification. Cladistics 32: 427–451. https://doi.org/10.1111/cla.12139

Brunke AJ, Żyła D, Yamamoto S, Solodovnikov A (2019) Baltic amber Staphylinini (Coleoptera: Staphylinidae: Staphylininae): a rove beetle fauna on the eve of our modern climate. Zoological Journal of the Linnaean Society 187: 166–197. https://doi.org/10.1093/zoolinnean/zlz021

Brunke AJ, Hansen AK, Salnitska M, Kypke JL, Predeus AV, Escalona HE, Chapados JT, Eyres J, Richter R, Smetana A, Ślipiński SA, Zwick A, Hájek J, Leschen RAB, Solodovnikov A, Dettman JR (2021) The limits of Quediini at last (Staphylinidae: Staphylininae): a rove beetle mega-radiation resolved by comprehensive sampling and anchored phylogenomics. Systematic Entomology 46: 396–421. https://doi.org/10.1111/syen.12468

Cameron M (1932) The fauna of British India including Ceylon and Burma. Coleoptera. Staphylinidae. Talyor and Francis, London, xii + 1–443 pp.

Cameron M (1937) Fauna Javanica. The Staphylinidae collected by Mr. F. C. Drescher. Part II. Tijdschrift voor Entomologie 80: 1–37.

Chatzimanolis S, Cohen IM, Schomann AS, Solodovnikov A (2010) Molecular phylogeny of the mega-diverse rove beetle tribe Staphylinini (Insecta, Coleoptera, Staphylinidae). Zoologica Scripta 39: 436–449. https://doi.org/10.1111/j.1463-6409.2010.00438.x

Hartert E (1901) William Doherty, Obituary. Novitates Zoologicae 8: 494–506.

Hatch MH (1957) The beetles of the Pacific Northwest. Part II: Staphyliniformia. University of Washington Press, Seattle, ix + 1–384 pp.

Hu J-Y, Li L-Z, Zhao M-J (2013) A new species of *Quwatanabius* Smetana (Coleoptera, Staphylinidae, Staphylininae) from Guangxi, South China. Zootaxa 3646: 297–299. https://doi.org/10.11646/zootaxa.3646.3.8

Hu F-S, Bogri A (2020) Taxonomic notes on the genus *Quwatanabius* in Taiwan (Coleoptera: Staphylinidae). Zootaxa 4743: 285–288. https://doi.org/10.11646/zootaxa.4743.2.12

Inger RF, Voris HR (2001) The biogeographical relations of the frogs and snakes of Sundaland. Journal of Biogeography 28: 863–891. https://doi.org/10.1046/j.1365-2699.2001.00580.x

Navarrete-Heredia JL, Newton AF, Thayer MK, Ashe JS, Chandler DS (2002) Guía ilustrada para los géneros de Staphylinidae (Coleoptera) de México. Illustrated guide to the genera of Staphylinidae (Coleoptera) of Mexico. Universidad de Guadalajara y Conabio, México, 401 pp.

Smetana A (1971a) Revision of the tribe Quediini of North America north of Mexico (Coleoptera: Staphylinidae). Memoirs of the Entomological Society of Canada No. 79: 1–303. https://doi.org/10.4039/entm10379fv

Smetana A (1971b) Revision of the tribe Quediini of America North of Mexico (Coleoptera: Staphylinidae). Supplementum 1. The Canadian Entomologist 103: 1833–1848. https://doi.org/10.4039/Ent1031833-12

Smetana A (1988) Revision of the tribes Quediini and Atanygnathinini. Part II. The Himalayan region (Coleoptera: Staphylinidae). Quaestiones Entomologicae 24: 163–464

Solodovnikov AY (2006a) Revision and phylogenetic assessment of *Afroquedius* gen. nov. from South Africa: toward new concepts of the genus *Quedius*, subtribe Quediina and reclassification of the tribe Staphylinini (Coleoptera: Staphylinidae: Staphylininae). Annals of

the Entomological Society of America 99: 1065–1084. https://doi.org/10.1603/0013-8746(2006)99[1064:RAPAOA]2.0.CO;2

Solodovnikov A (2006b) Adult and larval descriptions of a new termitophilous genus of the tribe Staphylinini with two species from South America (Coleoptera: Staphylinidae). Proceedings of the Russian Entomological Society St Petersburg 77: 274–283.

Tihelka E, Thayer MK, Newton AF, Cai C-Y (2020) New data, old story: molecular data illuminate the tribal relationships among rove beetles of the subfamily Staphylininae (Coleoptera: Staphylinidae). Insects 11: e164. https://doi.org/10.3390/insects11030164

Żyła D, Solodovnikov A (2020) Multilocus phylogeny defines a new classification of Staphylininae (Coleoptera, Staphylinidae), a rove beetle group with high lineage diversity. Systematic Entomology 45: 114–127. https://doi.org/10.111/syen.12382

ZooKeys 1076: 125–133 (2021)
doi: 10.3897/zookeys.1076.75846
https://zookeys.pensoft.net

RESEARCH ARTICLE

A peer-reviewed open-access journal
ZooKeys
Launched to accelerate biodiversity research

Discovery of the genus *Platycotylus* Olliff, 1883 (Coleoptera, Tenebrionidae) in Japan: Description of a new and remarkable species

Takahiro Yoshida[1], Kiyoshi Ando[2]

1 *Systematic Zoology Laboratory, Department of Biological Sciences, Graduate School of Science, Tokyo Metropolitan University, 1–1 Minami-osawa, Hachioji, Tokyo, 192–0397, Japan* **2** *Entomological Laboratory, Faculty of Agriculture, Ehime University, Tarumi 3–5–7, Matsuyama, 790–8566, Japan*

Corresponding author: Takahiro Yoshida (yoshida_toritoma@yahoo.co.jp)

Academic editor: Aaron Smith | Received 27 September 2021 | Accepted 30 October 2021 | Published 9 December 2021

http://zoobank.org/B653A0D3-C62F-4A17-813E-022EC2C2B5FE

Citation: Yoshida T, Ando K (2021) Discovery of the genus *Platycotylus* Olliff, 1883 (Coleoptera, Tenebrionidae) in Japan: Description of a new and remarkable species. ZooKeys 1076: 125–133. https://doi.org/10.3897/zookeys.1076.75846

Abstract

The genus *Platycotylus* Olliff, 1883 (Coleoptera: Tenebrionidae) is recorded from Japan (Nakanoshima Island, Tokara Islands) for the first time, through the discovery of a new and remarkable species, *Platycotylus merkli* **sp. nov.**, which is described herein. The male of this new species can be distinguished from all known males of other congeneric species by its long and asymmetrical epistomal horn. Although this new species is most similar to *Platycotylus parvicollis* (Pic, 1923), for which a male has not been examined, it can be distinguished from this species by its simple sparse pronotal punctation, smaller eyes, and acutely produced temples.

Keywords

Epistomal horn, Nakanoshima Island, Palorini, taxonomy, Tokara Islands, twisted aedeagus

Introduction

The tribe Palorini Matthews, 2003 was initially proposed by Matthews (2003a) as a new subfamily including 10 genera: *Platycotylus* Olliff, 1883, *Eutermicola* Lea, 1916, *Ulomotypus* Broun, 1886, and the seven genera of "the *Palorus* genus group"

of Halstead (1967), namely *Astalbus* Fairmaire, 1900, *Austropalorus* Halstead, 1967, *Palorinus* Blair, 1930, *Palorus* Mulsant, 1854, *Prolabrus* Fairmaire, 1897, *Pseudeba* Blackburn, 1903, and *Ulomina* Baudi di Selve, 1876. Later, it was downgraded to the rank of tribe by Bouchard et al. (2005), which was confirmed by subsequent authors (e.g., Matthews and Bouchard 2008; Matthews et al. 2010). Two additional palorine genera were later described: the extant genus *Paloropsis* Masumoto & Grimm, 2004 from Japan and the extinct genus *Vabole* Alekseev & Nabozhenko, 2015 from Eocene Baltic amber. Except for several cosmopolitan pest species of stored products, most species of Palorini are absent from the New World (Matthews and Bouchard 2008). Some genera are endemic to principal areas, i.e., two, three, and one genera are endemic to Madagascar, northern Australia, and New Zealand, respectively, suggesting that the ancestor of this tribe occurred in Gondwana before it broke up (Matthews and Bouchard 2008; Alekseev and Nabozhenko 2017).

The genus *Platycotylus* was established within the family Cucujidae by Olliff (1883) based on a single species, *Platycotylus inusiatus* Olliff, 1883. Doyen (1984) added *Doliema nitidula* Macleay, 1872 (= *Platycotylus nitidulus*) to this genus and implied that this genus was probably closely related to the genus *Lorelus* Sharp, 1876 (Tenebrionidae: Lagriinae). Subsequently, *Platycotylus* was finally assigned to the family Tenebrionidae and placed within the tribe Triboliini Gistel, 1848 (Tenebrioninae) by Doyen et al. (1990). Matthews (2003a, 2003b) included *Platycotylus* in the taxon currently regarded as Palorini (as presented above).

Platycotylus is composed of five species that are widespread in Africa, Southeast Asia, and Australia (Merkl 1992; Schawaller 2014). Two species, *Platycotylus ferrugineus* Kaszab, 1939 and *P. nitidulus*, have been recorded in Taiwan (Ando et al. 2016). All species have flattened bodies and are believed to live under hardly loosened bark of dead trees like laemophloeids, silvanids, and salpingids (Schawaller 2014; Alekseev and Nabozhenko 2017). In this study, we describe a new and morphologically remarkable species, *Platycotylus merkli* sp. nov., from Nakanoshima Island, Tokara Islands, Japan, which represents the first record of this genus in Japan.

Materials and methods

Morphology, dissection and photographic techniques

Observations of external characteristics and dissections were conducted using stereoscopic microscopes (Nikon SMZ1500 or Leica MZ16). The habitus images of the holotype (Fig. 1) were taken with a digital camera (Canon EOS 7D) fitted with a macro-objective (MP-E 65 mm) before dissection, and composite images of adults were produced using the automontage software Combine ZM and completed in Photoshop 6.0 (Adobe Systems Inc.). The abdomen of the holotype was removed and soaked in a 10% potassium hydroxide solution at room temperature overnight. After it was rinsed in water, the soaked abdomen was dissected under a stereoscopic

microscope (Nikon SMZ1500) using fine insect pins; specifically, the male genital organs were detached for observation. The dissected parts were mounted in Euparal on a slide and observed under an optical microscope (Nikon Eclipse E400). After observations were completed, the dissected genitalia and other abdominal segments were mounted in Euparal on a glass coverslip glued to a piece of cardboard and pinned with the relevant specimen.

Terminology, abbreviations and specimen deposition

Morphological terminology follows Matthews and Bouchard (2008). Examined specimens were deposited in the Ehime University Museum, Matsuyama, Japan (**EUMJ**).

Taxonomy

Order Coleoptera
Family Tenebrionidae
Tribe Palorini

***Platycotylus merkli* sp. nov.**
http://zoobank.org/324CF110-BE9C-400A-B497-AAA134298431
Figures 1–3
Japanese name: Tsuji-hirata-hime-kokunusutomodoki

Type specimen. ***Holotype:*** ♂, Japan, Kagoshima Prefecture, Toshima Village, Tokara Islands, Tokara-Nakanoshima Island, Nanatsuyama, 7.VII.2019, leg. Naomichi Tsuji, "under permission" (EUMJ).

Differential diagnosis. According to Merkl (1992), the epistome structures of males are important diagnostic characteristics for *Platycotylus* species. All known *Platycotylus* males present a pair of short tubercles at the middle of the epistome, except for *Platycotylus palmi* Ferrer, 1998 (absent; see Ferrer 1998). Therefore, aside from species of which males have not been examined [*Platycotylus parvicollis* (Pic, 1923) and *Platycotylus tenuicollis* (Fairmaire, 1893)], this new species can be distinguished from all other males of congeneric species by its long and asymmetrical epistomal horn.

The new species is most similar to *P. parvicollis*, of which a male has not yet been examined. It can be distinguished by the simple sparse punctation on the pronotum (laterally rugulose in *P. parvicollis*; see Merkl 1992) and by elytra that are scarcely striate, with elytral intervals that are neither convex nor carinate (striate in the original description of *P. parvicollis*; Pic 1923). Additionally, the smaller eyes and acutely produced temples of the new species differ from those of *P. parvicollis*.

In addition, the umbilical tubercle on the center of mentum may be one remarkable characteristic of this new species. At least, there is no such tubercle on the mentum of *P. nitidulus*, which has a small fovea in the middle.

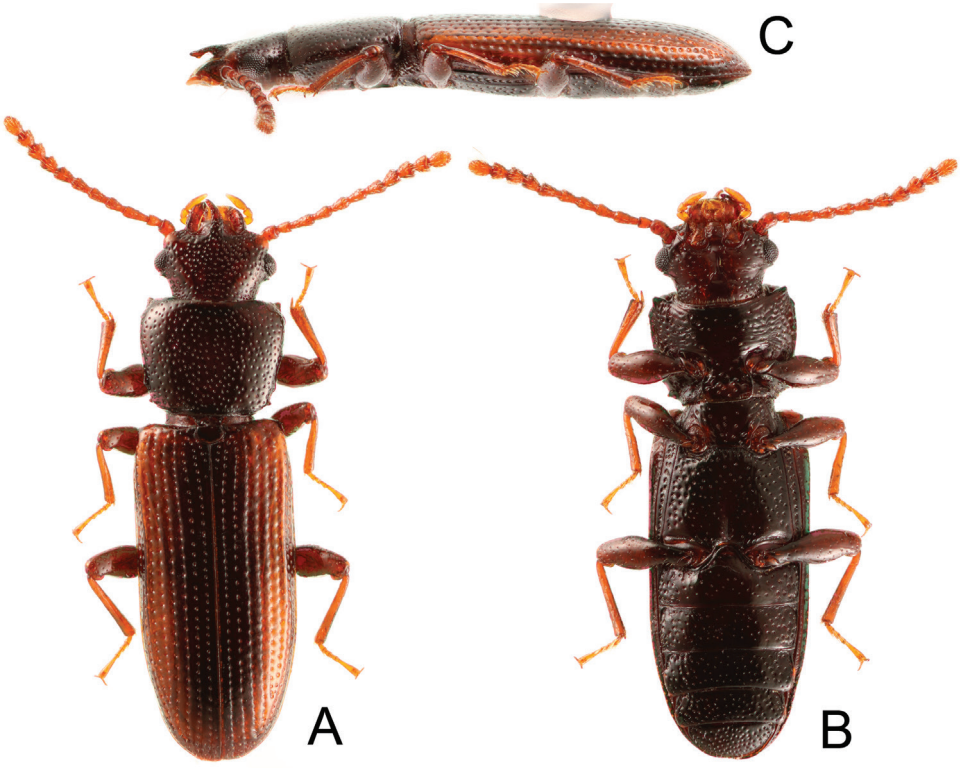

Figure 1. Habitus of *Platycotylus merkli* sp. nov., holotype, male **A** Dorsal **B** ventral **C** lateral.

Description. Body length: 3.40 mm. Male. Elongate and flattened, shiny; dark reddish brown, head and pronotum blackish brown, elytra darkened on sutural and lateral parts.

Head obtrapezoidal, weakly convex, without frontogenal and frontoclypeal sutures; punctures coarse and dense, partly piligerous; epistome with a large asymmetrical horn in middle, distinctly emarginate on both sides of the horn, which is distinctly curved to the left and acute at its apex, with a long yellow seta arising from each emarginated anterior margin, covered with punctures; genae convex, roundly produced laterad; frons broadened, weakly convex, slightly sloping forwards, 3.83 times as wide as width of eye in lateral view; eyes entirely lateral, strongly convex laterad, without inner ocular sulci; temples slender, acutely produced laterad, setiferous and finely punctate. Antennae slender, surpassing base of elytra, almost filiform though 7th antennomere dilated apicad and 8th to 10th ones dilated and nearly as long as wide; 11th antennomere elongate. Ultimate maxillary palpomeres fusiform. Mentum transversely quadrate, weakly convex, irregularly depressed at sides, with an umbilical tubercle at middle. Submentum flat, subquadrate, strongly emarginate at sides. Gula narrow, linguiform, unevenly flat and smooth.

Pronotum obtrapezoidal, widest at apical fifth and 1.30 times as wide as long; disc slightly convex, densely punctate, punctures piligerous laterally, nearly as large as and

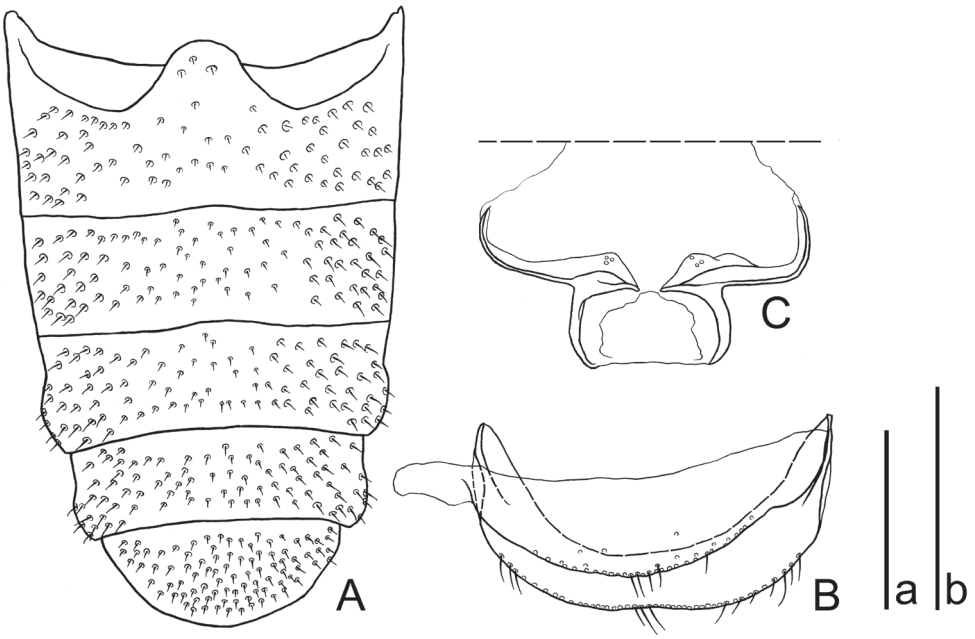

Figure 2. Abdominal segments of *Platycotylus merkli* sp. nov., holotype, male **A** Ventrites **B** 8th segment, ventral view **C** 9th sternite, ventral view. Scale bars: 1.0 mm **a** (**A**); 0.5 mm (**B, C**).

slightly sparser than on head; anterior margin subtruncate, unbeaded; anterior corners with an acutely pointed process; lateral margins slightly rounded and evenly convergent posteriad, almost invisible in dorsal view, roundly and weakly edged at apical fifth and basal fifth, slightly sinuate before base, very finely beaded; posterior corners with processes smaller than those on anterior corners and acutely pointed laterad; basal margin weakly rounded, moderately beaded. Scutellar shield transverse, 1.67 times as wide as long, surface flat and smooth.

Elytra elongate, subparallel-sided, widest at basal sixth and 2.14 times as long as their combined width, subvertical between 7th intervals and lateral margins; surface scarcely striate, with rows of punctures larger than on pronotum; intervals almost flat and impunctate; epipleura irregularly rugulose.

Prothoracic hypomera weakly depressed, with large and coarse piligerous punctures. Prosternum weakly convex, distinctly sulcate along apical bead, sparsely punctate in middle and moderately so laterally; prosternal process trapezoidal, depressed, coarsely punctate. Mesoventrite weakly convex, with large and sparse piligerous punctures. Metaventrite weakly convex, sparsely and evenly punctate though becoming denser and piligerous in each lateral fourth. Abdomen (Fig. 2A) with punctures piligerous, fine and dense; lateral margins of 3rd and 4th ventrites weakly and roundly produced in each apical half; 5th ventrite evenly rounded at posterior margin.

Abdominal sternites VIII and IX (Fig. 2B, C); sternite VIII thin, with short setae along posterior margin; sternite IX with a pair of horizontally elongate sclerites,

with an elongate protrusion on the apical third of each sclerite that is slightly curved inwards. Aedeagus (Fig. 3) lanceolate, very short, 0.11 times as long as elytra, slightly twisted towards left side of body, obsoletely margined between basale and apicale; basale 1.07 times as long as apicale; apicale rounded at apex.

Legs robust. Femora strongly dilated towards middle or distally, sparse with setiferous punctures. Tibiae short and slender; protibiae with two tibial spurs, one of which is very large and robust, curved posteriorly.

Female. Unknown.

Etymology. The new species is dedicated to the late Dr Ottó Merkl, who made a significant contribution to the taxonomy of Tenebrionidae.

Distribution. Japan: Tokara Islands (Nakanoshima Island).

Biological notes. The holotype was collected by beating the dead branches of an unidentified living tree.

Key to species of the genus *Platycotylus* (after Merkl 1992 and Schawaller 2014)

1 Pronotal surface between punctures and elytral intervals shagreened (microreticulated)..... ***P. ferrugineus*** **(Kaszab, 1939)**

– Pronotal surface and elytral intervals smooth and shiny **2**

2 Antennomere 11 elongate, at least 3 times longer than wide, pronotum flat . ..... ***P. tenuicornis*** **(Fairmaire, 1893)**

– Antennomere 11 only 2 times longer than wide, pronotum convex **3**

3 Pronotum more transverse, with distinctly prominent anterolateral corners .. .. ***P. nitidulus*** **(MacLeay, 1872)**

– Pronotum less transverse, subquadrate or trapezoidal, with short anterolateral corners..... **4**

4 Pronotum longer, trapezoidal, elytral interval 7 convex... *P. palmi* (Ferrer, 1998)

– Pronotum subquadrate or obtrapezoidal, elytral interval 7 keeled **5**

5 Eyes moderate in size, temple not produced, pronotum laterally with rugulose punctation, elytra striate ..... ***P. parvicollis*** **(Pic, 1923)**

– Eyes smaller, temple acutely produced, pronotum laterally with simple sparse punctation, elytra scarcely striate..... ***P. merkli*** **sp. nov.**

Abdominal pits and male genital morphology

Matthews and Bouchard (2008) regarded the abdominal pits of the palorine male and the inverted aedeagus as two autapomorphies of Palorini. However, the abdominal pits were absent on the males of *Platycotylus* examined by Masumoto and Grimm (2004). The male of *P. merkli* sp. nov. also does not possess these pits, indicating that they are lacking in the genus *Platycotylus*.

The male genital structures of *Platycotylus* have been poorly studied only in two species: *P. palmi* by Ferrer (1988) and *P. nitidulus*, with a simple illustration by Matthews and Bouchard (2005). The shapes of the aedeagi of these species are similar to each other and inverted, although the orientation of the aedeagus of *P. palmi* has yet

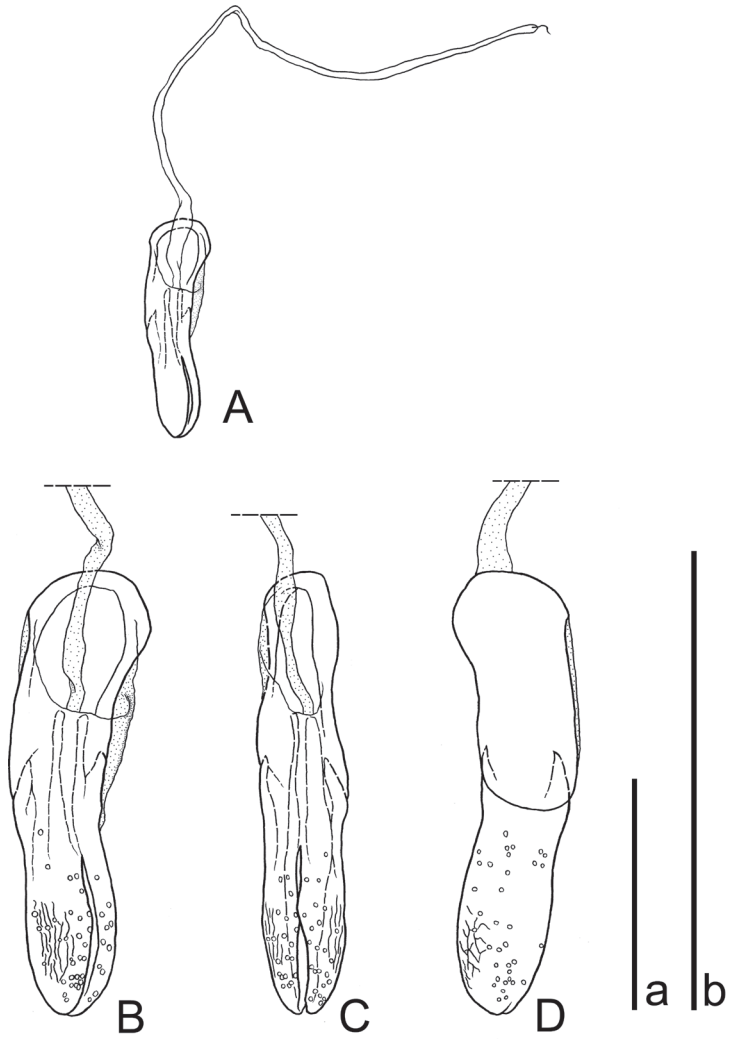

Figure 3. Aedeagus of *Platycotylus merkli* sp. nov., holotype **A, B** Dorsal **C** dorsolateral **D** ventral. Scale bars: 0.5 mm **a** for **A**; **b** for **B–D**.

to be examined. Nevertheless, the shape of the aedeagus of *P. merkli* sp. nov. is lanceolate, twisted in the middle, and with the basale slightly longer than the apicale (Fig. 3). Thus, the genital morphology of *P. merkli* sp. nov. is substantially different from that of its congeners, which highlights the systematic peculiarity of this new species.

A similar pattern of variation in male genital morphology is shown in a lineage of Erotylidae (Cucujoidea), which is mainly found on the male cones of cycad plants and contains three genera: *Cycadophila* Xu, Tang & Skelley, 2015, *Pharaxonotha* Reitter, 1875, and *Ceratophila* Tang, Skelley & Pérez-Farrera, 2018. Males of *Cycadophila* possess an aedeagus that is twisted towards the left side, whereas the other genera possess inverted male genitalia (Xu et al. 2015; Tang et al. 2020). Tang et al. (2020) suggested

that these shapes and orientations of the genitalia may be related to the mating position (side-to-side or end-to-end) as an adaptation to mating in the tight spaces of cycad cones. These authors also indicated that these morphological adaptations had evolved independently in each genus. The twisted aedeagus of the new species described here, as well as the inverted aedeagus of the tribe in general, may be associated with the habitat of the insect, i.e., under the hardly loosened bark of dead branches. Further studies on these habitats, as well as on the mating behavior and genital morphology of Palorini, are required.

Acknowledgements

We wish to express our hearty thanks to the late Dr Ottó Merkl for his valuable collaboration during the early stages of this project. We cordially thank Mr Naomichi Tsuji (Entomological Laboratory, Kyushu University, Fukuoka) for donating the important specimen to EUMJ and Dr Wolfgang Schawaller (Staatliches Museum für Naturkunde, Stuttgart) for providing valuable information on the genus *Platycotylus*. We also cordially thank Dr Wolfgang Schawaller and Dr Patrice Bouchard (Agriculture and Agri-Food Canada, Ottawa) for their improvement of the manuscript. We thank Enago (http://www.enago.jp) for the English language revision. Takahiro Yoshida was partly supported by a Research Fellowship of the Japan Society for the Promotion of Science for Young Scientists (JSPS Research Fellowships for Young Scientists, PD: JP19J00167).

References

Alekseev VI, Nabozhenko MV (2017) *Palorus platycotyloides* sp. n., the second fossil representative of the tribe Palorini (Coleoptera: Tenebrionidae) from Baltic amber. Acta Zoologica Bulgarica 69(2): 167–170.

Ando K, Merkl O, Jeng M-L, Chan M-L, Hayashi Y (2016) Catalogue of Formosan Tenebrionidae (Insecta: Coleoptera). Japanese Society of Systematic Entomology, Supplementary series 1: 1–112.

Bouchard P, Lawrence JF, Davies AE, Newton AF (2005) Synoptic classification of the world Tenebrionidae (Insecta: Coleoptera) with a review of family-group names. Annales Zoologici 55(4): 499–530.

Doyen JT (1984) Reconstitution of the Diaperini of North America, with new species of *Adelina* and *Sitophagus* (Coleoptera: Tenebrionidae). Proceedings of the Entomological Society of Washington 86(4): 777–789.

Doyen JT, Matthews EG, Lawrence JF (1990) Classification and annotated checklist of the Australian genera of Tenebrionidae (Coleoptera). Invertebrate Taxonomy 3: 229–260. https://doi.org/10.1071/IT9890229

Ferrer J (1998) *Thurea palmi* gen. & spec. nov. a new representative of the tribe Lagriini in Africa (Coleoptera, Tenebrionidae). Nouvelle Revue d'Entomologie (NS) 15: 151–154.

Halstead DGH (1967) A revision of the genus *Palorus* (sens. lat.) (Coleoptera: Tenebrionidae). Bulletin of the British Museum (Natural History) 19: 61–148. https://doi.org/10.5962/bhl.part.28300

Masumoto K, Grimm R (2004) A new genus and a species of Palorinae (Coleoptera: Tenebrionidae) from Japan. Entomological Review of Japan 59(1): 120–130.

Matthews EG (2003a) *Ulomotypus* Broun a member of the new subfamily Palorinae, with remarks on *Aphtora* Bates and *Demtrius* Broun (Coleoptera, Tenebrionidae). New Zealand Entomologist 26: 7–14. https://doi.org/10.1080/00779962.2003.9722104

Matthews EG (2003b) The *Palorus* group – a new subfamily of Tenebrionidae (Insecta, Coleoptera). Spixiana 26: 49–50. https://doi.org/10.1080/00779962.2003.9722104

Matthews EG, Bouchard P (2008) Tenebrionid beetles of Australia: description of tribes, keys to genera, catalogue of species. CSIRO Publishing, Canberra, 398 pp.

Matthews EG, Lawrence JF, Bouchard P, Steiner WE, Ślipiński A (2010) Tenebrionidae Latreille, 1802. In: Leschen RAB, Beutel RG, Lawrence JF (Eds) Handbook of Zoology, Coleoptera, Beetles. Vol. 2. Morphology and Systematics (Elateroidea, Bostrichiformia, Cucujiformia partim). Walter de Gruyter, Berlin/New York, 574–658. https://doi.org/10.1515/9783110911213.574

Merkl O (1992) Tenebrionidae (Coleoptera) from Laos and Vietnam, with reclassification of Old World 'Doliema'. Acta Zoologica Academiae Scientiarum Hungaricae 38: 261–280.

Olliff AS (1883) VIII. Remarks on a small collection of Clavicorn Coleoptera from Borneo, with descriptions of new species. Transactions of the Royal Entomological Society of London 31(2): 173–186. https://doi.org/10.1111/j.1365-2311.1883.tb02944.x

Pic M (1923) Nouveautés diverses. Mélanges Exotico-entomologiques, 40: 3–32.

Schawaller W (2014) The genus *Platycotylus* Olliff (*Thurea* Ferrer, syn. nov.) in Kenya and South Africa (Coleoptera: Tenebrionidae: Palorini). Annals of the Ditsong National Museum of Natural History 4(1): 51–53. https://hdl.handle.net/10520/EJC149082

Tang W, Xu G, Marler T, Khuraijam JS, Singh R, Lindström AJ, Radha P, Rich S, Nguyen KS, Skelley PE (2020) Beetles (Coleoptera) in cones of cycads (Cycadales) of the northern hemisphere: diversity and evolution. Insecta Mundi 0781: 1–19. https://journals.flvc.org/mundi/article/view/124503

Xu G, Tang W, Skelley P, Liu N, Rich S (2015) *Cycadophila*, a new genus (Coleoptera: Erotylidae: Pharaxonothinae) inhabiting *Cycas debaoensis* (Cycadaceae) in Asia. Zootaxa 3986: 251–278. https://doi.org/10.11646/zootaxa.3986.3.1

ZooKeys 1076: 135–150 (2021)
doi: 10.3897/zookeys.1076.75932
https://zookeys.pensoft.net

RESEARCH ARTICLE

A peer-reviewed open-access journal
ZooKeys
Launched to accelerate biodiversity research

The re-description of *Synoecnema hirsutum* Timm, 1959 (Synoecneminae, Ungellidae, Drilonematoidea) from a pheretimoid earthworm in Vietnam with the analysis of its phylogenetic relationships

Elena S. Ivanova[1], Boris D. Efeykin[1,2], Sergei E. Spiridonov[1,2]

1 *Centre of Parasitology of the Severtsov Institute of Ecology & Evolution, Russian Academy of Sciences, Leninski pr. 33, Moscow 119071, Russia* **2** *Joint Russian-Vietnamese Tropical Scientific and Technological Center, Cau Giay, Hanoi, Vietnam*

Corresponding author: Boris D. Efeykin (bocha19@yandex.ru)

Academic editor: Steven Nadler | Received 29 September 2021 | Accepted 15 November 2021 | Published 9 December 2021

http://zoobank.org/2A221BC4-5EE7-4603-AA6B-98C313CB3DCF

Citation: Ivanova ES, Efeykin BD, Spiridonov SE (2021) The re-description of *Synoecnema hirsutum* Timm, 1959 (Synoecneminae, Ungellidae, Drilonematoidea) from a pheretimoid earthworm in Vietnam with the analysis of its phylogenetic relationships. ZooKeys 1076: 135–150. https://doi.org/10.3897/zookeys.1076.75932

Abstract

Synoecnema hirsutum Timm, 1959 (Ungellidae, Drilonematoidea), found in the body cavity of the pheretimoid earthworm at the border of Laos and Vietnam, was re-described and illustrated. The mitochondrial genome of *S. hirsutum* obtained with Illumina HiSeq sequencing is the first annotated mitochondrial genome as a representative of the superfamily Drilonematoidea. The phylogeny inferred from the analysis of 12 mitochondrial genes has shown some similarity of *S. hirsutum* with a cephalobid *Acrobeloides varius*.

Keywords

Drilonematids, ungellids, earthworms, Vietnam, mitochondrial genome, phylogeny

Introduction

Recent phylogenetic analyses have shown that multiple (18 according to Viney 2017) separate occasions of transition to parasitic lifestyle had occurred in the evolutionary history of nematodes. Phylogenetic relationships of parasitic nematodes and free-living representatives of this phylum can reveal the evolutionary pathways of the acquisition of parasitism in this group of animals. However, the evolutionary history of the most numerous group of parasitic nematodes – the order Rhabditida (formerly the subclass or the class Secernentea) still remains a puzzle. The analysis of contemporary literature demonstrates that different groups of parasites have been studied in a very inconsistent manner with the bias on the parasitic nematodes of humans, domesticated animals and plants versus the parasitic nematodes of economically-unimportant invertebrates. The latter are also poorly presented in the mitochondrial genome phylogenetic research.

It is evident that evolutionary processes of parasitism acquisition are not anchored to the organisms important for humans and the study of neglected groups of parasites and their hosts can reveal interesting evolutionary patterns. One of such groups is the Drilonematoidea, one of the larger nematode taxa with still unresolved phylogeny. It hosts the highly specialised and diverse group of coelomic parasites of earthworms (Annelida, Clitellata). The impressive diversity of the nematodes, parasitic in earthworms, was discovered and described by R.W. Timm (1959, 1962, 1966, 1967), preceded by earlier reports by Dujardin (1845), Cobb (1928), Chitwood and Lucker (1934) and Baylis (1943). A separate superfamily Drilonematoidea was established to incorporate the species using the earthworms as the definitive and single hosts (Chitwood and Chitwood 1950). The first attempts to infer the phylogeny of the earthworm-parasitic nematodes from the analysis of nucleotide sequences demonstrated the polyphyletic nature of Drilonematoidea (Spiridonov et al. 2005; Ivanova and Spiridonov 2011, 2015, 2016). Based on the SSU phylogeny, the Creagrocercidae family was classified into Plectida i.e. outside Rhabditida, while the rest of the superfamily into the infraorder Cephalobomorpha within clade IV according to Blaxter et al. (1998), either to the suborder Tylenchina, together with Panagrolaimorpha and Tylenchomorpha (De Ley and Blaxter 2004). Today, the mitochondrial genome phylogeny is seen as a valuable tool in the resolution of the relationships between taxa (Zou et al. 2017; Kern et al. 2020; Kim et al. 2020), as well as in the understanding of nematode parasitism (Viney 2017). Viney emphasises the importance of comparing related forms with different lifestyles to identify genes or gene families that changed. The Drilonematoidea hosting exclusively parasitic forms represents the separate case within Cephalobomorpha with its majority of free-living forms inhabiting a variety of land habitats. To date, the only cephalobomorph mt complete genome sequenced is that of *Acrobeloides varius* Kim, Kim & Park, 2017 (Kim et al. 2020), a typical free-living nematode.

Within Drilonematoidea, the family Ungellidae (ungellids) is the most speciose taxon with the morphology profoundly changed by the parasitic lifestyle. These nematodes are characterised by the presence of cephalic hooks, expanded glandular structures in the enlarged tail portion of the body, degeneration of a spicular appara-

tus in males and thick-walled eggshells. They are very rare in earthworms inhabiting temperate regions, but found in the earthworm taxa of tropics and subtropics. Such geographical distribution of ungellids is a serious obstacle to the examination of this group with modern techniques.

The species of *Synoecnema* (Ungellidae) was found by S. E. Spiridonov in the body cavity of a pheretimoid earthworm collected in Vietnam at the border with Laos in April 2019. The genus *Synoecnema* had been established by de Magalhães in 1905 to accommodate a nematode species (*S. fragile*) found in the body cavity of an earthworm and characterised by the presence of a pair of cephalic hooks. Its taxonomic status was revised by Baylis and Daubney (1926) who assigned four species of *Dionyx* also recovered from the earthworm coelomic cavities and described by Pierantoni (1916), to *Synoecnema*. Later, Baylis (1943) had considered their decision unjustified because males of at least two of *Dionyx* species featured a spicular apparatus lacked by *S. fragile*. Since *Dionyx* had been a preoccupied name used for a coleopteran, Baylis (1943) proposed the new genus *Onychonema* for the accommodation of Pierantoni's *D. cognetti*, *D. minuta*, *D. guinensis* and *D. acutifrons*, leaving *S. fragile* as the type species of *Synoecnema* and describing four more species of the latter. Further on, Timm (1962), revising *Synoecnema*, transferred species *O. acutifrons* and *O. guinensis* back to *Synoecnema* noting that Baylis overlooked the lack of a spicular apparatus in the *O. acutifrons* male attached to a female in a permanent copula and the great similarity of *O. guinensis* females to that of all known species of *Synoecnema*. *Onychonema* Baylis, 1943 with its remaining *O. cognetti* and *O. minutum* was considered *insertae sedis* by Spiridonov and Ivanova (2005). The latter authors also synonymised *Siconemella* Timm, 1967, erected to accommodate related forms with larger cephalic hooks, with *Synoecnema*.

So far, all species of *Synoecnema* were found in coelomic cavities of tropical earthworms belonging to Megascolecoidae (mainly) and Drawidae and collected in South America, Papua New Guinea, India and Southeast Asia. To date, the genus *Synoecnema* Magalhães, 1905 accounts for 20 species: *S. fragile* Magalhães, 1905, *S. acutifrons* Pierantoni, 1916, *S. anseriforme* Timm, 1959, *S.* (= *Siconemella*) *burmensis* Timm, 1967, *S. drawidae* Baylis, 1943, *S. gatesi* Timm, 1962, *S. guinensis* Pierantoni, 1916, *S. hirsutum* Timm, 1959, *S. hoplochaetellae* Baylis, 1943, *S. laotense* Spiridonov, 1993, *S. modigliani* Ivanova & Spiridonov, 1989, *S. perionychis* Baylis, 1943, *S. pheretimae* Baylis, 1943, *S.* (= *Siconemella*) *philippinensis* Timm, 1967, *S. pingi* Ivanova & Spiridonov, 1989, *S. robustum* Ivanova & Spiridonov, 1989, *S. rodericensis* Ivanova & Spiridonov, 1989, *S. tsiliensis* Ivanova & Spiridonov, 1989, *S. tuliemense* Ivanova and Pham Van Luc, 1989 and *S. watinagii* Ivanova, Sumaya & Spiridonov, 2015.

To date, the latter species is the only member of the genus molecularly characterised. It is suggested that new discoveries in the morphology and genetics of the members of the genus may bring the need for further revision. The quantity of material collected allowed us to obtain enough material to provide the extended molecular analysis aimed at the resolution of relationships between higher taxa of Drilonematoidea, parasites of earthworms.

Materials and methods

Nematode material. Earthworms were collected at Muóng Lát, Thanh Hóa Province, VietNam (20°31'N, 104°56'E) in April 2019 and dissected alive. Fourteen specimens of the earthworm host species were examined and all were found infected by 2–80 nematodes (av. 14). All nematodes were presented by adult stages with the majority found in a state of a permanent copula, characteristic to the genus. Nematodes were located in the body cavity along the whole host body with the majority occupying anterior segments, were not attached to the septae, but were nearly immobile and responded to the dissection of the host by slight twitching soon followed by its distortion, bursting and death. For the morphological examination, about 20 specimens were fixed by hot 4% formalin and the rest by 96% ethanol for molecular studies.

Nematodes, preserved in formalin, were processed by anhydrous glycerine for light microscopy as described by Seinhorst (1959). Light microscopic studies and drawings were done using a Nikon Eclipse 200 microscope equipped with a drawing attachment. Illustrations were prepared using a WACOM Intuos A4 USB drawing tablet and Adobe Illustrator CS5. For the SEM studies, formalin-preserved material was dehydrated, critical point-dried and coated with gold. Images were taken on a Tescan CamScan MV 2300 and Mira3 Tescan. The voucher specimen (the female), under accession number 14283, was deposited in the Museum of the Helminthological Collections of the Centre of Parasitology at the Severtsov Institute of Ecology and Evolution, Moscow.

Molecular characterisation and phylogenetic analysis

DNA from the frozen nematode samples was isolated using the QiAmp Micro Kit (Qiagen) according to a standard protocol. DNA library preparation was implemented using the NEBNext Ultra II DNA Library Prep Kit for Illumina (New England Biolabs, Ipswich, MA, USA). The DNA quality was checked with Qubit 3.0, final library length distribution and checking for the absence of adapters was performed using Bioanalyzer 2100 (Agilent, Santa Clara, CA, USA). Sequencing was performed on Illumina HiSeq 4000 system with a 150 bp read length at the Skoltech Genomics Core Facility (https://www.skoltech.ru/research/en/shared-resources/gcf-2/).

The quality of raw reads was evaluated using FastQC (Andrews 2010). After filtering by quality, the remaining readings were cleared by removing cDNA synthesis adapters and sequence adapters by processing with the Trimmomatic programme. *De novo* assembly was implemented using Velvet (Zerbino et al. 2010) with the default settings. The resulting contigs were filtered by length and contigs with the most similarity in size to mitochondrial DNA were selected. Assembled sequences of protein-coding genes were checked for internal stops in PCGs manually. The contigs were annotated using the MITOS web server (Bernt et al. 2013), with the default settings. Prediction of protein-coding genes and rRNA genes was done by using a combination

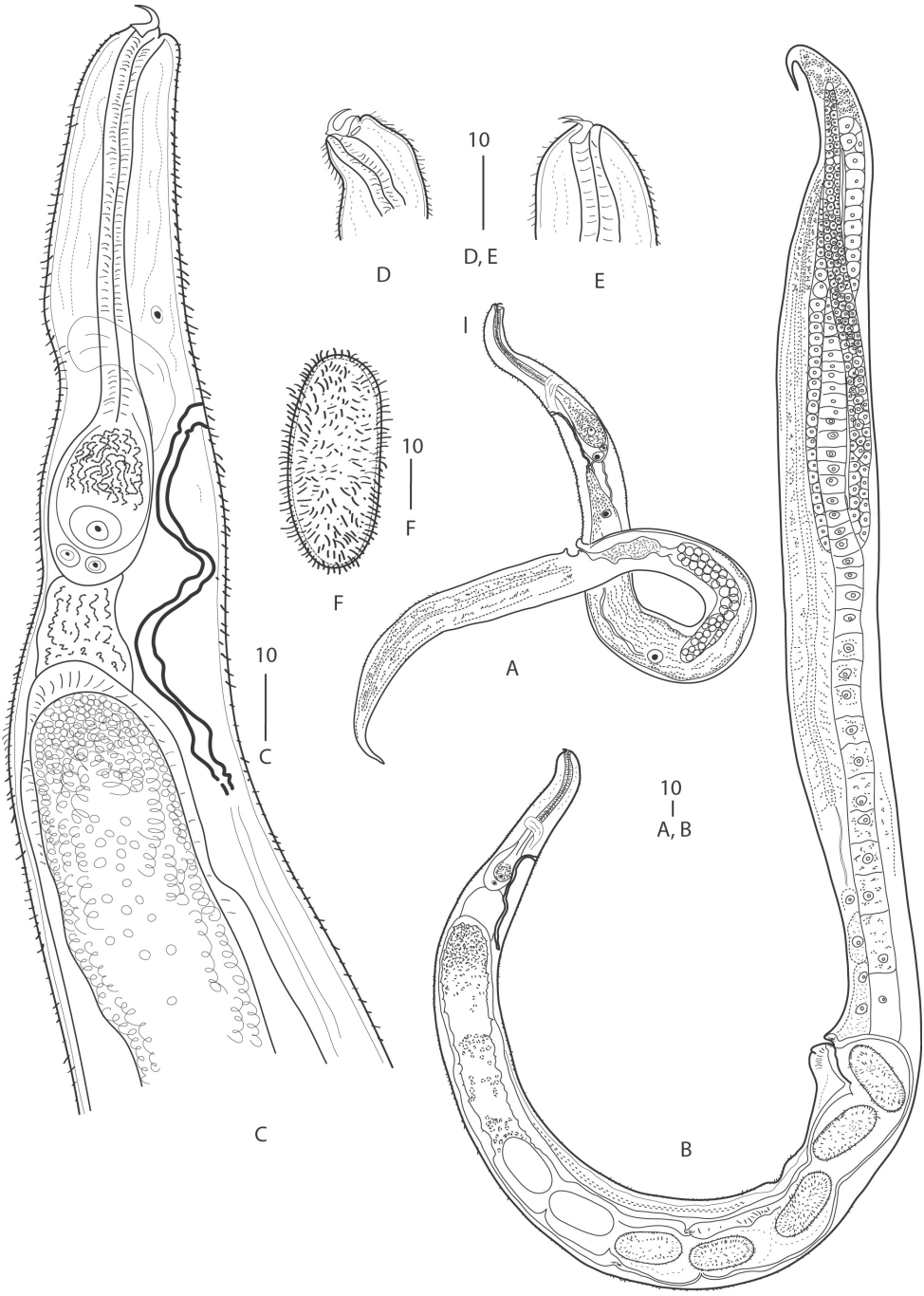

Figure 1. *Synoecnema hirsutum* Timm, 1959 **A** entire male **B** entire female **C** pharynx region of female **D-E** head region of females **F** egg. All in lateral position. Scales in μm.

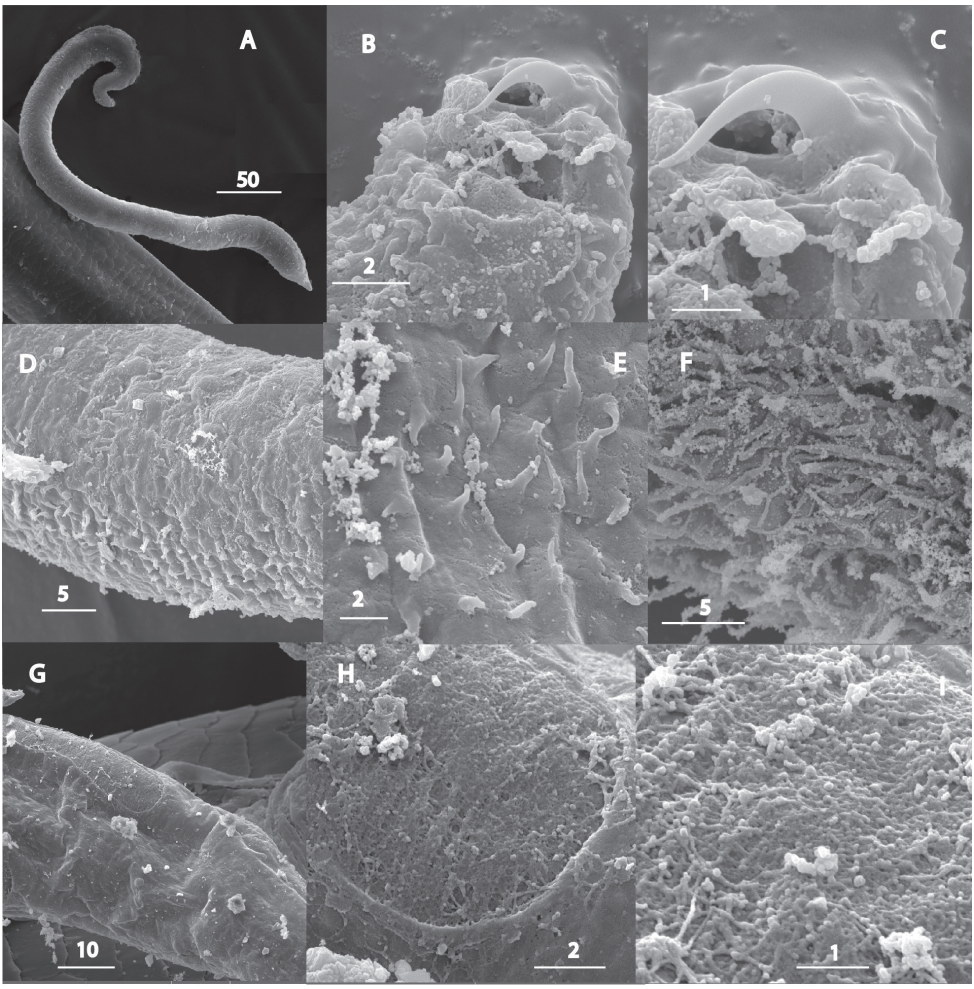

Figure 2. *Synoecnema hirsutum* Timm, 1959. SEM images. Male **A** entire worm **B-C** cephalic hooks **D-F** patches of cuticle covered with setae (**D-E** at mid-body **F** at anterior) **G-H** caudal organ at posterior **I** surface of caudal organ. Scales in μm.

of BLAST and MITOS online software. Concatenated nucleotide alignment of 12 protein-coding genes was performed using GENEIOUS PRIME 2019.1 (Biomatters Ltd., Auckland, New Zealand).

Phylogenetic reconstructions were conducted from the alignment of 12 protein-coding genes with *Limulus polyphemus* and *Lithobius forficatus* as outgroups. For multiple alignments of AA sequences, the nucleotide sequences of each of the protein-coding genes were initially translated into AA with MEGA6. Conserved regions in the alignments of the 12 PCGs were selected using the GUIDANCE2 server (Sela et al. 2015). The final alignment included 3568 out of 3926 AA, representing 90.8% of the original sequence alignment. Optimal evolutionary models were chosen by Parti-

tionFinder (Lanfear et al. 2012). Maximum Likelihood (ML) analysis was performed using IQ-TREE web server (Trifinopoulos et al. 2016) with 10,000 ultrafast bootstrap replicates (Hoang et al. 2018). Additionally, the coalescence-based analysis was carried out to test different phylogeny inference approaches. Phylogenetic analysis was performed for the datasets, based on separate protein-coding genes of the mitochondrial genome. The trees were visualised using TREEVIEW (Page 1996) and FIGTREE v.1.4.2 (http://tree.bio.ed.ac.uk/software/figtree/).

Description

Synoecnema hirsutum Timm, 1959

General. ***Adults.*** Small nematodes lacking sexual dimorphism in body shape and of anterior end structure. Body almost cylindrical, tapering to both ends. Cuticle thin, transversely striated, bearing diverse short setae and spike-like outgrowths variously distributed in different specimens. Epidermis thick. Lateral fields absent. Anterior end curved bearing small paired cephalic hooks. Hooks sub-terminal, curved, thickened and directed dorsad. Hook base ca. 2 μm long, hook blades ca. 3 μm long, closely positioned with distal tips slightly diverging and directed towards or parallel to hook base. Cephalic sensilla indistinct. Amphids discernible in several specimens; apertures situated closely to hook base, elliptical, 1–2 μm wide. Mouth shifted ventrad; stoma absent. Pharynx clavate with long thin muscular corpus and large muscular-glandular pear-shaped terminal bulb displaced dorsally. Isthmus not expressed. Nerve ring encircling posterior of corpus. Excretory pore 1 μm wide, level with nerve ring, excretory duct strongly cuticularised, extending beyond bulb base, paired excretory canals weakly cuticularised, passing through very large excretory gland which can be tracked at least to mid-body. Intestine discernible at anterior, cardia-like structure present. Caudal organs long shallow grooves situated mid-laterally on the surface of posterior half of body; grooves' surface lacking cuticle. No duct inside caudal organ observed. Tail extremity conical. Sexes often permanently in copula.

Female: N = 9. Body length = 1185 ± 138 (1014–1385) μm; a = 22.2 ± 3 (19–28); b = 11.2 ± 1.5 (9–13.2); max width = 64 ± 7 (55–75) μm; pharynx length = 107 ± 10 (93–123) μm; basal bulb height = 34 ± 3 (30–38) μm; basal bulb width = 19 ± 2 (16–22) μm; nerve ring from apex = 61 ± 10 (50–75) μm; excretory pore from apex = 74 ± 15 (54–101) μm; spermatheca from apex = 139 ± 18 (120–176) μm; V% = 44.5 ± 0 (36.1–49.5); egg length = 47 ± 2 (43–49) μm; egg width = 20 ± 1 (18–22) μm.

Anterior end tapering from pharyngeal base level. Pharyngeal procorpus 4–5 μm wide. Prodelphic, monodelphic. Postvulval body region very slightly swollen. Multilobed gland of obscure function present at posterior portion of body behind vulva, in some specimens hindering observation of gonad track and entwining gonad branches. Ovary distal cell situated close to tail extremity. Ovary running anteriad to the level of postvulval region, then turning posteriad to the point of distal

cell and then turning again anteriad where it runs straight ahead until reflexing at some distance (about corresponding body diameter) behind pharynx base. At reflexion, gonad forming large, not distinctly offset spermatheca (av. size 56 µm × 34 µm), followed by thick-walled oviduct and spacious thin-walled uterus. Spermatheca filled with large spermatozoa ca. 2 µm in diameter. Vulva pre-equatorial, on slight protuberance, anterior vulval flap enlarged, vagina absent and vulva opens immediately into uterus. No post-uterine sack present. Eggs ovoid, arranged in a single row, 3–5 with fully-developed eggshells at a time. Fully-developed eggshells 1 µm thick densely covered with spikes 2 µm long. Tail pointing posterior to ovary distal cell; portion of tail free of gonad short. Rectum and anus indiscernible. Caudal organs extending from vulva level to nearly end of tail.

Male: N = 5. Length = 624 ± 77 (517–725) µm; a = 18.5 ± 0.7 (17.8–19.1); b = 5.3 ± 1.1 (3.9–6.1); c = 2.8 ± 9.5 (2.2–3.1); c' = 7.9 ± 2.7 (6–10.9); max width = 36 ± 3 (32–38) µm; pharynx length = 129 ± 25 (103–167) µm; basal bulb height = 36 ± 3 (32–40) µm; basal bulb width = 18 ± 2 (15–20) µm; nerve ring from apex = 73 ± 1 (72–74) µm; excretory pore from apex = 73 ± 11 (60–82) µm; testis reflexion from apex = 316 ± 102 (260–497) µm; testis reflexion length = 64 ± 18 (40–83) µm; tail length = 240 ± 51 (201–328) µm.

Very similar to females in general appearance and morphology of anterior end and caudal organs, but much smaller and slimmer, especially at posterior. Monorchic. Testis reflexed at anterior third of body level. Flexure short and wide. Spermatocytes rounded, ca. 5 µm in diameter, arranged distally in two rows. Proximal part of reproductive system not distinctly differentiated into *vas deferens* and ejaculatory duct. Spicular apparatus and gubernaculum absent. Anal flaps developed unequally, anterior flap inflated and hook-like, while posterior one much smaller, partly overhanging indentation posterior to anus. No caudal sensilla detected. Caudal organ structure and position similar to that of females.

Remarks on morphology

The examination of the present species has shown its strong similarity to *S. hirsutum* Timm, 1959 in the general morphology, i.e. body proportions, the shape and size of cephalic hooks and eggs and the cuticle appearance. In terms of morphometrics, there are a few smaller differences which include: the slightly larger body size (1014–1385 µm vs. 0.70–1.09 mm, females and 517–725 µm vs. 512–654, males), the longer male tail (201–328 µm vs. 160–244 µm) and the slightly more posterior vulva position (36.1–49.5 vs. 34.8–46.5%) (see Table 1). Contrary to Timm (1959), we did not observe an anus in any female specimen. Therefore, we concluded it was absent or indistinct. Describing *S. anseriforme* and *S. hirsutum*, Timm (1959) discovered in females a median ventral pore located posterior to a vulva. The pore was interpreted by the author as an additional excretory pore due to the absence of a distinct intestine and rectum in these nematodes. Later, Timm (1966) re-appraises such a ventral pore

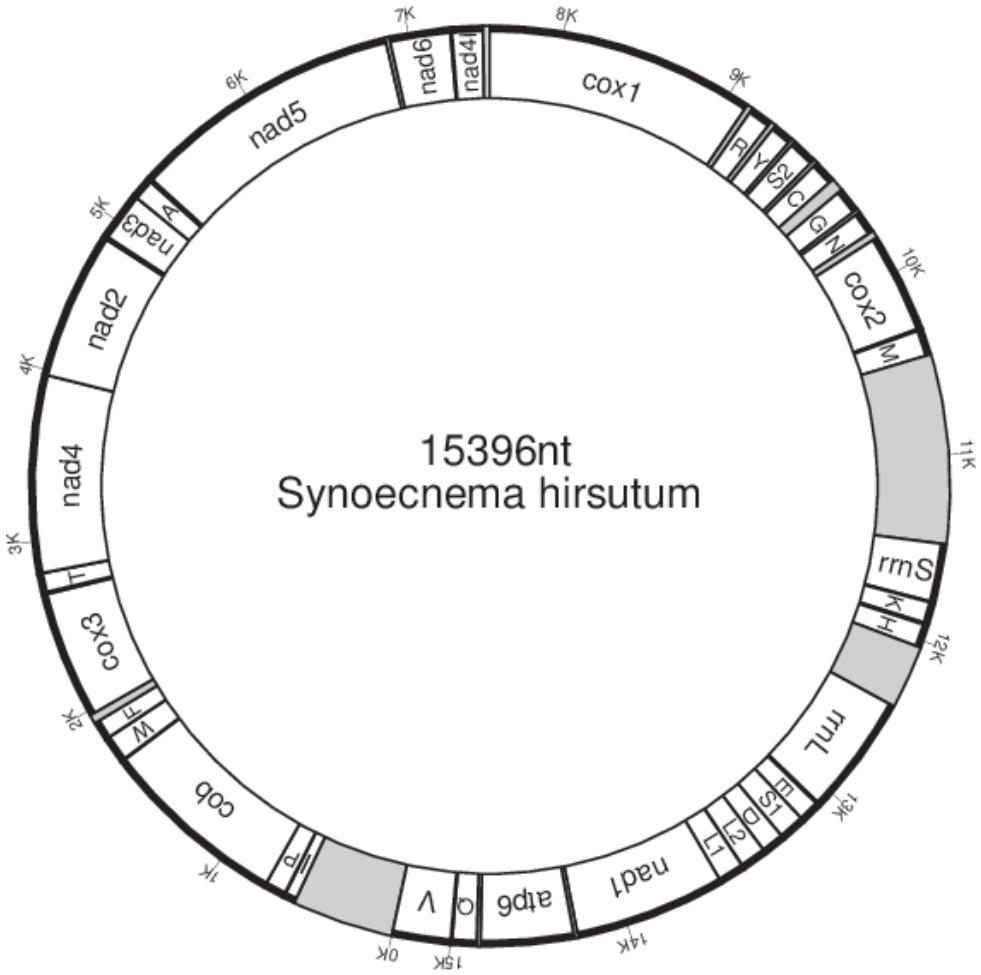

Figure 3. Map of the mitochondrial genome of *Synoecnema hirsutum*. Non-coding areas are shaded.

of *S. anseriforme* as an anal aperture, but does not mention *S. hirsutum*. He also notes that an anal aperture is absent in the rest of the *Synoecnema*.

For *S. anseriforme* females, Timm (1959) also describes pocket-like phasmids or "suckers" and depicts similar structures for a female of *S. hirsutum*, but after re-examination of all known *Synoecnema* species of Baylis (1934) and Timm (1959, 1962), comes to the conclusion that "all have small cephalic hooks and lack distinct suckers in both sexes, with the exception of *S. drawidae* Baylis, 1934 in which the female has long narrow suckers with a slit-like opening". In many illustrations to the species of *Synoecnema*, both of Baylis and Timm, the long narrow slits were depicted (though not explained) extending along the posterior body portion of a nematode. Further on, Ivanova and Spiridonov (1987), Ivanova and Pham Van Luc (1989) and Spiridonov (1993) described similar structures in *Synoecnema* species using light microscopy as

long, slit-like caudal organs surrounded by a modified (fibrous) tissue. Structure of similar slits/grooves in *S. watinagii* and an undescribed *Synoecnema* from pheretimoid hosts was examined with the aid of scanning microscopy (Ivanova et al. 2017; unpubl.). The slits were deep (immersed in body wall) or shallow, all located mid-laterally and extended from mid-body to near end of the tail. The surface of a slit was devoid of a cuticle. No sucker-like structures were observed.

As the chief diagnostic feature of *S. hirsutum* seems to be the presence of setae covering the body of the nematode which also is a characteristic trait of the *Synoecnema* from our material, we tend to assume that both nematodes belong to the same species.

The term "caudal organ" was used when describing caudal structures of yet unknown function in nematodes of Drilonematoidea (Spiridonov et al. 2007; Ivanova and Neuhaus 2009; Ivanova and Bain 2013). Ivanova et al. (2017) discussed its possible function and pointed out the uniqueness of this structure in *Synoecnema* along with the simplifying of many other morphological traits.

Multigene analysis of *Synoecnema hirsutum* phylogenetic relationships

The results of the multigene phylogenetic analysis of *Synoecnema hirsutum* relationships are presented in Fig. 4. The monophyly of Chromadoria nematodes, included in this analysis, is strongly supported as also the monophyly of the phylum Nematoda (Fig. 4). In this ML phylogenetic tree, *S. hirsutum* formed a clade under maximal bootstrap support with a soil free-living nematode *Acrobeloides varius* (Kim et al. 2020). As the mitochondrial data for the only other acrobelid studied, *A. complexus* (KM192361), are incomplete, they were not used in the analysis. The clade *Synoecnema+Acrobeloides* clustered with tylenchids under maximal bootstrap support. Contrary to expectations, the combined clade of tylenchids + *Synoecnema* + *Acrobeloides* remained outside of the larger clade containing all other Rhabditida (sensu De Ley and Blaxter 2002) and the two studied Plectidae (*Plectus aquatilis* and *P. acuminatus*). Additionally, a clade containing oxyurids and spirurids was in a similarly detached position. Such topology with the basal position of the clade (tylenchids + *Synoecnema* + *Acrobeloides*) was also observed in the trees inferred from the analysis of single mitochondrial genes *atp*6, *cox*I, *co*b, *nad*3, *nad*5 and *nad*6 (data not shown). The phylograms inferred from analyses of other mitochondrial genes (*cox*2, *cox*3, *nad*1 *nad*2, *nad*4 and *nad*4*L*) demonstrated more traditional basal position of plectids vs. all other representatives of Rhabditida. Coalescent analysis (not shown) demonstrated the great similarity with the ML tree (Fig. 4).

An arrangement of the genes in the mitochondrial genome of *Synoecnema hirsutum*

The circular molecule of complete mitochondrial genome has been reconstructed from separate contigs (Fig. 3). With the length of 15396 bp, this circular genome contains 12 protein-encoding genes, 22 transport RNA genes, two ribosomal sequences and three non-coding regions.

Figure 4. Phylogenetic relationships of *Synoecnema hirsutum* inferred from Maximum Likelihood analysis of concatenated dataset of 12 mitochondrial protein-coding genes.

Discussion

The superfamily Drilonematoidea is a taxon representing a quite exotic and not easily obtainable group of parasites. Due to little or no molecular data available for the majority of their taxa, relationships within four families constituting Drilonematoidea

are still not phylogenetically resolved. Likewise, it is true concerning two subfamilies of Ungellidae (Ungellinae and Synoecneminae) where the present species belongs. The family Ungellidae has been split into Synoecneminae accommodating species lacking male spicular apparatus and Ungellinae housing ones with spicules and a gubernaculum (Spiridonov and Ivanova 2005). While no molecular data are available for Ungellinae, a limited number of molecular data was obtained for three out of 10 genera of Synoecneminae, namely *Synoecnema*, *Siconema* and *Drasico* Ivanova, Ganin & Spiridonov, 2014. The phylogenetic analysis, based on the D2-D3 region, confirmed the validity of all three genera (Ivanova et al. 2014, 2015).

Limited molecular data are available for some of the other higher taxa of Drilonematoidea and include several SSU and LSU sequences for two representatives of Homungellidae and representatives of three genera of Drilonematidae. The previous phylogenetic analyses were not in full agreement with the classification, based on morphology and topologies, showing the different positions on the phylogenetic tree for parasites from lumbricid and non-lumbricid earthworm hosts. The 'lumbricid' parasites were presented by *Dicelis* species from the Drilonematidae family (*D. lovatiana* Ivanova, 1993; *D. kimmeriensis* Ivanova, 1993; *D. rubidi* Ivanova, 1994; *D. caledoniensis* Spiridonov, Ivanova & Wilson, 2005; *D. ussuriensis* Spiridonov, Ivanova & Wilson, 2005) and were separated from the rest of Drilonematoidea phylogenetically representing a terminal branch of cephalobid phylogeny (Spiridonov et al. 2005; Ivanova and Spiridonov 2016). The rest of the sequences presented by 'non-lumbricid' parasites grouped together, uniting different families of Drilonematoidea.

In the present study, we aimed to overcome the limitations of the previous molecular phylogenetic analyses using a multigene analysis, based on 12 protein-encoding genes. Earlier, it has been shown that some mitochondrial genes are not suitable for the analysis of phyletic links between higher taxa because of saturation (Blouin et al. 1998). Still, we expected the wider set of genes to bring sufficient discriminatory power to reveal the phylogenetic relationships within Drilonematoidea. The close position of the ungellid *Synoecnema hirsutum* to the cephalobid *Acrobeloides varius* in the present analysis corresponds to the previous topologies (Ivanova et al. 2014, 2015), based on 18S and 28S rDNA. Some details of the phylogenetic tree contradict the traditional views on the nematode phylogeny. Thus, in the multigene phylogram (Fig. 4), plectids were found clustering only with a certain part of the order Rhabditida (precisely with the representatives of infraorders Ascaridomorpha, Diplogasteromorpha, Panagrolaimomorpha, Rhabditomorpha and aphelenchids). Oxyuridomorpha, Spiruromorpha and tylenchids, along with the cephalobid *Acrobeloides varius* and the ungellid *Synoecnema hirsutum*, were closer to the base of the nematode tree, thus making the order Rhabditida (sensu De Ley and Blaxter 2002) polyphyletic. Such topology was supported in some phylograms inferred from single mitochondrial genes (*atp*6, *cox*I, *co*b, *nad*3, *nad*5 and *nad*6), but not supported in other (*cox*2, *cox*3, *nad*1 *nad*2, *nad*4 and *nad*4*L*). The multigene tree also demonstrated several patterns not common for traditional (pre-molecular) taxonomy of nematodes. In this tree, Tylenchoidea and Aphelenchoidea formed independent, not closely related clades, thus showing the polyphyly of Tylenchina. Such a phylogenetic pattern was reported in other analyses of

nematode phylogeny, based on complete mitochondrial genomes (Sun et al. 2014; Kim et al. 2015). It can be added that, in the phylogenies inferred from the analysis of 18S rDNA sequences (van Megen 2009), the tylenchid nematodes and the majority of aphelenchids formed two independent clades (clade 10B vs. 12A+12B). The previously-reported polyphyly of Spirurina (Liu et al. 2013) is even less surprising, as very few (if any) morphological features speak in favour of the entity of this morphologically- and ecologically-diverse group. In our phylogram, previously reported splitting of true spirurids vs. the clade (ascaridids + cucullanids + heterakids) was also evident.

Previous attempts to find the place for ungellids and other Drilonematoidea in the system of Nematoda were based on nuclear ribosomal sequences only (Spiridonov et al. 2005, 2007; Ivanova and Spiridonov 2011; Ivanova et al. 2012; 2014;). First, LSU and SSU analyses had confirmed that the earthworm parasites from the family Creagrocercidae were not related to the rest of Drilonematoidea (Drilonematomorpha of De Ley and Blaxter 2002), but appeared to be close to *Domorganus* Goodey, 1947 (Ohridiidae, Plectida) (Ivanova, Spiridonov 2011). Further on, it was shown that at least two evolutionary lines of Drilonematoidea were related to Cephalobomorpha. Each of the lines, according to these phylogenetic reconstructions, evidently has independent roots in the free-living representatives of this infra-order. The obtained results, inferred from the multigene analysis of *S. hirsutum* in this study, support the previous topology, showing its close relations to the cephalobid *A. varius*. The clade, consisting of these two nematodes, was strongly supported (100%) in the ML tree. The length of branches leading to these nematodes and related tylenchids is quite long, which can be regarded as a sign of lengthy independent evolution. As biological traits of *S. hirsutum* and *A. varius* are markedly different, it is reasonable to question whether they can be the result of so-called a 'long branch attraction'. Still, we believe that the obtained topology reflects the true phylogenetic relationships between ungellids and cephalobids. Common features in the arrangement of genes in the mitochondrial genome can be considered as an additional argument in this case. Indeed, only *A. varius* and *S. hirsutum* have a joint cluster of genes *nad*5 - *nad*6 - *nad*4L (Fig. 5). Though joint genes *nad*6 and *nad*4L are characteristic for different Rhabditomorpha, Ascaridomorpha and Diplogasteromorpha (Kim et al. 2020), the junction of three genes without intermittent transport RNA genes makes it a unique feature of these ungellids and cephalobids.

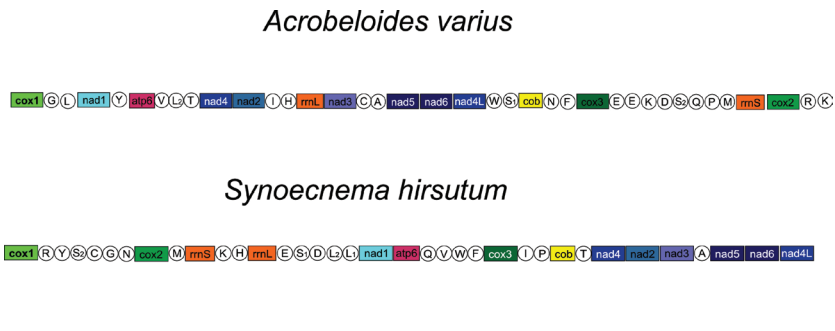

Figure 5. Linear maps of the mitochondrial genomes of *Synoecnema hirsutum* and *Acrobeloides varius.*

Data availability

The assembled mitochondrial genome is deposited in NCBI GenBank under accession MG294556. Protocols are deposited in protocols.io under: https://doi.org/10.17504/protocols.io.bv4gn8tw

Acknowledgements

We gratefully acknowledge the financial support from the Russian Science Foundation grant [19-74-20147].

References

Andrews S (2010) FastQC: a quality control tool for high throughput sequence data. http://www.bioinformatics.babraham.ac.uk/projects/fastqc

Baylis HA (1943) Some nematode parasites of earthworms from the Indo-Malay region. Parasitology 35: 112–127. https://doi.org/10.1017/S0031182000021491

Baylis HA, Daubney R (1926) A synopsis of the families and genera of Nematoda. London. 277 pp. London: Printed by Order of the Trustees of the British Museum. https://doi.org/10.2307/3271710

Bernt M, Donath A, Jühling F, Externbrink F, Florentz C, Fritzsch G, Pütz J, Middendorf M, Stadler PF (2013) MITOS: improved de novo metazoan mitochondrial genome annotation. Molecular Phylogenetics and Evolution 69: 313–319. https://doi.org/10.1016/j.ympev.2012.08.023

Blaxter ML, De Ley P, Garey JR, Liu LX, Scheldeman P, Vierstraete A, Vanfleteren JR, Mackey LY, Dorris M, Frisse LM, Vida JT, Thomas WK (1998) A molecular evolutionary framework for the phylum Nematoda. Nature 392: 71–75. https://doi.org/10.1038/32160

Chitwood BG, Chitwood MB (1950) An introduction to nematology (Revised edition). Monumental Printing Co. Baltimore. 213 pp.

Chitwood BG, Lucker JT (1934) *Dicelis nira*, new species (Nematoda: Drilonematidae). Proceedings of Helminthological Society of Washington 1: 39–44.

Dujardin F (1845) *Histoire naturelle des helminthes ou vers intestinaux*. Paris, XVI + 654 pp. https://doi.org/10.5962/bhl.title.10123

Cobb NA (1928) *Ungella secta* gen. nov., sp. nov., a nemic parasite of the Burmese Oligochaete (earthworm) *Eutyphoeus rarus*. Journal of the Washington Academy of Sciences. Contribution to the Science of Nematology 18: 394–397.

De Ley P, Blaxter ML (2004) A new system for Nematoda: combining morphological characters with molecular trees, and translating clades into ranks and taxa. Nematology Monographs and Perspectives 2: 633–653. https://doi.org/10.1163/9789004475236_061

De Ley P, Blaxter ML (2002). Systematic position and phylogeny. In D Lee (Ed.)The Biology of Nematodes (pp. 1–30). London: Taylor & Francis. https://doi.org/10.1201/b12614-2

Hoang DT, Chernomor O, Von Haeseler A, Minh BQ, Vinh LS (2018) UFBoot2: improving the ultrafast bootstrap approximation. Molecular Biology and Evolution 35: 518–531. https://doi.org/10.1093/molbev/msx281

Ivanova ES, Spiridonov SE (1989) New species of *Synoecnema* (Drilonematoidea, Ungellidae) – parasitic nematodes of tropical earthworms *Pheretima* (Oligochaeta, Megascolecidae). In: Ryss, A Yu (Ed.). Tylenchidy i rhabditidy rasteniy i nasekomykh. Trudy Zoologicheskogo Instituta AN SSSR 194: 106–120.

Ivanova ES, Pham Van Luc (1989) *Synoecnema tuliemense* sp.n. (Nematoda, Ungellidae) from earthworms of Vietnam. Vestnik Zoologii 3: 7–11.

Ivanova ES, Pham Van Luc, Spiridonov SE (2012) Two new species of *Siconema* (Drilonematoidea: Ungellidae) parasitic in earthworms in Vietnam, and systematic relationships as inferred from ribosomal sequence data. Zootaxa 3344: 47–59. https://doi.org/10.11646/zootaxa.3344.1.3

Ivanova ES, Bain O (2012) A new genus and six new species of Ungellidae (Rhabditida: Drilonematoidea) parasitic in earthworms from West Africa and Haiti. Nematology 14: 457–481. https://doi.org/10.1163/156854111X612180

Ivanova ES, Ganin GN, Spiridonov SE (2014) A new genus and two new nematode species (Drilonematoidea, Ungellidae, Synoecneminae) parasitic in two morphs of *Drawida ghilarovi* Gates, 1969, endemic earthworm from the Russian Far East. Systematic Parasitology 87: 231–248. https://doi.org/10.1007/s11230-014-9471

Ivanova ES, Sumaya NH, Spiridonov SE (2015) *Synoecnema watinagii* (Drilonematoidea: Ungellidae: Synoecneminae), a new nematode species parasitic in earthworms from the Philippines with the first molecular and SEM data for the genus Zootaxa 3957: 120–130. http://dx.doi.org/10.11646/zootaxa.3957.1.10

Ivanova ES, Spiridonov SE (2015) Four new species of Iponematinae (Drilonematidae, Drilonematoidea, Cephalobomorpha) parasitic in earthworms: description and molecular affiliations Nematology. 17: 1207–1227. https://doi.org/10.1163/15685411-00002936

Ivanova ES, Spiridonov SE (2016) New data on morphology and molecular affiliations of two species of *Dicelis* Dujardin, 1845 (Cephalobomorpha, Drilonematoidea) parasitic in lumbricids. Russian Journal of Nematology 24: 117–126.

Ivanova ES, Spiridonov SE (2011) Two new species of creagrocercid nematodes parasitic in earthworms, with comments on the phylogenetic affiliations of the Creagrocercidae Baylis, 1943. Systematic Parasitology 78: 81–94. https://doi.org/10.1007/s11230-010-9276-5

Kern E, Kim T, Park J (2020) The Mitochondrial Genome in Nematode Phylogenetics. Frontiers in Ecology and Evolution https://doi.org/10.3389/fevo.2020.00250

Kim J, Lee S, Gazi M, Kim T, Jung D, Chun JY, Kim S, Seo TK, Park C, Baldwin JG, Nadler SA, Park J (2015) Mitochondrial genomes advance phylogenetic hypotheses for Tylenchina (Nematoda: Chromadorea). Zoologica Scripta 44: 1–17. https://doi.org/10.1111/zsc.12112

Kim T, Kim J, Park J (2017) *Acrobeloides varius* sp. n. (Rhabditida: Cephalobidae) from South Korea. Nematology 19: 43–52. https://doi.org/10.1163/15685411-00003064

Kim T, Lee Y, Kil HJ, Park J (2020) The mitochondrial genome of *Acrobeloides varius* (Cephalobomorpha) confirms non-monophyly of Tylenchina (Nematoda). PeerJ 8: e9108. http://doi.org/10.7717/peerj.9108

Lanfear R, Calcott B, Ho SY, Guindon S (2012) Partitionfinder: combined selection of partitioning schemes and substitution models for phylogenetic analyses. Molecular Biology and Evolution, 29: 1695–1701. https://doi.org/10.1093/molbev/mss020

Liu GH, Shao R , Li JY, Zhou DH, Li H, Zhu XQ (2013) The complete mitochondrial genomes of three parasitic nematodes of birds: a unique gene order and insights into nematode phylogeny. BMC Genomics 14: 414–427. https://doi.org/10.1186/1471-2164-14-414

Magalhães PS (1905) Notes d'helminthologie brasillienne. Archives de parasitologie. Paris. 9: 305–318.

Pierantoni U (1916) I nematodi parassiti degli oligocheti. Bolletino della Società dei naturalisti in Napoli 28: 139–163.

Page RD (1996) TreeView: an application to display phylogenetic trees on personal computers. Computer Applications in the Biosciences 12: 357–358. https://doi.org/10.1093/bioinformatics/12.4.357

Sela I, Ashkenazy H, Katoh K, Pupko T (2015) GUIDANCE2: accurate detection of unreliable alignment regions accounting for the uncertainty of multiple parameters. Nucleic Acids Research 43 (Web Server issue): W7-W14. https://doi.org/10.1093/nar/gkv318

Spiridonov SE (1993) Nematodes of the family Ungellidae Chitwood, 1950 from Laotian earthworms Russian Journal of Nematology 1: 31–40.

Spiridonov SE, Ivanova ES (2005) The nematodes of the superfamily Drilonematoidea, parasites of earthworms. Moscow, Russia, Tovarischestvo nauchnyh izdaniy KMK, 296 pp.

Spiridonov SE, Ivanova ES, Wilson MJ (2005) The nematodes of the genus *Dicelis* Dujardin, 1845 parasitic in earthworms: the interrelationships of four Eurasian populations. Russian Journal of Nematology 13: 61–81.

Spiridonov SE, Ivanova ES, Pham Van Luc (2007) Two new species of Ungellidae and Homungelidae (Drilonematoidea; Rhabditida) from Vietnamese earthworms and the phylogenetic links of these families. Russian Journal of Nematology 15: 101–108.

Seinhorst JW (1959) A rapid method for the transfer of nematodes from fixative to anhydrous glycerin. Nematologica 4: 54–60. https://doi.org/10.1163/187529259X00381

Sun L, Zhuo K, Lin B, Wang Hb, Liao J (2014) The complete mitochondrial genome of *Meloidogyne graminicola* (Tylenchina): A unique gene arrangement and its phylogenetic implications. PLoS ONE 9(6): e98558. https://doi.org/10.1371/journal.pone.0098558

Timm RW (1959) Observations on *Synoecnema* (Nematoda, Ungellidae), with a description of two new species. Pakistan Journal of Scientific Research 11: 58–62.

Timm RW (1962) Nematode parasites of the coelomic cavity of earthworms. I. The genera *Synoecnema* and *Ungella*. Biologia (Dacca) 8: 1–7.

van Megen H, van den Elsen S, Holterman M, Karssen G, Mooyman P, Bongers T, Holovachov O, Bakker J, Helder J (2009) A phylogenetic tree of nematodes based on about 1200 full-length small subunit ribosomal DNA sequences. Nematology 11: 927–950. https://doi.org/10.1163/156854109X456862

ZooKeys 1076: 151–182 (2021)
doi: 10.3897/zookeys.1076.69025
https://zookeys.pensoft.net

RESEARCH ARTICLE

A peer-reviewed open-access journal
ZooKeys
Launched to accelerate biodiversity research

Gems of the southern Japanese seas – four new species of *Edwardsianthus* (Anthozoa, Actiniaria, Edwardsiidae) with redescriptions of two species

Takato Izumi[1], Takuma Fujii[2,3,4]

1 *Molecular Invertebrate Systematics and Ecology Laboratory, Department of Biology, Chemistry, and Marine Sciences, Faculty of Science, University of the Ryukyus, 1 Senbaru, Nishihara, Okinawa 903-0213, Japan* **2** *Kagoshima City Aquarium, 3-1 Honko-shinmachi, Kagoshima, 892-0814, Japan* **3** *International Center for Island Studies Amami Station, Kagoshima University,15-1 Naze-Minatomachi, Amami, Kagoshima 894-0026, Japan* **4** *The Kagoshima University Museum, 1-21-30 Korimoto, Kagoshima 890-0065, Japan*

Corresponding author: Takato Izumi (iz.takato@gmail.com)

Academic editor: Bert W. Hoeksema | Received 22 May 2021 | Accepted 30 August 2021 | Published 10 December 2021

http://zoobank.org/7B4E1271-0B60-4504-80B3-68028E4B1AD6

Citation: Izumi T, Fujii T (2021) Gems of the southern Japanese seas – four new species of *Edwardsianthus* (Anthozoa, Actiniaria, Edwardsiidae) with redescriptions of two species. ZooKeys 1076: 151–182. https://doi.org/10.3897/zookeys.1076.69025

Abstract

Edwardsianthus England, 1987 is a genus of Edwardsiidae, a family of burrowing and worm-like sea anemones characterized by lacking four mesenteries in the first cycle and containing only one type of nematocysts in nemathybomes. Until now, this genus has accommodated only two species since its establishment and has been recorded only from Indo-West Pacific regions. In this study, six species are reported from Japan: two are previously known species, *E. pudicus* (Klunzinger, 1877) and *E. gilbertensis* (Carlgren, 1931); four are new species, *E. carbunculus* **sp. nov.**, *E. sapphirus* **sp. nov**., *E. smaragdus* **sp. nov.**, and *E. amethystus* **sp. nov.** Based on these results, the diagnostic features of the genus are revised.

Keywords

Cnidaria, cnidae, Kochi, Nansei Islands, nemathybomes, northernmost distribution limit, Pacific Ocean, phylogeny, taxonomy

Introduction

The superfamily Edwardsioidea, re-established by Rodríguez et al. (2014), consists of only one family, Edwardsiidae Andres, 1881. This family is a large taxon in the order Actiniaria with ca. 95 nominal species (Gusmão et al. 2020). Most edwardsiids are burrowers in a broad range of soft substrates, such as sand or mud, others can bore into skeletons of dead coral in caves or rock crevices (Carlgren, 1892; Dnyansagar et al. 2018; Izumi and Fujita, 2018; Sanamyan et al. 2018), whereas a few species can live in ice (Daly et al. 2013) or in homoscleomorph sponges (Izumi et al. 2018). Edwardsiids are characterized by worm-like bodies, absence of basal disks, and eight perfect mesenteries in the first cycle, unlike almost all other sea anemones, which have 12 perfect mesenteries, excluding a few exceptional taxa (e.g., Halcampulactidae Gusmão et al. 2019). This simplified mesenterial arrangement of edwardsiids is similar to that of "Edwardsia-stage" larvae (Duerden, 1899) of several actiniarian species that have 12 or more mesenteries as adults (Uchida and Soyama, 2001). As a result, worm-like edwardsiids had been hypothesized to be the common ancestral form of actiniarians (McMurrich, 1891; Hyman, 1940). However, several studies have asserted that Edwardsiidae is a derived lineage and that the simplified mesenterial arrangement of this family is a derived character (Manuel, 1981; Daly, 2002). Recent phylogenetic studies by Rodríguez et al. (2014) and Gusmão et al. (2019) have reinforced the latter hypothesis.

The genus *Edwardsianthus* England, 1987 was established in order to rearrange the type genus of Edwardsiidae, *Edwardsia* de Quatrefages, 1842. England (1987) divided *Edwardsia* into three genera: *Edwardsia*, *Edwardsioides* Danielessen, 1890, and *Edwardsianthus* England, 1987. *Edwardsioides* was synonymized with *Edwardsia* by Carlgren (1921), which was revoked by England (1987). *Edwardsioides* was again synonymized with *Edwardsia* (Fautin, 2007) and thus only *Edwardsianthus and Edwardsia* remain as valid genera (Daly & Fautin, 2021). Since the establishment by England (1987), no additional species of *Edwardsianthus* have been discovered, and currently this genus still contains only two species (Daly & Fautin, 2021): *E. pudicus* (Klunzinger, 1877) and *E. gilbertensis* (Carlgren, 1931). Consequently, the genus *Edwardsia* remains the largest genus in the family with more than 60 species (Fautin, 2016; Daly & Fautin, 2021).

Edwardsianthus specimens have been collected from a broad range in the Indo-West Pacific region (Fautin, 2013). However, until now there has been only one record of an *Edwardsianthus* species from Japanese waters; *E. gilbertensis* from Ishigaki Island, Okinawa (Uchida & Soyama, 2001). This reference also mentioned *Edwardsianthus* cf. *pudica* from Onagawa, Miyagi as reported in Uchida (1941), but this observation has not been confirmed (Yanagi, 2006).

During recent surveys of Japanese waters, we recorded two previously described species of *Edwardsianthus* and also collected specimens of four undescribed species. These undescribed species have tentacles in more vivid colors than the two other ones, and they share the same particular morphological genus characters. Moreover, in our

phylogenetic analysis, these undescribed species were found within the clade of *Edwardsianthus* and monophyletic with the other two species.

We formally describe the new species as *Edwardsianthus carbunculus* sp. nov., *E. smaragdus* sp. nov., *E. sapphirus* sp. nov., and *E. amethystus* sp. nov., and redescribe the two existing species, *E. pudicus* and *E. gilbertensis*. Furthermore, we revise the definition of *Edwardsianthus* to accommodate the four new species. Since neither the family, the genus, nor its species had names in the Japanese language, we designate Japanese names to all these taxa.

Materials and methods

Specimen collection and preservation

Specimens of *Edwardsianthus* used in the present study were collected from southern Japan (Fig. 1). Specimens of *E. gilbertensis* were collected by digging in shallow, submerged areas at low tides, whereas the other species were sampled during scuba diving. They were dug out by using a shovel and a sieve, or by hand. The specimens were generally kept undisturbed in aquaria for several hours to several days after collection, as long possible, until they were completely relaxed and had their tentacles extended. Then, specimens were anesthetized with magnesium chloride solution, magnesium sulfate solution or l-menthol, and finally fixed in 5–10% (v/v) seawater formalin solution. The examined specimens were eventually deposited in the National Museum of Nature and Science, Tokyo (**NSMT**) or in the Coastal Branch of the Natural History Museum and Institute, Chiba (**CMNH**).

Preparation of histological sections

Histological sections of all specimens were made following standard protocols (Presnell and Schreibman, 1997); The materials were dissected by scissors, serially dehydrated by ethanol and xylene, embedded in paraffin, and sliced into serial sections each 8–10 μm thick. Thereafter, sections were mounted on glass slides. All sections were stained by hematoxylin and eosin, and finally they were mounted using the medium EUKITT (ORSAtec).

Observation of cnidae

Cnidae were extracted from the tentacles, actinopharynx, nemathybomes, column, and filaments. Concerning the column of some *Edwardsianthus* species, no or few cnidocytes were observed, and the few observed capsules were broken or almost of the same type as those observed in their nemathybomes. In those cases, we did not describe the cnidom of column because it is possible that these cnidae were contaminants from broken nemathybomes. Images of the cnidae were obtained by differen-

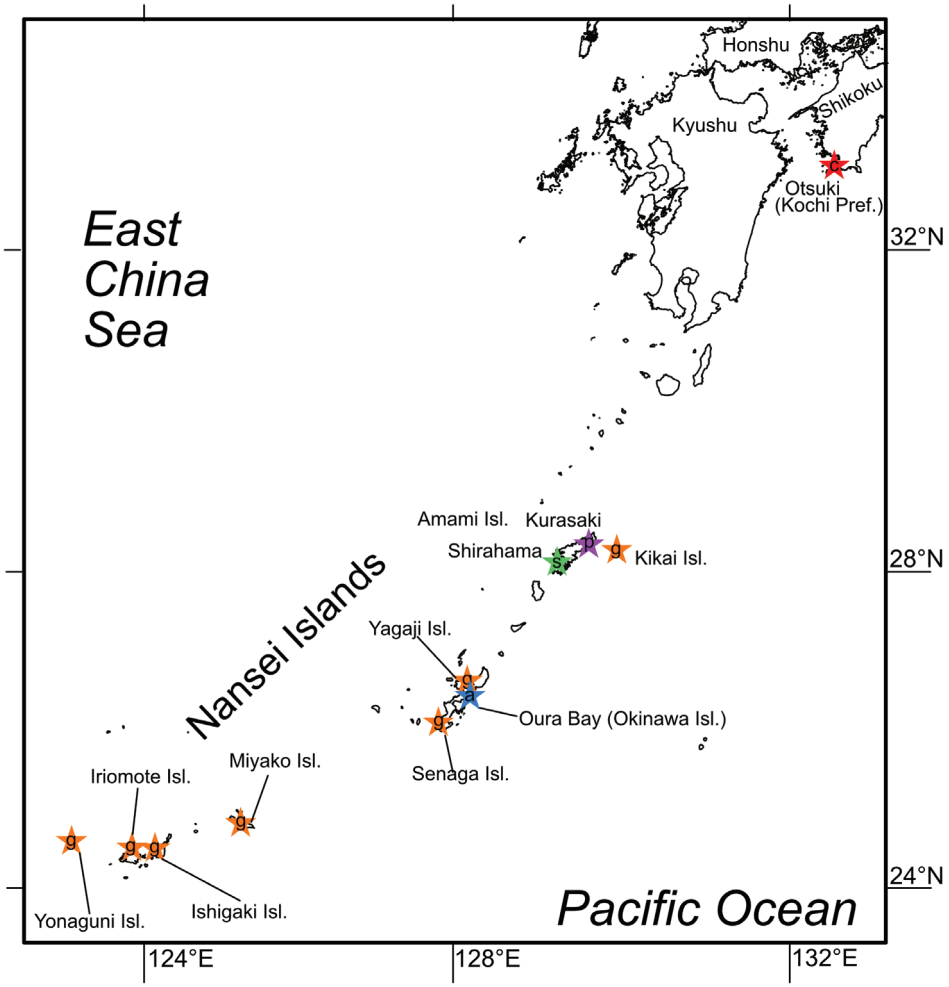

Figure 1. Localities of the specimens of the *Edwardsianthus* species collected in this study. Purple star marked by p indicates collection locality of *Edwardsianthus pudicus*; orange stars are those of *E. gilbertensis*; red star marked by c is *E. carbunculus* sp. nov.; blue star marked by a is *E. sapphirus* sp. nov.; green star marked by s is *E. smaragdus* sp. nov.

tial interference contrast microscopy following the method of Yanagi et al. (2015). For each capsule, length and width were measured from the images using ImageJ v. 1.49 (Rasband, 1997–2012). Size distributions were processed and values of means and standard deviations were calculated in Microsoft Excel 2013. The nomenclature of cnidae followed Mariscal (1974). Thus, although England (1987) designated the large basitrichs in nemathybomes as "pterotrichs" and "microbasic t-mastigophores", we unified the name of such cnidocysts as "basitrichs" following the nomenclature of Mariscal (1974).

PCR and DNA sequencing

DNA was extracted from subsamples of each tissue that were preserved in 99% ethanol by using ChargeSwitch gDNA Micro Tissue Kit (Invitrogen). In addition, some tissue samples for DNA were processed following the guanidine extraction protocol (Sinniger et al. 2010). PCR amplifications were performed in 10 μL (or 25 μL) reaction volume, consisting of 0.4 (1.0) μL of 25 μM forward and reverse primers, 2.0 (5.0) μL of EmeraldAmp PCR Master Mix (TaKaRa), and 3.4 (8.5) μL of distilled water. For PCR amplifications, two mitochondrial markers, 12S, 16S rDNA, and a nuclear marker, 18S rDNA, were amplified. The primers and amplification conditions are shown in Table 1. Amplifications were performed using traditional molecular markers of Actiniaria; mitochondrial 12S rDNA and 16S rDNA, and nuclear 18S rDNA. PCR methods and protocols followed methods of preceding phylogenetic studies (Medlin et al. 1988; Apakupakul et al. 1999; Geller and Walton, 2001; Medina et al. 2001; Sinniger et al. 2005) referring to Rodríguez et al. (2014). The PCR products were processed using exonuclease I and shrimp alkaline phosphate (ExoSAP-IT; Thermo Fisher) before sequencing. Sequencing reactions were performed using BigDye Terminator Cycle Sequencing Ready Reaction Kit v3.1 (Applied Biosystems) and using PCR primers (12S, 16S) or PCR primers and internal primers (18S; Table 1). We used four internal primers (two forward and two reverse) for 18S (Apakupakul et al. 1999). Sequencing was performed using an ABI 3500xL Genetic Analyzer (Applied Biosystems). The sequence of each marker was individually assembled using GeneStudio ver. 2.2.0.0 (http://genestudio.com).

Phylogenetic analyses

The phylogenetic analyses were performed on the family Edwardsiidae. The base sequences used in phylogenetic analyses are shown in Table 2. Each dataset was aligned using MAFFT ver. 7.402 (Katoh and Standley, 2013) under the default settings. Ambiguously aligned regions were eliminated using Gblocks ver. 0.91b (Castresana, 2002) with the type of DNA sequences and in default parameters except allowing small final blocks and gap positions within the final blocks. The obtained data were processed using Kakusan 4 (Tanabe, 2011) to select the appropriate substitution models for the RAxML and MrBayes analyses (Table 3). In the concatenated dataset, substitution parameters were estimated separately for each gene partition. The maximum-likelihood (ML) analysis was performed using RAxML-VI-HPC (Stamatakis, 2006), with substitution models recommended by Kakusan 4 and evaluated using 100 bootstrap replicates. Bayesian inference (BI) was conducted using MrBayes ver. 3.2.6 (Ronquist and Huelsenbeck, 2003) with substitution models recommended by Kakusan 4. Two independent runs of the Markov Chain Monte Carlo were performed simultaneously for 5×10^6 generations; trees were sampled every 100 generations, and the average standard deviation of split frequencies (ASDSF) every 100,000 generations were calculated. As the ASDSF was

Table 1. Primers and protocols of polymerase chain reactions of every molecular marker.

Marker	Primer	Sequences (5'-3')	PCR protocol	Reference
12S	12S1a	TAAGTGCCAGCAGACGCGGT	(95 °C for 4 min) + 4 × [(94°C for 30 sec) → (50°C for 1 min) → (72°C for 2 min)]+30 × [(94°C for 30 sec) → (55°C for 1 min) → (72°C for 2 min)] + (72°C for 4 min)	Sinniger et al. (2005)
	12S3r	ACGGGCAATTTGTACTAACA		
16S	ANEM16SA	CACTGACCGTGATAATGTAGCGT	(95°C for 4 min) + 30 × [(95°C for 30 sec) → (46°C for 45 sec) → (72°C for 1 min)] + (72°C for 5 min)	Geller and Walton (2001)
	ANEM16SB	CCCCATGGTAGCTTTTATTCG		
	16Sant1a	GCCATGAGTATAGACGCACA	(95°C for 4 min) + 30 × [(95°C for 30 sec) → (46°C for 45 sec) → (72°C for 1 min)] + (72°C for 5 min)	Sinniger et al. (2005)
	16SbmoH	CGAACAGCCAACCCTTGG		
18S PCR	18SA	AACCTGGTTGATCCTGCCAGT	(94°C for 4 min) + 35 × [(94°C for 20 sec) → (57°C for 20 sec) → (72°C for 1 min 45 sec)] + (72°C for 7 min)	Medlin et al. (1988)
	18SB	TGATCCTTCCGCAGGTTCACCT		
Only sequence	18SL	CCAACTACGAGCTTTTTAACTG		Apakupakul et al. (1999)
	18SC	CGGTAATTCCAGCTCCAATAG		
	18SY	CAGACAAATCGCTCCACCAAC		
	18SO	AAGGGCACCACCAGGAGTGGAG		

Table 2. Base sequences in the phylogenetic analyses. Sequences indicated by accession numbers were obtained from GenBank, and those indicated by bold were newly obtained in this study. *Synactinernus churaumi* (Actinernidae) were for the outgroups of phylogenetic analysis of Edwardsiidae.

Higher taxon	Family	Genus	Species	Localities	Catalog numbers	12S	16S	18S
Actiniaria, Anenthemonae, Edwardsioidea	Edwards	*Edwardsianthus*	*pudicus*	Amami Island	NSMT-Co 1702	**LC649467**	**LC649475**	**LC649483**
			gilbertensis	Ishigaki Island	CMNH-ZG 6527	–	**LC649481**	**LC649489**
			gilbertensis	Kataburu_ Yonaguni	NSMT-Co 1701	**LC649468**	**LC649476**	**LC649484**
			carbunculus	Otsuki_Kochi	CMNH-ZG 05954	**LC649472**	**LC649480**	**LC649488**
			sapphirus	Oura Bay	CMNH-ZG 09761	**LC649469**	**LC649477**	**LC649485**
			smaragdus	Amami Island	CMNH-ZG 09762	**LC649471**	**LC649479**	**LC649487**
			amethystus	Oura Bay	CMNH-ZG 09763	**LC649470**	**LC649478**	**LC649486**
		Tempuractis	*rinkai*	Misaki	NSMT-Co 1573	**LC649473**	**LC649482**	**LC649490**
		Edwardsia	*japonica*			GU473274	GU473288	GU473304
			timida			GU473281	-	GU473315
		Edwardsianthus	*gilbertensis*			EU190728	EU190772	EU190859
		Scolanthus	*shrimp*			MN200242	MN200264	MN200245
			celticus			MN200251	MN200244	MN200240
		Nematostella	*vectensis*			EU190750	AY169370	AF254382
	Actinernidae	*Synactinernus*	*churaumi*	Off Ishigaki Island	NSMT-Co 1661	**LC649474**	LC484641	LC484636

Table 3. The substitution models of phylogenetic analyses on each marker.

	Mitochondrial		Nuclear
	12S rDNA	16S rDNA	18S rDNA
ML analysis	GTR+Gamma	GTR+Gamma	GTR+Gamma
Bayesian inference	HKY85+Gamma	HKY85+Gamma	K80+Gamma

calculated on the basis of the last 75% of the samples, the initial 25% of the sampled trees were discarded as burn-in.

All constructed Maximum Likelihood and Bayesian trees were rooted and combined using FigTree ver. 1.4.3 (http://tree.bio.ed.ac.uk/software/figtree/).

Results and discussion

Order Actiniaria Hertwig, 1882
Suborder Anenthemonae Rodriguez & Daly, 2014
Superfamily Edwardsioidea Andres, 1881
Family Edwardsiidae Andres, 1881

Genus *Edwardsianthus* England, 1987
New Japanese name: nanyo-mushimodoki-ginnchaku-zoku

Diagnosis (revised from the diagnosis given by England, 1987). Body divisible into physa, scapus, and capitulum. physa short, without nemathybomes or cuticle. Scapus long, generally with nemathybomes but sometimes without, sunk in mesoglea; cuticle present. Tentacles usually 20, inequal number at inner and outer cycle: five-eight inner and 12–15 outer. Siphonoglyph weak or absent, ventral. Mesenteries eight macrocnemes and six pairs of microcnemes, minute and restricted to distal part of column. Microcnemes never paired with macrocnemes. Gametogenic tissue, filaments, and parietal and retractor muscles on macrocnemes only. Parietals well developed; retractors strong-diffuse to restricted-reniform. Cnidom: spirocysts, basitrichs, microbasic *p*-mastigophores.

Type species. *Edwardsia pudica* Klunzinger, 1877 (currently recognized as *Edwardsianthus pudicus* (Klunzinger, 1877); the genus name is masculine). Type locality is Egypt, Red Sea.

Derivation of Japanese name. This name is constructed from *nanyo* (south sea), *mushimodoki-ginchaku* (worm-like sea anemone).

Remarks. Since England (1987) established this genus, no new species were described in addition to the two that were already known. This study revises the diagnosis of the genus for the first time in the 30 years since its original description, including new evidence for four new species.

In the present study, sea anemones resembling *Edwardsianthus* were collected from several Japanese localities (Fig. 1). According to our analyses, these edwardsiids were shown to belong to the same phylogenetic clade as *E. pudicus* and *E. gilbertensis* (Fig. 10) and also shared the same mesenterial arrangement, i.e., lacking four microcnemes on the first mesenterial cycle. Therefore, these new species fit well with the definition of *Edwardsianthus* given by England (1987). Thus, we have placed these four new species within *Edwardsianthus* as *Edwardsianthus carbunculus* sp. nov., *E. sapphirus* sp. nov., *E. smaragdus* sp. nov., and *E. amethystus* sp. nov..

England (1987) also stated that the genus *Edwardsianthus* has only one type of basitrich in the nemathybomes. However, *Edwardsianthus carbunculus* sp. nov., *Edwardsianthus sapphirus* sp. nov., and *Edwardsianthus smaragdus* sp. nov. have two types of basitrichs in their nemathybomes, and *Edwardsianthus amethystus* has no nemathybomes at all. Consequently, we have now added a new character to the diagnosis of this genus: an inequal number of inner and outer tentacles. Species of this genus have a peculiar tentacular arrangement as “5 inner and 15 outer” or “8 inner and 12 outer”. The ten-

tacular arrangement is useful to distinguish *Edwardsianthus* from the genus *Edwardsia* de Quatrefages, 1842 of the same family, as *Edwardsia* species have equal numbers of tentacles in their inner and outer cycles (Carlgren, 1949; Izumi & Fujita, 2019).

Edwardsianthus pudicus (Klunzinger, 1877)

New Japanese name: nanyo-mushimodoki-ginchaku
Figs 2, 3A–E; Table 4

Edwardsia pudica Klunzinger, 1877: 80–81, pl. 6, fig. 3; Carlgren, 1931: 18–20, figs 16, 17.
Edwardsiella pudica Andres, 1883: 309.
Edwardsia adenensis Faurot, 1895: 121, pl. 6, fig. 5, pl. 7, fig. 6.
Edwardsia bocki Carlgren, 1931: 7–9, figs 5, 6.
Edwardsia stephensoni Carlgren, 1950: 128–129, figs 1, 2.
Edwardsianthus pudica: England, 1987: 224–229, fig. 10.

Material examined. NSMT-Co 1702: histological sections, dissected tissues, and prepared nematocysts, collected by SCUBA diving on 7 November 2015 off Kurasaki seashore, Amami-Oshima Island, Kagoshima, Japan, at ca. 20 m depth, by Takuma Fujii.

Description. ***External anatomy.*** Size: ca. 120–200 mm in whole length, and ca. 12–15 mm in width in living specimen, and ca. 80–130 mm in length and ca. 8–10 mm in width in preserved specimen (Fig. 2A). Column: cylinder-like form, and the proximal part narrower to some extent; consisting of capitulum, scapus, and physa. The distal-most part capitulum, translucent and visible magenta mesenteries within, short, without nemathybomes. Scapus with very thick and easily removed peridermlike cuticle, dark gray color in living and preserved animals, and with tiny, pale white in color, densely scattered nemathybomes (Fig. 2A). Tentacles: 20 in number in two cycles, inner tentacle 8 and outer 12, magenta pink or purple in color with brown obscure patches in living animals (Fig. 2B; these colors are lost in preserved specimen), without acrospheres. Inner tentacles short, slender, ca. 5–6 mm in length, and outer ones long and slender, 10–14 mm in length in preserved. Mouth: at the center of oral disc, apparently swollen, showing white color in live specimens. ***Internal anatomy.*** Mesenterial arrangement: eight perfect mesenteries, all macrocnemes. Four dorsal and ventral directives, and four lateral mesenteries not paired with other macrocnemes. All macrocnemes present along whole length of the body from oral to aboral end and bearing distinct retractor and parietal muscles. Twelve tiny microcnemes, without muscles, confined only in distal-most part. Four microcnemes between dorsal directives and dorso-lateral mesenteries, four between dorso-and ventro-lateral mesenteries, and four between ventro-lateral mesenteries and ventral directives. Retractor muscles: at the mid part of column, strongly developed and diffused (Fig. 2F), pennon-like, arranged with ca. 100 muscular processes. Processes except some basal ones simple or slightly branched, and pinnate in some parts. Some processes nearest to body wall extremely well-branched, with secondary and tertiary branches (Fig. 2F; England, 1981: fig. 10).

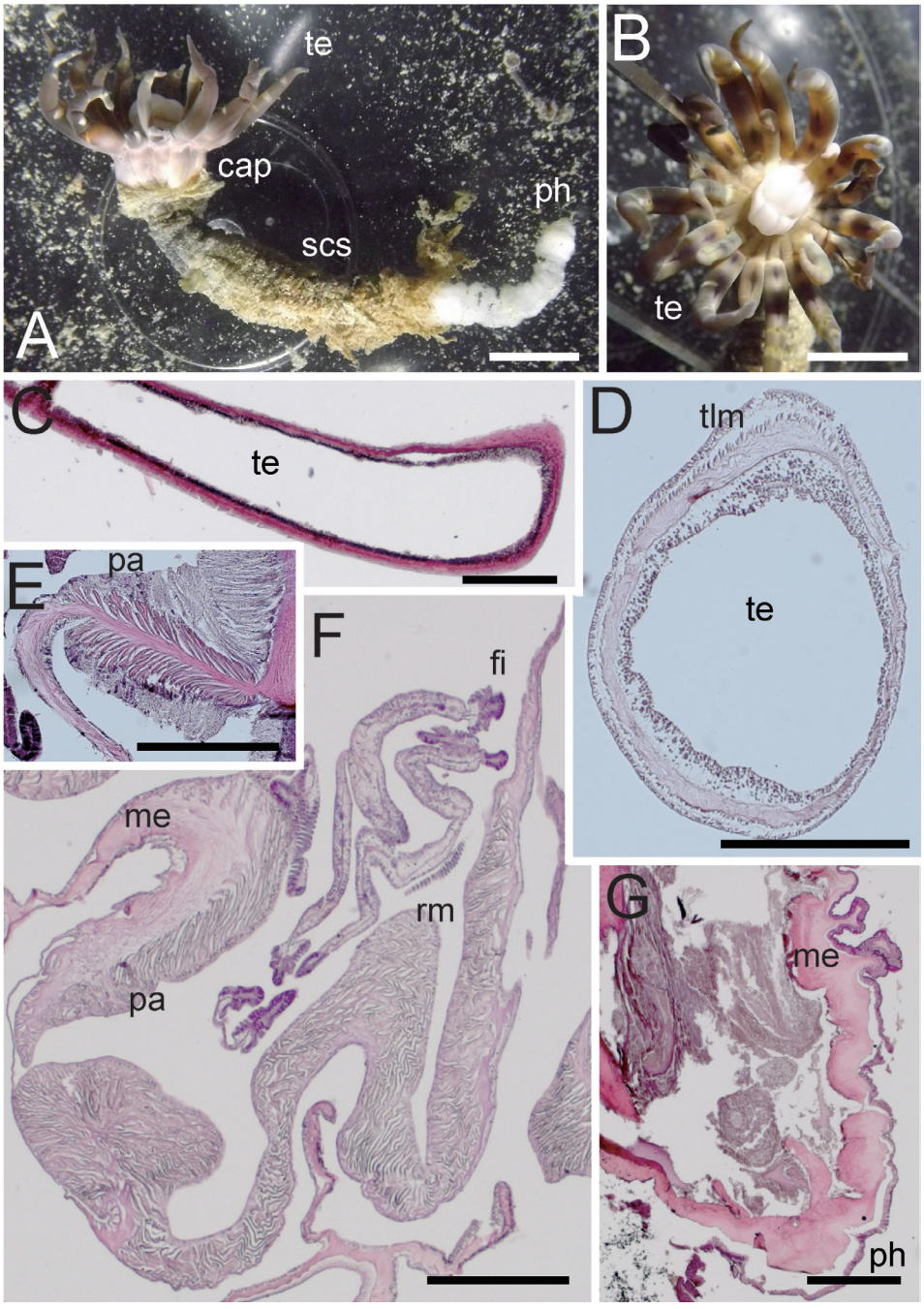

Figure 2. External and internal morphology of *Edwardsianthus pudicus* (NSMT-Co 1702) **A** outer view of living specimen **B** oral view of living specimen **C** longitudinal section of tentacle **D** transverse section of tentacle **E** transverse section of parietal muscle **F** transverse section of macrocnemes **G** longitudinal section of physa. Abbreviations: cap, capitulum; fi, filament; me, mesoglea; pa, parietal muscle; ph, physa; rm, retractor muscle; scs, scapus; te, tentacle; tlm, tentacular longitudinal muscle. Scale bars: 5 mm (**A, B**); 1 mm (**C**); 500 μm (**D, F, G**); 100 μm (**E**).

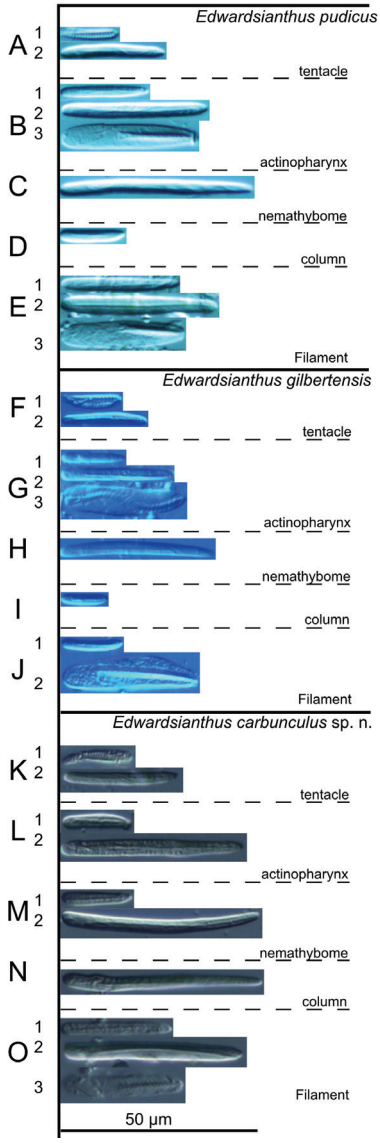

Figure 3. Cnidae of *Edwardsianthus* species **A–E** *E. pudicus* (NSMT-Co 1702) **A1** spirocyst in tentacle; **A2** basitrich in tentacle **B1** small basitrich in actinopharynx **B2** large basitrich in actinopharynx **B3** microbasic *p*-mastigophore in actinopharynx **C** basitrich in nemathybome **D** basitrich in column **E1** small basitrich in filament **E2** large basitrich in filament **E3** microbasic *p*- mastigophore in filament **F–J** *E. gilbertensis* (CMNH-ZG 06527) **F1** spirocyst in tentacle **F2** basitrich in tentacle **G1** small basitrich in actinopharynx **G2** large basitrich in actinopharynx **G3** microbasic *p*-mastigophore in actinopharynx **H** basitrich in nemathybome **I** basitrich in nemathybome **J1** basitrich in filament **J2** microbasic *p*- mastigophore in filament **K–O** *E. carbunculus* sp. nov. (CMNH-ZG 05954) **K1** spirocyst in tentacle **K2** basitrich in tentacle **L1** small basitrich in actinopharynx **L2** large basitrich in actinopharynx **M1** small basitrich in nemathybome **M2** large basitrich in nemathybome **N** basitrich in column **O1** small basitrich in filament **O2** large basitrich in filament **O3** microbasic *p*-mastigophore in filament.

Table 4. Cnidoms of the species of *Edwardsianthus pudicus*, *Edwardsianthus gilbertensis* and *Edwardsianthus carbunculus* sp. nov.

		Edwardsianthus pudicus					***Edwardsianthus gilbertensis***					***Edwardsianthus carbunculus* sp. n.**				
		NSMT-Co 1702					**CMNH-ZG 06527**					**CMNH-ZG 05954**				
		Length × Width (μm)	Mean (μm)	SD (μm)	n	frequency	Length × Width (μm)	Mean (μm)	SD (μm)	n	frequency	Length × Width (μm)	Mean (μm)	SD (μm)	n	frequency
Tentacle																
basitrichs		20.1–34.0 × 2.9–4.2	27.4 × 3.6	3.09 × 0.30	57	numerous	13.2–26.4 × 2.8–4.6	20.5 × 3.6	3.23 × 0.44	50	numerous	25.9–34.6 × 2.7–4.3	30.0 × 3.3	2.05 × 0.29	94	numerous
spirocysts		11.9–20.1 × 2.2–3.6	15.1 × 2.9	1.88 × 0.32	25	numerous	8.5–14.3 × 3.0–4.4	11.0 × 3.4	1.43 × 0.35	12	few	11.8–21.0 × 2.5–3.7	16.6 × 3.1	1.83 × 0.28	57	numerous
Actinopharynx																
basitrichs	S	17.4–24.2 × 1.9–3.0	20.8 × 2.5	2.02 × 0.44	15	numerous	16.3–21.1 × 2.4–3.9	18.4 × 3.1	1.24 × 0.39	12	few	14.3–16.9 × 3.5–3.9	16.0 × 3.7	0.99 × 0.19	4	rare
	L	34.8–42.6 × 3.3–5.4	38.4 × 4.5	1.80 × 0.44	47	numerous	26.5–34.3 × 3.0–4.5	30.8 × 3.7	1.71 × 0.35	66	numerous	36.1–48.8 × 3.2–5.0	42.5 × 4.2	2.85 × 0.40	76	numerous
microbasic *p*-mastigophores		30.3–35.6 × 6.6–7.1	33.4 × 6.7	1.92 × 0.17	5	few	28.9–35.5 × 6.6–8.4	32.5 × 7.6	2.71 × 0.78	3	rare	–	–	–	–	–
Nemathybome																
basitrichs	S	–	–	–	–	–	–	–	–	–	–	16.6–19.9 × 3.9–4.1	18.4 × 4.0	1.35 × 0.08	4	rare
	L	46.8–56.6 × 3.2–5.6	41.7 × 51.7	1.95 × 0.43	44	numerou	34.0–45.2 × 3.0–4.8	39.6 × 3.8	2.02 × 0.38	75	numerous	46.8–56.6 × 3.2–5.6	51.7 × 4.3	2.08 × 0.47	44	numerous
Column																
basitrichs		15.8–17.5 × 3.4–3.8	16.8 × 3.7	0.72 × 0.18	3	rare	9.8–14.4 × 2.8–4.1	12.0 × 3.3	1.12 × 0.41	12	few	47.9–53.8 × 3.4–4.8	50.8 × 4.0	1.62 × 0.33	24	numerous
Filament																
basitrichs	S	25.1–31.7 × 2.4–4.1	29.0 × 3.3	1.69 × 0.34	49	numerous	12.9–19.2 × 2.8–4.2	14.8 × 3.4	1.32 × 0.33	61	numerous	22.4–32.2 × 3.2–5.0	28.3 × 4.0	2.29 × 0.43	43	numerous
	L	29.4–42.7 × 4.2–5.9	37.3 × 4.9	3.09 × 0.31	29	numerous	–	–	–	–	–	27.6–44.3 × 4.1–5.8	34.8 × 4.8	5.87 × 0.51	11	few
microbasic *p*-mastigophores		29.7–34.1 × 5.2–7.6	31.6 × 6.2	1.26 × 0.62	11	few	33.0–38.4 × 8.2–10.9	36.3 × 9.3	1.63 × 0.72	12	few	30.1–31.8 × 5.3–5.9	30.9× 5.6	0.87 × 0.29	2	rare

Parietal muscles: developed, comparatively distinct, egg-shaped, elongated along mesenteries, with ca. 15–20 simple or slightly branched muscular processes on each side (Fig. 2E). Others: existence of siphonoglyph unknown because of the contracted state of the specimen. Each with one tentacle from each endo- or exocoels. Tentacular circular muscle indistinct (Fig. 2C), and longitudinal muscle distinct, ectodermal (Fig. 2D). Mesoglea thickest in body wall, > 200 μm in thickness in some parts, and comparatively thick in physa and mesenteries, but thinner in parietal muscles and tentacles (Fig. 2C–E). Nemathybomes sunk into mesoglea. Marginal sphincter muscle and basilar muscle absent (Fig. 2G). Gametogenic tissue not attached to retractor muscles, distinct, but no mature gametocytes observed in our specimen (Fig. 2F). ***Cnidom.*** Basitrichs, spirocysts, and microbasic *p*-mastigophores. See Fig. 3A–E and Table 4 for sizes and distributions of cnidae on this study.

Derivation of Japanese name. see the derivation of genus name.

Remarks. This specimen from Amami Oshima Island resembled the features of *Edwardsianthus pudicus* as stated by England (1987); he redescribed this species as *Edwardsianthus pudica* (Klunzinger, 1877), but the appropriate name is *Edwardsianthus pudicus* following nomenclatural rules (ICZN 31.2 and 34.2; Ride et al., 1999), as in WoRMS (Daly & Fautin, 2021). England (1987) redescribed *E. pudicus* in detail and designated this species as the type of *Edwardsianthus* England, 1987. England (1987) mentioned that *E. pudicus* had a large body, reaching 200 mm in length and 15 mm in width, a thick walled scapus with easily stripped periderm, scattered small nemathybomes, long slender tapered tentacles, swelled mouth, extremely developed and diffused retractor muscles composed of 70–90 muscular processes, well-developed parietal muscle with 20–30 simple or slightly branched processes, and dioecious gametogenic tissue. These features almost completely correspond to the specimen obtained in this study. The tentacles being translucent purple or magenta-pink in color (England, 1987) were also similar to the tentacles and capitulum of our specimen. Moreover, *E. pudicus* inhabits a broad area of the Indo-Pacific region (Fautin, 2013; Daly & Fautin, 2021), so it is not unexpected to find this species in Japanese waters.

Edwardsianthus gilbertensis Carlgren, 1931

Japanese name: minami-mushimodoki-ginchaku: Uchida & Soyama, 2001
Figs 3F–J, 4; Table 4

Edwardsia gilbertensis Carlgren, 1931: 10–12, figs 7–9.
Edwardsianthus gilbertensis: England, 1987: 218, 231, fig. 10; Uchida and Soyama, 2001: 49.

Material examined. CMNH-ZG 06527: dissected specimen, histological sections, tissues in paraffin, and prepared nematocysts, collected by wading on 7 June 2013 from the intertidal zone of Kabira Bay, Ishigaki Island, Okinawa Pref., Japan, by Kensuke Yanagi; NSMT-Co 1701: dissected specimens (2 individuals), collected by hand dur-

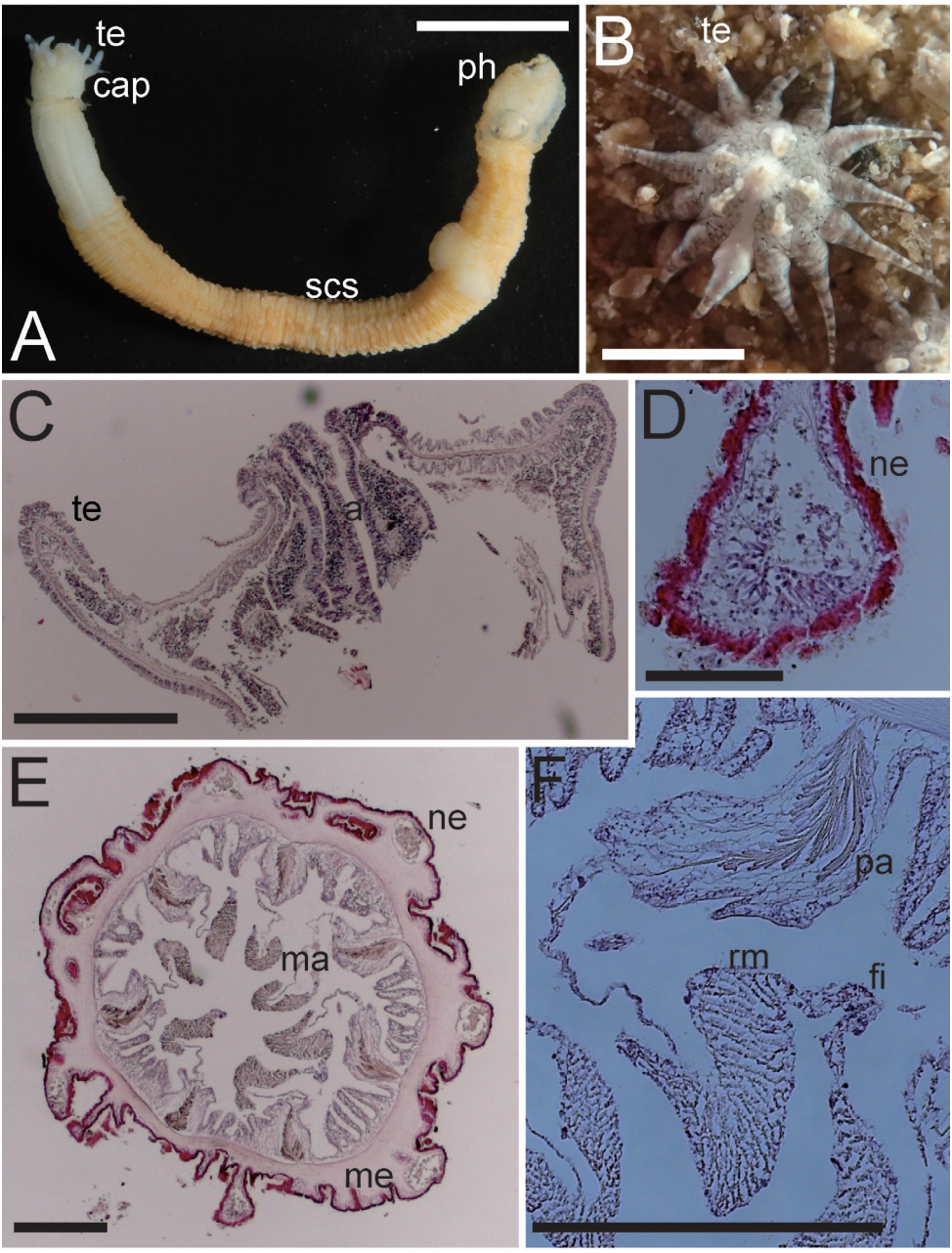

Figure 4. External and internal morphology of *Edwardsianthus gilbertensis* (CMNH-ZG 06527 except for B) **A** outer view of preserved specimen **B** oral view of living specimen with 18 tentacles in the habitat **C** longitudinal section of oral end **D** transverse section of nemathybome **E** transverse section of column in lower part; **F**. Enlarged view of transverse section of mesenteries. Abbreviations: a, actinopharynx; cap, capitulum; fi, filament; ma, macrocneme; ne, nemathybomes; pa, parietal muscle; ph, physa; rm, retractor muscle; scs, scapus; te, tentacle. Scale bars: 5 mm (**A**); 1 mm (**B**); 500 μm (**C, E, F**); 100 μm (**D**). Photograph B by Kensuke Yanagi.

ing wading on 26 March 2015 from the intertidal zone of Funaura Bay, Iriomote Island, Okinawa Pref., Japan, by Takato Izumi; NSMT-Co 1781: dissected or whole specimens (3 individuals), collected by wading on 17 March 2015 from the intertidal zone of Yonaha Bay, Miyako Island, Okinawa Pref., Japan, by Takato Izumi; NSMT-Co 1782: histological sections, tissues in paraffin, and prepared nematocysts, collected by wading on 19 March 2014 from the intertidal zone of Kataburu Beach, Yonaguni Island, Okinawa Pref., Japan, by Takato Izumi; NSMT-Co 1783: histological sections, tissues in paraffin, and prepared nematocysts, collected by wading on 23 March 2015 from the intertidal zone of Kataburu Beach, Yonaguni Island, Okinawa Pref., Japan, by Takato Izumi; NSMT-Co 1784–NSMT-Co 1789: whole or dissected specimens, collected by wading on 17 March 2016 from the intertidal zone of Kataburu Beach, Yonaguni Island, Okinawa Pref., Japan, by Takato Izumi; NSMT-Co 1790: dissected specimens (3 individuals), collected by wading on 24 March 2015 from the intertidal zone of Higawa Bay, Yonaguni Island, Okinawa Pref., Japan, by Takato Izumi; NSMT-Co 1791: histological sections, tissues in paraffin, collected by wading on 23 September 2014 from the intertidal zone of Senaga Island, Okinawa Pref., Japan, by Takato Izumi; NSMT-Co 1792: histological sections, tissues in paraffin, collected by wading on 21 September 2014 from the intertidal zone of Yagaji Island, Okinawa Pref., Japan, by Takato Izumi; NSMT-Co 1793: histological sections, tissues in paraffin, collected by hand during snorkeling on 9 November 2015 from Shio-michi, Kikai Island, Kagoshima Pref., Japan, 1 m depth, by Takato Izumi.

Description. ***External anatomy.*** Size: preserved specimens ca. 20–60 mm in whole length, and 2.5–3.5 mm in width, with worm-like form, and equal width along whole body. Column: consisting of capitulum, scapus, and physa. The distal-most part capitulum, translucent or opaque gray in color in living specimens, short, without nemathybomes. Scapus with thick periderm-like cuticle, brownish orange in color, both in living and preserved specimens, and with tiny, pale white in color, more or less in 8 rows nemathybomes. Aboral end apparent physa (Fig. 4A). Tentacles: 20 in number in two cycles; inner tentacles four or five and outer 10–15, opaque whitish gray in color in living animals (Fig. 4B; this color is lost in preserved specimen), without acrospheres. Inner tentacles slender, ca. 1 mm in length, and outer ones long, slender, short, with sparse white spots on surface, 2–3 mm in length. Mouth: at the center of oral disc, a little swollen. ***Internal anatomy.*** Mesenterial arrangement: eight perfect mesenteries, all macrocnemes. Four dorsal and ventral directives, and four lateral mesenteries not paired with other macrocnemes, (Fig. 4E). All macrocnemes are present along the whole body length from oral to aboral end, and bear distinct retractor and parietal muscles. Approximately seven to twelve tiny microcnemes, without muscles, only confined to distal-most part. Four microcnemes between dorsal directives and dorso-lateral mesenteries, four between dorso-and ventro-lateral mesenteries, and four between ventro-lateral mesenteries and ventral directives. Retractor muscles: at the mid part of column, distinct and diffused (Fig. 4E, F), pennon-like, consist of ca. 15–35 simple or slightly branched muscular processes (Fig. 4F). Parietal muscles: distinctly developed, leaf-like shape elongated along mesenteries, with ca. ten simple or slightly

branched muscular processes in each side (Fig. 4F). Others: each with one tentacle from each endo- or exocoel. Actinopharynx short, limited in uppermost part (Fig. 4C), without siphonoglyph. Tentacular circular muscle indistinct, and longitudinal muscle distinct, ectodermal. Mesoglea thickest in body wall (Fig. 4E), and comparatively thick in tentacles (Fig. 4C), but thinner in mesenteries and parietal muscles (Fig. 4F). Nemathybomes protruding from mesoglea (Fig. 4D). Marginal sphincter muscle and basilar muscle absent. Gametogenic tissue not attached to retractor muscles, distinct, but no mature gametocyte. Zooxanthellae sparsely distributed on endoderm of mesenteries (Fig. 4F). ***Cnidom.*** Basitrichs, spirocysts, and microbasic *p*-mastigophores. See Fig. 3F–J and Table 4 for sizes and distributions of cnidae.

Remarks. *Edwardsia gilbertensis* was originally described from the Gilbert Islands, Kiribati (Carlgren, 1931), and there have been several reports from other localities in the tropical/subtropical zone in the Pacific (Fautin, 2013). However, there were no records of *E. gilbertensis* from Japan except for a fieldguide (Uchida & Soyama, 2001), which reported this species from Kabira Bay, Ishigaki Island. In this research we discovered many individuals of *E. gilbertensis* living not only in the intertidal zone of Kabira Bay in Ishigaki Island (Fig. 4B), but also across a broad area of the Nansei Islands, from Kikai Island, Amami Islands (Kagoshima Pref.) to Yonaguni Island, Yaeyama Islands (Okinawa Pref.). The morphological features of these specimens almost completely correspond to the original description of Carlgren (1931): 6.5 cm in length and 0.2 cm in width in fixed specimens; 16–20 tentacles; nemathybomes more or less in rows; 20–30 muscular processes on retractors. The cnidom of our specimen also agrees well with the original description, especially concerning the point that there is only one type of cnidae, "31–41 × (2)2.5(3) μ" in size (Carlgren, 1931) in the nemathybomes. Thus, it is confirmed that *Edwardsianthus gilbertensis* is widely distributed in the southern islands of Japan including Ishigaki Island.

***Edwardsianthus carbunculus* sp. nov.**
http://zoobank.org/8AA70F27-89FB-447A-8758-73C0928F8F0E
Japanese name: rubi-mushimodoki-ginchaku
Figs 3K–O, 5; Table 4

Material examined. ***Holotype***. CMNH-ZG 05954, histological sections, tissues in paraffin, and prepared nematocysts, collected by SCUBA diving on 10 July 2013, Nishidomari (in front of Kuroshio Biological Institute), Kochi Pref., Japan, 5 m depth, by Kensuke Yanagi.

Description. ***External anatomy.*** Size: preserved specimen ca. 60 mm in whole length, and 10–15 mm in width (but distal side strongly contracted and aboral side torn off during sampling, so body length estimated > 100 mm when living), with cylinder-like form, and the proximal side a little narrower. Column: consisting of capitulum and scapus. The distal-most part of capitulum, transparent and visible scarlet color inside, short, without nemathybomes. Scapus with very thick periderm-like cuti-

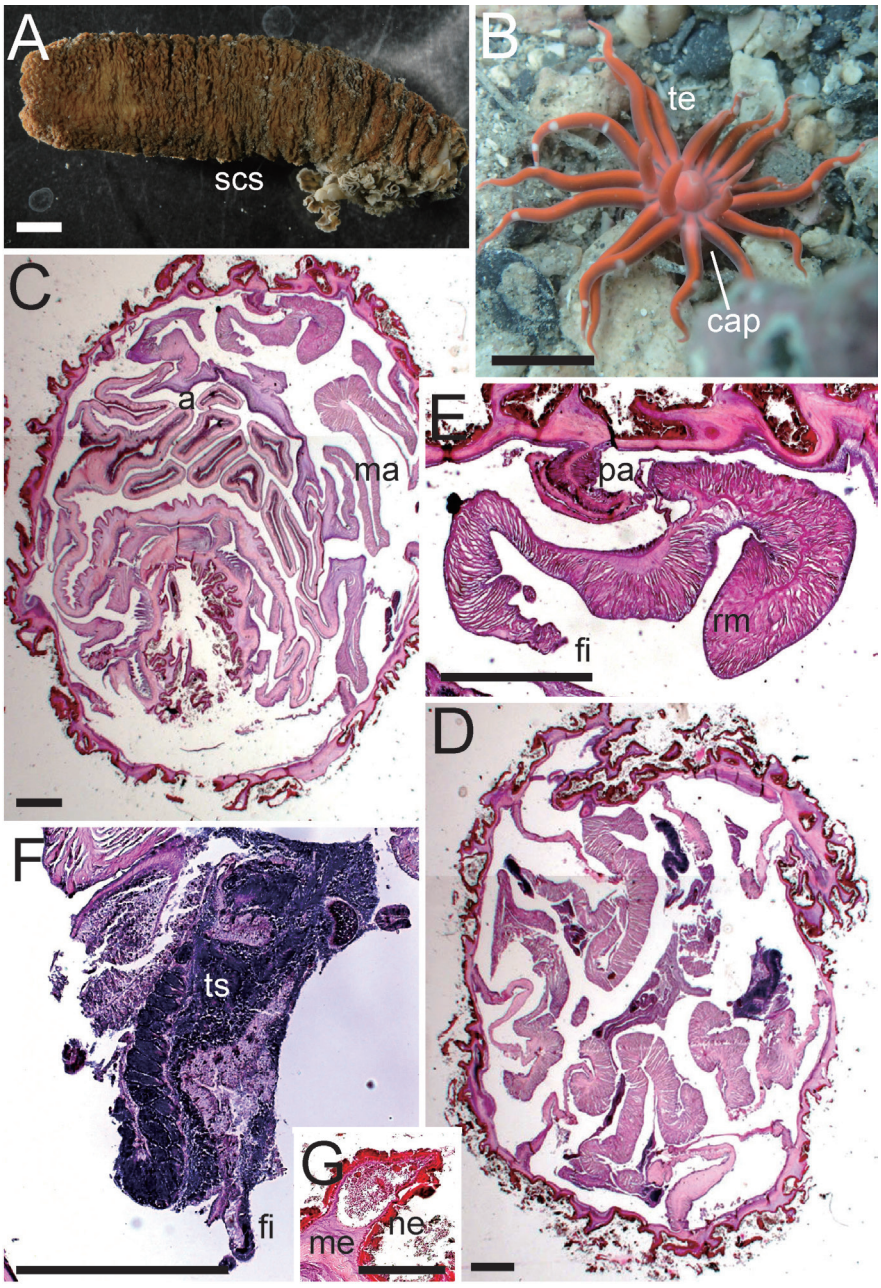

Figure 5. External and internal morphology of *Edwardsianthus carbunculus* sp. nov. (CMNH-ZG 05954) **A** outer view of preserved specimen (aboral end is damaged) **B** oral view of living specimen in the habitat (photograph Kensuke Yanagi) **C** transverse section of column in upper part **D** transverse section of lower column in lower part **E** transverse section of the macrocneme **F** transverse section of testis **G** transverse section of nemathybomes. Abbreviations: a, actinopharynx; cap, capitulum; fi, filament; me, mesoglea; ne, nemathybomes; pa, parietal muscle; rm, retractor muscle; scs, scapus; te, tentacle. Scale bars: 5 mm (**A, B**); 500 μm (**C–F**); 100 μm (**G**). Picture B taken by Kensuke Yanagi.

cle, dark brown in color in living specimen (Fig. 5B; this color lost in preserved specimen), and with tiny, pale white in color, densely scattered nemathybomes (Fig. 5A). Tentacles: 20 in number in two cycles: inner tentacles five and outer 15, vivid scarlet in color (Fig. 5B), without acrospheres. Inner tentacles short, blunt, ca. 6 mm in length, and outer ones long, slender, with sparse white spots on surface, 15–20 mm in length in the living specimen. Mouth: at the center of oral disc apparently swollen in living animal (Fig. 5B). ***Internal anatomy.*** Mesenterial arrangement: eight perfect mesenteries, all macrocnemes. Four dorsal and ventral directives, and four lateral mesenteries not paired with other macrocnemes, arranged in normal *Edwardsia* pattern (Fig. 5C, D). All macrocnemes are present along the whole body length from oral to aboral end and bear distinct retractor and parietal muscles. Twelve tiny microcnemes, without muscles, only confined to distal-most part. Four microcnemes between dorsal directives and dorso-lateral mesenteries, four between dorso-and ventro-lateral mesenteries, and four between ventro-lateral mesenteries and ventral directives. Retractor muscles: at the mid part of column, strongly developed and diffused (Fig. 5E), pennon-like, arranged with 60–90 muscular processes, simple or slightly branched, and pinnated in some parts. Some processes nearest to body wall extremely well-branched, into secondary and thirdly branches (Fig. 5E). Parietal muscles: not so well developed, apparently elongated to direction of mesenteries, with ca. 20–30 simple to muscular processes in each side (Fig. 5E). Others: each with one tentacle from each endo- or exocoels. Existence of siphonoglyph unknown because of contracted state of specimen. Tentacular circular muscle indistinct, and longitudinal muscle distinct, ectodermal. Mesoglea thickest in body wall, > 200 μm in thickness in some parts (Fig. 5C, D), and comparatively thick in tentacles and mesenteries (nearby retractor), but thinner in parietal muscles (Fig. 5E). Nemathybomes protruding from mesoglea (Fig. 5G). Marginal sphincter muscle and basilar muscle absent. Gametogenic tissue apart from retractor muscles, distinct, with dense immature testes (Fig. 5F). ***Cnidom.*** Basitrichs, spirocysts, and microbasic *p*-mastigophores. See Fig. 3K–O and Table 4 for sizes and distributions of cnidae.

Etymology. The species epithet refers to ruby, a kind of gemstone, and is named so after the scarlet, vivid red, color of its tentacles. Derivation of the Japanese name is the same as that of the Latin species name.

Remarks. This species can be distinguished from *Edwardsianthus* not only by the scarlet tentacles, the most characteristic feature of this species, and their arrangement, but also by the species' cnidom: *E. carbunculus* can be distinguished from *E. gilbertensis* and *E. pudicus* by having two types of basitrichs in its nemathybomes (Table 4), and from the other three new species by containing only one type of basitrich in its filaments (Tables 4, 5). In the phylogenetic tree (Fig. 10), *E. carbunculus* sp. nov. is closely related to *E. pudicus*, but there are differences in their morphology as described above and in the separation of their localities: *E. pudicus* inhabits tropical and subtropical waters while *E. carbunculus* were only lives in temperate seas. Therefore, we concluded that this sea anemone is a new species. The genus *Edwardsianthus* is also traditionally characterized by nemathybomes containing only one type of nematocysts, but this

definition needs revision because this species has two types of nematocysts in nemathybomes (Fig. 3M, Table 4; compare with the remarks given for the genus *Edwardsianthus*).

To complete the description of this species, it is necessary to collect and examine specimens with complete proximal ends. However, this species was collected only once from the type locality, and no additional field observations are known, even despite the presence of its characteristic red tentacles. This species is the only *Edwardsianthus* species inhabiting the temperate zone: the other *Edwardsianthus* species live in tropical or subtropical zones (Fig. 1; Fautin, 2013). Thus, the locality, Kochi, becomes the northernmost distribution limit of this genus.

***Edwardsianthus sapphirus* sp. nov.**

http://zoobank.org/84D8919D-0CF0-4C90-BD92-896482C4D206

Japanese name: safaia-mushimodoki-ginchaku

Figs 6, 7A–D; Table 5

Material examined. ***Holotype***. CMNH-ZG 09761: histological sections, tissues in paraffin, and prepared nematocysts, collected by SCUBA diving on 24 June 2012, in Oura Bay, Okinawa Island, Okinawa Pref., Japan, 10 m depth, by Takuma Fujii.

Description. ***External anatomy.*** Size: preserved specimen ca. 150 mm in whole length, and 20 mm (narrower part)–35 mm (broader part) in width, and > 300 mm in living animal. Column: cylinder-like form, and the proximal part swollen to some extent in preserved specimen. The column consisting of capitulum, scapus and quite small physa. The distal-most part of the capitulum transparently blue, short, without nemathybomes. Scapus with thin and easily stripped periderm, brown in color, and with quite numerous, tiny, pale white in color, scattered nemathybomes (Fig. 6B). Nemathybomes. Aboral end differentiated small, tapered physa. Tentacles: 20 in number in two cycles: inner tentacles 5 and outer 15, metallic greenish blue in color with no pattern in living specimen (Fig. 6A; this color lost in preserved specimen), slender, without acrospheres. Inner tentacles ca. 10 mm and outer ones 15–25 mm in length in the living specimen. Mouth: at the center of oral disc, apparently swollen in living animal (Fig. 6A). ***Internal anatomy.*** Mesenterial arrangement: eight perfect mesenteries, all macrocnemes. Four dorsal and ventral directives, and four lateral mesenteries not paired with other macrocnemes, arranged in normal *Edwardsia* pattern (Fig. 6C). All macrocnemes are present along the whole body length from oral to aboral end and bear distinct retractor and parietal muscles. Twelve tiny microcnemes, without muscles, only confined to distal-most part. Four microcnemes between dorsal directives and dorso-lateral mesenteries, four between dorso-and ventro-lateral mesenteries, and four between ventro-lateral mesenteries and ventral directives. Retractor muscles: at the mid part of column, strongly developed and diffused (Fig. 6E), pennon-like, arranged with 120–150 muscular processes, simple or slightly branched. One process nearest to body wall extremely well-branched, with > 100 secondary and thirdly branched pro-

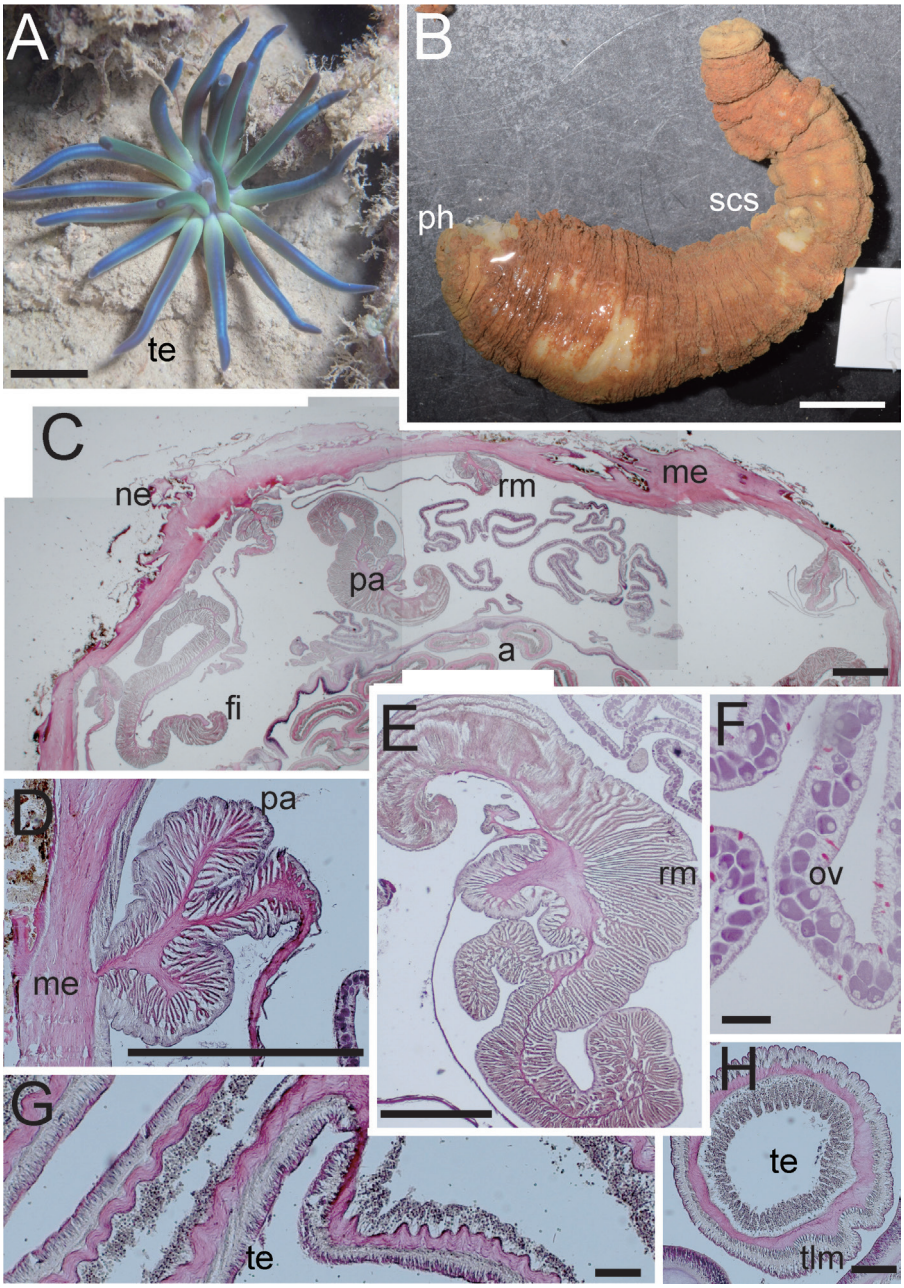

Figure 6. External and internal morphology of *Edwardsianthus sapphirus* sp. nov. (CMNH-ZG 09761). **A** oral view of living specimen in the habitat **B** outer view of preserved specimen; **C**. Transverse section of column in upper part **D** enlarged view of transverse section of parietal muscle **E** enlarged view of transverse section of retractor muscle **F** transverse section of ovary **G** longitudinal section of tentacle **H** transverse section of tentacle. Abbreviations: a, actinopharynx; fi, filament; me, mesoglea; ne, nemathybome; oo, oocytes; pa, parietal muscle; ph, physa; rm, retractor muscle; scs, scapus; te, tentacle; tlm, tentacular longitudinal muscle. Scale bars: 1 cm (**A, B**); 500 μm (**C–E**); 100 μm (**F–H**).

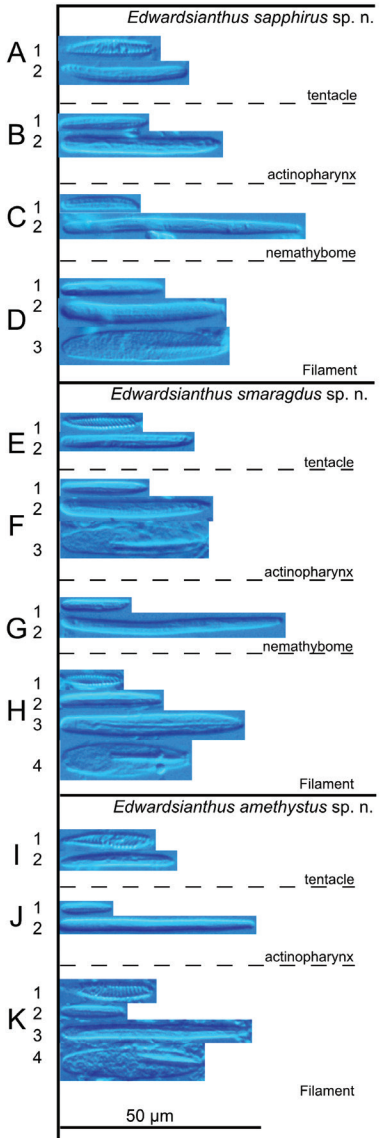

Figure 7. Cnidae of *Edwardsianthus* species **A–D** *E. sapphirus* sp. nov. (CMNH-ZG 09761) **A1** spirocyst in tentacle **A2** basitrich in tentacle **B1** small basitrich in actinopharynx **B2** large basitrich in actinopharynx **C1** small basitrich in nemathybome **C2** large basitrich in nemathybome **D1** small basitrich in filament **D2** large basitrich in filament **D3** microbasic *p*-mastigophore in filament **E–H** *E. smaragdus* sp. nov. (CMNH-ZG 09762) **E1** spirocyst in tentacle **E2** basitrich in tentacle **F1** small basitrich in actinopharynx **F2** large basitrich in actinopharynx **F3** microbasic *p*-mastigophore in actinopharynx **G1** small basitrich in nemathybome; **G2** large basitrich in nemathybome; **H1** spirocyst in filament; **H2** small basitrich in filament **H3** large basitrich in filament **H4** microbasic *p*-mastigophore in filament **I–K** *E. amethystus* sp. nov. (CMNH-ZG 09763) **I1** spirocyst in tentacle **I2** basitrich in tentacle **J1** small basitrich in actinopharynx **J2** large basitrich in actinopharynx **K1** spirocyst in filament **K2** small basitrich in filament **K3** large basitrich in filament **K4** microbasic *p*-mastigophore in filament.

Table 5. Cnidoms of the species of *Edwardsianthus sapphirus* sp. nov., *Edwardsianthus smaragdus* sp. nov., and *Edwardsianthus amethystus* sp. nov.

		***Edwardsianthus sapphirus* sp. nov.**					***Edwardsianthus smaragdus* sp. nov.**					***Edwardsianthus amethystus* sp. nov.**				
		CMNH-ZG 09761					CMNH-ZG 09762					CMNH-ZG 09763				
		Length × Width (μm)	Mean (μm)	SD (μm)	n	frequency	Length × Width (μm)	Mean (μm)	SD (μm)	n	frequency	Length × Width (μm)	Mean (μm)	SD (μm)	n	frequency
Tentacle																
basitrichs		27.5–37.3 × 3.0–4.8	33.1 × 3.9	2.27 × 0.40	55	numerous	25.4–40.3 × 3.0–4.7	30.4 × 3.8	2.72 × 0.41	67	numerous	17.0–32.6 × 2.7–4.3	27.7 × 3.6	3.15 × 0.38	55	numerous
spirocysts		14.9–23.6 × 2.8–4.9	19.1 × 3.9	1.78 × 0.46	64	numerous	12.1–21.7 × 2.5–5.1	18.0 × 3.8	2.07 × 0.49	61	numerous	14.6–24.1 × 3.0–4.9	20.6 × 4.0	1.96 × 0.37	53	numerous
Actinopharynx																
basitrichs	S	20.2–25.9 × 2.3–3.6	22.1 × 3.1	1.49 × 0.40	13	few	20.5–23.6 × 2.5–3.0	22.2 × 2.7	1.03 × 0.20	6	few	12.3–18.2 × 2.7–4.7	14.2 × 3.7	1.18 × 0.48	48	numerous
	L	34.1–44.1 × 3.6–5.6	39.1 × 4.7	2.24 × 0.42	44	numerous	34.9–47.7 × 3.5–5.9	40.0 × 4.5	2.46 × 0.44	71	numerous	28.9–49.1 × 3.8–4.7	38.6 × 4.1	9.60 × 0.34	4	rare
microbasic *p*-mastigophores		–	–	–	–	–	35.1–42.0 × 7.2–8.5	38.3 × 7.8	2.73 × 0.49	5	few	–	–	–	–	–
Nemathybome												(No nematocyst was observed)				
basitrichs	S	16.9–20.5 × 3.2–3.9	18.5 × 3.4	1.05 × 0.22	8	few	16.5–17.1 × 3.0–3.7	16.8 × 3.3	0.31 × 0.35	2	rare					
	L	39.8–75.2 × 2.8–4.9	56.0 × 3.7	4.98 × 0.47	43	numerous	48.7–61.6 × 3.0–4.7	54.4 × 3.8	2.75 × 0.41	59	numerous					
Filament																
basitrichs	S	25.2–29.8 × 2.6–3.9	27.1 × 3.4	1.71 × 0.48	4	few	18.6–32.2 × 2.5–4.1	28.2 × 3.1	2.23 × 0.33	61	numerous	12.6–17.3 × 2.9–4.8	15.2 × 3.6	1.15 × 0.45	42	numerous
	L	38.4–50.5 × 4.3–6.2	44.6 × 5.1	2.97 × 0.41	54	numerous	39.3–52.0 × 4.6–7.1	46.1 × 5.8	2.77 × 0.51	45	numerous	27.4–46.3 × 3.6–5.2	36.7 × 4.3	5.98 × 0.41	23	numerous
spirocysts		–	–	–	–	–	15.6–18.2 × 3.0–4.2	16.9 × 3.7	1.31 × 0.57	2	rare	13.3–23.6 × 3.2–6.1	19.5 × 4.8	2.14 × 0.57	27	numerous
microbasic *p*-mastigophores		33.1–42.3 × 5.9–8.3	36.9 × 7.4	2.69 × 0.55	16	numerous	30.9–41.2 × 6.6–8.6	35.0 × 7.8	2.91 × 0.70	13	few	35.1 × 7.8	–	–	1	rare

cesses (Fig. 6E). Parietal muscles: distinct, developed peculiarly: consisted of ca. 20–30 processes in each side, and only one of them extremely developed, branched into secondary 15–25 processes, and expanded broadly. Thus, parietals in entirety appearing in a characteristic shape like the club symbol of cards (Fig. 6D). Others: each with one tentacle from each endo- or exocoels. Existence of siphonoglyph unknown because of contracted state of specimen. Tentacular circular muscle endodermal, indistinct (Fig. 6G), and longitudinal muscle ectodermal, distinct, and sometimes pinnated (Fig. 6H). Mesoglea thickest in body wall, sometimes reaching 1 mm in thickness (Fig. 6C), but thinner in mesenteries, parietal muscle, and tentacles (Fig. 6E–H). Nemathybomes protruding from mesoglea. Marginal sphincter muscle and basilar muscle absent. Gametogenic tissue apart from retractor muscles, distinct (Fig. 6C, F), with matured oocytes. ***Cnidom.*** Basitrichs, spirocysts, microbasic *p*-mastigophores. See Fig. 7A–D and Table 5 for sizes and distribution.

Etymology. The species epithet refers to a sapphire, a gemstone, and is named so after the brilliant metallic blue color of the species' tentacles. Derivation of the Japanese name is the same as that of the Latin species name.

Remarks. This species is one of the largest species of its family. It is not only characterized by its gigantic body size, and bluish metallic tentacle coloration, but also by the strange club-like shape of its parietal muscles. Congeneric species have parietal muscles with simple or slightly branched processes, and there are no confirmed cases of parietal muscles with such secondary branched muscular processes in other species. Thus, the shape of parietal muscle of this species is very conspicuous within its genus, allowing *E. sapphirus* to be distinguished easily from its congeners.

There have been several observations of the metallic blue tentacles resembling this species reported during SCUBA diving in Amami Oshima by Takuma Fujii and some other divers (Atetsu Bay and some other places). However, it was too difficult to dig out such large edwardsiid sea anemones that are buried deeply in the substrate, as they usually retract their whole bodies quickly into the substrate. Therefore, we think that the difficulty in collecting multiple specimens is the most serious issue that needs to be overcome in order to make additional progress in the study of edwardsiids.

Edwardsianthus smaragdus sp. nov.

http://zoobank.org/05B8173F-21FB-4429-B5BB-5371E3EB144F
Japanese name: emerarudo-mushimodoki-emeginchaku
Figs 7E–H, 8; Table 5

Material examined. ***Holotype***. CMNH-ZG 09762: histological sections, tissues in paraffin, and prepared nematocysts, collected by SCUBA diving on 31 January 2016, off Shirahama seashore, Amami-Oshima Island, Kagoshima, Japan, 15 m depth, by Daisuke Uyeno.

Description. ***External anatomy.*** Size: preserved specimen ca. 70 mm in whole length, and ca. 15 mm in width, and ca. 100 mm in living specimen. Column: cylin-

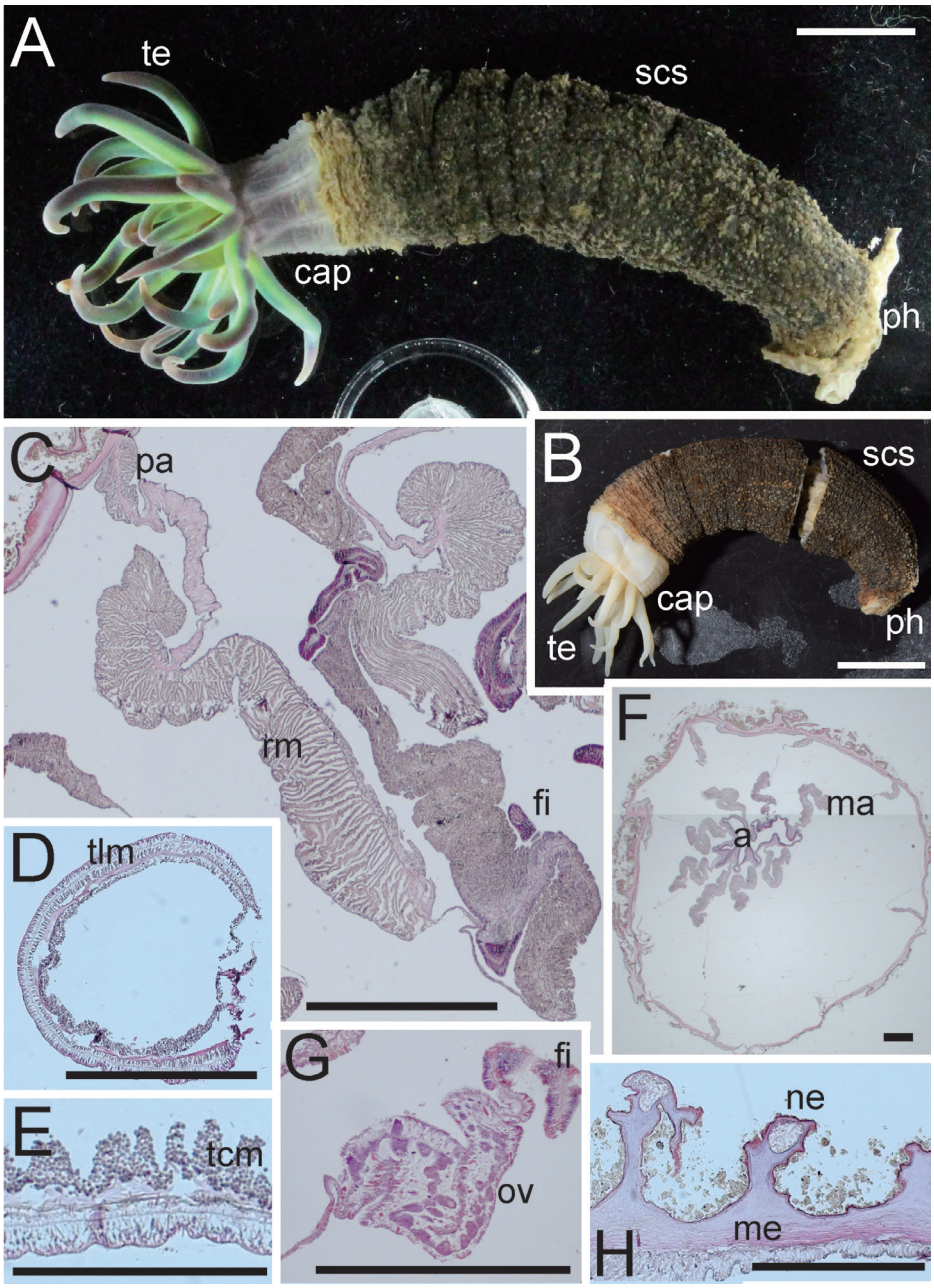

Figure 8. External and internal morphology of *Edwardsianthus smaragdus* sp. nov. (CMNH-ZG 09762). **A** outer view of living specimen **B** outer view of preserved specimen **C** transverse section of retractor muscle **D** transverse section of the tentacle **E** longitudinal section of the tentacle **F** transverse section of column **G** enlarged view of transverse section of ovary **H** transverse section of a nemathybome. Abbreviations: a, actinopharynx; cap, capitulum; fi, filament; ma, macrocneme; me, mesoglea; ne, nemathybomes; ov, ovary; pa, parietal muscle; ph, physa; rm, retractor muscle; scs, scapus; te, tentacle; tcm, tentacular circular muscle; tlm, tentacular longitudinal muscle. Scale bars: 1 cm (**A, B**); 500 μm in (**C**–**H**).

der-like in form, and the middle part swollen to some extent (Fig. 8A, B). The column consisting of capitulum, scapus and quite small physa. The distal-most part of the capitulum whitish transparent in living animals, short, without nemathybomes. Scapus with thick periderm, brownish black in color, and with protruding scattered tiny, dingy grey color nemathybomes in the living specimen (Fig. 8A). Aboral end differentiated small, tapered physa. Tentacles: 20 in number in two cycles: inner tentacles five and outer 15, brilliant green in color and pale purple at the tips, no pattern, comparatively slender, without acrospheres. Inner tentacles ca. 7 mm and outer ones ca. 10–15 mm in length in the living specimen. Mouth: at the center of oral disc, slightly swollen both in living and preserved specimen. ***Internal anatomy.*** Mesenterial arrangement: eight perfect mesenteries, all macrocnemes. Four dorsal and ventral directives, and four lateral mesenteries not paired with other macrocnemes, arranged in normal *Edwardsia* pattern (Fig. 8F). All macrocnemes are present along the whole body length from oral to aboral end and bear distinct retractor and parietal muscles. Twelve tiny microcnemes, without muscles, only confined to distal-most part. Four microcnemes between dorsal directives and dorso-lateral mesenteries, four between dorso-and ventro-lateral mesenteries, and four between ventro-lateral mesenteries and ventral directives. Each tentacle exo- or endocoelic. Retractor muscles: at the mid part of column, weakly developed but distinct, diffused (Fig. 8C), pennon-like, arranged with 50–60 muscular processes, simple or slightly branched. One process nearest to body wall well-branched (Fig. 8C). Parietal muscles indistinct, elongated in direction of mesenteries, consisted of short and slightly branched processes, sparsely, < ten on each side (Fig. 8C). Others: each with one tentacle from each endo- or exocoels. Existence of siphonoglyph unknown because of contracted state of specimen. Tentacular circular muscle endodermal, distinct, and longitudinal muscle ectodermal, both distinct. Mesoglea thickest in body wall and actinopharynx, maximum 400 μm in thickness (Fig. 8F), but far thinner in parietal muscle and tentacles (Fig. 8C–E), and thinnest, < 10 μm, in mesenteries. Nemathybomes protruding from mesoglea (Fig. 8H). Marginal sphincter muscle and basilar muscle absent. Gametogenic tissue apart from retractor muscles, distinct (Fig. 8G), with matured oocytes. ***Cnidom.*** Basitrichs, spirocysts, microbasic *p*-mastigophores. See Fig. 7E–H and Table 5 for sizes and distribution.

Etymology. This species epithet refers to an emerald, a gemstone, and is named so after the bright green coloration of its tentacles. Derivation of the Japanese name is the same as that of the Latin species name.

Remarks. *Edwardsianthus* species usually have strongly developed and diffused retractor and parietal muscles (Figs 2F, 4F, 5E, 6E, 9E), but those of *Edwardsianthus smaragdus* form an exception by their less distinct development (Fig. 8F). This character is clear in addition to its brilliant light green tentacles. Concerning the cnidom, *E. smaragdus* can be distinguished from *E. pudicus* and *E. gilbertensis* by containing two types of basitrichs in its nemathybomes, and from the other three new species of *Edwardsianthus* by having microbasic *p*-mastigophores in its actinopharynx (Tables 4, 5).

In the phylogenetic tree (Fig. 10; Suppl. material 1 Fig. S1), *E. smaragdus* sp. nov. has a far longer branch than the other species, and therefore its phylogenetic position is not stable; the ML bootstrap value was 57, which is comparatively low, and not supported by BI posterior probability; Fig. 10). Nevertheless, it is most probable that *E. smaragdus* n. sp. belongs to this genus (ML bootstrap value was 79) despite the BI posterior probability not being well-supported. Considering that the morphology of this species corresponds completely with the diagnosis of *Edwardsianthus*, this species is classified as *E. smaragdus*.

***Edwardsianthus amethystus* sp. nov.**
http://zoobank.org/E472474A-8E8B-4B30-93CC-B46005F3F8F0
Japanese name: amejisuto-mushimodoki-ginchaku
Figs 7I–K, 9; Table 5

Material examined. ***Holotype***. CMNH-ZG 09763: histological sections, tissues in paraffin, and prepared nematocysts, collected by SCUBA diving on 28 March 2013, in Oura Bay, Okinawa Island, Okinawa Pref., Japan, 15 m depth, by Takuma Fujii.

Description. ***External anatomy.*** Size: preserved specimen ca. 200 mm in whole length, and 7 mm (narrower part)–20 mm (broader part) in width, and > 300 mm in living animal, one of the largest species in edwardsiids (Fig. 9B). Column: worm-like in form, and the distal part swollen to some extent (maybe because of condition during preservation). The column consisting of capitulum, scapus and quite small physa. The distal-most part a short capitulum, without nemathybomes. Scapus with thin and easily stripped periderm, light brown in color, and surface completely smooth, with extremely small nemathybome-like spots (Fig. 9B). Aboral end differentiated with small, rounded physa. Tentacles: 20 in number in two cycles: inner tentacles five and outer 15, slender, pale purple in color with several dark purple spots (Fig. 9A; this color is lost in preserved specimen: Fig. 9B). Inner tentacles ca. 10 mm and outer ones ca. 15–20 mm in length in the living specimen. Mouth: at the center of oral disc, apparently swollen in living animal. ***Internal anatomy.*** Mesenterial arrangement: eight perfect mesenteries, all macrocnemes. Four dorsal and ventral directives, and four lateral mesenteries not paired with other macrocnemes, arranged in the normal *Edwardsia* pattern. All macrocnemes are present along the whole body length from oral to aboral end and bear distinct retractor and parietal muscles. Twelve tiny microcnemes, without muscles, only confined to distal-most part. Four microcnemes between dorsal directives and dorso-lateral mesenteries, four between dorso-and ventro-lateral mesenteries, and four between ventro-lateral mesenteries and ventral directives. Retractor muscles: at the mid part of column, strongly developed and diffused (Fig. 9E), pennon-like, arranged with 100–150 muscular processes, simple to well branched. Processes near filament short and highly branched, and one process nearest

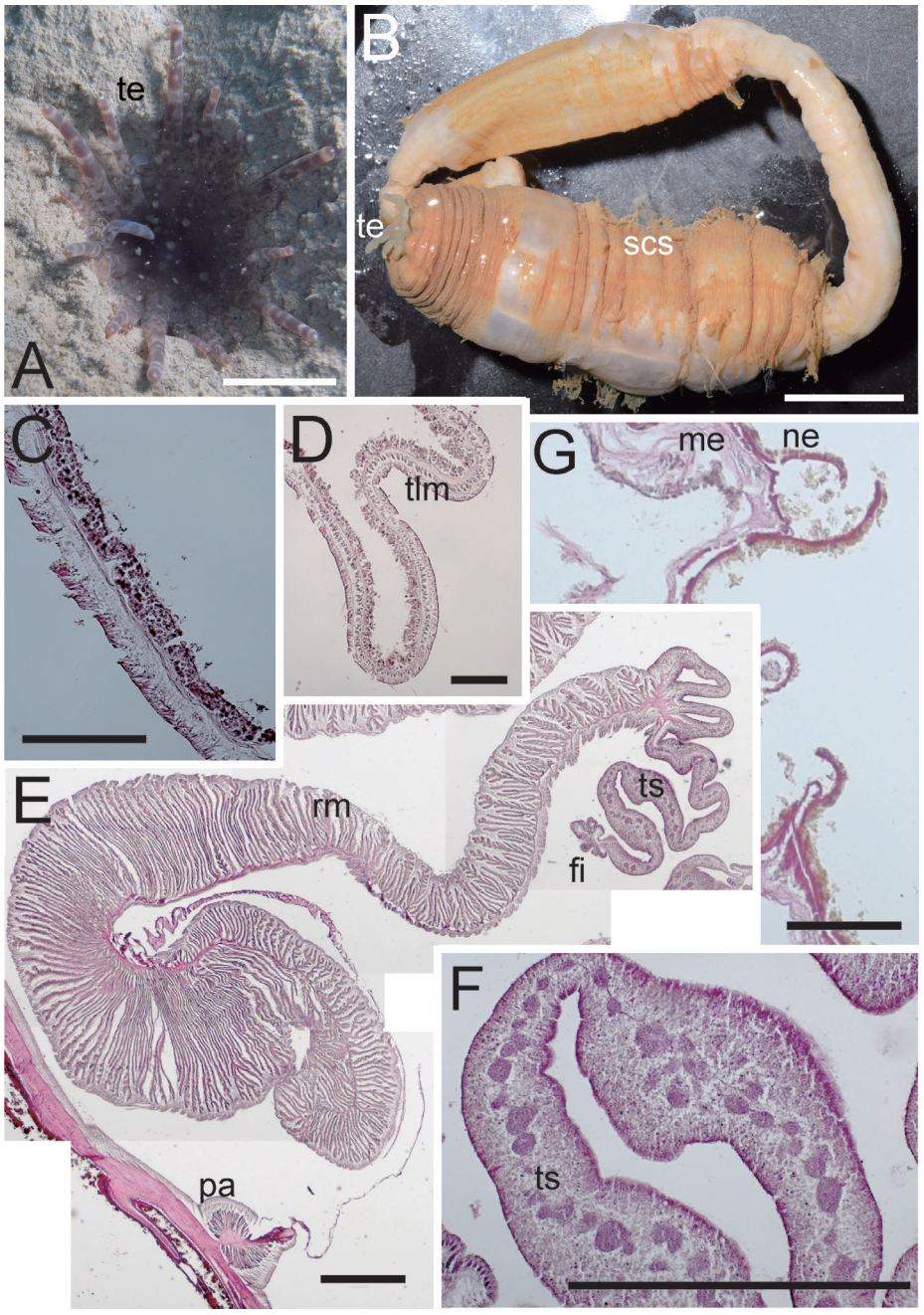

Figure 9. External and internal morphology of *Edwardsianthus amethystus* sp. nov. (CMNH-ZG 09763) **A** oral view of living specimen in the habitat **B** outer view of preserved specimen **C** longitudinal section of tentacle **D** transverse section of tentacle **E** transverse section of retractor muscle **F** transverse section of testis **G** transverse section of trace of nemathybome. Abbreviations: fi, filament; me, mesoglea; ne, nemathybome-like structure; pa, parietal muscle; rm, retractor muscle; scs, scapus; te, tentacle; tlm, tentacle longitudinal muscle; ts, testis. Scale bars: 1 cm (**A, B**); 500 μm (**E, F**); 100 μm (**C, D, G**).

to the body wall extremely well-branched, with ca. 80 secondary and thirdly branched processes (Fig. 9E). Parietal muscles: distinct, rounded shape, consisting of 10–15 simple processes on each side (Fig. 9E). Others: each with one tentacle from each endo- or exocoels. Existence of siphonoglyph unknown because of contracted state of specimen. Tentacular circular muscle indistinct (Fig. 9C), and longitudinal muscle ectodermal, distinct (Fig. 9D). Mesoglea thickest in body wall and actinopharynx, ca. 200 μm in thickness (Fig. 9E), but far thinner in mesenteries, retractor muscles, and tentacles (Fig. 9C, D). Nemathybome-like structures protruding from mesoglea, but without any nematocysts (Fig. 9G). Marginal sphincter muscle and basilar muscle absent. Gametogenic tissue apart from retractor muscles, distinct (Fig. 9F), with matured oocytes. ***Cnidom.*** Basitrichs, spirocysts, and microbasic *p*-mastigophores. There are no nematocysts in nemathybome-like structures. See Fig. 7I–K and Table 5 for sizes and distributions.

Etymology. This species epithet refers to amethyst, a kind of gemstone, and is named after this species' dark purple tentacle coloration. Derivation of the Japanese name is the same as that of the Latin species name.

Remarks. The most characteristic feature of this species is the nemathybome-like features without nematocysts. Nemathybomes are pocket-like features on columns of some genera of Edwardsiidae, and they always contain large nematocysts (Carlgren, 1949; Brandão et al. 2019). Thus, the structures of *Edwardsianthus amethystus* cannot be called nemathybomes because they lack nematocysts. This is the first case of confirmation of this nemathybome-like feature in *Edwardsianthus* anemones, and by these *E. amethystus* can be easily distinguished from its congeners. We placed this sea anemone in the genus *Edwardsianthus* because of the characteristic arrangement of tentacles and mesenteries, but the generic diagnosis has now been modified to "sometimes without" nemathybomes (see the Remarks for the genus).

Phylogenetic analyses. The concatenated phylogenetic tree of 12S, 16S, and 18S rDNA (total 2886 bp) is shown in Fig. 10. All *Edwardsianthus* specimens formed a clade (indicated in red box) supported by a ML bootstrap value of 79%, but not well supported by BI posterior probability. In this clade, *E. pudicus*, *E. carbunculus* sp. nov., *E. sapphirus* sp. nov., and *E. amethystus* sp. nov. were closely related with high support (ML bootstrap value = 83%; BI posterior probability = 0.98), *Edwardsianthus smaragdus* sp. nov. was indicated as their sister group, but was only slightly supported by ML (bootstrap value = 57%) and not supported by the BI method. *Edwardsianthus gilbertensis* was nested with the other five species and positioned at the most basal node of this genus.

In addition, the most basal position of our phylogenetic tree of Edwardsiidae is taken by *Tempuractis rinkai* Izumi, Ise, & Yanagi, 2018. This edwardsiid is the only species of the genus *Tempuractis* Izumi, Ise, & Yanagi, 2018. It has a simple morphology compared to other edwardsiid species by showing a smooth body wall without particular structures, like nemathybomes, a simple aboral end without any apparent physa, and simple tentacles without any structures (Izumi et al., 2018). This topology suggests that nemathybomes of Edwardsiidae were obtained within the family lineage (Fig. 10).

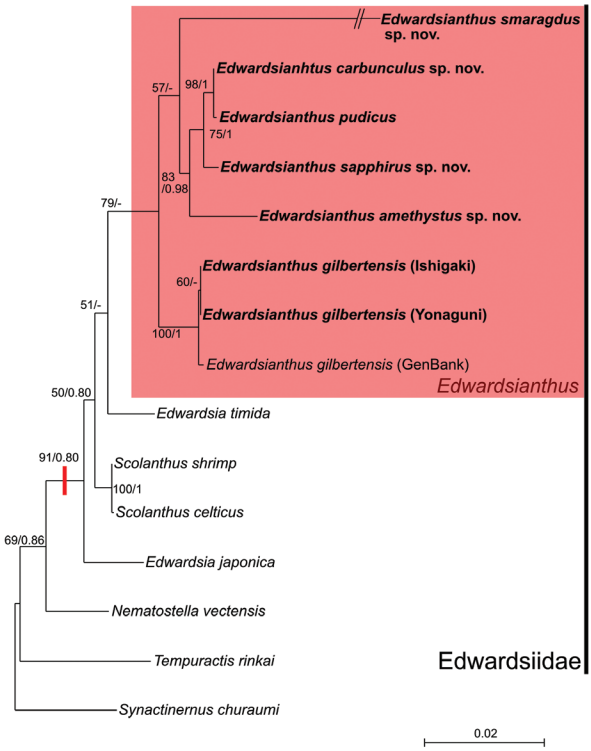

Figure 10. Maximum-likelihood tree of the order Actiniaria based on the combined dataset of mitochondrial 12S and 16S and nuclear 18S rDNA (total 2866 bp). The clade of the genus *Edwardsianthus* is colored in a red box. Red bar at node indicates the position at which nemathybomes would be obtained. Numbers indicate ML bootstrap support values followed by BI posterior probabilities of the nodes (bootstrap values of ≥ 50% and posterior probabilities ≥ 0.5 are shown).

Acknowledgements

We thank the researchers below for sample collection as indicated in parentheses: Kensuke Yanagi (Coastal Branch of Natural History Museum and Institute, Chiba; *E. carbunculus* and some specimens of *E. gilbertensis*), Daisuke Uyeno (Kagoshima University; *E. smaragdus*). Regarding the collection of specimens, we also thank the following people: research members of Umisawa collections (*E. pudicus*), Takuma Mezaki (Kuroshio Biological Research Institute; *E. carbunculus*), Shin Nishihira and the members of the diving team Diving Team Snuck Snufkin (*E. sapphirus*). In addition, we are greatful to Kensuke Yanagi and Toshihiko Fujita (National Science Museume, Tsukuba) for their advice and help for research, and James Davis Reimer (University of the Ryukyus) for editing an early draft of the manuscript. Finally, we thank two reviewers and the editor of this paper for providing us with helpful comments and suggestions. We also thank the financial support from several groups for our research: The Sasakawa

Scientific Research Grant from the Japan Science Society (No. 27–528), JSPS KAKENHI (JP17J03267), and Grant-in-Aid for JSPS Fellow DC2 to TI; JSPS KAKENHI (24–3048, JP17K15198, JP17H01913, and 21H03651) and the "Establishment of Research and Education Network on Biodiversity and Its Conservation in the Satsunan Islands" project of Kagoshima University adopted by the Ministry of Education, Culture, Sports, Science and Technology, Japan to TF.

References

Andres A (1881) Prodromus neapolitanae actiniarum faunae addito generalis actiniarum bibliographiae catalogo. Mitteilungen aus der Zoologischen Station zu Neape 2: 305–371.

Apakupakul K, Siddall ME, Burreson EM (1999) Higher level relationships of leeches (Annelida: Clitellata: Euhirudinea) based on morphology and gene sequences. Molecular Phylogenetics and Evolution 12: 350–359. https://doi.org/10.1006/mpev.1999.0639

Carlgren O (1892) Beiträge zur Kenntnis der Edwardsien. Öfversigt af Kongliga Vetenskaps-Akademiens Förhandlingar 1892: 451–461.

Carlgren O (1921) Actiniaria Part I. Danish Ingolf-Expedition 5: 1–241.

Carlgren O (1931) Zur Kenntnis der Actiniaria Abasilaria. Arkiv für Zoologi 23: 1–48.

Carlgren O (1949) A survey of the Ptychodactiaria, Corallimorpharia and Actiniaria. Kungliga Svenska Vetenskapsakademiens Handlingar 1: 1–121.

Castresana, J. (2002) Gblocks Server. http://molevol.cmima.csic.es/castresana/Gblocks_server.html [Accessed 2 January 2002]

Daly M (2002) A systematic revision of Edwardsiidae (Cnidaria: Anthozoa). Invertebrate Biology 121: 212–225. https://doi.org/10.1111/j.1744-7410.2002.tb00061.x

Daly M, Fautin DG (2021) World List of Actiniaria. http://www.marinespecies.org/ [Accessed 18 July 2021]

Daly M, Rack F, Zook R (2013) *Edwardsiella andrillae*, a new species of sea anemone from Antarctic ice. PLoS ONE 8: 1–8. https://doi.org/10.1371/journal.pone.0083476

Danielssen DC (1890) Actinida. Den Norske Nordhavs-Expedition 1876–1878. Zoologi. Grøndahl and Søn, Christiania, 184 pp.

Dnyansagar R, Zimmermann B, Moran Y, Praher D, Sundberg P, Møller LF, Technau U (2018) Dispersal and speciation: The cross Atlantic relationship of two parasitic cnidarians. Molecular Phylogenetics and Evolution 126: 346–355. https://doi.org/10.1016/j.ympev.2018.04.035

Duerden JE (1899) The Edwardsia-stage of the Actinian *Lebrunia*, and the formation of the gastro-coelomic cavity. Journal of the Linnean Society of London, Zoology 27: 269–316. https://doi.org/10.1111/j.1096-3642.1899.tb00249.x

England KW (1987) Certain Actiniaria (Cnidaria, Anthozoa) from the Red Sea and tropical Indo-Pacific Ocean. Bulletin of the British Museum (Natural History) 53: 205–292.

Fautin DG, Zelenchuck T, Rveendran D (2007) Genera of orders Actiniaria and Corallimorpharia (Cnidaria, Anthozoa, Hexacorallia), and their type species. Zootaxa 1668: 183–244. https://doi.org/10.11646/zootaxa.1668.1.12

Fautin DG (2013) Hexacollarians of the World. ttp://hercules.kgs.ku.edu/hexacoral/anemone2/index.cfm [Accessed 2 January 2013]

Fautin DG (2016) Catalog to families, genera, and species of orders Actiniaria and Corallimorpharia (Cnidaria: Anthozoa). Zootaxa 4145: 1–449. https://doi.org/10.11646/zootaxa.4145.1.1

Geller JB, Walton ED (2001) Breaking up and getting together: evolution of symbiosis and cloning by fission in sea anemones (genus *Anthopleura*). Evolution 55: 1781–1794. https://doi.org/10.1111/j.0014-3820.2001.tb00827.x

Gusmão LC, Berniker, L, Van Deusen V, Harris O, Rodríguez E (2019). Halcampulactidae (Actiniaria, Actinostoloidea), a new family of burrowing sea anemones with external brooding from Antarctica. Polar Biology 42(7): 1271–1286. https://doi.org/10.1007/s00300-019-02516-1

Gusmão LC, Qu C, Burke SL, Rodríguez E (2020). Two new deep-sea species of burrowing anemones (Cnidaria: Actiniaria: Edwardsiidae) from Whittard Canyon off the southwestern coast of Ireland. American Museum Novitates 2020(3945): 1–25. https://doi.org/10.1206/3945.1

Hertwig R (1882) Die Actinien der Challenger Expedition. Gustav Fischer, Jena, 119 pp.

Hyman L (1940) The Invertebrates I. McGraw-Hill, New York, 724 pp.

Izumi T, Fujita T (2018) Description of three new species of *Scolanthus* (Cnidaria, Anthozoa, Actiniaria, Edwardsiidae): first records of the genus from Japan. ZooKeys 794: 1–21. https://doi.org/10.3897/zookeys.794.25243

Izumi T, Fujita T (2019) Two species of Edwardsia having gigantic nematocysts, *E.* aff. *tuberculata* and *E. alternobomen* sp. nov. (Cnidaria; Anthozoa; Actiniaria; Edwardsiidae) from Japan. Zootaxa 4661: 533–544. https://doi.org/10.11646/zootaxa.4661.3.7

Izumi T, Ise Y, Yanagi K, Shibata D, Ueshima R (2018) First detailed record of symbiosis between a sea anemone and homoscleromorph sponge, with a description of *Tempuractis rinkai* gen. et sp. nov. (Cnidaria: Anthozoa: Actiniaria: Edwardsiidae). Zoological Science 35: 188–198. https://doi.org/10.2108/zs170042

Katoh K, Standley DM (2013) MAFFT multiple sequence alignment software version 7: improvements in performance and usability. Molecular Biology and Evolution 30: 772–780. https://doi.org/10.1093/molbev/mst010

Klunzinger CB (1877) Die Korallthiere des Rothen Meeres. 1: Die Alcyonarien und Malacodermen. Gutmann'schen Buchhandlung, Berlin, 98 pp.

Manuel RL (1981) British Anthozoa. Academic Press, New York, 241 pp.

Mariscal RN (1974) Nematocysts. In "Coelenterate Biology: Reviews and New Perspectives" Ed by L Muscatine, HM Lenhoff, Academic Press, New York, 129–178. https://doi.org/10.1016/B978-0-12-512150-7.50008-6

McMurrich JP (1891) Contributions on the morphology of the Actinozoa. Journal of Morphology 5: 125–165. https://doi.org/10.1002/jmor.1050050105

Medina M, Collins AG, Silberman, JD, Sogin, ML (2001) Evaluating hypotheses of basal animal phylogeny using complete sequences of large and small subunit rRNA. Proceedings of the National Academy of Sciences 98(17): 9707–9712. https://doi.org/10.1073/pnas.171316998

Medlin L, Elwood HJ, Stickel S, Sogin ML (1988) The characterization of enzymatically amplified eukaryotic 16S-like rRNA-coding regions. Gene 71: 491–499. https://doi.org/10.1016/0378-1119(88)90066-2

Presnell JK, Schreibman MP (1997) Humason's Animal Tissue Techniques 5th Edition. Johns Hopkins University Press, Baltimore, ## pp.

Rasband WS (1997–2012) ImageJ, U.S. National Institutes of Health, Bethesda, Maryland, USA. http://imagej.nih.gov/ij/

Ride WH, Cogger G, Dupuis C, Kraus O, Minelli A, Thompson FC, Tubbs PK (1999) International Code of Zoological Nomenclature. London, 4th ed., 305 pp. https://www.iczn.org/the-code/the-international-code-of-zoological-nomenclature/the-code-online/

Rodríguez E, Barbeitos MS, Brugler MR, Crowley LM, Grajales A, Gusmão L, Häussermann V, Reft A, Daly M. (2014) Hidden among sea anemones: the first comprehensive phylogenetic reconstruction of the Order Actiniaria (Cnidaria, Anthozoa, Hexacorallia) reveals a novel group of hexacorals. PLoS ONE 9: 1–17. https://doi.org/10.1371/journal.pone.0096998

Ronquist F, Huelsenbeck JP (2003) MrBayes 3: Bayesian phylogenetic inference under mixed models. Bioinformatics 19: 1572–1574. https://doi.org/10.1093/bioinformatics/btg180

Sanamyan NP, Sanamyan KE, McDaniel N, Bocharova ES (2018) First record of two genera of sea anemones (Cnidaria: Actiniaria), *Octineon* and *Edwardsiella*, from the North Pacific Ocean. Invertebrate Zoology 15: 1–18. https://doi.org/10.15298/invertzool.15.1.01

Sinniger F, Montoya-Burgos JI, Chevaldonné P, Pawlowski J (2005) Phylogeny of the order Zoantharia (Anthozoa, Hexacorallia) based on the mitochondrial ribosomal genes. Marine Biology 147: 1121–1128. https://doi.org/10.1007/s00227-005-0016-3

Sinniger F, Reimer JD, Pawlowski J (2010) The Parazoanthidae (Hexacorallia: Zoantharia) DNA taxonomy: Description of two new genera. Marine Biodiversity 40: 57–70. https://doi.org/10.1007/s12526-009-0034-3

Stamatakis A (2006) RAxML-VI-HPC: maximum likelihood-based phylogenetic analyses with thousands of taxa and mixed models. Bioinformatics 22: 2688–2690. https://doi.org/10.1093/bioinformatics/btl446

Tanabe AS (2011) Kakusan4 and Aminosan: two programs for comparing nonpartitioned, proportional and separate models for combined molecular phylogenetic analyses of multilocus sequence data. Molecular Ecology Resources 11: 914–921. https://doi.org/10.1111/j.1755-0998.2011.03021.x

Uchida H, Soyama I (2001) Sea Anemones in Japanese Waters. TBS, Japan, 157 pp. [in Japanese]

Uchida T (1941) Actiniaria collected in the vicinity of Onagawa Bay. The Science Reports of the Tôhoku University 16: 383–390.

Yanagi K (2006) Sea anemones around the Sagami Sea with the list of Japanese species. Memoirs of the National Science Museum 40: 113–173. [in Japanese]

Yanagi K, Fujii T, Hirose M (2015) Redescription of the sea anemone *Exocoelactis actinostoloides* (Cnidaria: Anthozoa: Actiniaria) based on a topotypic specimen collected from Tokyo Bay, Japan. Species Diversity 20: 199–209. https://doi.org/10.12782/sd.20.2.199

Supplementary material 1

The correct shape of Maximum-likelihood tree of the order Actiniaria based on the combined dataset of mitochondrial 12S and 16S and nuclear 18S rDNA (total 2866 bp)

Authors: Takato Izumi, Takuma Fujii

Data type: phylogenetic tree

Link: https://doi.org/10.3897/zookeys.1076.69025.suppl1